Evidence-Based Complementary and Alternative Medicine

Therapeutic Strategies for the Treatment of Cardio/ Cerebrovascular-Related Diseases

Lead Guest Editor: Joen-Rong Sheu
Guest Editors: Thanasekaran Jayakumar and Periyakali Saravana Bhavan

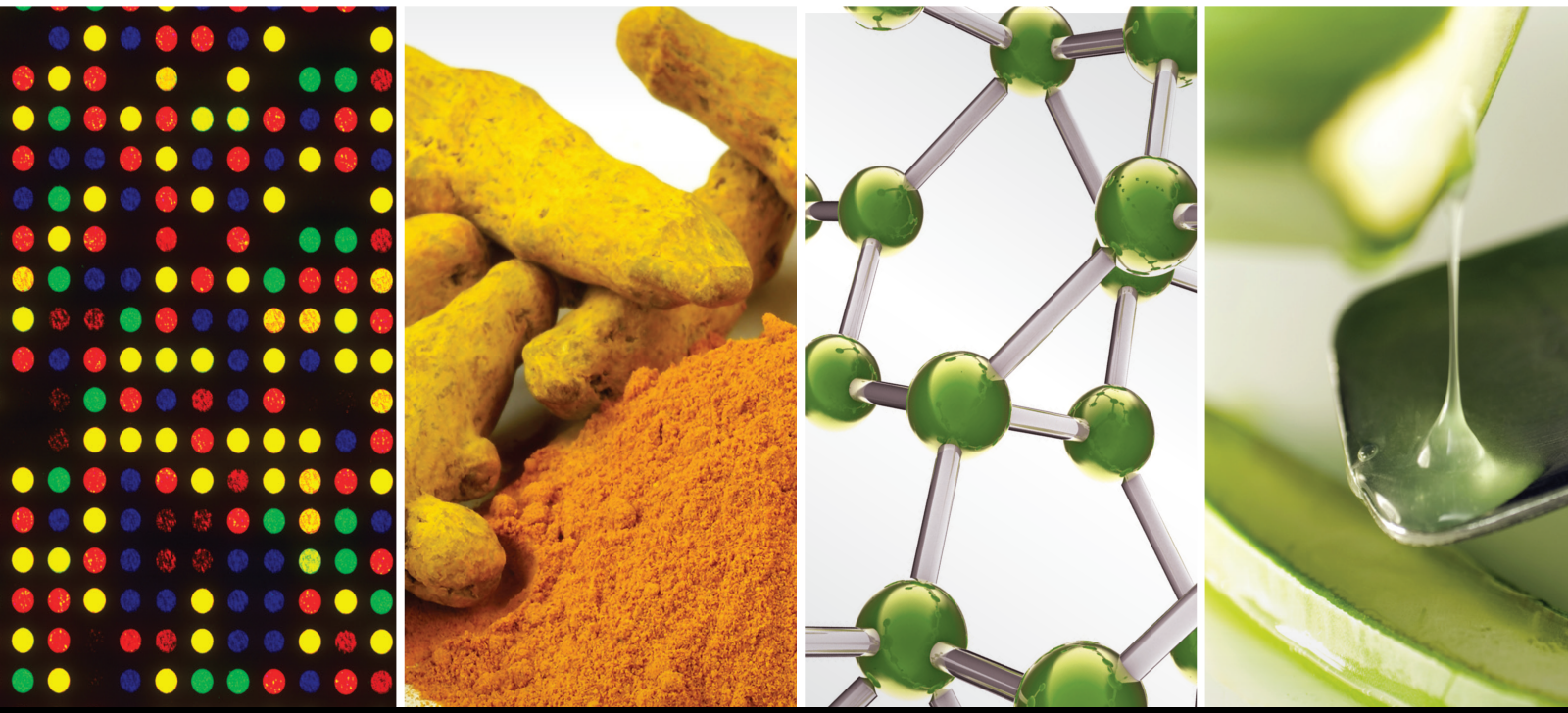

Therapeutic Strategies for the Treatment of Cardio/Cerebrovascular-Related Diseases

Evidence-Based Complementary and Alternative Medicine

Therapeutic Strategies for the Treatment of Cardio/Cerebrovascular-Related Diseases

Lead Guest Editor: Joen-Rong Sheu
Guest Editors: Thanasekaran Jayakumar and Periyakali Saravana Bhavan

Chief Editor

Associate Editors

Academic Editors

Contents

Hindawi
Evidence-Based Complementary and Alternative Medicine
Volume 2022, Article ID 2056630, 14 pages
https://doi.org/10.1155/2022/2056630

Research Article

Integrated Bioinformatics Analysis and Verification of Gene Targets for Myocardial Ischemia-Reperfusion Injury

Jianru Wang,[1] **Xiaohui Li**,[1] **Guangcao Peng**,[1] **Genhao Fan**,[1] **Mengmeng Zhang**,[1] **and Jian Chen**[2,3]

[1]*Department of Cardiovascular, The First Affiliated Hospital of Henan University of CM, Zhengzhou, Henan 450099, China*
[2]*Department of Vascular Disease, Shanghai TCM-Integrated Hospital, Shanghai University of Traditional Chinese Medicine, Shanghai 200082, China*
[3]*Institute of Vascular Anomalies, Shanghai Academy of Traditional Chinese Medicine, Shanghai 200082, China*

Correspondence should be addressed to Jian Chen; alexandercj@126.com

Received 16 September 2021; Revised 11 March 2022; Accepted 28 March 2022; Published 15 April 2022

Academic Editor: Thanasekaran Jayakumar

Background. Myocardial ischemia-reperfusion injury (MIRI) has become a thorny and unsolved clinical problem. The pathological mechanisms of MIRI are intricate and unclear, so it is of great significance to explore potential hub genes and search for some natural products that exhibit potential therapeutic efficacy on MIRI via targeting the hub genes. *Methods*. First, the differential expression genes (DEGs) from GSE58486, GSE108940, and GSE115568 were screened and integrated via a robust rank aggregation algorithm. Then, the hub genes were identified and verified by the functional experiment of the MIRI mice. Finally, natural products with protective effects against MIRI were retrieved, and molecular docking simulations between hub genes and natural products were performed. *Results*. 230 integrated DEGs and 9 hub genes were identified. After verification, Emr1, Tyrobp, Itgb2, Fcgr2b, Cybb, and Fcer1g might be the most significant genes during MIRI. A total of 75 natural products were discovered. Most of them (especially araloside C, glycyrrhizic acid, ophiopogonin D, polyphyllin I, and punicalagin) showed good ability to bind the hub genes. *Conclusions*. Emr1, Tyrobp, Itgb2, Fcgr2b, Cybb, and Fcer1g might be critical in the pathological process of MIRI, and the natural products (araloside C, glycyrrhizic acid, ophiopogonin D, polyphyllin I, and punicalagin) targeting these hub genes exhibited potential therapeutic efficacy on MIRI. Our findings provided new insights to explore the mechanism and treatments for MIRI and revealed new therapeutic targets for natural products with protective properties against MIRI.

1. Introduction

Coronary heart disease (CHD) as a global public health problem is one of the main causes of decreased quality of life and death worldwide [1]. Acute myocardial infarction (AMI) is a kind of acute and critical manifestation of CHD with high morbidity and mortality. Early rapid restoration of coronary blood flow can reduce the size of myocardial infarction and prevent further cardiac injury. With the development of reperfusion strategies such as thrombolysis and percutaneous coronary intervention, the mortality rate of AMI has been greatly reduced [2]. However, myocardial reperfusion can further cause secondary myocardial injury, which can account for 50% of the final myocardial infarct area [3]. This phenomenon, termed myocardial ischemia-reperfusion injury (MIRI), has become an unsolved clinical problem and a major cause of cardiac insufficiency. Currently, there is no specific treatment for MIRI in pharmacopeia [4]. Therefore, clinical and basic studies in the prevention and treatment of MIRI are active areas in the medical field.

It is currently believed that the pathogenesis of MIRI is a multi-factorial complex process. The latest evidence indicates that epigenetic regulation including histone modification, DNA methylation, non-coding RNAs, and N6-methyladenosine (m6A) methylation plays a key role in MIRI and can be used as new therapeutic targets for MIRI [5]. Iron, as an essential mineral, is an important player in

the physiological functions of many tissues and organs in the human body. Studies in recent years have shown that imbalance in iron metabolism homeostasis is intimately related to the pathological process of MIRI [6]. Ferroptosis, a newly discovered form of regulated cell death, results from the imbalance in iron metabolism [6]. The occurrence of ferroptosis plays an important role during MIRI and can serve as a potential therapy for MIRI [7]. Furthermore, there are numerous other reported pathological mechanisms of MIRI including immunoreaction, autophagy, cell-derived exosomes, dysfunctional mitochondria, different forms of cell death, inflammation, oxidative stress, intracellular calcium overload, and so on [4, 8–10]. Although the pathological mechanisms of MIRI have been extensively explored, its specific pathogenesis has not been fully elucidated. Therefore, plentiful work is still required to better understand the potential pathologic mechanism of MIRI at the molecular level, which may be imperative to develop more effective treatments and seek early diagnostic markers.

In recent years, with the help of bioinformatics and high-throughput techniques, a comprehensive understanding of the molecular mechanism and progression of various diseases has become possible [11]. Molecular docking, a very popular and useful tool, is used to research the interaction between a small-molecule ligand and a target receptor in the drug discovery arena [12]. In our previous study, the molecular docking technique was successfully used to predict the binding modes between 12 COVID-19 targets and the 20 compounds of Qingfei Paidu decoction that have been widely used to treat COVID-19 in China [13]. The analyses of microarray and RNA-seq gene expression data by bioinformatics have been extensively used not only to explore the diagnostic and prognostic biomarkers but also to probe crucial genes and biological processes in many diseases [14–17]. However, some reasons, including the limited sample quantities, the heterogeneity of experimental samples, the use of different detection platforms, and so on, may generate deviation in the results [18, 19]. The integration of the results of multiple gene expression data sets by a robust rank aggregation (RRA) algorithm based on a statistical model that naturally allows evaluating the significance of the results is a promising strategy to overcome these shortcomings [20]. RRA has been widely used in the comprehensive analysis of multiple data sets for both oncology and non-oncology diseases [18, 19, 21]. However, there are no reports on the use of the RRA algorithm in MIRI.

In this study, expression profile analyses and bioinformatics methods were combined to explore hub genes and their functions in MIRI. We subsequently performed the validation of the results via the functional experiment of the MIRI mice. Meanwhile, we retrieved the natural products in Chinese herbal medicine exerting protection for MIRI from the PubMed database. Finally, molecular docking simulations between natural products and hub genes were performed (Figure 1). To sum up, the ultimate goal of the research is to provide novel insights into new potential therapeutic targets and the pathogenesis of MIRI and develop more effective anti-MIRI drugs.

2. Materials and Methods

2.1. Affymetrix Microarray Data. We collected the expression profile data of GSE58486 (GPL18802), GSE108940 (GPL7202), and GSE115568 (GPL16570) from the Gene Expression Omnibus (GEO) database (https://www.ncbi.nlm.nih.gov/geo/). GSE58486 contains six MIRI samples and three sham surgery samples. GSE108940 contains six MIRI samples and six sham surgery samples. GSE115568 contains three MIRI samples and three sham surgery samples. All samples were collected from murine hearts.

2.2. Screening for Differential Expression Genes (DEGs) and Functional Enrichment Analyses. GEO2R online analysis (https://www.ncbi.nlm.nih.gov/geo/geo2r/) was firstly used to obtain the .txt files of the DEGs for the three microarray data sets. The p-value <0.01 and the absolute fold-change (FC) >1.5 were set to determine DEGs. Then, multi-list enrichment analysis of the three gene lists was performed using Metascape (https://metascape.org) [22]. $p < 0.01$, a minimum count of 3, and the enrichment factor >1.5 were set as the thresholds for enrichment analyses.

2.3. Integration of DEGs in Three Data Sets. The TXT files of all gene lists ranked by logFC in three data sets were collected for RRA analysis (https://www.icesi.edu.co/CRAN/web/packages/RobustRankAggreg/) in R version 3.5.3 (https://cran.rproject.org/), and the p-value <0.01 was set to define the significant integrated DEGs. The code used for the RRA analysis is presented in Supplementary Table 1. Gene ontology (GO) and pathway enrichment analyses of integrated DEGs were performed using Metascape. For pathway enrichment analyses, the KEGG pathway, Reactome gene sets, and WikiPathways were employed. The bubble plots were drawn with the ggplot2 package.

2.4. PPI Network and TFs Analysis. The interaction network of the integrated DEGs was performed based on the Search Tool for the Retrieval of Interacting Genes (STRING) [23] to mine their target genes, and interaction pairs with a combined score of >0.4 were considered significant. Then, Cytoscape (version 3.2.1) [24] was applied to visualize the molecular interactions. Next, MCODE analysis [25] was carried out to find densely connected modules in the PPI network. Finally, transcription factors (TFs) analysis of the MCODE modules were analyzed by the iRegulon plugin [26] of Cytoscape with the default criteria. The top five TFs of each module with the higher normalized enrichment scores (NES > 4) were listed.

2.5. Hub Protein Analysis. CytoHubba app [27] was used to identify the top 20 ranking genes using the degree, closeness, edge percolated component (EPC), maximum neighborhood component (MNC), and maximal clique centrality (MCC). The overlapping genes from five algorithms were taken as hub genes. At last, the functional enrichment analyses of hub genes were performed in Metascape, using GO

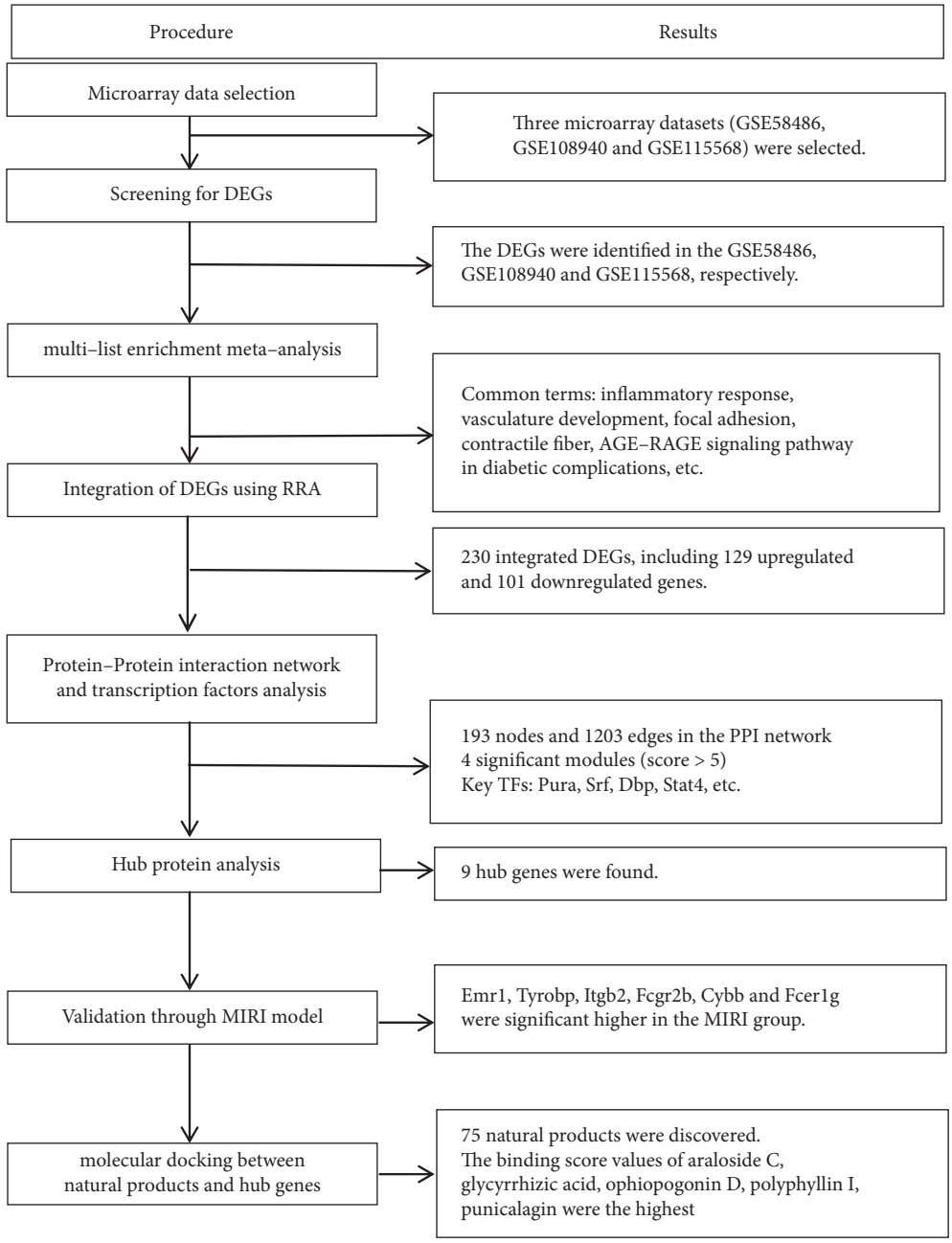

Figure 1: Flowchart of the study design. First, the differential expression genes (DEGs) from three arrays were screened for myocardial ischemia-reperfusion injury (MIRI) and integrated to explore the potential pathogenesis of MIRI using the RRA algorithm. Second, protein-protein interaction network and transcription factors analysis of the integrated DEGs were performed. Then, the most significant DEGs were identified and verified by the functional experiment of the MIRI mice. Finally, natural products exerting protection for MIRI were retrieved and molecular docking simulations were performed.

biological processes, KEGG pathway, Reactome gene sets, and WikiPathways.

2.6. Establishment of MIRI Model in Mice. The animal experiments were approved by the Experimental Animal Welfare Ethics Review Committee of the First Affiliated Hospital of Henan University of CM (approval number, YFYDW2020004) and followed the National Institutes of Health Guide for the Care and Use of Laboratory Animals (NIH Publications No. 8023, revised 1978). Male C57BL/6 J mice (6–8 weeks) were purchased from Huaxing Experimental Animal Farm (Zhengzhou, China; qualified production number, SCXK-(Yu)-2019-0002). The mice were fed under a 12 h cycle of light/dark in IVC condition and had free access to food and water. Before modeling, the mice were randomly divided into two groups ($n = 9$/group), namely sham group and MIRI group. MIRI mouse model was established by ligating the left anterior descending coronary artery, as previously described [28]. After ischemia

for 30 min, the ligation was released to allow reperfusion. Mice were sacrificed following reperfusion 24 h. Sham-operated mice underwent the same procedure without ligation. Blood samples were collected for measurement of lactate dehydrogenase (LDH) activities using a kit (Nanjing Jiancheng Bioengineering Institute, Nanjing, China) following the manufacturer's instructions. The infarct area was determined by staining the heart tissues with 2% triphenyl tetrazolium chloride (TTC; Beijing Solarbio Science & Technology Co. Ltd., Beijing, China) for 15 min at 37°C. The infarct size was evaluated according to the method reported in previous literature by Image-Pro Plus 6.0 software (Media Cybernetics, Silver Spring, MD, USA) [29, 30].

2.7. Verifying of Hub Genes by Quantitative Real-Time Polymerase Chain Reaction (RT-qPCR). Total RNA was extracted from each myocardial tissue using TRIzol (Invitrogen Corporation, CA, USA). cDNA was synthesized using NovoScript® Plus1st Strand cDNA Synthesis SuperMix (Novoprotein Scientific Inc., Shanghai, China). RT-qPCR was performed using SYBR High-Sensitivity qPCR SuperMix (Novoprotein Scientific Inc., Shanghai, China). The primers were synthesized by Shanghai Sangon Biological Engineering Technology (Shanghai, China; Table 1). The mRNA expression level was normalized to that of β-actin in the same sample. The relative mRNA expression level was calculated using the $2^{-\Delta\Delta CT}$ method.

2.8. Molecular Docking Simulation. The natural products in Chinese herbal medicine exerting protection for MIRI were retrieved from the PubMed database (https://pubmed.ncbi.nlm.nih.gov/). Then, the 2D chemical structures of natural products were obtained from PubChem (https://pubchem.ncbi.nlm.nih.gov/). The 3D structures of hub genes were obtained from the Protein Data Bank (PDB) database (https://www.rcsb.org/). Molecular docking simulation of each hub gene with natural products was performed using AutoDock Vina software.

2.9. Statistical Analysis. All data were presented as mean ± SEM and analyzed using IBM SPSS statistics 21.0 software. The Student's t-test was utilized to compare data between two groups. A p value < 0.05 was accepted as statistically significant.

3. Results

3.1. Identification and Functional Enrichment Analyses of DEGs. After screening with the threshold of |FC| >1.5 and $p < 0.01$, 1986, 1703, and 402 DEGs were identified in the GSE58486, GSE108940, and GSE115568, respectively (Figure 2(a)–2(c)). To facilitate the understanding of the functional mechanisms that are shared between, or selectively ascribed to, specific gene lists, a multi-gene-list meta-analysis was performed. Figure 2(d) shows that eight GO terms were common in all studies. Figure 2(e) shows that eight pathways were common in all studies.

Table 1: Primer sequence of RT-qPCR.

Gene name	Primer sequence
β-actin	Forward 5'-CCCATCTACGAGGGCTAT-3'
	Reverse 5'-TGTCACGCACGATTTCC-3'
Fcer1g	Forward 5'-CGTGATCTTGTTCTTGCTCCT-3'
	Reverse 5'-TTCGGACCTGGATCTTGAGT-3'
Cybb	Forward 5'-GCTATGAGGTGGTGATGTTAGT-3'
	Reverse 5'-GCTGAGGAAGTTGGCATTGT-3'
Fcgr2b	Forward 5'-AATCCTGCCGTTCCTACTGAT-3'
	Reverse 5'-AGTGTCACCGTGTCTTCCTT-3'
Cd68	Forward 5'-CCTTCACGATGACACCTACAG-3'
	Reverse 5'-AACAGTGGAGGATCTTGGACTA-3'
Itgb2	Forward 5'-TGTCCTCCTCCTGGTCATCT-3'
	Reverse 5'-CCGTTGTCGTAGCACTCTTG-3'
Ptprc	Forward 5'-GGTTGTTCTGTGCCTTGTTCA-3'
	Reverse 5'-ATCCTGCTTGCCTCCATCC-3'
Emr1	Forward 5'-CAGGAGTGGAATGTCAAGATGT-3'
	Reverse 5'-CACAGAGTTAGAGCAGTTGGAA-3'
Tyrobp	Forward 5'-TCTGTTCCTTCCTGTCCTCCT-3'
	Reverse 5'-CTCAGTCTCAGCAATGTGTTGT-3'
Fcgr1	Forward 5'-TCAGGACAGTGGCGAATACAG-3'
	Reverse 5'-GAATGGCGACCTCCGAATCT-3'

3.2. Identification of Integrated DEGs in MIRI. Table 2 presents that 230 integrated DEGs were identified using the RRA ($p < 0.01$). The top 20 up- and downregulated hub genes were drawn into a heatmap (Figure 3(a)). The top five BP terms showed that integrated DEGs were mainly related to inflammatory response, cell chemotaxis, and so on (Figure 3(b)). The top five CC terms showed that integrated DEGs were mainly related to the extracellular matrix, external encapsulating structure, and so on (Figure 3(b)). The top five MF terms showed that integrated DEGs were mainly related to extracellular matrix structural constituent, cell adhesion molecule binding, and so on (Figure 3(b)). We enriched 35, 55, and 15 pathways from the KEGG, Reactome, and WikiPathways databases, respectively, setting a p-value < 0.01, a minimum count of 3, and an enrichment factor >1.5 as screening thresholds. The top 10 enriched Reactome pathways closely associated with MIRI were mainly neutrophil degranulation, extracellular matrix organization, collagen degradation, and so on (Figure 3(c)). The top 10 enriched KEGG pathways closely associated with MIRI were mainly IL-17 signaling pathway, AGE-RAGE signaling pathway, ECM-receptor interaction, and so on (Figure 3(d)). The top 10 enriched WikiPathways closely associated with MIRI were mainly focal adhesion, PI3K-Akt-mTOR signaling pathway, inflammatory response pathway, and so on (Figure 3(e)).

3.3. PPI Network and TFs Analysis. There were 193 nodes and 1,203 edges in the PPI network of the 230 integrated DEGs in MIRI (Figure 4). MCODE analysis showed that four meaningful functional modules were selected (score > 5). The top 5 TFs were predicted to target these MCODE modules, including Pura, Srf, Dbp, Stat4, and so on (Figure 5(a)–5(d)).

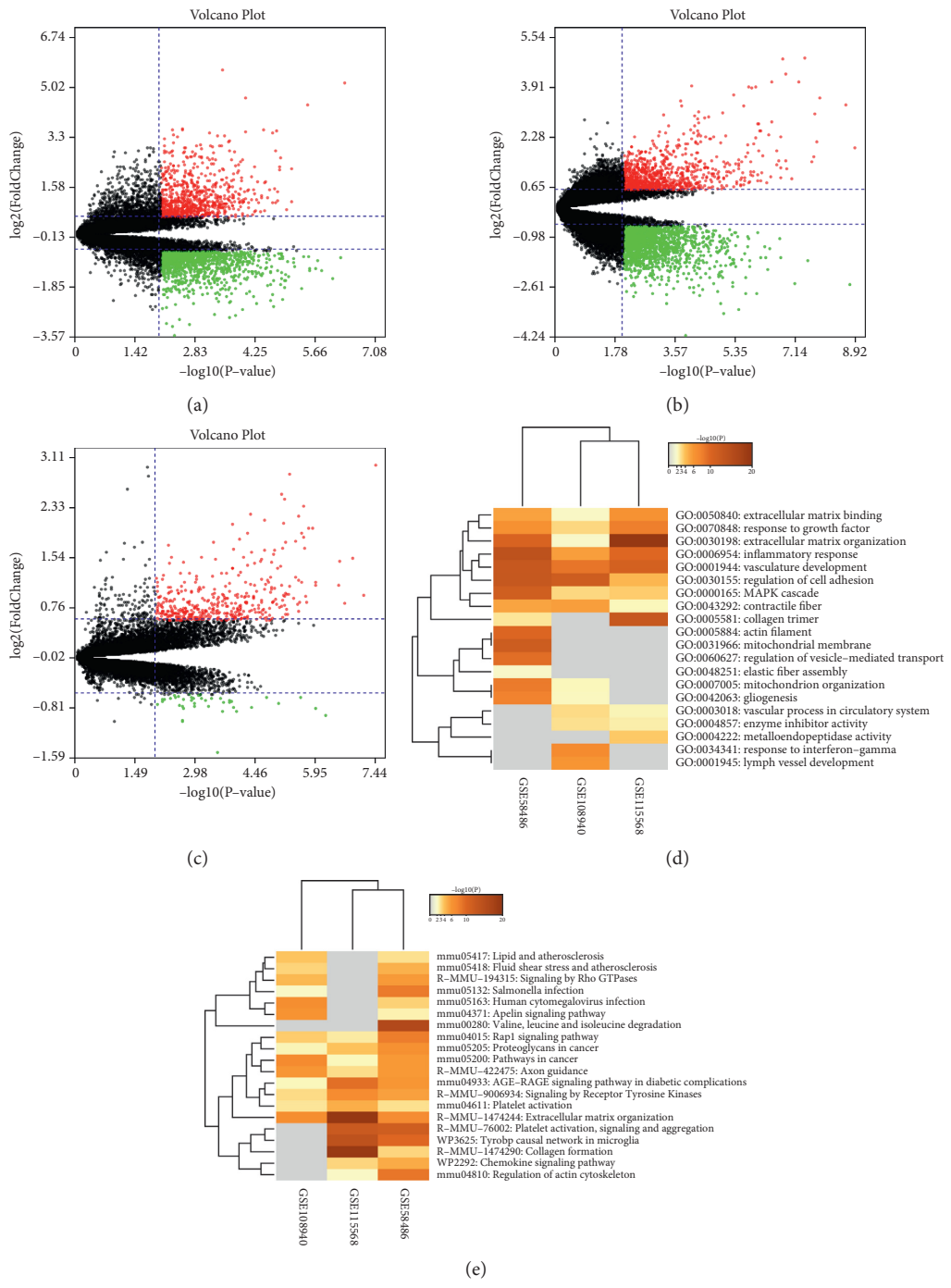

Figure 2: Identification and functional enrichment analyses of DEGs: (a)–(c) volcano plot for GSE58486, GSE108940, and GSE115568; (d) heatmap visualization of the results of GO enrichment analyses across multiple gene lists; and (e) heatmap visualization of the results of pathways enrichment analyses using KRGG, Reactome, and WikiPathways databases across multiple gene lists. The gray color indicates a lack of significance.

3.4. Hub Protein Analysis. The hub genes were identified by CytoHubba from 230 integrated DEGs. The top 20 ranking genes, which were selected based on closeness, degree, EPC, MCC, and MNC, are displayed in Figure 6(a)–6(e). There were 9 intersection genes (Tyrobp, Itgb2, Emr1, Fcer1g, Fcgr1, Fcgr2b, Cybb, Cd68, and Ptprc) among 5 algorithms (Figure 6(f)). These genes, also known as hub genes, were selected for further validation in the MIRI model. In addition, Metascape results showed that 9 genes were mainly related to neutrophil degranulation, inflammatory response,

Table 2: Integrated DEGs in MIRI by RRA.

DEGs	Gene names
Upregulated	Timp1, Serpina3n, Lox, Ccl6, Ccl7, Postn, Ccl9, Ccl2, Ctgf, Fn1, Bcl2a1b, Angptl4, Clec4n, Ms4a6d, Nmrk2, Thbs4, S100a6, Cd53, Hmox1, Col3a1, Adam8, Emp1, Ctss, Ltbp2, Sprr1a, Spp1, Cdkn1a, Col1a1, Mmp14, Aldh1a2, Aebp1, Lcn2, Ugdh, Fxyd5, Efhd2, Mpeg1, Lgals3, Col8a1, Lilrb4, Il4ra, Ccl8, Il33, Uck2, Fgl2, Ptprc, Ccr2, Tmem173, Car13, Mt2, Tnc, Snora75, Hp, Fcgr2b, Ch25h, Myo5a, Col1a2, Anxa1, Fcer1g, Fbn1, Alox5ap, Col5a2, Clic1, Thbs1, Ly86, Il1r1, Saa3, Cd68, Cybb, Pla2g4a, Tyrobp, Clec4d, Cxcl5, Nckap1l, Myof, Ifi30, Igsf6, Pdpn, Cd84, Vcan, Emr1, Chil3, Lcp1, Loxl1, P2ry6, Fstl1, Tnfaip6, Col12a1, Tlr13, Adamts2, Fcgr1, Mmp3, Il1b, Selplg, Col5a1, Clec7a, Mki67, Cyth4, Sulf1, C3ar1, Wisp1, Anxa2, Mfap5, Frzb, Apobec1, Nppb, Itgb2, Serpinb1a, Trem2, Ccna2, Loxl2, Retnlg, Loxl3, Soat1, Itgam, Eif1a, Tgfbi, S100a8, Hbegf, Wfdc17, Runx1, S100a9, Fgr, Emb, Bst1, Mmp8, Msr1, Fhl1, Acta1, Wfdc21
Downregulated	Kcnd2, Gpr22, Ldhd, Il15, Ces1d, Kcnip2, 1700040L02Rik, Cdnf, Epm2a, Pfkfb1, Dusp18, A530016L24Rik, Lrrc39, Asb15, Hrasls, Mccc1, Rtn4ip1, Kcnj2, Actr3b, Plxnb1, Tarsl2, Letm2, Fsd2, P2ry1, Dnajc28, Intu, Kcnv2, Ccdc141, Magix, Asb14, Rbm20, Kcnj3, Cmya5, Acacb, Angpt1, Suclg2, Dbt, Wnk2, Rpl3l, Abcc9, Gm10336, Efcab2, Cpeb3, A930018M24Rik, Gca, Slc38a3, Adra1a, Itgb6, Ppm1k, Pdpr, Mylk4, Mettl7a1, Arhgap20, Rnf207, Krt222, Mccc2, Gm31251, Klf9, Epha4, Tcp11l2, Aldh4a1, Efnb3, Akr1c14, Ppp2r3a, Tmem143, Isoc2a, Btnl9, Fyco1, Jmy, Helt, Tcaim, Pank1, Osbpl3, Slc16a10, Klra21, Pkd2l2, Cacna1c, Osbp2, Ppm1l, Cyfip2, Hlf, Gm30307, Lmod3, Slc2a12, Nebl, Pm20d1, Ppara, Mmp15, C1qtnf9, Tmem25, Ank2, Mitf, Colgalt2, Pitpnc1, Mlxipl, Ppargc1b, Lrtm1, Rps6ka2, Apol10b, Dsg2, Ucp3

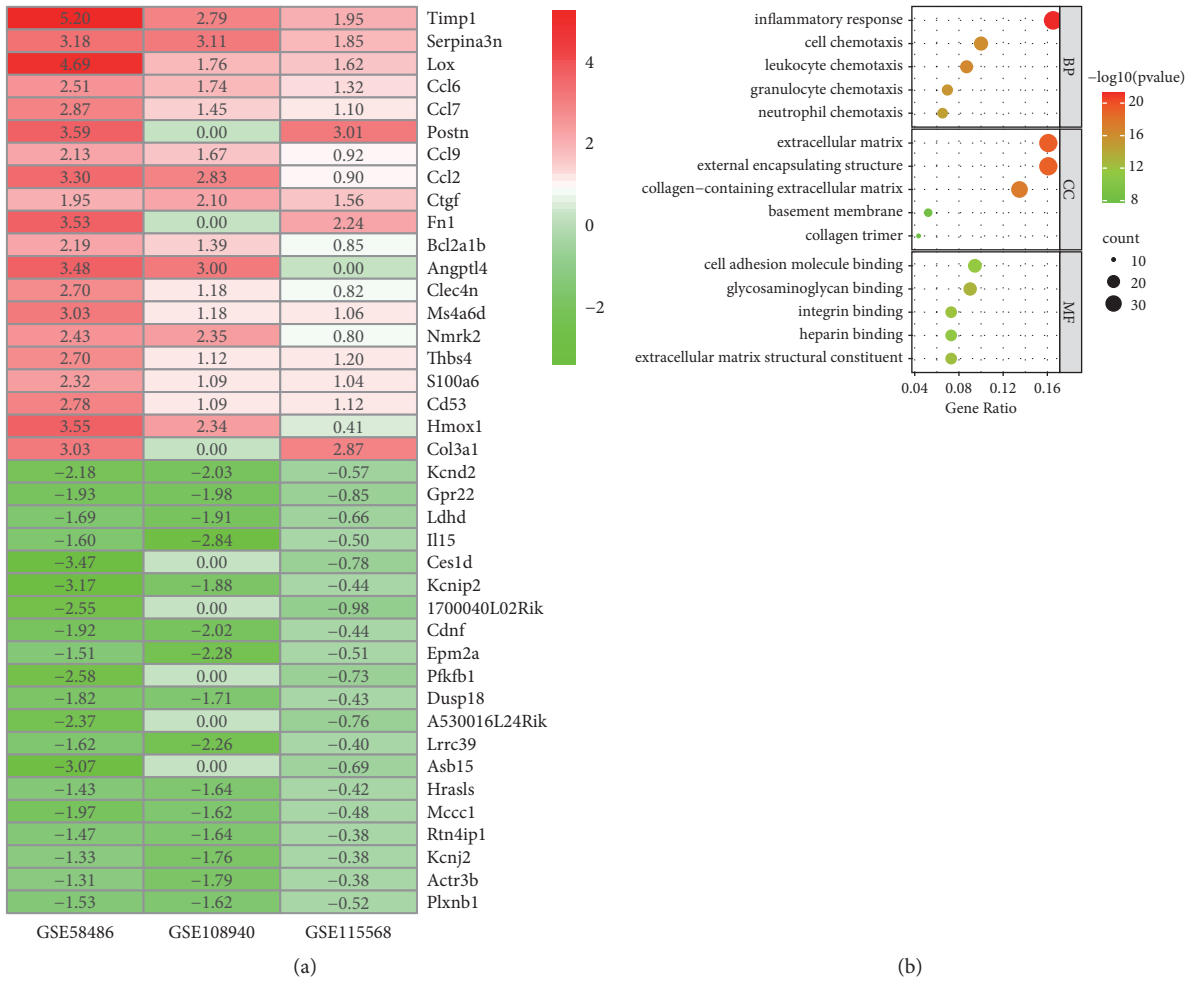

(a) (b)

Figure 3: Continued.

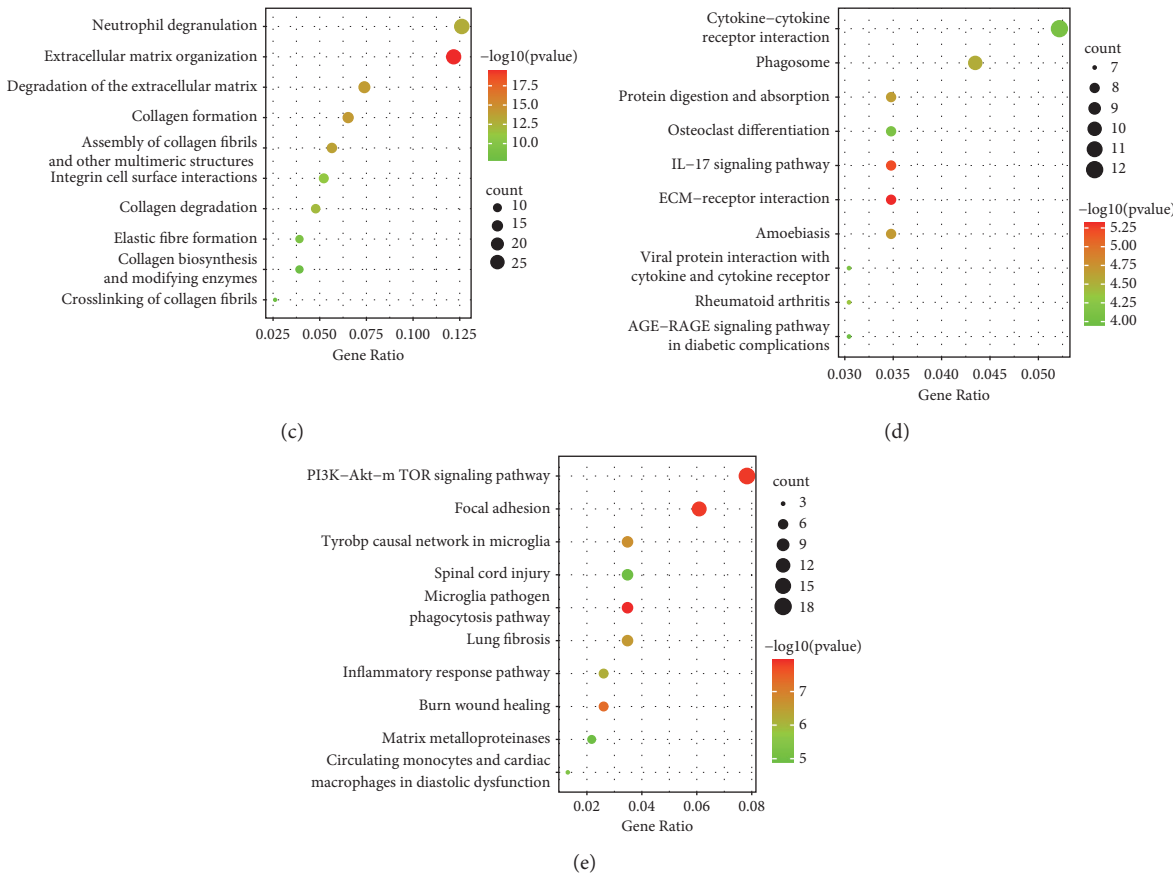

Figure 3: Identification and functional enrichment analyses of integrated DEGs. (a) Heatmap of top 20 up- and downregulated DEGs of three microarrays screening by RRA. Red boxes represent upregulated genes and green boxes represent downregulated genes. The values in the boxes represent logFC values. (b) The top five enriched GO terms for integrated DEGs in biological process, molecular function, and cellular component categories. (c) The top ten enriched Reactome pathways for integrated DEGs. (d): The top ten enriched KEGG pathways for integrated DEGs. (e) The top ten enriched WikiPathways for integrated DEGs.

superoxide anion generation, leukocyte mediated cytotoxicity, and so on (Figure 6(g)).

3.5. The Successful Establishment of the MIRI Model in Mice. As illustrated in Figure 7(a)–7(b), the infarct areas of hearts in the MIRI group were significantly larger than those in the sham group. Moreover, the serum LDH activities were significantly increased in mice subjected to MIRI (Figure 7(c)). Taken together, the obtained data suggested that the MIRI mouse model was successfully established.

3.6. The mRNA Expression Levels of Six Hub Genes Were Upregulated in the MIRI Model. To verify the results of bioinformatics analysis, we detected the mRNA expression level of hub genes by RT-qPCR in the myocardial tissues. Compared with the sham group, the mRNA expression levels of Emr1, Tyrobp, Itgb2, Fcgr2b, Cybb, and Fcer1g were higher in the MIRI group (Figure 7(d)). Unexpectedly, CD68, Ptprc, and Fcgr1 were not markedly differentially expressed. However, the changing trend was consistent with the result of bioinformatics results (Figure 7(d)).

3.7. Molecular Docking Results. A total of 75 natural products were discovered, and their multiple mechanisms of action for treating MIRI were complex (Supplementary Table 2). To verify the effect of natural products on hub genes, molecular docking was performed. Unfortunately, the 3D structure of Emr1 was not obtained from the PDB database. The molecular docking results showed that there were different degrees of binding between natural products and hub genes, and most of the natural products showed a good ability to bind the hub genes, particularly araloside C, glycyrrhizic acid, ophiopogonin D, polyphyllin I, and punicalagin (Figure 8).

4. Discussion

MIRI, as an inevitable phenomenon, is a major challenge to the treatment of AMI and plays a crucial role in the damage, repair, and remodeling of myocardial tissue. MIRI not only can contribute to myocardial infarction but also can lead to myocardial stunning, the no-reflow phenomenon, reperfusion arrhythmia, lethal reperfusion injury, coronary capillary rupture, and hemorrhages [10, 31]. Despite remarkable progress in understanding the pathogenesis of MIRI, the

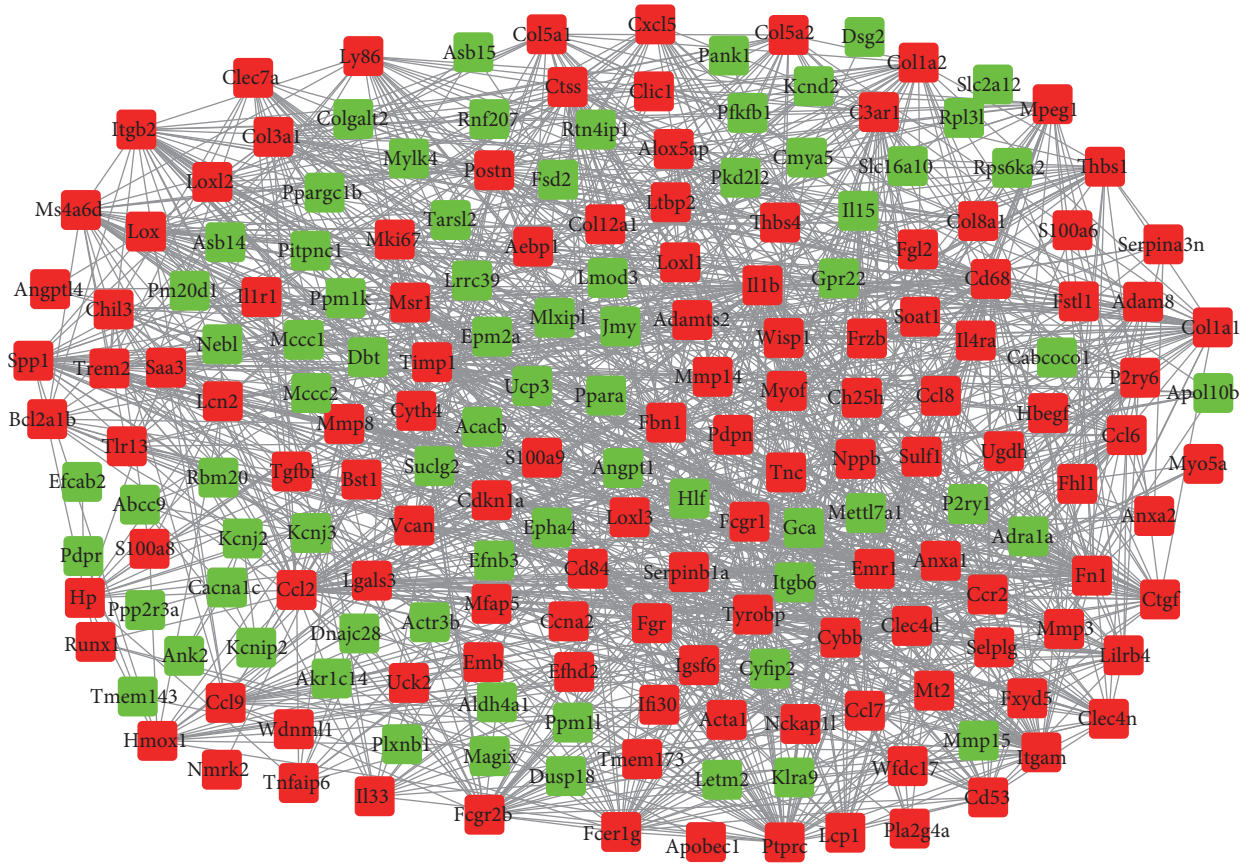

Figure 4: The PPI network of the 230 integrated DEGs. Red boxes represent upregulated genes, and green boxes represent downregulated genes.

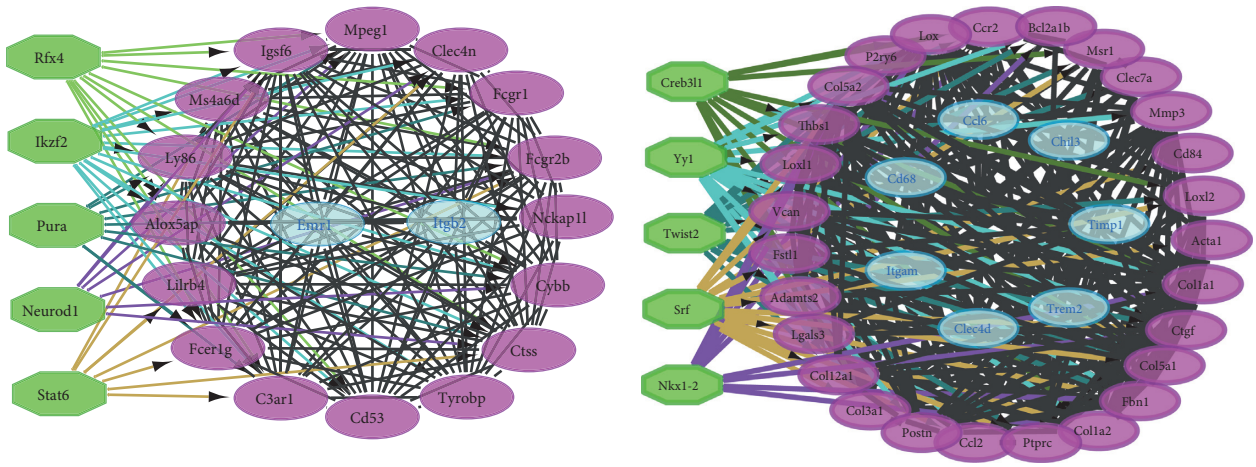

(a) (b)

Figure 5: Continued.

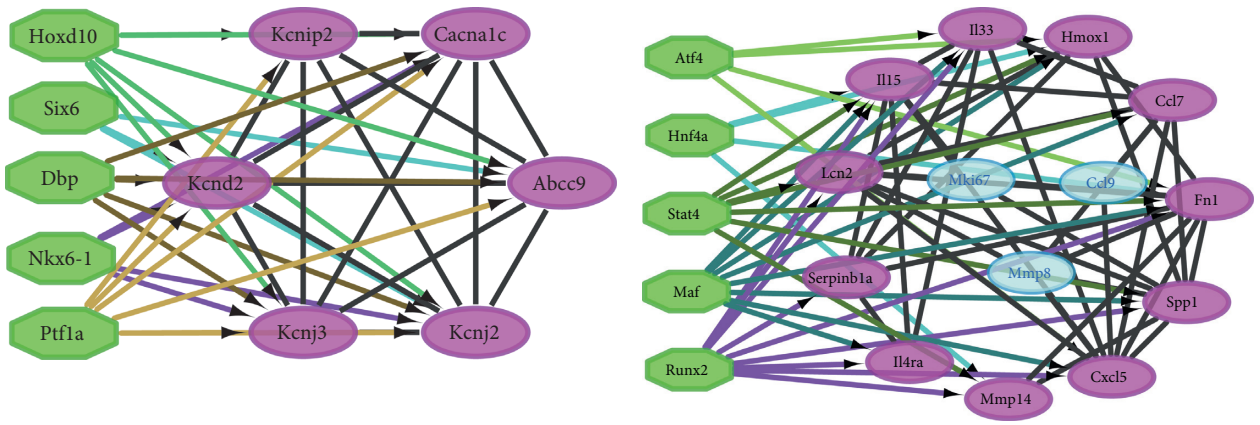

(c) (d)

Figure 5: TFs analysis of MCODE modules: (a)–(d) TFs analysis of modules 1–4. Green stands for the predicted TF; purple stands for the TF-binding protein; and blue stands for the unbound protein.

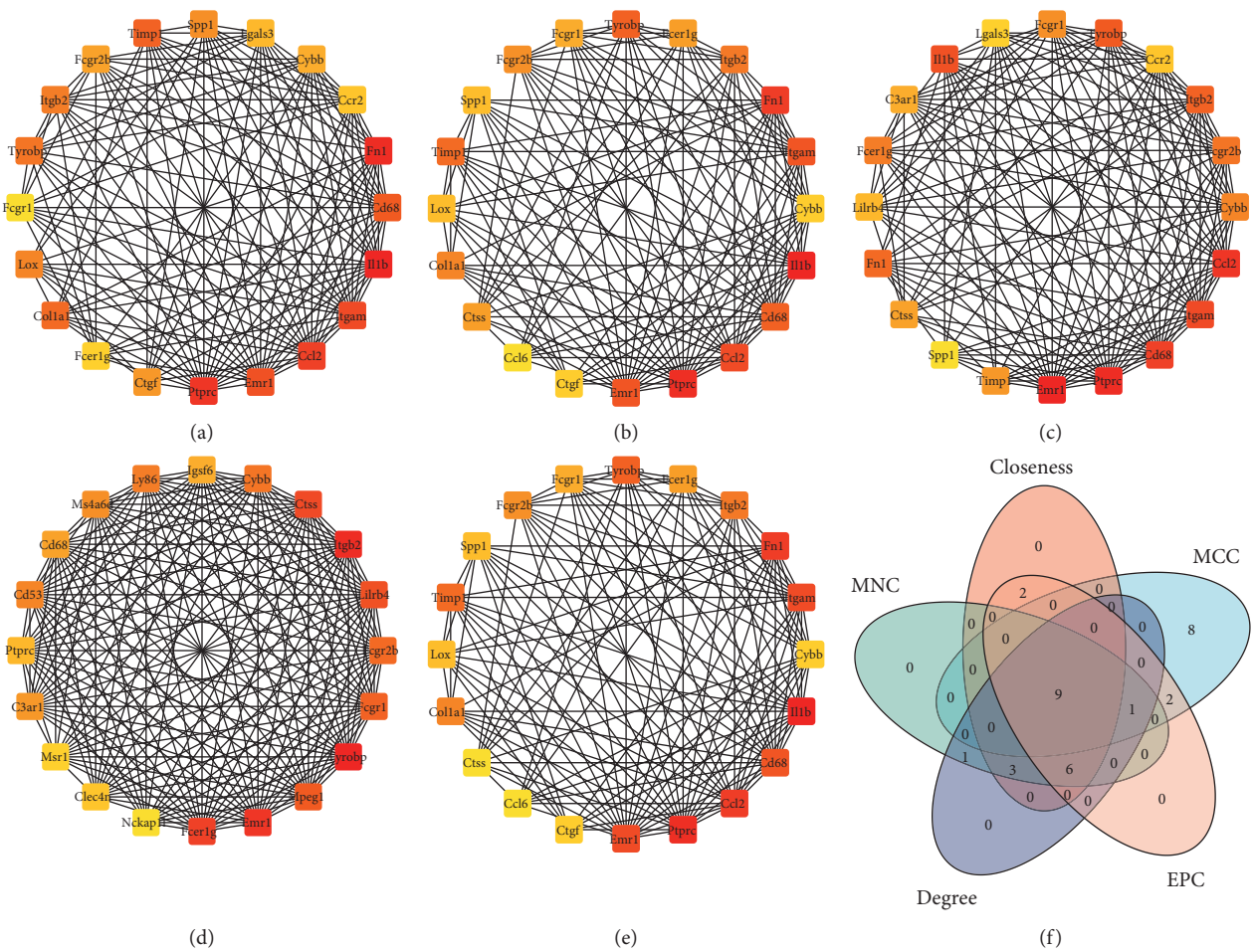

(a) (b) (c)

(d) (e) (f)

Figure 6: Continued.

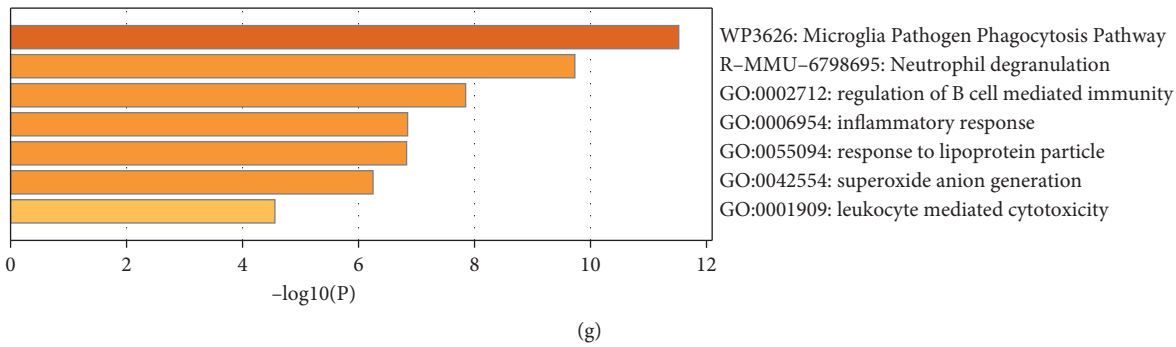

FIGURE 6: Identification and functional enrichment analysis of hub genes; (a–e) top 20 genes were calculated from the PPI network of the 230 integrated DEGs by the closeness, degree, EPC, MCC, and MNC, respectively; (f) the Venn diagram showing the hub genes identified by the CytoHubba plugin; and (g) functional enrichment analysis of the hub genes.

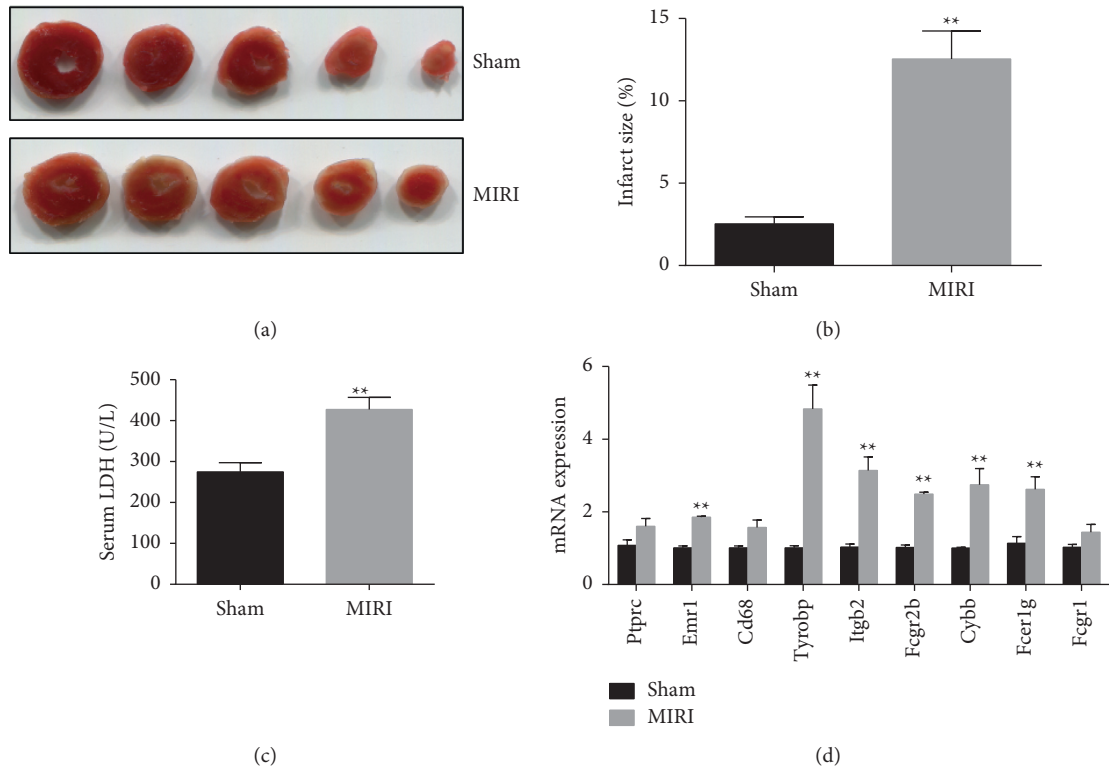

FIGURE 7: The hub genes were validated in the MIRI model: (a) representative slices stained by TTC, (b) quantitative analysis of myocardial infarct size ($n = 5$), (c) the activities of LDH in serum ($n = 6$), and (d) validation of the mRNA expression levels of hub genes ($n = 3$). $^{**}p < 0.01$ versus the sham group.

optimal treatment strategies to effectively restrict MIRI remain elusive [32]. It has been very disappointing to translate effective strategies that have been proven in many preclinical studies into better clinical outcomes [32]. There is an undisputed unmet need between therapy and understanding the pathophysiological mechanism of MIRI. Only with a better understanding of the mechanisms of MIRI, more appropriate strategies to reduce myocardial damage can be developed. Therefore, researching the mechanisms underlying MIRI development is very important.

In this study, GSE58486, GSE108940, and GSE115568 data sets were firstly downloaded from the GEO database, and DEGs were determined. Then, the multi-gene-list meta-analyses were performed to find the common GO and KEGG terms of the DEGs. Moreover, the three data sets were analyzed using the RRA method, and integrated DEGs were found. Function annotation and pathway enrichment analyses of integrated DEGs were then conducted. The results of the above functional enrichment analyses showed that DEGs might be mainly involved in regulating the extracellular

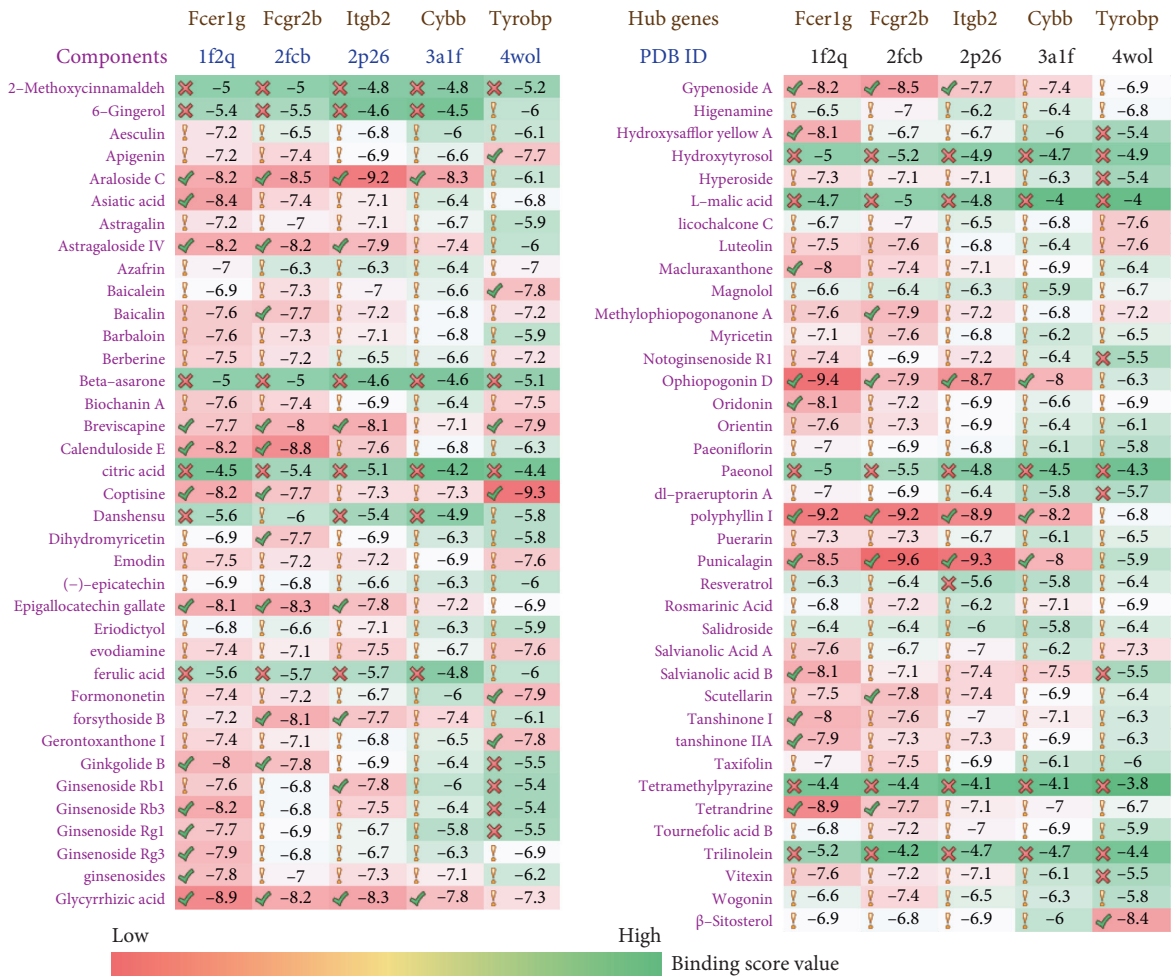

Figure 8: The Molecular Docking Results.

matrix, cell adhesion, cell chemotaxis, inflammatory response, AGE-RAGE signaling pathway, and PI3K-Akt-mTOR signaling pathway. MIRI induces a series of sterile inflammatory reactions, which can lead to further myocardial injury. Many risk factors, including chemokines, inflammatory cytokines, inflammatory cells, complement cascades, inflammatory pathways, and so on, play important roles in the inflammatory response during MIRI through multiple interacting pathways [33, 34]. Adhesion molecules are transmembrane glycoproteins with a variety of biological activities, which are produced by cells. They can mediate the interaction and binding between cells and cells and between cells and extracellular matrix. Adhesion molecules E-selectin and intercellular cell adhesion molecule-1 expressed on activated endothelial cells can regulate the leukocyte adhesion cascade and thus aggravate tissue inflammation in the pathological process of MIRI [35]. A study has shown that HMGB1/TLR4 signaling, as an inflammatory signaling pathway, promotes the release of inflammatory factors and aggravates MIRI by regulating the migration, adhesion, and aggregation of dendritic cells to the myocardium [36]. Substantial evidence implies the AGE-RAGE signaling pathway plays a crucial role in MIRI [37]. AGE-RAGE pathway can regulate ventricular arrhythmias, cardiomyocyte apoptosis, and contractile impairment following MIRI, which is a potential therapeutic strategy for ameliorating MIRI [37]. More recent evidence suggests that PI3K/Akt/mTOR signaling pathway protects cardiac injury from MIRI by regulating apoptosis and autophagy in cardiomyocytes [38, 39]. Thus, it can serve as a potential target in the setting of MIRI. According to the above studies, the results of the identified enrichment analyses in the current research play a recognized role in the pathogenesis of MIRI.

We also constructed a PPI network with integrated DEGs and identified the following nine hub genes: Tyrobp, Itgb2, Emr1, Fcer1g, Fcgr1, Fcgr2b, Cybb, Cd68, and Ptprc. Consistent with the bioinformatics results, MIRI mouse model results proved that Emr1, Tyrobp, Itgb2 (synonym: CD18), Fcgr2b, Cybb, and Fcer1g were significantly higher in the MIRI group. The changing trend of CD68, Ptprc, and Fcgr1 was consistent with the bioinformatics results. These results suggest that the results of our bioinformatics analysis may provide a reliable basis for the study of the mechanism of MIRI. The results of pathway and process enrichment analysis showed that hub genes were mainly related to microglia pathogen phagocytosis pathway, neutrophil degranulation, regulation of B-cell-mediated immunity, inflammatory response, response to lipoprotein particle,

superoxide anion generation, leukocyte mediated cytotoxicity, and so on. Neutrophils, as the primary responders of MIRI, represent an important component in the protracted inflammatory response and severity related to MIRI [40]. Early research suggested that specific neutrophils degranulation within the ischemic myocardium occurred in MIRI [41]. In addition, superoxide anion generation that occurs during MIRI can further augment MIRI by enhancing the pro-oxidant activity of aconitase [42]. In summary, the enriched pathway and process of these hub genes were, in part, consistent with the pathological process of MIRI shown in previous studies.

It is noticeable that the role of several hub genes in MIRI has been reported in the literature. Palazzo et al. [43] found that $CD18^{-/-}$ mice subjected to MIRI showed a marked reduction in neutrophils accumulation and myocardial necrosis. The results clearly demonstrate that deficiency of CD18 protects MIRI. Cybb expression levels were found to increase with MIRI [44]. Fortunately, myocardial ischemic postconditioning, melatonin, and RIPerC have protective effects on the myocardium by decreasing Cybb expression in the rat model of MIRI [45]. Fcer1g, adapter protein containing an immunoreceptor tyrosine-based activation motif, plays a pivotal role in the extension of MIRI at least partly through mediating collagen-induced platelet activation [46]. Tyrobp expressed in circulating immune cells is a cell membrane-associated protein, which has been reported to be involved in ischemia-reperfusion injury including the liver, lung, and kidney, but not the heart [47–49]. There are no reports on the involvement of Emr1 and Fcgr2b in MIRI. However, our findings suggest otherwise. Thus, Emr1, Tyrobp, and Fcgr2b are fascinating therapeutic targets, the inhibition of which may protect the myocardium from ischemia-reperfusion injury. Moreover, some important TFs, such as Pura, Srf, Dbp, and Stat4 were uncovered in the present study. Among these TFs, Srf has been reported to mediate MIRI by regulating its target genes (Tagln, Fos, NCX1, Slc8a1, and Egr1) [50]. To sum up, these TFs can further enhance our understanding of MIRI pathogenesis and have the potential to offer novel treatment strategies for MIRI.

Currently, there remains an unmet clinical need for the treatment methods and drugs for MIRI. Natural products especially the extracts of Chinese herbal medicine have been an important source of medicines and drug templates with proven success, which has increasingly drawn widespread attention [51, 52]. In the study, we searched the natural products in Chinese herbal medicine exerting protection for MIRI and discovered 75 natural products. To validate the therapeutic efficacy of natural products against MIRI via targeting the hub genes identified in this research, molecular docking simulations were performed. The results showed that most of the natural products showed a good binding ability to the hub genes, and the binding score values of araloside C, glycyrrhizic acid, ophiopogonin D, polyphyllin I, and punicalagin were the highest. We summarized the mechanism of action of natural products for the treatment of MIRI and found that anti-apoptosis, anti-inflammatory, anti-oxidative stress, regulating energy metabolism, reducing Ca^{2+} overload, and so on were principal mechanisms, especially araloside C, glycyrrhizic acid, ophiopogonin D, polyphyllin I, and punicalagin (Supplementary Table 2). Interestingly, the pathways and processes of the hub genes enrichment analyses were basically consistent with the mechanism of action of natural products. In summary, these natural products (especially araloside C, glycyrrhizic acid, ophiopogonin D, polyphyllin I, and punicalagin) provide a broad application prospect for developing more effective anti-MIRI drugs and will undoubtedly deserve in-depth investigation in the future.

The following are the novelties and multiple strengths of our current research. First, the RRA algorithm, a promising strategy used in the integrated analysis of multiple data sets, was first applied to explore DEGs in MIRI. Second, the functional experiment of the MIRI mice was accomplished to validate the obtained hub genes, which could avoid the bias from the results of pure bioinformatics analysis and thus yield more reliable results. Third, the molecular docking simulations of hub genes and natural products retrieved from the PubChem database were performed to analyze the potential binding effects, which could lead to better prevention and treatment for MIRI. However, our results had several limitations, which should be taken into consideration. On the one hand, our findings are based on currently available gene expression data from the microarray. Some genes, although playing potential roles in pathological processes of MIRI, were ignored in our study because they were not detected by the microarray. On the other hand, further molecular biology experiments are required to validate the function of hub genes in the progression of MIRI and the protective effects of natural products that showed a good ability to bind the hub genes against MIRI.

In conclusion, this study identified several key candidate genes, TFs, and biological pathways and searched for some natural products that exhibited potential therapeutic efficacy on MIRI via targeting the hub genes. Through our research is a preliminary investigation, the findings help us acquire a better understanding of pathogenesis, biomarkers discovery, and therapeutic targets for MIRI, reveal new therapeutic targets for natural products with protective properties against MIRI, and develop more effective anti-MIRI drugs.

Data Availability

GSE58486, GSE108940, and GSE115568 data sets used in this study were downloaded from the GEO database (https://www.ncbi.nlm.nih.gov/geo). The data used to support the findings of this study are included in the article.

Conflicts of Interest

The authors declare that they have no conflicts of interest in the paper.

Authors' Contributions

Jian Chen conceived and designed the study. Jianru Wang analyzed the data and wrote the manuscript. Xiaohui Li

completed the molecular docking simulation. Genhao Fan and Mengmeng Zhang contributed significantly to the functional experiment of the MIRI mice, and Guangcao Peng provided important suggestions.

Acknowledgments

The authors would like to thank the authors of those data sets and the people who manage them. This work was supported by the Key R&D and Promotion Special Project of Henan Province (Scientific Problem Tackling) Project (No. 202102310492), the National Natural Science Foundation of China (Nos. 82004311 and 82104873), the Traditional Chinese Medicine Scientific Research Special Project of Henan Province (Nos. 2019JDZX2013 and 20–21ZY2187), the Shanghai Sailing Program (No. 20YF1445900), the Budgetary Projects of Shanghai University of Traditional Chinese Medicine (No. 2019LK046), the Special Clinical Research Project of Health Profession of Shanghai Municipal Commission of Health (20194Y0081), and Scientific Research Project of Traditional Chinese Medicine of Hongkou District Health (HKQ-ZYY-2020-19).

Supplementary Materials

Supplementary Table 1. The R code used for the RRA analyses. Supplementary Table 2. Summary of natural products in Chinese herbal medicine exerting protection for MIRI. (*Supplementary Materials*)

References

[1] J. Schmidt-RioValle, M. Abu Ejheisheh, M. J. Membrive-Jiménez et al., "Quality of life after coronary artery bypass surgery: a systematic review and meta-analysis," *International Journal of Environmental Research and Public Health*, vol. 17, no. 22, p. 8439, 2020.

[2] P. K. Thrombolysis, "In ST-elevation myocardial infarction is not dead," *EuroIntervention*, vol. 16, no. 14, pp. 1129-1130, 2021.

[3] D. M. Yellon and D. J. Hausenloy, "Myocardial reperfusion injury," *New England Journal of Medicine*, vol. 357, no. 11, pp. 1121–1135, 2007.

[4] C. D. Sánchez-Hernández, L. A. Torres-Alarcón, A. González-Cortés, and A. N. Peón, "Ischemia/reperfusion injury: pathophysiology, current clinical management, and potential preventive approaches," *Mediators Inflamm*, vol. 2020, Article ID 8405370, 2020.

[5] K. Wang, Y. Li, T. Qiang, J. Chen, and X. Wang, "Role of epigenetic regulation in myocardial ischemia/reperfusion injury," *Pharmacological Research*, vol. 170, Article ID 105743, 2021.

[6] J.-y. Li, S.-q. Liu, R.-q. Yao, Y.-p. Tian, and Y.-m. Yao, "A novel insight into the fate of cardiomyocytes in ischemia-reperfusion injury: from iron metabolism to ferroptosis," *Frontiers in Cell and Developmental Biology*, vol. 9, Article ID 799499, 2021.

[7] X. Li, N. Ma, J. Xu et al., "Targeting ferroptosis: pathological mechanism and treatment of ischemia-reperfusion injury," *Oxidative Medicine and Cellular Longevity*, vol. 2021, Article ID 1587922, 14 pages, 2021.

[8] C.-L. Chen, L. Zhang, Z. Jin, T. Kasumov, and Y.-R. Chen, "Mitochondrial redox regulation and myocardial ischemia-reperfusion injury," *American Journal of Physiology–Cell Physiology*, vol. 322, no. 1, pp. C12–c23, 2022.

[9] M. Cui, Y. Han, J. Yang, G. Li, and C. Yang, "A narrative review of the research status of exosomes in cardiovascular disease," *Annals of Palliative Medicine*, vol. 11, no. 1, pp. 363–377, 2022.

[10] G. Heusch, "Myocardial ischaemia-reperfusion injury and cardioprotection in perspective," *Nature Reviews Cardiology*, vol. 17, no. 12, pp. 773–789, 2020.

[11] M. Yousef, A. Kumar, and B. Bakir-Gungor, "Application of biological domain knowledge based feature selection on gene expression data," *Entropy*, vol. 23, p. 1, 2020.

[12] H. Yu, C. Li, X. Wang et al., "Techniques and strategies for potential protein target discovery and active pharmaceutical molecule screening in a pandemic," *Journal of Proteome Research*, vol. 19, no. 11, pp. 4242–4258, 2020.

[13] J. Chen, Y.-k. Wang, Y. Gao et al., "Protection against COVID-19 injury by qingfei paidu decoction via anti-viral, anti-inflammatory activity and metabolic programming," *Biomedicine & Pharmacotherapy*, vol. 129, Article ID 110281, 2020.

[14] M. H. Rahman, S. Peng, X. Hu et al., "A network-based bioinformatics approach to identify molecular biomarkers for type 2 diabetes that are linked to the progression of neurological diseases," *International Journal of Environmental Research and Public Health*, vol. 17, no. 3, 2020.

[15] M. H. Rahman, H. K. Rana, S. Peng et al., "Bioinformatics and system biology approaches to identify pathophysiological impact of COVID-19 to the progression and severity of neurological diseases," *Computers in Biology and Medicine*, vol. 138, Article ID 104859, 2021.

[16] M. H. Rahman, H. K. Rana, S. Peng et al., "Bioinformatics and machine learning methodologies to identify the effects of central nervous system disorders on glioblastoma progression," *Briefings in Bioinformatics*, vol. 22, no. 5, 2021.

[17] H.-Q. Mu, Z.-Q. Liang, Q.-P. Xie et al., "Identification of potential crucial genes associated with the pathogenesis and prognosis of prostate cancer," *Biomarkers in Medicine*, vol. 14, no. 5, pp. 353–369, 2020.

[18] J. Niu, T. Yan, W. Guo et al., "Identification of potential therapeutic targets and immune cell infiltration characteristics in osteosarcoma using bioinformatics strategy," *Frontiers in Oncology*, vol. 10, p. 1628, 2020.

[19] Y. Tang, Y. Zhang, and X. Hu, "Identification of potential hub genes related to diagnosis and prognosis of hepatitis B virus-related hepatocellular carcinoma via integrated bioinformatics analysis," *BioMed Research International*, vol. 2020, Article ID 4251761, 19 pages, 2020.

[20] R. Kolde, S. Laur, P. Adler, and J. Vilo, "Robust rank aggregation for gene list integration and meta-analysis," *Bioinformatics*, vol. 28, no. 4, pp. 573–580, 2012.

[21] H. Zeng, Y. Fu, L. Shen, and S. Quan, "Integrated analysis of multiple microarrays based on raw data identified novel gene signatures in recurrent implantation failure," *Frontiers in Endocrinology*, vol. 13, Article ID 785462, 2022.

[22] Y. Zhou, B. Zhou, L. Pache et al., "Metascape provides a biologist-oriented resource for the analysis of systems-level datasets," *Nature Communications*, vol. 10, no. 1, p. 1523, 2019.

[23] D. Szklarczyk, A. L. Gable, D. Lyon et al., "STRING v11: protein-protein association networks with increased coverage, supporting functional discovery in genome-wide

experimental datasets," *Nucleic Acids Research*, vol. 47, no. D1, pp. D607–d613, 2019.

[24] M. Kohl, S. Wiese, and B. Warscheid, "Cytoscape: software for visualization and analysis of biological networks," *Methods in Molecular Biology*, vol. 696, pp. 291–303, 2011.

[25] G. D. Bader and C. W. Hogue, "An automated method for finding molecular complexes in large protein interaction networks," *BMC Bioinformatics*, vol. 4, no. 1, p. 2, 2003.

[26] R. s. Janky, A. Verfaillie, H. Imrichová et al., "iRegulon: from a gene list to a gene regulatory network using large motif and track collections," *PLoS Computational Biology*, vol. 10, no. 7, Article ID e1003731, 2014.

[27] C. H. Chin, S. H. Chen, H. H. Wu, C. W. Ho, M. T. Ko, and C. Y. L. cytoHubba, "Identifying hub objects and sub-networks from complex interactome," *BMC Systems Biology*, vol. 8, 2014.

[28] X. Fang, H. Wang, D. Han et al., "Ferroptosis as a target for protection against cardiomyopathy," *Proceedings of the National Academy of Sciences*, vol. 116, no. 7, pp. 2672–2680, 2019.

[29] J. Zhang, Y. Zhou, Y. Sun et al., "Beneficial effects of oridonin on myocardial ischemia/reperfusion injury: insight gained by metabolomic approaches," *European Journal of Pharmacology*, vol. 861, Article ID 172587, 2019.

[30] H. C. Fang, B. Q. Wu, Y. L. Hao et al., "KRT1 gene silencing ameliorates myocardial ischemia-reperfusion injury via the activation of the Notch signaling pathway in mouse models," *Journal of Cellular Physiology*, vol. 234, no. 4, pp. 3634–3646, 2019.

[31] C.-F. Yang, "Clinical manifestations and basic mechanisms of myocardial ischemia/reperfusion injury," *Tzu Chi Medical Journal*, vol. 30, no. 4, pp. 209–215, 2018.

[32] A. Rout, U. S. Tantry, M. Novakovic, A. Sukhi, and P. A. Gurbel, "Targeted pharmacotherapy for ischemia reperfusion injury in acute myocardial infarction," *Expert Opinion on Pharmacotherapy*, vol. 21, no. 15, pp. 1851–1865, 2020.

[33] M. Algoet, S. Janssens, U. Himmelreich et al., "Myocardial ischemia-reperfusion injury and the influence of inflammation," *Trends in Cardiovascular Medicine*, 2022.

[34] N. J. Pluijmert, D. E. Atsma, and P. H. A. Quax, "Post-ischemic myocardial inflammatory response: a complex and dynamic process susceptible to immunomodulatory therapies," *Frontiers in Cardiovascular Medicine*, vol. 8, Article ID 647785, 2021.

[35] L. Arnold, M. Weberbauer, M. Herkel et al., "Endothelial BMP4 promotes leukocyte rolling and adhesion and is elevated in patients after survived out-of-hospital cardiac arrest," *Inflammation*, vol. 43, no. 6, pp. 2379–2391, 2020.

[36] J. Xue, H. Ge, Z. Lin et al., "The role of dendritic cells regulated by HMGB1/TLR4 signalling pathway in myocardial ischaemia reperfusion injury," *Journal of Cellular and Molecular Medicine*, vol. 23, no. 4, pp. 2849–2862, 2019.

[37] T.-W. Lee, Y.-H. Kao, Y.-J. Chen, T.-F. Chao, and T.-I. Lee, "Therapeutic potential of vitamin D in AGE/RAGE-related cardiovascular diseases," *Cellular and Molecular Life Sciences*, vol. 76, no. 20, pp. 4103–4115, 2019.

[38] L. Gong, X. Wang, J. Pan et al., "The co-treatment of rosuvastatin with dapagliflozin synergistically inhibited apoptosis via activating the PI3K/AKt/mTOR signaling pathway in myocardial ischemia/reperfusion injury rats," *Open Medicine*, vol. 15, no. 1, pp. 47–57, 2021.

[39] F. F. Ramli, A. Ali, and N. I. Ibrahim, "Molecular-signaling pathways of ginsenosides Rb in myocardial ischemia-reperfusion injury: a mini review," *International Journal of Medical Sciences*, vol. 19, no. 1, pp. 65–73, 2022.

[40] Z. V. Schofield, T. M. Woodruff, R. Halai, M. C.-L. Wu, and M. A. Cooper, "Neutrophils-A key component of ischemia-reperfusion injury," *Shock*, vol. 40, no. 6, pp. 463–470, 2013.

[41] P. Dhôte-Burger, A. Vuilleminot, T. Lecompte et al., "Neutrophil degranulation related to the reperfusion of ischemic human heart during cardiopulmonary bypass," *Journal of Cardiovascular Pharmacology*, vol. 25, pp. S124–S129, 1995.

[42] Y.-R. Chen and J. L. Zweier, "Cardiac mitochondria and reactive oxygen species generation," *Circulation Research*, vol. 114, no. 3, pp. 524–537, 2014.

[43] A. J. Palazzo, S. P. Jones, W. G. Girod, D. C. Anderson, D. N. Granger, and D. J. Lefer, "Myocardial ischemia-reperfusion injury in CD18- and ICAM-1-deficient mice," *American Journal of Physiology - Heart and Circulatory Physiology*, vol. 275, no. 6, pp. H2300–H2307, 1998.

[44] G. Aslan, A. Atessahin, and E. Sahna, "The inhibition of apoptosis through myocardial postconditioning by affecting Fas/FasIg signaling through miR139-3p and miR181a-1," *Journal of Cardiac Surgery*, vol. 35, no. 3, pp. 564–570, 2020.

[45] K. Gul-Kahraman, M. Yilmaz-Bozoglan, and E. Sahna, "Physiological and pharmacological effects of melatonin on remote ischemic perconditioning after myocardial ischemia-reperfusion injury in rats: role of Cybb, Fas, NfκB, Irisin signaling pathway," *Journal of Pineal Research*, vol. 67, no. 2, Article ID e12589, 2019.

[46] N. Takaya, Y. Katoh, K. Iwabuchi et al., "Platelets activated by collagen through the immunoreceptor tyrosine-based activation motif in the Fc receptor γ-chain play a pivotal role in the development of myocardial ischemia-reperfusion injury," *Journal of Molecular and Cellular Cardiology*, vol. 39, no. 6, pp. 856–864, 2005.

[47] J. H. Spahn, W. Li, A. C. Bribriesco et al., "DAP12 expression in lung macrophages mediates ischemia/reperfusion injury by promoting neutrophil extravasation," *The Journal of Immunology*, vol. 194, no. 8, pp. 4039–4048, 2015.

[48] T. Nakao, Y. Ono, H. Dai et al., "DNAX activating protein of 12 kDa/triggering receptor expressed on myeloid cells 2 expression by mouse and human liver dendritic cells: functional implications and regulation of liver ischemia-reperfusion injury," *Hepatology*, vol. 70, no. 2, pp. 696–710, 2019.

[49] D. N. Grigoryev, D. I. Cheranova, D. P. Heruth et al., "Meta-analysis of molecular response of kidney to ischemia reperfusion injury for the identification of new candidate genes," *BMC Nephrology*, vol. 14, no. 1, p. 231, 2013.

[50] K. M. O'Shea, R. Ananthakrishnan, Q. Li et al., "The formin, DIAPH1, is a key modulator of myocardial ischemia/reperfusion injury," *EBioMedicine*, vol. 26, pp. 165–174, 2017.

[51] A. A. Izzo, M. Teixeira, S. P. H. Alexander et al., "A practical guide for transparent reporting of research on natural products in the British Journal of Pharmacology: reproducibility of natural product research," *British Journal of Pharmacology*, vol. 177, no. 10, pp. 2169–2178, 2020.

[52] C. Zhao, S. Li, J. Zhang et al., "Current state and future perspective of cardiovascular medicines derived from natural products," *Pharmacology & Therapeutics*, vol. 216, Article ID 107698, 2020.

Hindawi
Evidence-Based Complementary and Alternative Medicine
Volume 2022, Article ID 7708781, 7 pages
https://doi.org/10.1155/2022/7708781

Research Article

Vasorelaxant Effects of the *Vitex Agnus-Castus* Extract

Shpëtim Thaçi,[1] Berat Krasniqi,[1] Miribane Dërmaku-Sopjani,[2] Arleta Rifati-Nixha,[2] Sokol Abazi,[3] and Mentor Sopjani[1]

[1]*Faculty of Medicine, University of Prishtina, Prishtina 10000, Kosovo*
[2]*Faculty of Natural Sciences and Mathematics, University of Prishtina, Prishtina 10000, Kosovo*
[3]*Canadian Institute of Technology, Tirana 100, Albania*

Correspondence should be addressed to Mentor Sopjani; mentor.sopjani@uni-pr.edu

Received 30 April 2021; Revised 26 January 2022; Accepted 1 March 2022; Published 22 March 2022

Academic Editor: Thanasekaran Jayakumar

This study was undertaken to describe and characterize the relaxing effects of the medicinal plant *Vitex agnus-castus* (VAC) extract on isolated rabbit arterial rings. The VAC extracts (VACE) were extracted with ethanol and tested in aorta rings (3-4 mm) of rabbits suspended in an organ bath (Krebs, 37°C, 95% O_2/5% CO_2) under a resting tension of 1 g to record isometric contractions. After the stabilization period (1-2 hours), contractions were induced by the addition of phenylephrine (0.5 μM) or high KCl (80 mM) and VACE was added on the plateau of the contractions. Experiments were performed to determine the effects and to get insights into the potential mechanism involved in VACE-induced relaxations. The cumulative addition of VACE (0.15–0.75 mg/mL) relaxed, in a concentration-dependent manner, the rabbit aorta rings precontracted either with phenylephrine- or with high KCl thus suggesting calcium channel blocking activities. The VACE effect appeared to be endothelium-dependent. The preincubation with L-NAME (the inhibitor of nitric oxide synthases (NOS)), ODQ (the selective inhibitor of guanylyl cyclase), and indomethacin (the cyclooxygenase inhibitor), downregulated VACE-induced relaxation of aorta rings precontracted with phenylephrine, whereas the bradykinin (stimulator of NOS) and zaprinast (phosphodiesterase inhibitor) further upregulated relaxant effects induced by VACE. These results revealed that the aorta relaxation effect of VACE was mainly endothelium-dependent and mediated by NO/cGMP and prostaglandins synthesis. This vasodilator effect of VACE may be useful to treat cardiovascular disorders, including hypertensive diseases.

1. Introduction

Herbal medicine has been commonly used throughout human history for the treatment of various conditions, or diseases [1]. Medicinal herbs have been widely used for both culinary and medicinal purposes and played an important role in the development of human culture. Herbal medicine-derived natural products have been used in traditional medicine for the prevention and treatment of various human conditions, including cardiovascular diseases [2, 3].

Numerous plant-derived natural products have already been isolated [1, 4–7], with a great potential to be used for healing purposes in a variety of disorders [7–11]; many of them have already been approved for therapeutic use in the last years [12, 13]. However, the effects of some of them still need to be mechanistically characterized. Therefore, pharmacological characterization of their effects, and especially the underlying intracellular mechanism involved, may help to better understand their roles and can be used as a strategy for identifying new applicable and more potent drugs.

The genus *Vitex* L. (family *Lamiaceae*) has about 250 different species. These are deciduous shrubs, mainly native throughout the tropic and subtropics regions. One of the *Vitex* species is *Vitex agnus-castus* (chaste tree, VAC) [14, 15]. It is an aromatic, ornamental, and deciduous shrub native to the Mediterranean and Western Asia. The chemical composition of VACE (*Vitex agnus-castus* extract) was reported [16] in 2016, revealing the presence of 47 different components accounting for about 99% essential oils from the leaves, fruit, and inflorescence, respectively. Lately, our team published the tracheorelaxant properties and mode of

action of VACE fruits, as well as their phytochemical composition [17]. Fruits of VACE have been used for the treatment of many female conditions, including hormonal imbalances, pain, and menstrual cycle problems [14, 15, 18–20]. Noteworthily, in Albanian folk medicine, VAC fruits and leaves are often used for increasing milk and female reproductive disorders treatment.

Additionally, the extracts from genus *Vitex* have been reported to have cardiovascular activities [15] and were used to treat hypertension. However, these functions are mainly not scientifically assessed. Recently, the leaf extracts of *Vitex pubescens* have been reported to have antihypertensive and vasorelaxant action in the aorta [21]. Therefore, this study was aimed to investigate the vascular effects of *Vitex agnus-castus* extract on rabbit aorta rings under various experimental conditions.

2. Materials and Methods

2.1. Preparation of the Crude Plant Extract. The fruits of VAC (*Vitex agnus-castus*, L) were collected carefully from Albania. Plant materials were professionally determined by a botanist and then manually picked, cleaned up of adulterants, and shade-dried away from strong winds [17, 22]. Then, it was further grinded to a coarse powder by a grinding machine. The resulting material was soaked in 80% ethanol for 24 hours at room temperature under constant shaking and then filtered by passing through a filter paper. After that, the filtered liquid (filtrate) was concentrated in a rotary evaporator under pressure, dried out, and transferred to containers. The extract was standardized with 0.13–0.15% casticin and kept in a refrigerator (4°C). Appropriate dilutions of the crude plant extract from the stock were freshly made on the day of the experiment.

2.2. Reagents. Phenylephrine (PE, a vasoconstrictor), N^G-nitro-L-arginine methyl ester (L-NAME, an inhibitor of nitric oxide synthases (NOS)), bradykinin (a stimulator of NOS), indomethacin (a cyclooxygenase (COX) inhibitor), ODQ (1H- (1,2,4) oxadiazolo (4,3-a) quinoxalin-1-one, a selective inhibitor of soluble guanylyl cyclase (sGC)), and zaprinast (a selective inhibitor of cGMP-specific phosphodiesterases V and VI (PDE5/6)) were purchased from Sigma Aldrich, Germany. All chemicals and reagents used for making physiological salt solutions and other analyses were of analytical grade. Bradykinin was dissolved in 0.1 M acetic acid; indomethacin was dissolved in ethanol, while zaprinast was dissolved in DMSO at 10 mM. Unless otherwise specified, all the drugs were dissolved in distilled water [17, 22]. Of note, all experimental solutions of drugs were made fresh daily.

2.3. Treatment and Sensitization of Rabbits. Adult rabbits (standard chinchilla rabbits), local breed and either sex, weighing about 800–1200 g (Gram), were treated according to the law of animals' protection of the Republic of Kosova (ethics committee approval no. AUV-03; 1557). The experiments were performed according to the national and international standards for animal research [23, 24], in compliance with the European Council Directive of November 24, 1986 (86/609/EEC). Rabbits were kept in proper conditions, 19–23°C, 12 hours light/dark regimen cycle, and given ad libitum food and water. Animals were housed in the animal facility of the Faculty of Medicine of the Uni. of Prishtina. Rabbits of either sex were sacrificed following a blow on the back of the head and their thoracic aorta was taken out by dissection and kept in the normal Krebs–Henseleit solution (KHS) in the following composition (mM): NaCl (118), KCl (4.7), $CaCl_2$ (2.52), $MgSO_4$ (1.64), KH_2PO_4 (1.18), $NaHCO_3$ (7), and glucose (5.5). Aorta was then cut vertically in 2-3 mm width rings. Each isolated aorta ring was then mounted between two stainless-steel hooks in the thermostatically controlled (37°C) organ baths. The lower hook was fixed at the bottom of the organ bath, while the upper one was connected to an isometric transducer (DMT 750, Danish Myo Technology, Denmark) connected to an ink writing recorder. The mounted aorta tissue was kept in the organ bath (10 ml) containing KHS (pH 7.4) and continuously aerated with 5% CO_2 and 95% O_2.

2.4. Experimental Protocols. Changes in isometric tension of aortic rings were continuously measured with a force transducer (DMT 750, Danish Myo Technology, Denmark). An optimal preload of 1 g was applied to each aorta ring and allowed to equilibrate for about 1 h, during which the preparations were regularly washed out with KHS every 15 min and resting tension of 1 g was readjusted. After equilibration, rings were stimulated with PE (0.5 μM) or K+ (80 mM) until a sustained response was obtained. Then, VACE was added on the plateau of either PE- or K+-induced contraction in a cumulative manner (VACE 0.15 to 0.75 mg/mL) or in a single maximal concentration (VACE 0.75 mg/mL). Control preparations were treated with a drug vehicle only.

Endothelium-derived relaxing factors are known to induce aorta smooth muscle (ASM) relaxation [25]. Accordingly, we hypothesized the involvement of endothelium in the relaxant effects of VACE. To this end, in a series of experiments with aorta rings, the endothelium was removed by gently rubbing the intimal surface of the vessel with a smooth wooden stick in an appropriate condition. After preparation, successful removal of the endothelium was assessed by the significant decrease of acetylcholine (ACh, 1 μM) ability to elicit the aortic ring relaxation, while smooth muscle integrity was tested with KCl (80 mM)-induced contraction in both, endothelium-intact and endothelium-denuded aorta rings. The relaxant effect of VACE was tested as explained above. To deeper investigate the endothelium-dependent mechanisms of VACE relaxation [5, 25], the endothelium-intact aortic rings were treated with PE, in presence or absence of 0.75 mg/mL of VACE, and without (PE + VACE alone) or with bradykinin, L-NAME, ODQ, zaprinast, or indomethacin, respectively [26, 27]. All abovementioned inhibitors and the stimulator were added 5 min prior to induce contraction by PE. The aortic rings evoked a constriction effect that reached the plateau level for

about 30 minutes after PE treatment. The tested aortic rings were performed in parallel without or with the specific inhibitor, stimulator, respectively.

2.5. Statistical Analysis. The relaxant function of VACE in the aorta is expressed as a value of PE-KCl-induced maximal contractions compared to 1 g of contraction force. The data are representative of at least four independent experiments ($n = 4$) for each series of experiments and expressed as means ± SEM. Statistical analysis was made by one-way ANOVA and Dunnett's post-test. A value of $p < 0.05$ was considered statistically significant (GraphPad Prism Software, La Jolla, CA).

3. Results

VACE significantly relaxed the PE, -high K^+, -precontracted aortic rings in a dose-dependent manner.

In the first series of experiments, the effect of increasing concentrations of VACE on the basal tone of isolated rabbit aortic rings was assessed. As shown in Figures 1(a), 1(b), concentrations of VACE higher than 0.15 mg/mL significantly relaxed the PE-induced contraction.

In the next series of experiments, we tested the effects of cumulative concentration of VACE on high (80 mM) K^+-induced contraction of rabbit aortic rings. As reported in Figure 1(c), concentration of VACE higher than 0.3 mg/mL significantly reduced the high K^+-evoked aortic contraction.

3.1. Vasorelaxant Effects of VACE Are Partially Endothelium-Dependent. The presence or absence of an intact endothelium in all preparations was assessed by testing the capacity of ACh to induce relaxation of rings precontracted with phenylephrine. Figure 2(a) shows almost complete loss of relaxing response of aorta rings to ACh on endothelium-denuded as compared to endothelium-intact preparations, which were used to test the role of the endothelium in VACE-induced ASM relaxation. The steady contraction of rabbit aortic rings precontracted with PE was similar in the endothelium-intact and endothelium-denuded rings. The addition of VACE (0.15–0.75 mg/mL) induced a concentration-dependent relaxation, which was significantly higher in endothelium-intact than in endothelium-denuded aortic rings (Figure 2(b)). Thus, the vasorelaxant effect of VACE appears to be at least partly endothelium-dependent.

3.2. Involvement of NO/cGMP Signaling Pathway in VACE-Induced Vasorelaxant Activity. To further explore the endothelium participation in VACE-induced vasodilatation, we tested the involvement of the nitric oxide (NO)-cyclic GMP (cGMP) pathway. Therefore, as presented in Figure 3, the relaxant effect of VACE (0.75 mg/mL) on PE-induced arterial contraction was significantly increased by tissue incubation with bradykinin (nitric oxide synthase stimulator, 100 nM) ($p < 0.05$, $n = 9$) or zaprinast a selective inhibitor of cGMP-specific phosphodiesterases V and VI (PDE5/6, 10 μM) ($p < 0.05$, $n = 9$), whereas L-NAME (a nonspecific nitric oxide (NO) synthase inhibitor, 100 μM) ($p < 0.05$, $n = 10$) or ODQ (a selective inhibitor of sGC, 10 μM) ($p < 0.05$, $n = 5$), significantly decreased the VACE-induced dilatation ($p < 0.001$, $n = 12$) of isolated rabbit aortic rings as compared to VACE following PE-induced aortic precontraction alone.

Another mechanism of vascular relaxation involves prostaglandins (PG) production [28, 29], mediated by COX induction [30]. To determine whether PG was also involved in VACE-induced relaxation of rabbit aorta, the effect of the extract was evaluated in PE-contracted rings preincubated with indomethacin (10 μM). The nonselective cyclooxygenase inhibitor significantly reduced the vasodilatory response of the vessels to VACE (Figure 4) ($p < 0.01$, $n = 4$–8).

4. Discussion

This study showed for the first time that the VACE has vasorelaxant effects on rabbit aortic rings contracted by either PE or high K^+ (Figures 1(a), 1(b) and 1(c)), which indicated that the *Vitex agnus-castus* contains bioactive compounds capable of regulating the function of blood vessels. Extracts or specific isolated compounds of genus *Vitex* have been previously shown to exert numerous functions and used for treating certain menstrual disorders, infertility, hyperprolactinemia, acne, corpus luteum insufficiency, PMDD, menopause, cyclical mastalgia, inflammatory conditions, and cyclic breast pain, disrupted lactation, diarrhea, and flatulence [14, 15, 18–20]. In Albanian folk medicine, fruits and leaves of VAC are frequently used for the treatment of numerous female reproductive problems. The phytochemical composition of VACE has been previously reported [16], including a paper from our team on their tracheorelaxant properties and underlying mechanisms [15]. The extracts from other species (*Vitex pubescens*) of genus *Vitex* have been reported to have cardiovascular activities [15]. However, to our best knowledge, the vascular relaxant effects and underlying mechanisms of *Vitex agnus-castus* described in the present work have not been reported earlier. The effect of VACE was observed at a relatively narrow range of concentrations.

VACE-mediated vasorelaxant effects may be both endothelium-dependent and endothelium-independent. The present study showed that PE and high K+-induced contraction of aortic smooth muscle is associated with increased intracellular calcium levels [5, 31, 32]. Calcium can regulate either the production or release of various endothelial-derived relaxing factors [33]. Nonspecific inhibition of both PE and high K+ by VACE suggests that its nonspecific vasorelaxant role, at least partly, may involve calcium channel blockade mechanisms. These results are consistent with our previous study reporting a tracheorelaxant function of VACE [17]. This VACE relaxant function may partly be endothelium-independent, potentially through the inhibition of calcium receptors, either extracellular and/or intracellular, and by activation of K_{ATP} channels [21]. This does not exclude the involvement of other potential mechanisms, such as inhibition of β-adrenergic receptors in

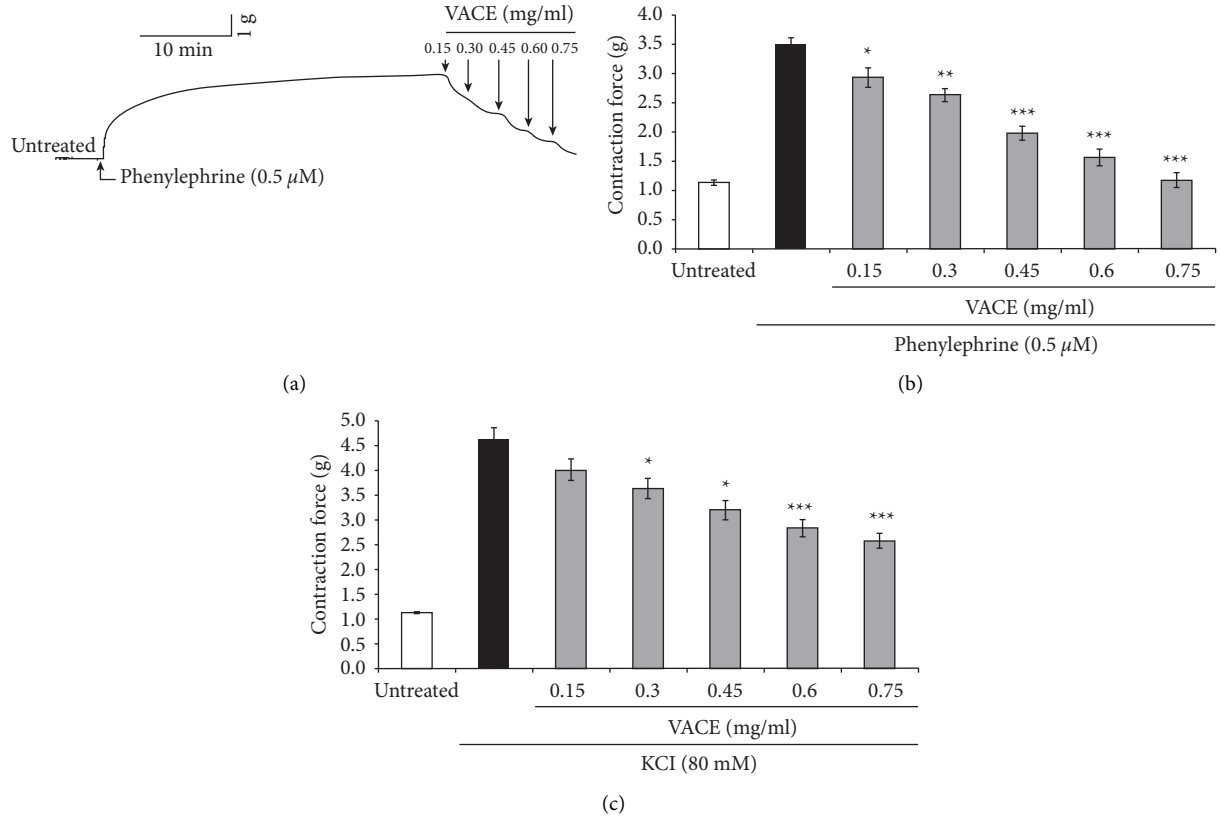

Figure 1: Concentration-dependent relaxant effect of VACE on PE-, KCl, -induced ASM contractions. (a). Original representative tracings in force/time of isolated rabbit ASM before (untreated) and after PE (0.5 μM)-induced contraction followed by the addition of cumulative concentrations (0.15–0.75 mg/mL) of VACE. Arithmetic means ± SEM (n = 4-5 aortic rings, each from a different animal) of the relaxant effects of VACE cumulative concentrations (0.15–0.75 mg/mL, gray bars) on rabbit ASM induced by PE (0.5 μM, black bar) (b) and KCl (80 mM, black bar), respectively (c). All results are shown as a value of the 1 g of contraction response. Statistically significant difference from the respective VACE concentration in rabbit aorta compared to PE and KCl alone, respectively. $^{*}p < 0.05$, $^{**}p < 0.01$, and $^{***}p < 0.001$.

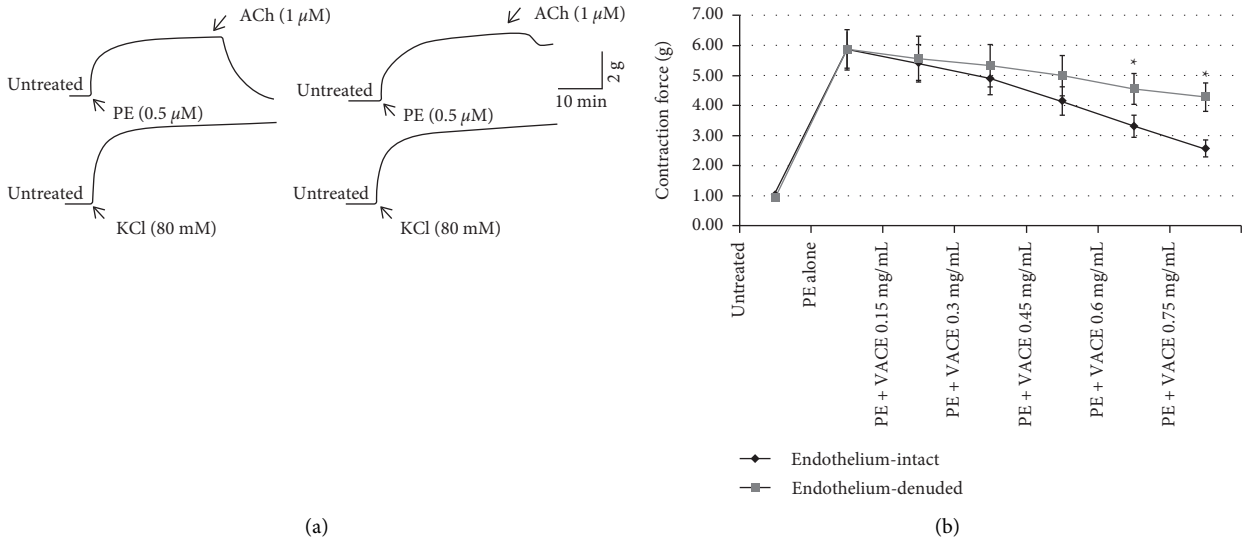

Figure 2: Effect of endothelial denudation on VACE relaxant effect after the PE-induced muscle contraction in isolated rabbit aorta. (a). Original representative tracings in force/time of isolated rabbit ASM before (untreated) and after PE (0.5 μM)-induced, and after reaching the plateau, following the ACh (1 μM)-induced relaxation to determine endothelium integrity in endothelium-intact ((a) upper left) and endothelium-denuded ((a) upper right). To test the integrity of smooth muscle after the endothelium removal, the aorta rings were precontracted with KCl (80 mM) integrity in endothelium-intact ((a) lower left) and endothelium-denuded ((a) lower right). (b) Data are shown as the arithmetic means ± SEM (n = 7-8) and expressed as the contraction force (g) of maximal contraction induced by PE (0.5 μM) followed with VACE treatment (0.15–0.75 mg/mL) of aortic rings with or without endothelium, respectively. n indicates the number of different rabbits from which descending thoracic aortic rings were derived. $^{*}p < 0.05$ compared between endothelium-denuded and endothelium-intact aortic rings.

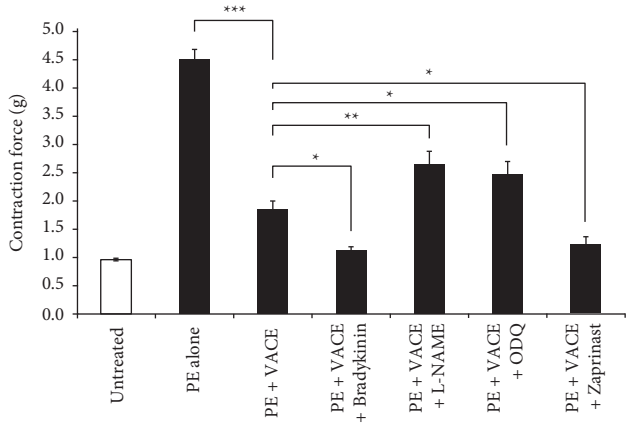

Figure 3: Bradykinin and zaprinast upregulated, whereas L-NAME and ODQ downregulated the relaxant effects of VACE in aorta rings precontracted with PE. Arithmetic means ± SEM ($n = 5$–12) of the basal tonus (1-st bar) and the relaxation responses precontracted with PE (0.5 μM) alone (2-nd bar) PE and (0.75 mg/mL) VACE (3-rd bar) PE and (100 nM) bradykinin and VACE (4-rth bar, PE and (100 μM) L-NAME and VACE (5-th bar) PE and (10 μM) ODQ and VACE (6-th bar), or PE and (10 μM) zaprinast and VACE (7-th bar). In all cases where indicated, bradykinin, L-NAME, ODQ, and zaprinast were preincubated for 5 min. Statistical significance ($^{*}p < 0.05$, $^{**}p < 0.01$, and $^{***}p < 0.001$) between treatments, was as indicated in the figure. VACE-induced aortic relaxation involves prostaglandins production.

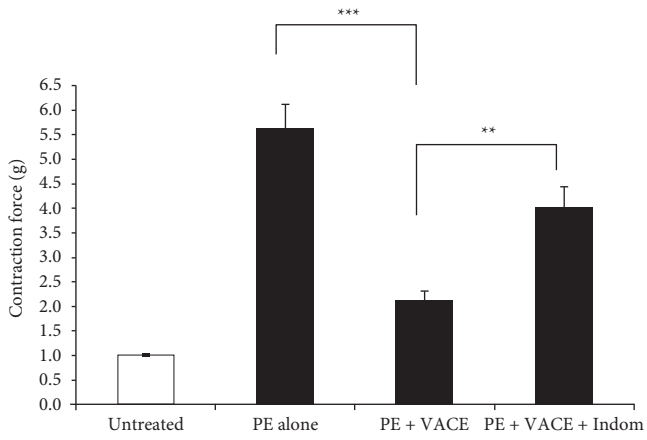

Figure 4: Indomethacin inhibited the VACE-induced relaxant effects of rabbit aortic rings precontracted with PE. Arithmetic means ± SEM ($n = 4$–8 aortic rings, each from a different rabbit) of the measurements recorded in rabbit ASM with PE (0.5 μM) and treated with VACE 0.75 mg/mL without (PE + VACE) or with (after 5 min pretreatment) 10 μM indomethacin (PE + VACE + Indomethacin). Significant differences from the absence of VACE, as well as from the absence of indomethacin: $^{**}p < 0.01$, $^{***}p < 0.001$.

ASM cells [33]. Calcium channel blocking properties of VACE in ASM may have antioxidant functions [7, 15].

Endothelial cells are essential in the control and regulation of various physiological cardiovascular functions [34]. Endothelium deregulation is associated with diseases, including cardiovascular diseases [35]. In this regard, the endothelial cells appear to be the main site of the relaxant action of the bioactive compounds present in the VACE. Although the effect of VACE was observed in both preparations; however, VACE-induced relaxation at higher concentrations-in denuded aortic rings precontracted by PE was significantly lower than intact aortic rings (Figure 2). The presence of the VACE effect in both types of preparations might be due to either endothelium was not fully absent in endothelium-denuded preparations or the involvement of endothelium-independent mechanisms in VACE effects. Herein, it may be that VACE could be acting on the ASM cells to increase responsiveness to endothelium relaxing factors [36]. The VACE-induced endothelium-mediated ASM relaxation effects seem to be particularly associated with a synergic induction of NO/cGMP and PG signaling pathways. This particular VACE endothelium-dependent activity suggested a potential role for NO release or activation and the cyclooxygenase signaling pathway and/or their interactions on vascular smooth muscles [37].

Accordingly, we found the effect of L-NAME, ODQ, bradykinin, and zaprinast (Figure 3), as well as indomethacin on VACE relaxation (Figure 4). In line with this, one of the well-known mechanisms that induce vascular smooth muscle cell relaxation, including vascular smooth muscle cells, is the NO/cGMP pathway [37, 38]. Nitric oxide is a ubiquitous molecule, an endogenous vasorelaxant mediator that under normal conditions or in response to a variety of agonists can be generated by the NOS isoforms, which use L-arginine, oxygen, and NADPH as substrates to generate NO and L-citrulline [39]. sGC is the receptor for NO in vascular smooth muscles. NO activates sGC, which in turn catalyzes the conversion of guanosine triphosphate (GTP) to the intracellular second messenger cyclic guanosine monophosphate (cGMP) in vascular smooth muscle cells, and thereby increased levels of cGMP induces muscle relaxation [37, 39, 40]. On the contrary, PDE5-catalyzed cGMP degradation to GMP accounts for ending vasorelaxation [25, 40]. As a deduction, PDE5 inhibitors, such as zaprinast, inhibit the degradation of cGMP leading to induced muscle relaxation. Accordingly, we preincubated isolated aortic rings with either bradykinin or L-NAME or ODQ or zaprinast to find the putative involvement of the NO/cGMP-dependent signaling pathway for the inhibitory effect of VACE following PE-induced aorta muscle contractions. Specifically, our findings showed that treatment with NOS stimulator bradykinin and PDE5 inhibitor zaprinast further increased the ASM relaxant effects of VACE. Indeed, relaxation to VACE was significantly decreased by the presence of a NOS inhibitor L-NAME and an inhibitor of sGC ODQ. These results suggested the involvement of the NO-sGC-cGMP pathway in the vasorelaxant effects of VACE, by stimulating NO and cGMP synthesis and/or inhibiting cGMP degradation [41]. These may also explain the relaxation mechanism of VACE more pronounced on endothelium-intact and less effective on endothelium-denuded ASM.

Prostacyclin is an endothelium-derived specific mediator and factor contributing to vasorelaxation [42], as it has been reported in circulatory failure cases in sepsis. An

important endothelium-dependent pathway participating in vascular relaxation is the PG-cAMP pathway [28, 29]. Production of PG in the endothelium is catalyzed by COX enzyme isoforms [30]. To determine whether the PG pathway is involved in VACE-induced ASM relaxation, we tested the role of indomethacin, COX-1, and COX-2 inhibitor and blocker of the PG-cAMP pathway. Indomethacin blocks PG synthase and the PG-cAMP pathway. As we have shown, pretreatment with indomethacin (Figure 4) significantly inhibited the relaxant effect of VACE in aortic rings precontracted with PE. Thus, suggesting that the aorta relaxation effect induced by VACE might be partly realized through prostaglandins' formation.

5. Conclusions

This study finding has proven that VACE exerts vascular relaxant properties that are endothelium-dependent and, at least partly, are mediated by NO/cGMP- and COX-1-PG-dependent mechanisms. Also, VACE may act through directly relaxing the ASM cells, by inhibiting cGMP, hydrolyzing PDEs, and other endothelium-independent mechanisms involved in vascular relaxation. Taken together, our findings might give reasons to explain the effects of VACE that seem to have a potential therapeutic value in the treatment of cardiovascular diseases, including hypertensive heart disease.

Data Availability

The data results used to support the findings of this study are included within the article, while the original database is deposited in our laboratory (Fac. of Medicine, Uni. Prishtina).

Conflicts of Interest

The authors declare that there are no conflicts of interest regarding the publication of this paper.

Acknowledgments

The authors thank the project donor Department of Science and Technology. of the Republic of Kosova. This work was supported by the Small Research Project (Ref. no. 2-3214/2, 2015, granted to M. Sopjani) financed by the Department of Science and Technology of the Republic of Kosova.

References

[1] D. C. Favarin, J. R. de Oliveira, C. J. de Oliveira, and A. P. Rogerio, "Potential effects of medicinal plants and secondary metabolites on acute lung injury," *BioMed Research International*, vol. 2013, Article ID 576479, 12 pages, 2013.

[2] A. Malik, M. H. Mehmood, H. Channa, M. S. Akhtar, and A.-H. Gilani, "Pharmacological basis for the medicinal use of polyherbal formulation and its ingredients in cardiovascular disorders using rodents," *BMC Complementary and Alternative Medicine*, vol. 17, no. 1, p. 142, 2017.

[3] J. Matsumoto-Miyazaki, H. Ushikoshi, S. Miyata et al., "Acupuncture and traditional herbal medicine therapy prevent deliriumin patients with cardiovascular disease in intensive care units," *The American Journal of Chinese Medicine*, vol. 45, no. 02, pp. 255–268, 2017.

[4] G. Alam, S. Wahyuono, I. G. Ganjar, L. Hakim, H. Timmerman, and R. Verpoorte, "Tracheospasmolytic activity of viteosin-A and vitexicarpin isolated fromVitex trifolia," *Planta Medica*, vol. 68, no. 11, pp. 1047–1049, 2002.

[5] A. B. Dongmo, A. G. B. Azebaze, F. M. Donfack et al., "Pentacyclic triterpenoids and ceramide mediate the vasorelaxant activity of Vitex cienkowskii via involvement of NO/cGMP pathway in isolated rat aortic rings," *Journal of Ethnopharmacology*, vol. 133, no. 1, pp. 204–212, 2011.

[6] C. N. Gabrieli, P. G. Kefalas, and E. L. Kokkalou, "Antioxidant activity of flavonoids from Sideritis raeseri," *Journal of Ethnopharmacology*, vol. 96, no. 3, pp. 423–428, 2005.

[7] A. Srancikova, E. Horvathova, and K. Kozics, "Biological effects of four frequently used medicinal plants of Lamiaceae," *Neoplasma*, vol. 60, pp. 585–597, 2013.

[8] F. P. Santana, N. M. Pinheiro, M. I. Mernak et al., "Evidences of herbal medicine-derived natural products effects in inflammatory lung diseases," *Mediators of Inflammation*, vol. 2016, Article ID 2348968, 14 pages, 2016.

[9] D. Stagos, N. Portesis, C. Spanou et al., "Correlation of total polyphenolic content with antioxidant and antibacterial activity of 24 extracts from Greek domestic Lamiaceae species," *Food and Chemical Toxicology*, vol. 50, no. 11, pp. 4115–4124, 2012.

[10] M. Fukahori, S. Kobayashi, Y. Naraki et al., "Quality evaluation of medicinal products and health foods containing chaste berry (*Vitex agnus-castus*) in Japanese, European and American markets," *Chemical and Pharmaceutical Bulletin*, vol. 62, no. 4, pp. 379–385, 2014.

[11] M. M. Bernareggi, M. G. Belvisi, H. Patel, P. J. Barnes, and M. A. Giembycz, "Anti-spasmogenic activity of isoenzyme-selective phosphodiesterase inhibitors in Guinea-pig trachealis," *British Journal of Pharmacology*, vol. 128, no. 2, pp. 327–336, 1999.

[12] Y.-T. Cheng, C.-C. Yang, and L.-F. Shyur, "Phytomedicine-Modulating oxidative stress and the tumor microenvironment for cancer therapy," *Pharmacological Research*, vol. 114, pp. 128–143, 2016.

[13] V. Romanucci, G. Di Fabio, D. D'Alonzo, A. Guaragna, G. Scapagnini, and A. Zarrelli, "Traditional uses, chemical composition and biological activities of Sideritis raeseri Boiss. & Heldr," *Journal of the Science of Food and Agriculture*, vol. 97, no. 2, pp. 373–383, 2017.

[14] M. Rafieian-Kopaei and M. Movahedi, "Systematic review of premenstrual, postmenstrual and infertility disorders of Vitex agnus castus," *Electronic Physician*, vol. 9, no. 1, pp. 3685–3689, 2017.

[15] A. Rani and A. Sharma, "The genus Vitex: a review," *Pharmacognosy Reviews*, vol. 7, no. 14, pp. 188–198, 2013.

[16] R. C. S. Neves and C. A. G. D. Camara, "Chemical composition and acaricidal activity of the essential oils from *Vitex agnus-castus* L. (Verbenaceae) and selected monoterpenes," *Anais da Academia Brasileira de Ciências*, vol. 88, no. 3, pp. 1221–1233, 2016.

[17] S. Thaçi, B. Krasniqi, D. Cela et al., "Mechanisms underlying the tracheorelaxant effect of Vitex agnus-castus extract," *Rev.Bras.Farmacogn.*vol. 30, no. 1, pp. 103–110, 2020.

[18] H. Kikuchi, B. Yuan, Y. Nishimura et al., "Cytotoxicity of Vitex agnus-castus fruit extract and its major component, casticin, correlates with differentiation status in leukemia cell

lines," *International Journal of Oncology*, vol. 43, no. 6, pp. 1976–1984, 2013.

[19] B. J. Tesch, "Herbs commonly used by women:an evidence-based review," *Disease-a-Month*, vol. 48, no. 10, pp. 671–696, 2002.

[20] M. Weisskopf, W. Schaffner, G. Jundt, T. Sulser, S. Wyler, and H. Tullberg-Reinert, "AVitex agnus-castusExtract inhibits cell growth and induces apoptosis in prostate epithelial cell lines," *Planta Medica*, vol. 71, no. 10, pp. 910–916, 2005.

[21] A. A. Al Akwaa, M. Z. Asmawi, A. Dewa, and R. Mahmud, "Antihypertensive activity and vascular reactivity mechanisms of Vitex pubescens leaf extracts in spontaneously hypertensive rats," *Heliyon*, vol. 6, Article ID e04588, 2020.

[22] B. Krasniqi, S. Thaci, M. Dermaku-Sopjani, A. Rifati-Nixha, S. Abazi, and M. Sopjani, "Insight into the mechanisms underlying the tracheorelaxant properties of the sideritis raeseri extract," *Evid Based Complement Alternat Med*, vol. 2020, Article ID 6510708, 8 pages, 2020.

[23] L. Carbone, "The utility of basic animal research," *Hastings Center Report*, vol. 42, no. s1, pp. S12–S15, 2012.

[24] L. Carbone, "Pain management standards in the eighth edition of the guide for the care and use of laboratory animals," *Journal of the American Association for Laboratory Animal Science*, vol. 51, pp. 322–328, 2012.

[25] F. Mullershausen, A. Lange, E. Mergia, A. Friebe, and D. Koesling, "Desensitization of NO/cGMP signaling in smooth muscle: blood vessels versus airways," *Molecular Pharmacology*, vol. 69, no. 6, pp. 1969–1974, 2006.

[26] T. Kaya, S. Gursoy, B. Karadas, B. Sarac, H. Fafali, and A. S. Soydan, "High-concentration tramadol-induced vasodilation in rabbit aorta is mediated by both endothelium-dependent and -independent mechanisms," *Acta Pharmacologica Sinica*, vol. 24, pp. 385–389, 2003.

[27] J. D. Raffetto, F. Calanni, P. Mattana, and R. A. Khalil, "Sulodexide promotes arterial relaxation via endothelium-dependent nitric oxide-mediated pathway," *Biochemical Pharmacology*, vol. 166, pp. 347–356, 2019.

[28] A.-M. Hristovska, L. E. Rasmussen, P. B. L. Hansen et al., "Prostaglandin E2Induces vascular relaxation by E-prostanoid 4 receptor-mediated activation of endothelial nitric oxide synthase," *Hypertension*, vol. 50, no. 3, pp. 525–530, 2007.

[29] J.-i. Suzuki, M. Ogawa, R. Watanabe et al., "Roles of prostaglandin E2 in cardiovascular diseases," *International Heart Journal*, vol. 52, no. 5, pp. 266–269, 2011.

[30] C. Capone, G. Faraco, J. Anrather, P. Zhou, and C. Iadecola, "Cyclooxygenase 1-derived prostaglandin E 2 and EP1 receptors are required for the cerebrovascular dysfunction induced by angiotensin II," *Hypertension*, vol. 55, no. 4, pp. 911–917, 2010.

[31] M. Dermaku-Sopjani, F. Kurti, N. T. Xuan, and M. Sopjani, "Klotho-dependent role of 1,25 (OH) 2D3 in the brain," *Neurosignals*, vol. 29, pp. 14–23, 2021.

[32] M. Sopjani and M. Dërmaku-Sopjani, "Klotho-dependent cellular transport regulation," *Klotho*, vol. 101, pp. 59–84, 2016.

[33] J. Akter, M. Z. Islam, M. A. Hossain et al., "Endothelium-independent and calcium channel-dependent relaxation of the porcine cerebral artery by different species and strains of turmeric," *Journal of Traditional and Complementary Medicine*, vol. 9, no. 4, pp. 297–303, 2019.

[34] W. C. Aird, "Phenotypic heterogeneity of the endothelium," *Circulation Research*, vol. 100, no. 2, pp. 158–173, 2007.

[35] J. Barthelmes, M. P. Nägele, V. Ludovici, F. Ruschitzka, I. Sudano, and A. J. Flammer, "Endothelial dysfunction in cardiovascular disease and Flammer syndrome-similarities and differences," *EPMA Journal*, vol. 8, no. 2, pp. 99–109, 2017.

[36] L. Belemnaba, S. Ouédraogo, C. Auger et al., "Endothelium-independent and endothelium-dependent vasorelaxation by a dichloromethane fraction from Anogeissus Leiocarpus (DC) Guill. Et Perr. (Combretaceae): possible involvement of cyclic nucleotide phosphodiesterase inhibition," *African Journal of Traditional, Complementary, and Alternative Medicines: AJTCAM*, vol. 10, no. 2, pp. 173–179, 2013.

[37] M. Sausbier, R. Schubert, V. Voigt et al., "Mechanisms of NO/cGMP-dependent vasorelaxation," *Circulation Research*, vol. 87, no. 9, pp. 825–830, 2000.

[38] S. Moncada, R. M. Palmer, and E. A. Higgs, "Nitric oxide: physiology, pathophysiology, and pharmacology," *Pharmacological Reviews*, vol. 43, pp. 109–142, 1991.

[39] S. Moncada, R. M. J. Palmer, and E. A. Higgs, "Biosynthesis of nitric oxide from l-arginine," *Biochemical Pharmacology*, vol. 38, no. 11, pp. 1709–1715, 1989.

[40] R. Feil, S. M. Lohmann, H. de Jonge, U. Walter, and F. Hofmann, "Cyclic GMP-dependent protein kinases and the cardiovascular system," *Circulation Research*, vol. 93, no. 10, pp. 907–916, 2003.

[41] S. H. Francis, J. L. Busch, J. D. Corbin, and D. Sibley, "cGMP-dependent protein kinases and cGMP phosphodiesterases in nitric oxide and cGMP action," *Pharmacological Reviews*, vol. 62, no. 3, pp. 525–563, 2010.

[42] A. V. Araújo, C. Z. Ferezin, G. J. Rodrigues et al., "Prostacyclin, not only nitric oxide, is a mediator of the vasorelaxation induced by acetylcholine in aortas from rats submitted to cecal ligation and perforation (CLP)," *Vascular Pharmacology*, vol. 54, no. 1-2, pp. 44–51, 2011.

Hindawi
Evidence-Based Complementary and Alternative Medicine
Volume 2022, Article ID 9805697, 1 page
https://doi.org/10.1155/2022/9805697

Corrigendum

Corrigendum to "Auraptene, a Monoterpene Coumarin, Inhibits LTA-Induced Inflammatory Mediators via Modulating NF-κB/MAPKs Signaling Pathways"

Chih-Hsuan Hsia,[1,2] **Thanasekaran Jayakumar**,[1] **Wan-Jung Lu**,[3,4,5] **Joen-Rong Sheu**,[1] **Chih-Wei Hsia**,[1] **Periyakali Saravana Bhavan**,[6] **Manjunath Manubolu**,[7] **Wei-Chieh Huang**,[1] **and Yi Chang**[1,8,9]

[1]*Graduate Institute of Medical Sciences, College of Medicine, Taipei Medical University, Taipei 110, Taiwan*
[2]*Translational Medicine Center, Shin Kong Wu Ho-Su Memorial Hospital, Taipei 111, Taiwan*
[3]*Department of Pharmacology, School of Medicine, College of Medicine, Taipei Medical University, Taipei 110, Taiwan*
[4]*Department of Medical Research, Taipei Medical University Hospital, Taipei 110, Taiwan*
[5]*Graduate Institute of Metabolism and Obesity Sciences, College of Nutrition, Taipei Medical University, Taipei 110, Taiwan*
[6]*Department of Zoology, Bharathiar University, Coimbatore 641046, Tamil Nadu, India*
[7]*Department of Evolution, Ecology and Organismal Biology, Ohio State University, Columbus, OH 43212, USA*
[8]*School of Medicine, Fu Jen Catholic University, New Taipei City 242, Taiwan*
[9]*Department of Anesthesiology, Shin Kong Wu Ho-Su Memorial Hospital, Taipei 111, Taiwan*

Correspondence should be addressed to Yi Chang; m004003@ms.skh.org.tw

Received 19 January 2022; Accepted 19 January 2022; Published 21 February 2022

In the article titled "Auraptene, a Monoterpene Coumarin, Inhibits LTA-Induced Inflammatory Mediators via Modulating NF-κB/MAPKs Signaling Pathways" [1], the corresponding author's affiliations were listed incorrectly. The correct affiliation list is as shown above.

References

[1] C.-H. Hsia, T. Jayakumar, W.-J. Lu et al., "Auraptene, a monoterpene coumarin, inhibits LTA-induced inflammatory mediators via modulating NF-κB/MAPKs signaling pathways," *Evidence-based Complementary and Alternative Medicine*, vol. 2021, Article ID 5319584, 11 pages, 2021.

Hindawi
Evidence-Based Complementary and Alternative Medicine
Volume 2022, Article ID 8653697, 21 pages
https://doi.org/10.1155/2022/8653697

Research Article

Exploring the Mechanism of Edaravone for Oxidative Stress in Rats with Cerebral Infarction Based on Quantitative Proteomics Technology

Guozuo Wang,[1] Xiaomei Zeng,[2] Shengqiang Gong,[1] Shanshan Wang,[1] Anqi Ge,[3] Wenlong Liu,[1] Jinwen Ge ,[1] and Qi He[2]

[1]*Hunan University of Chinese Medicine, Changsha, Hunan, China*
[2]*People's Hospital of Ningxiang City, Ningxiang, Hunan, China*
[3]*The First Affiliated Hospital of Hunan University of Chinese Medicine, Changsha, Hunan, China*

Correspondence should be addressed to Jinwen Ge; 001267@hnucm.edu.cn

Received 3 August 2021; Revised 23 October 2021; Accepted 10 November 2021; Published 4 January 2022

Academic Editor: Thanasekaran Jayakumar

Objective. To explore the mechanism of edaravone in the treatment of oxidative stress in rats with cerebral infarction based on quantitative proteomics technology. *Method*. The modified Zea Longa intracavitary suture blocking method was utilized to make rat CI model. After modeling, the rat was intragastrically given edaravone for 7 days, once a day. After the 7-day intervention, the total proteins of serum were extracted. After proteomics analysis, the differentially expressed proteins are analyzed by bioinformatics. Then chemoinformatics methods were used to explore the biomolecular network of edaravone intervention in CI. *Result*. The neurological scores and pathological changes of rats were improved after the intervention of edaravone. Proteomics analysis showed that in the model/sham operation group, 90 proteins in comparison group were upregulated, and 26 proteins were downregulated. In the edaravone/model group, 21 proteins were upregulated, and 41 proteins were downregulated. Bioinformatics analysis and chemoinformatics analysis also show that edaravone is related to platelet activation and aggregation, oxidative stress, intercellular adhesion, glycolysis and gluconeogenesis, iron metabolism, hypoxia, inflammatory chemokines, their mediated signal transduction, and so on. *Conclusion*. The therapeutic mechanism of edaravone in the treatment of CI may involve platelet activation and aggregation, oxidative stress, intercellular adhesion, glycolysis and gluconeogenesis, iron metabolism, hypoxia, and so on. This study revealed the serum protein profile of edaravone in the treatment of cerebral infarction rats through serum TMT proteomics and discovered the relevant mechanism of edaravone regulating iron metabolism in cerebral infarction, which provides new ideas for the study of edaravone intervention in cerebral infarction and also provides reference information for future research on the mechanism of edaravone intervention in iron metabolism-related diseases.

1. Introduction

Stroke is the second most common cause of death in the world, and it is also the main cause of adult disability [1]. As the American Heart Association and the National Institute of Neurological Diseases and Stroke reported, about 795,000 Americans suffer from ischemic stroke (such as cerebral infarction, CI) each year, and 220,000 die from ischemic stroke each year [2, 3]. The "China Cardiovascular Disease Report 2018" compiled by the National Center for Cardiovascular Diseases showed that the prevalence of cardiovascular disease in China is on the rise. It is estimated that there are 290 million people suffering from cardiovascular disease, of which 13 million have stroke and 11 million have coronary heart disease [4]. According to the China Stroke Prevention Report (2015), about 15% of people over 40 years old are high-risk groups. From 2011 to 2013, the comprehensive standardized prevalence rate of ischemic stroke was about 2%, and the prevalence rate increased by 8.1% [5]. According to data from the World Bank, by 2030, China will have 31.77 million patients with ischemic stroke, which will cost US$40 billion each year [6]. Current research

showed that oxidative stress plays an important role in the pathological process of ischemic brain injury. After cerebral ischemia, the production of superoxide anions, hydrogen peroxide, hydroxyl free radicals and peroxynitrite anions increases due to factors such as excitotoxicity, inflammatory response, and hypoxic environment inhibiting cell respiration, especially during reperfusion [7–9]. Hydroxyl free radicals and peroxynitrite anions can promote protein nitrification and oxidation, lipid peroxidation, mitochondrial and DNA damage, inflammatory activation, cell necrosis, and apoptosis, which can cause brain damage [10, 11].

As a scavenger of oxidative stress, edaravone is widely used in China and other Asian countries, but it has not been approved for use in Western countries [12]. A systematic review involving 49 animal experiments showed that the functional and cognitive prognosis of edaravone in an animal model of focal cerebral ischemia increased by 30.3% and 25.5%, respectively [13]. A systematic review published by Yang et al. included 18 randomized controlled trials involving 1802 patients, and the results showed that edaravone can significantly reduce the mortality or long-term disability rate of acute ischemic stroke (AIS) [14]. Both of these systematic reviews support the effectiveness of edaravone for acute ischemic stroke. Although the current research shows that edaravone can mainly improve the oxidative stress in CI [15], there is no systematic research on the mechanism of edaravone in the treatment of ischemic brain injury such as proteomics and chemoinformatics. In particular, with the rapid development and rapid iteration of current proteomics technology, the large amount of data obtained from proteomics detection and analysis represents all the processes and changes that occur in the cell [16, 17]. Therefore, in this research, proteomics and bioinformatics analysis strategies would be utilized to observe the changes of related indicators after edaravone in the treatment of CI and further explore the mechanism of edaravone to protect ischemic brain injury.

2. Material and Methods

2.1. Experimental Materials. SPF-grade male SD rats, weighing 200~230 g, were provided by Laboratory Animal Technology Co., Ltd., and the certificate number is SCXK: (Xiang) 2017–0012 (edaravone injection, article number, company batch number 1511001Y). RIPA lysate was obtained from Thermo Inc.; iodoacetamide was obtained from IAM, Sigma Aldrich; trypsin was obtained from Promega; ammonium bicarbonate was obtained from Sigma Aldrich Inc.; SOD, MDA, and GSH-px kits were obtained from Shanghai Enzyme Linked Biotechnology Co., Ltd.; rat angiotensinogen (AGT) ELISA kit (E-EL-M0013c) was purchased from Elabscience Inc. The Catalase (CAT) kit was purchased from Nanjing Jiancheng Biotechnology Research Institute. Protein quantification kit, Exactive Plus mass spectrometer, EASY-n LC 1000 liquid analyzer, C18 analytical column, EASY-Spray Column, AcclaimPep Map 100 were obtained from Thermo Inc. Nano Vue UV-Visible Spectrophotometer was obtained from GE Healthcare. Laser Doppler flow meter was obtained from Mo or VMS-LDF, Moor Instruments, Aminster, Devon, UK.

2.2. Experimental Methods

2.2.1. Animal Grouping and Intervention. Thirty male healthy SD rats were randomly divided into 3 groups by random number table method: sham operation group (CN group), CI model group (CI group), and edaravone group (CE group), 10 rats in each group. The rats in the model administration group were given edaravone by gavage with a dose of 3.5 g/kg. The sham operation group and the model group were given distilled water by gavage with a volume of 10 mL/kg. The drug was administered once a day at 14 : 00 for 7 consecutive days. All animals' care and experimental procedures were approved by the Animal Ethics Committee of Hunan University of Chinese Medicine and were in accordance with the National Institute of Health's Guide for the Care and Use of Laboratory Animals.

2.2.2. Animal Modeling. After drug administration, according to the method of Longa et al. [18], the right middle cerebral artery occlusion (MCAO) model of rats was prepared by the suture method. First, the rats were anesthetized by intraperitoneal injection of 1% sodium pentobarbital (50 mg/kg), and then the right common carotid artery was carefully separated. Then, a 5–0 suture was used to insert a blunt nylon thread from the right external carotid artery of the rat. The thread enters the intracranial segment of the internal carotid artery from the side of the external carotid artery through the bifurcation of the common carotid artery and the extracranial segment of the internal carotid artery and reaches the branch of the middle cerebral artery for circular ligation. During the model preparation process of rats in the sham operation group, except that the nylon thread did not block the middle cerebral artery, the other operations were the same as those in the model group and edaravone group. After the rats were awake, the neurological function was scored according to Longa's 5-point system.

Zero points meant no neurological deficits. One point meant mild loss of nerve function: limited extension of the left forelimb, flexion when the tail is lifted. Two points meant moderate neurological deficit: rotating to the paralyzed side (left side) when crawling. Three points meant severe neurological deficit: falling into the paralyzed side (left side) while crawling. Four points meant difficulty in crawling and performance of decreased consciousness. Rats with a score of 1 to 3 were included in the experiment.

2.2.3. Immunofluorescence Staining. After BrdU was dissolved in normal saline, the dose was determined at 100 mg/kg/d, and intraperitoneal injection was performed. The sections of brain tissue were immersed in 3% H2O2 deionized water for 10 min, washed with PBS for 5 min × 3 times, and immersed in 2 mol/L HCl at 37°C for 15 min. Then, the sections were washed with PBS for 5 min × 3 times; 5% goat serum was blocked at room temperature for 30 min,

and the liquid was aspirated. After that, BrdU monoclonal antibody (1 : 100) of 10 μL was added and incubated in 37°C water bath. Rhodamine (light emission wavelength 570 ~ 590 nm, red light) staining was performed, 37°C water bath for 30 min. Finally, the slices were packaged with glycerin and observed with an OLYMPUS BX51 fluorescence microscope by the corresponding color filters at 520 and 580 nm, respectively. Rhodamine is red.

2.3. Protein Sample Processing

2.3.1. Serum Protein and Brain Tissue Protein Extraction. After the rats were anesthetized with 1% pentobarbital sodium, blood was taken from the abdominal aorta, and the preserum was left standing. The rats were then sacrificed by cervical dislocation under anesthesia. Then, the brain tissue was taken out and washed with physiological saline, the brain tissue was put in the EP tube, RIPA lysis solution was added, and the brain tissue was cut into pieces with ophthalmological scissors and put it in a glass homogenizer for homogenization. The brain tissue homogenate was placed in a centrifuge at 4°C and centrifuged at 13,000 r/min for 30 minutes, and the precipitate was discarded. The upper liquid was the whole brain tissue protein.

2.3.2. Enzymatic Hydrolysis of Protein. The protein sample was added with TCEP with a final concentration of 5 mmol/L, 37°C water bath for 30 minutes, and allowed to cool in room temperature. IAA with a final concentration of 10 mmol/L was added and kept in a 37°C dark water bath for 30 minutes. The enzyme solution was added to a water bath at a ratio of protein content to trypsin solution of 25 : 1 at 37°C overnight. On the second day, formic acid was added to the digested protein sample, and 0.1% was added to terminate the digestion reaction. The digested product was transferred to a 10 k Da ultrafiltration tube and centrifuged at 4°C at 10,000 r/min for 30 min. The protein in the lower layer of the ultrafiltration tube can be directly analyzed by mass spectrometry.

2.3.3. TMT Labeling and High-Performance Liquid Chromatography (HPLC) Classification. The protein extract was used to remove the high-abundance proteins, and the BCA kit was used to determine the protein concentration. 20 μg of the eluate was taken for SDS-PAGE electrophoresis to detect the removal of high-abundance proteins. Trypsin enzymatically hydrolyze peptides with Strata X C18 (Phenomenex) desalting and freeze-drying in vacuum. The peptide was dissolved with 0.5 M TEAB, and the peptide was labeled according to the TMT kit operating instructions. The peptides were fractionated by high pH reverse HPLC, and the column was Agilent 300Extend C18.

2.3.4. LC-LTQ-MS/MS Analysis and Mass Spectrum Data Retrieval. In mass spectrometry analysis, the peptides were separated using the EASY-nLC 1000 ultra-high performance liquid system, and the Thermo ScientificTM Q ExactiveTM Plus was simultaneously used for detection and analysis. The peptides are separated and ionized and then enter the Q ExactiveTM Plus mass spectrometer for analysis. Peptide precursor ions and their secondary fragments are detected and analyzed by Orbitrap. The secondary mass spectrum data is retrieved by Maxquant (v1.5.2.8), and the mass spectrum quality control is performed at the same time.

2.4. Bioinformatics and Chemical Informatics Analysis. All the proteins retrieved from the database are analyzed, and the proteins whose expression changes are more than 1.3 times (fold change greater than 1.5 for upregulation and less than 0.67 for downregulation) are selected as differential proteins. Pubchem (https://pubchem.ncbi.nlm.nih.gov/) was used to retrieve the molecular structure of edaravone and saved as the "sdf" structure. Then, it was imported into Pharmmapper (http://lilab-ecust.cn/pharmmapper/) for potential target prediction [19]. The GeneCards database (https://www.genecards.org/) [20] and OMIM (https://omim.org/) [21] were used to retrieve genes related to CI and establish disease gene data sets.

The UniProt database is used to correct the names of differential proteins and official gene symbols (Table S1, see supplementary materials). David Ver 6.8 was used for gene ontology (GO) annotation analysis and functional clustering analysis of differential proteins, edaravone potential, and CI genes [22]. The online tool STRING (http://www.string-db.org) was used for protein interaction analysis of differential proteins [23].

2.5. Detection of Oxidative Stress Indicators in Brain Tissue. After the brain tissue was homogenized with physiological saline, the contents of SOD, MDA, GSH, and NO were determined according to the instructions of the kit.

2.6. Detection of Serum AGT and CAT by ELISA. The serum of each group of rats was collected, placed in an anticoagulation tube, shaken, centrifuged (3000 r/min) for 15 min, and the upper serum was collected. Serum AGT and CAT levels were detected by ELISA according to the instructions of the kit. Firstly, the AGT and CAT monoclonal antibodies are coated on the ELISA plate, and the standards and samples are added to make the AGT and CAT bound to the corresponding monoclonal antibodies. Biotinylated anti-rat AGT and CAT antibodies are added to form an immune complex and connect to the plate. Then, streptavidin labeled with horseradish peroxidase is combined with biotin, the enzyme substrate OPD is added, and after the yellow color appears, the stop solution sulfuric acid is added. The sample is detected by the microplate reader at a wavelength of 450 nm in accordance with the ELISA kit procedure. After the blank hole is zeroed, read the optical density (OD) value of each hole.

2.7. Statistical Analysis. The measurement data were expressed as mean ± standard deviation (SD). The neurological function score (mNSS score) of the rats was analyzed by one-way analysis of variance using SPSS software 19.0. $P < 0.05$ was considered to be statistically significant.

3. Results

3.1. Neurological Score and Pathological Changes. The neurological function score of each model group was in the range of 1–3 points, which can indicate to a certain extent that the model is successful. The neurological function scores of the CN group and the CE group were lower than those of the CI group, indicating that the neurological function after drug intervention was better than the cerebral infarction model without drug intervention and to a certain extent that the drug has an intervention effect on CI (Table 1).

Under immunofluorescence, the BrdU signals appeared in the edaravone group, and it was considered that there were newborn nerve cells. The number of positive signals in the edaravone group was higher than that in the model group, indicating that the number of newborn nerve cells increased after drug treatment (Figure 1).

Table 1: Neurological score.

Group	Score ($X \pm S$)	P value
CN	0	—
CI	2.813 ± 0.403	—
CE	2.067 ± 0.799	0.0012

3.2. Proteomics Analysis Results

3.2.1. Differential Expressed Protein. A total of 1,340 proteins were identified in this study, of which 1,138 proteins contained quantitative information. With 1.3 times as the change threshold and t-test P value<0.05 as the standard, then among the quantified proteins, the expression of 90 proteins in the CI/CN comparison group was upregulated, and the expression of 26 proteins was downregulated (Table 2). In the CE/CI comparison group, the expression of 21 proteins was upregulated, and the expression of 41 proteins was downregulated (Table 3). The difference fold value change more than 1.5 times was regarded as a significant increase, and less than 0.77 was regarded as a significant decrease. There are overlapping proteins between CE/CI group and CI/CN group (Figure 2). They were considered to be the adjustable targets of edaravone after CI. The expression matrix of these proteins is shown in Figure 3.

3.2.2. Proteomics Findings Validated by ELISA. Compared with sham operation group, the AGT and CAT in model group were increased ($P < 0.05$). Compared with model group, the AGT and CAT in edaravone group were decreased ($P < 0.05$). This is consistent with the findings of proteomics (Figure 4).

3.2.3. Bioinformatics Analysis. One hundred and fifty-three (153) differentially expressed proteins were introduced into String to construct PPI network (Figure 5) and subjected to enrichment analysis. The enrichment results show that these 153 differentially expressed proteins are related to 12 signaling pathways, 84 biological processes, 41 cell components, and 29 molecular functions. Their fold enrichment, P value and count of each signaling pathway, biological process, cell component, and molecular function are shown in Figure 6. The biological processes is mainly related to response to muscle filament sliding, platelet degranulation, muscle contraction, cellular oxidant detoxification, proteolysis, negative regulation of endopeptidase activity, response to drug, response to zinc ion, response to ethanol, protein refolding, retina homeostasis, response to unfolded protein, cell-cell adhesion, cardiac muscle contraction, response to hydrogen peroxide, skeletal muscle contraction, canonical glycolysis, defense response to fungus, response to selenium ion, and so on. The cell component is related to extracellular exosome, extracellular space, extracellular region, cytosol, extracellular matrix, blood microparticle, focal adhesion, muscle myosin complex, membrane, sarcomere, melanosome, stress fiber, platelet alpha granule lumen, actin filament, cell-cell adherens junction, myosin filament, Z disc, basement membrane, and so on. The molecular function is related to structural constituent of muscle, glycoprotein binding, identical protein binding, antioxidant activity, calcium ion binding, serine-type endopeptidase activity, actin binding, cadherin binding involved in cell-cell adhesion, MHC class II protein complex binding, protein binding, poly(A) RNA binding, unfolded protein binding, virion binding, endopeptidase inhibitor activity, actin filament binding, cytoskeletal protein binding, serine-type endopeptidase inhibitor activity, and so on. The signaling pathway is mainly related to metabolic pathways, biosynthesis of amino acids, glycolysis/gluconeogenesis, arginine biosynthesis, carbon metabolism, and so on (Figure 6). Their details were shown in Table S2.

3.3. Chemoinformatics Analysis Results

3.3.1. Edaravone-CI PPI Network. Edaravone target and CI gene were introduced into String to construct edaravone-CI PPI network. This network is composed of 141 nodes and 1324 edges. The average node degree is 18.8, and the average local clustering coefficient is 0.526 (Figure 7).

3.3.2. Enrichment Analysis Results. The Edaravone target and CI gene were input into David for enrichment analysis and returns 14 CI-related signaling pathways, 63 biological processes, 21 cell components, and 21 molecular function. Their P value, fold enrichment and count of each signaling pathway, biological process, cell component, and molecular function are shown in Figure 8. The biological process is related to blood coagulation, platelet activation, proteolysis, platelet degranulation, fibrinolysis, response to hypoxia, and so on. The cell component is related to extracellular space, extracellular region, platelet alpha granule lumen, cell surface, extracellular matrix, extracellular exosome, and so on. The molecular function is related to serine-type endopeptidase activity, protease binding, protein binding, heparin binding, glycoprotein binding, receptor binding, and so on.

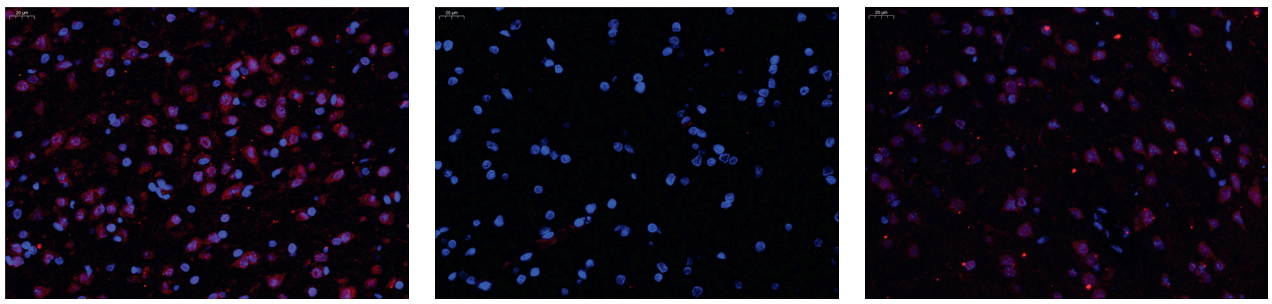

(a) (b) (c)

Figure 1: Pathological changes (400X). (a) Sham operation group. (b) Model group. (c) Edaravone group.

Table 2: Differential expressed protein of CI/CN group.

Protein description	Gene name	CI/CN ratio	Regulated type
Endoplasmin	Hsp90b1	1.395	Up
4-Trimethylaminobutyraldehyde dehydrogenase	Aldh9a1	1.67	Up
Betaine-homocysteine S-methyltransferase 1	Bhmt	4.005	Up
Creatine kinase M-type	Ckm	2.532	Up
Calpastatin	Cast	1.368	Up
Pyruvate kinase	Pkm	1.667	Up
Protein IGHM	IGHM	0.707	Down
COP9 signalosome complex subunit 1	Gps1	1.65	Up
Transgelin	Tagln	1.605	Up
Insulin-like growth factor I	Igf1	0.632	Down
Protein P4ha2	P4ha2	1.457	Up
Polyadenylate-binding protein 1	Pabpc1	1.544	Up
“6-Phosphofructo-2-kinase/fructose-2,6-bisphosphatase 1”	Pfkfb1	1.723	Up
Protein F5	F5	0.692	Down
Protein Myh1	Myh1	2.155	Up
Protein Ugp2	Ugp2	1.635	Up
Protein LOC103691744	LOC103691744	4.174	Up
Protein Myom1	Myom1	1.745	Up
Protein RGD1564614	RGD1564614	0.711	Down
Protein LOC299282	Serpina3n	1.632	Up
Protein S100-A9	S100a9	1.873	Up
Haptoglobin	Hp	1.9	Up
Filamin-C	Flnc	1.991	Up
“Ubiquilin 1, isoform CRA_a”	Ubqln1	1.658	Up
Myl9 protein	Myl9	1.792	Up
Filamin alpha	Flna	1.81	Up
Matrix metalloproteinase 19	Mmp19	0.724	Down
Glycerol kinase	Gk	2.08	Up
Protein papln	Papln	0.734	Down
Calponin	Cnn2	0.714	Down
Protein aldh8a1	Aldh8a1	1.784	Up
Neutrophilic granule protein (predicted)	Ngp	1.729	Up
Protein col14a1	Col14a1	2.295	Up
Protein Atp6v1a	Atp6v1a	1.341	Up
Protein LOC100362751	LOC498555	2.379	Up
Leukocyte cell-derived chemotaxin 2 (predicted)	Lect2	0.739	Down
Protein Rsu1	Rsu1	0.675	Down
“Fructose-1,6-bisphosphatase 1”	Fbp1	1.709	Up
Heat shock 70 kDa protein 4	Hspa4	1.526	Up
Protein Myh1	Myh1	1.987	Up
S-adenosylmethionine synthase	Mat1a	1.787	Up
Protein Igkv8-27	Igkv8-27	0.536	Down
Protein Lama2	Lama2	1.429	Up
Protein Rrbp1	Rrbp1	2.254	Up

Table 2: Continued.

Protein description	Gene name	CI/CN ratio	Regulated type
Protein Lamc1	Lamc1	2.232	Up
"Nitrilase 1, isoform CRA_a"	Nit1	1.789	Up
Protein Myh1	Myh2	2.763	Up
Myomesin 2	Myom2	2.09	Up
"ATPase, H+ transporting, V1 subunit E isoform 1, isoform CRA_a"	Atp6v1e1	1.351	Up
Lamin-B1	Lmnb1	2.227	Up
"Prolactin induced protein, isoform CRA_d"	Pip	2.152	Up
Myosin-7	Myh7	2.873	Up
"Lamin A, isoform CRA_b"	Lmna	2.146	Up
Integrin alpha M	Itgam	1.393	Up
"RCG39455, isoform CRA_a"	Tsku	0.602	Down
Acylamino-acid-releasing enzyme	Apeh	0.65	Down
ATP-citrate synthase	Acly	1.686	Up
Protein Sec24d	Sec24d	1.551	Up
"Protein S (alpha), isoform CRA_b"	Pros1	0.679	Down
40S ribosomal protein S6	Rps6	0.535	Down
Ras-related protein Rab-11B	Rab11b	1.566	Up
Bifunctional purine biosynthesis protein PURH	Atic	1.777	Up
Ribonuclease 4	Rnase4	0.762	Down
Anionic trypsin 1	Prss1	4.631	Up
Angiotensinogen	Agt	1.777	Up
"Myosin light chain 1/3, skeletal muscle isoform"	Myl1	2.052	Up
"Myosin regulatory light chain 2, skeletal muscle isoform"	Mylpf	2.39	Up
Tropomyosin alpha-1 chain	Tpm1	2.41	Up
Catalase	Cat	1.669	Up
Protein disulfide-isomerase	P4hb	1.408	Up
Fructose-bisphosphate aldolase A	Aldoa	1.927	Up
Elongation factor 2	Eef2	1.652	Up
Delta-aminolevulinic acid dehydratase	Alad	1.858	Up
Alcohol dehydrogenase 1	Adh1	2.348	Up
"Carbamoyl-phosphate synthase [ammonia], mitochondrial"	Cps1	4.184	Up
Tropomyosin alpha-4 chain	Tpm4	0.647	Down
"Glycogen phosphorylase, liver form"	Pygl	1.704	Up
Adenosylhomocysteinase	Ahcy	1.729	Up
Galectin-1	Lgals1	0.599	Down
Serotransferrin	Tf	1.471	Up
cAMP-dependent protein kinase type II-beta regulatory subunit	Prkar2b	0.506	Down
Insulin-like growth factor-binding protein 2	Igfbp2	0.661	Down
"Phospholipase A2, membrane associated"	Pla2g2a	0.562	Down
Phosphoglycerate kinase 1	Pgk1	1.581	Up
60S acidic ribosomal protein P0	Rplp0	2.136	Up
Insulin-like growth factor-binding protein 1	Igfbp1	0.56	Down
Cytosolic 10-formyltetrahydrofolate dehydrogenase	Aldh1l1	1.968	Up
Protein S100-A8	S100a8	1.535	Up
Ficolin-2	Fcn2	1.54	Up
Tropomyosin beta chain	Tpm2	3.257	Up
14-3-3 protein epsilon	Ywhae	1.607	Up
Heat shock cognate 71 kDa protein	Hspa8	2.161	Up
"60 kDa heat shock protein, mitochondrial"	Hspd1	1.749	Up
"Actin, alpha cardiac muscle 1"	Actc1	1.579	Up
"Actin, alpha skeletal muscle"	Acta1	3.221	Up
Heat shock protein HSP 90-alpha	Hsp90aa1	1.606	Up
Pleckstrin	Plek	0.638	Down
Interleukin-1 receptor-associated kinase-like 2	Irak2	0.447	Down
Argininosuccinate lyase	Asl	1.607	Up
Aspartyl aminopeptidase	Dnpep	1.473	Up
Tubulin alpha-4A chain	Tuba4a	0.683	Down
Ras-related protein Rap-1b	Rap1b	0.691	Down
Secreted phosphoprotein 24	Spp2	0.521	Down
Nucleobindin-1	Nucb1	1.625	Up

Table 2: Continued.

Protein description	Gene name	CI/CN ratio	Regulated type
Receptor-type tyrosine-protein phosphatase F	Ptprf	1.443	Up
COP9 signalosome complex subunit 4	Cops4	1.441	Up
COP9 signalosome complex subunit 3	Cops3	1.787	Up
Group specific component	Gc	2.016	Up
Carboxypeptidase	Ctsa	1.415	Up
Phenylalanine hydroxylase	Pah	2.261	Up
Nucleotide exchange factor SIL1	Sil1	1.666	Up
Desmin	Des	2.285	Up
Alpha-2 antiplasmin	Serpinf1	1.488	Up
Aflatoxin B1 aldehyde reductase member 2	Akr7a2	1.647	Up
"Tropomyosin 1, alpha, isoform CRA_a"	Tpm1	3.376	Up
Hepcidin	Hamp	1.643	Up
Guanine deaminase	Gda	1.566	Up
Peroxiredoxin-4	Prdx4	1.601	Up

Table 3: Differential expressed protein of CE/CI group.

Protein description	Gene name	CE/CI ratio	Regulated type
4-Trimethylaminobutyraldehyde dehydrogenase	Aldh9a1	0.739	Down
Betaine-homocysteine S-methyltransferase 1	Bhmt	0.42	Down
Creatine kinase M-type	Ckm	0.637	Down
Galectin	Lgals3	1.564	Up
Thyroglobulin	Tg	2.708	Up
"6-Phosphofructo-2-kinase/fructose-2,6-bisphosphatase 1"	Pfkfb1	0.62	Down
Complement factor I	Cfi	0.574	Down
Protein TNC	TNC	1.606	Up
Peptidyl-prolyl cis-trans isomerase	Ppia	0.729	Down
Protein F11	F11	1.337	Up
Protein LOC103691744	LOC103691744	0.204	Down
Protein RGD1310507	RGD1310507	0.697	Down
Histidine-rich glycoprotein	Hrg	5.24	Up
Coagulation factor XII	F12	0.669	Down
LOC683667 protein	Sri	1.321	Up
Glycerol kinase	Gk	0.537	Down
Protein Fat4	Fat4	1.45	Up
Carboxylic ester hydrolase	Ces1c	0.421	Down
RCG21066	rCG_21066	0.686	Down
Protein IGHM	IGHM	1.411	Up
"Sushi, Von Willebrand factor type A, EGF and pentraxin domain-containing protein 1"	Svep1	1.454	Up
"Procollagen, type XVIII, alpha 1, isoform CRA_a"	Col18a1	1.499	Up
Serine protease inhibitor A3M	Serpina3m	0.616	Down
"Fructose-1,6-bisphosphatase 1"	Fbp1	0.602	Down
Serine protease hepsin	Hpn	1.413	Up
S-adenosylmethionine synthase	Mat1a	0.521	Down
"Troponin I, fast skeletal muscle"	Tnni2	0.722	Down
"Fibulin 2, isoform CRA_a"	Fbln2	1.354	Up
Apolipoprotein C-II (predicted)	Apoc2	2.066	Up
Heat shock 27 kDa protein 1	Hspb1	1.671	Up
"Protein S (alpha), isoform CRA_b"	Pros1	1.448	Up
Protein LOC691828	LOC691828	0.718	Down
Glutathione peroxidase	Gpx1	0.399	Down
40S ribosomal protein S6	Rps6	2.075	Up
Peroxiredoxin-6	Prdx6	0.582	Down
Lysozyme C-1	Lyz1	0.675	Down
Anionic trypsin 1	Prss1	0.272	Down
Angiotensinogen	Agt	0.687	Down
Serum albumin	Alb	0.67	Down
Catalase	Cat	0.658	Down

Table 3: Continued.

Protein description	Gene name	CE/CI ratio	Regulated type
Alcohol dehydrogenase 1	Adh1	0.442	Down
Beta-2-microglobulin	B2m	0.656	Down
"Carbamoyl-phosphate synthase [ammonia], mitochondrial"	Cps1	0.297	Down
Galectin-1	Lgals1	1.658	Up
Cysteine-rich secretory protein 1	Crisp1	0.439	Down
Serotransferrin	Tf	0.471	Down
Cystatin-C	Cst3	0.625	Down
Carbonic anhydrase 2	Ca2	0.533	Down
Cytosolic 10-formyltetrahydrofolate dehydrogenase	Aldh1l1	0.599	Down
C-reactive protein	Crp	1.454	Up
Cadherin-17	Cdh17	1.512	Up
Ficolin-2	Fcn2	0.724	Down
Interleukin-1 receptor-associated kinase-like 2	Irak2	0.556	Down
Argininosuccinate lyase	Asl	0.707	Down
Apolipoprotein H	Apoh	0.644	Down
Protein Serpina4	Serpina4	0.727	Down
Protein Hbb-b1	LOC103694855	0.507	Down
Secreted phosphoprotein 24	Spp2	1.849	Up
BPI fold-containing family a member 2	Bpifa2	0.46	Down
Phenylalanine hydroxylase	Pah	0.491	Down
Cathepsin D	Ctsd	1.466	Up
Alpha-2 antiplasmin	Serpinf1	0.713	Down

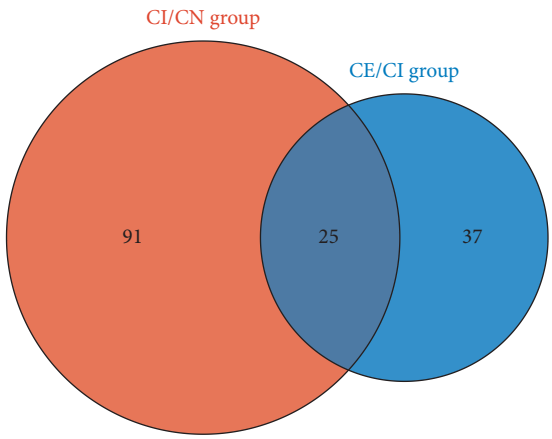

Figure 2: Venn diagram of CE/CI group and CI/CN group.

The signaling pathway is related to complement and coagulation cascades, platelet activation, TNF signaling pathway, insulin resistance, HIF-1 signaling pathway, FoxO signaling pathway, and so on (Figure 8). Their details were shown in Table S3.

3.4. Expression of Differentially Expressed Proteins in Brain Tissue. The expression of DEPs in each organ in each comparison group was analyzed, and the obtained DEPs were analyzed by Expression Atlas. After the tissue specificity is set to "brain," the protein with the number 10 in descending order or the protein with number ≧10 is matched. The brain tissue specificity of these proteins is ranked according to their expression strength in brain tissue and other tissues, and the detailed information is listed in Tables 4 and 5.

Different proteins with upregulated expression and high brain specificity in the CI/CE comparison group are cathepsin D, LOC683667 protein, galectin-1, C-reactive protein, and 40S ribosomal protein S6.

Different proteins with downregulated expression and high brain specificity in the CI/CN comparison group are cystatin-C, serotransferrin, peptidyl-prolyl cis-trans isomerase, beta-2-microglobulin, carbonic anhydrase2, angiotensinogen, peroxiredoxin-6, glutathione peroxidase, 4-trimethylaminobutyraldehyde dehydrogenase, and catalase.

3.5. Oxidative Stress Indicators in Brain Tissue. Compared with the sham operation group, the MDA content of the model group was significantly increased, while the SOD and GSH content were significantly decreased ($P < 0.05$), indicating that the model was successful. Compared with the model group, the MDA content of the edaravone administration group significantly decreased, and the SOD and GSH content significantly increased ($P < 0.05$), indicating that edaravone can improve the brain SOD, MDA, and GSH content of rats (Figure 9).

4. Discussion

CI is a cerebrovascular disease characterized by brain blood supply disorder, local avascular necrosis, or softening of brain tissue caused by ischemia and hypoxia. Among them, neuronal programmed death (apoptosis, autophagy, iron death, scorch death, etc.) and necrosis exist simultaneously. The main pathological mechanisms include energy exhaustion, excitotoxicity, oxidative stress, endoplasmic reticulum dysfunction, and a large amount of immune cell infiltration and aggregation. Various cytokines are involved in a series of "cascade-like" cascade events, such as

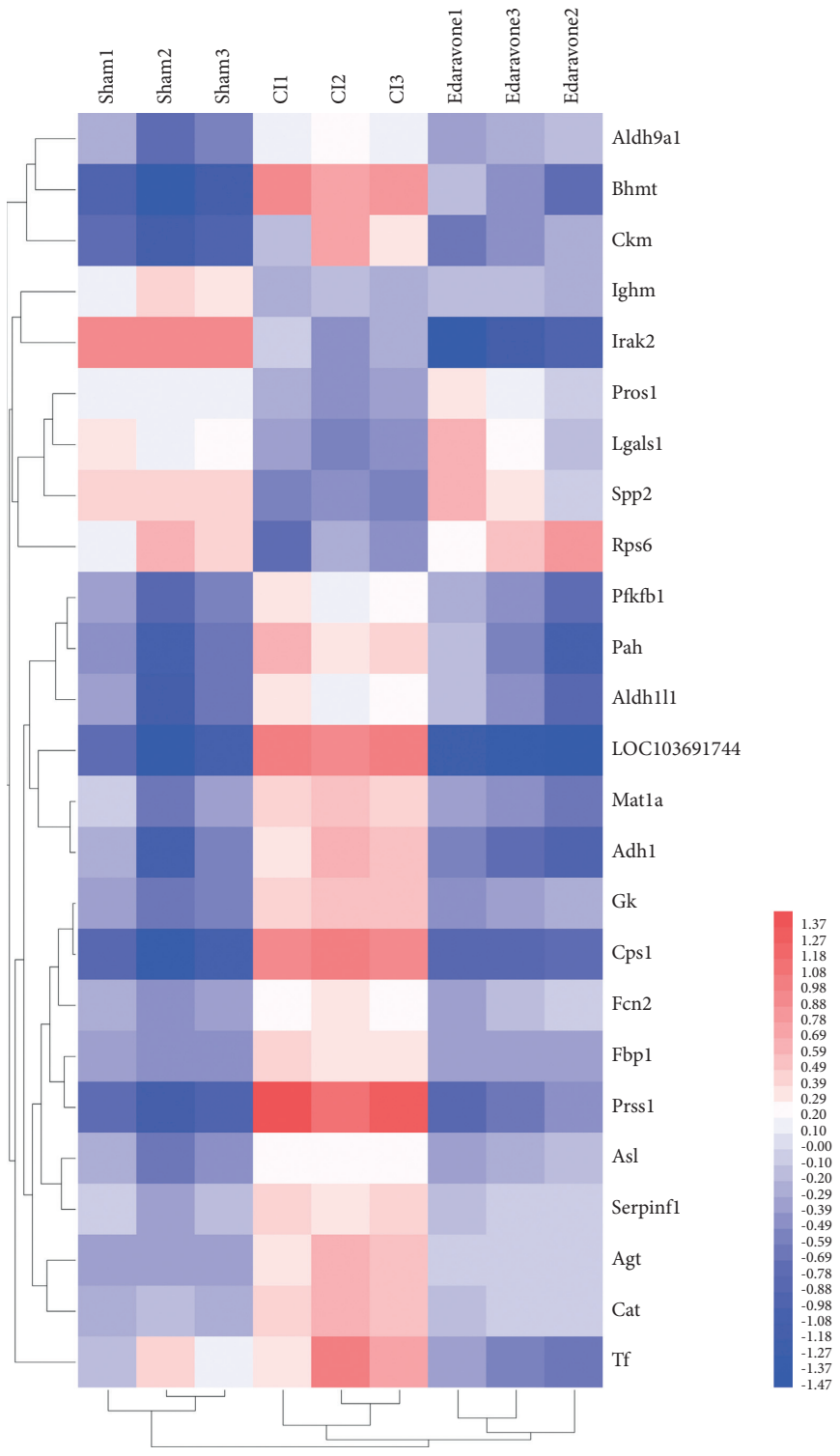

Figure 3: The expression matrix the 26 proteins.

neuroinflammation in the infarct area, which ultimately leads to the death of nerve cells. The damage caused by free radicals induced by oxidative stress is considered to be an important pathological basis for brain neuron damage in the onset of stroke. The chain reaction of free radicals causes excessive oxidation of cell membrane lipids and nuclear proteins and damages the structure and function of mitochondria, resulting in insufficient cell energy production, leading to cell death or apoptosis. Therefore, antioxidative stress response and scavenging excess free radicals may be important strategies for early CI to protect neurons and reduce damage.

Edaravone, as a free radical scavenger, has the effects of antioxidative stress and inhibiting lipid peroxidation.

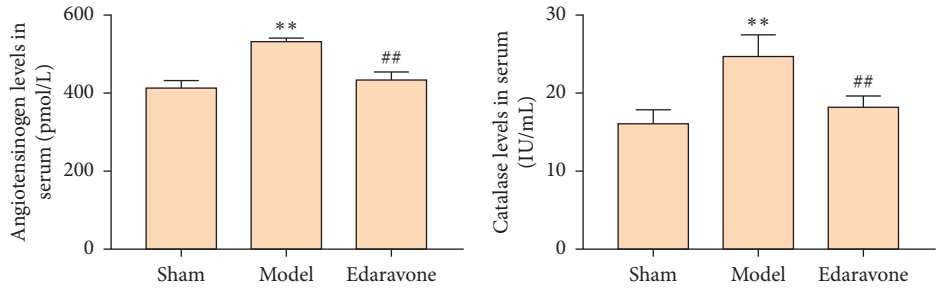

Figure 4: Serum AGT and CAT level (**compared with sham operation group, $P < 0.05$; ##compared with model group, $P < 0.05$).

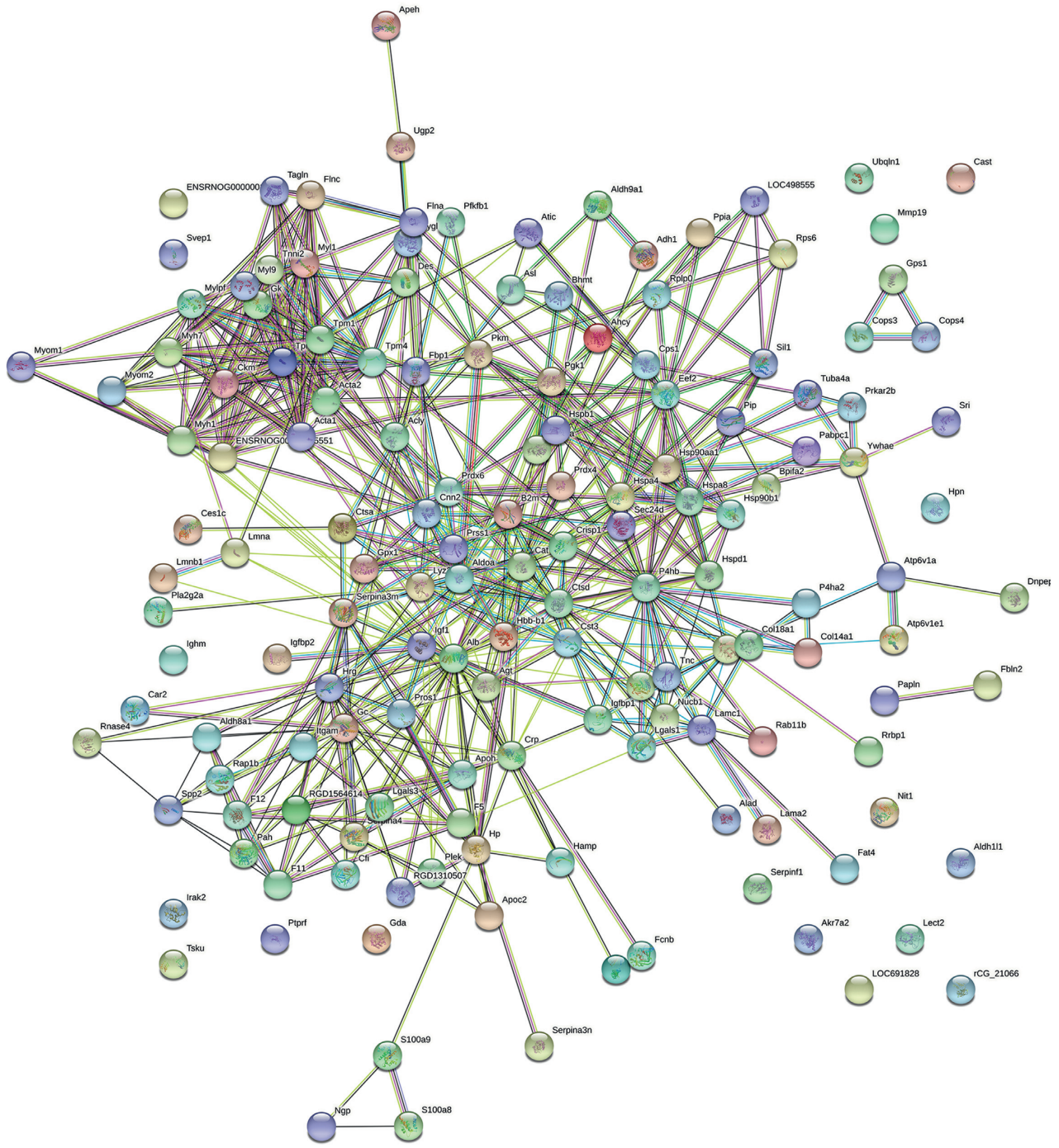

Figure 5: The PPI network of differentially expressed proteins.

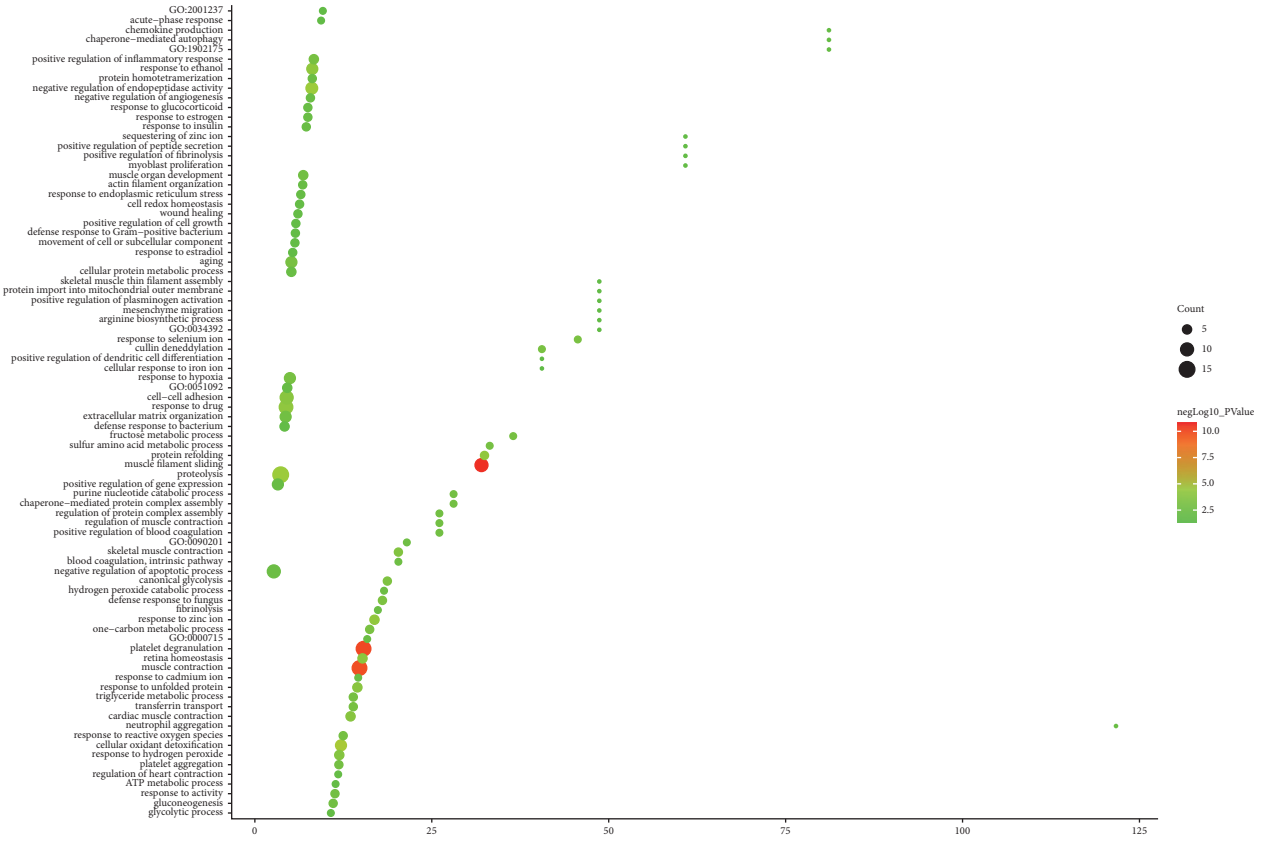

(a)

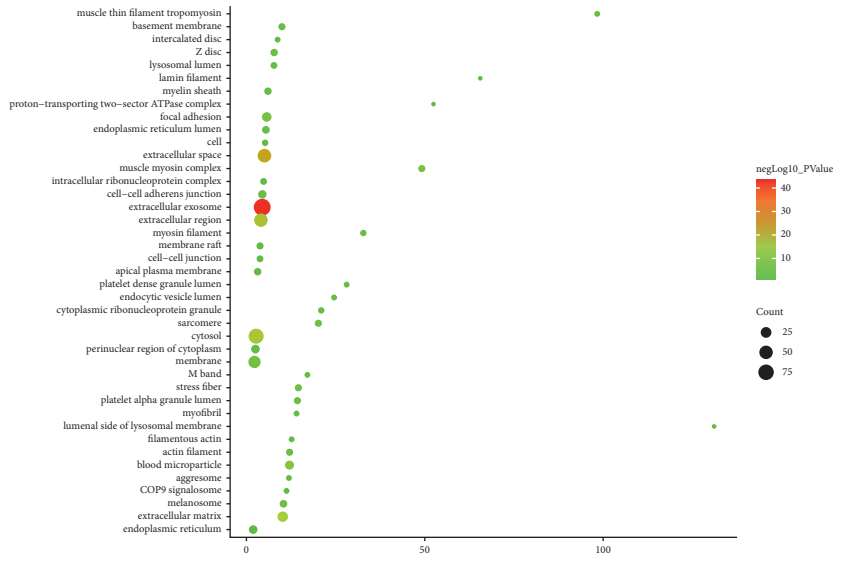

(b)

Figure 6: Continued.

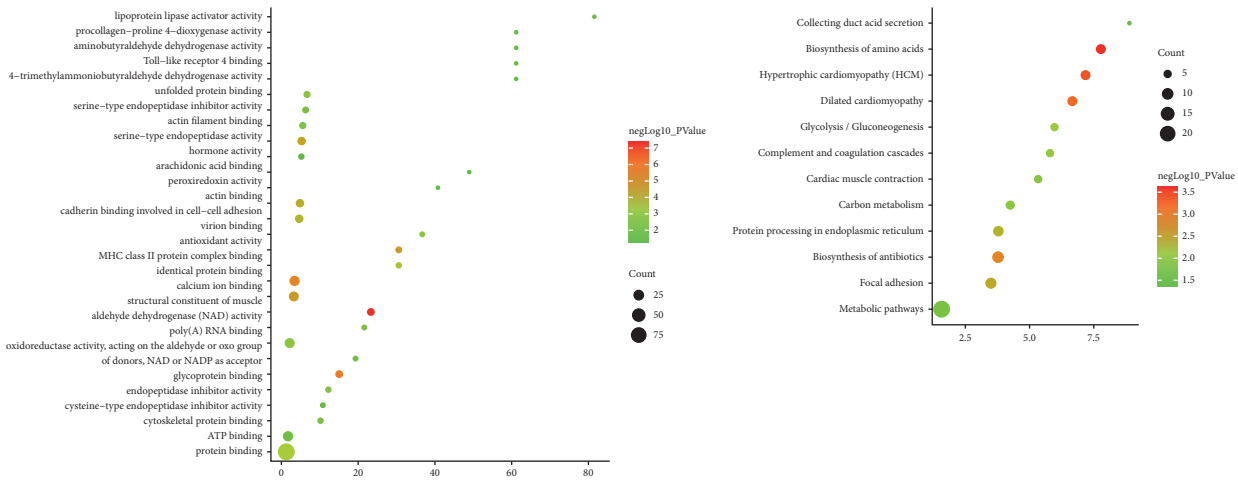

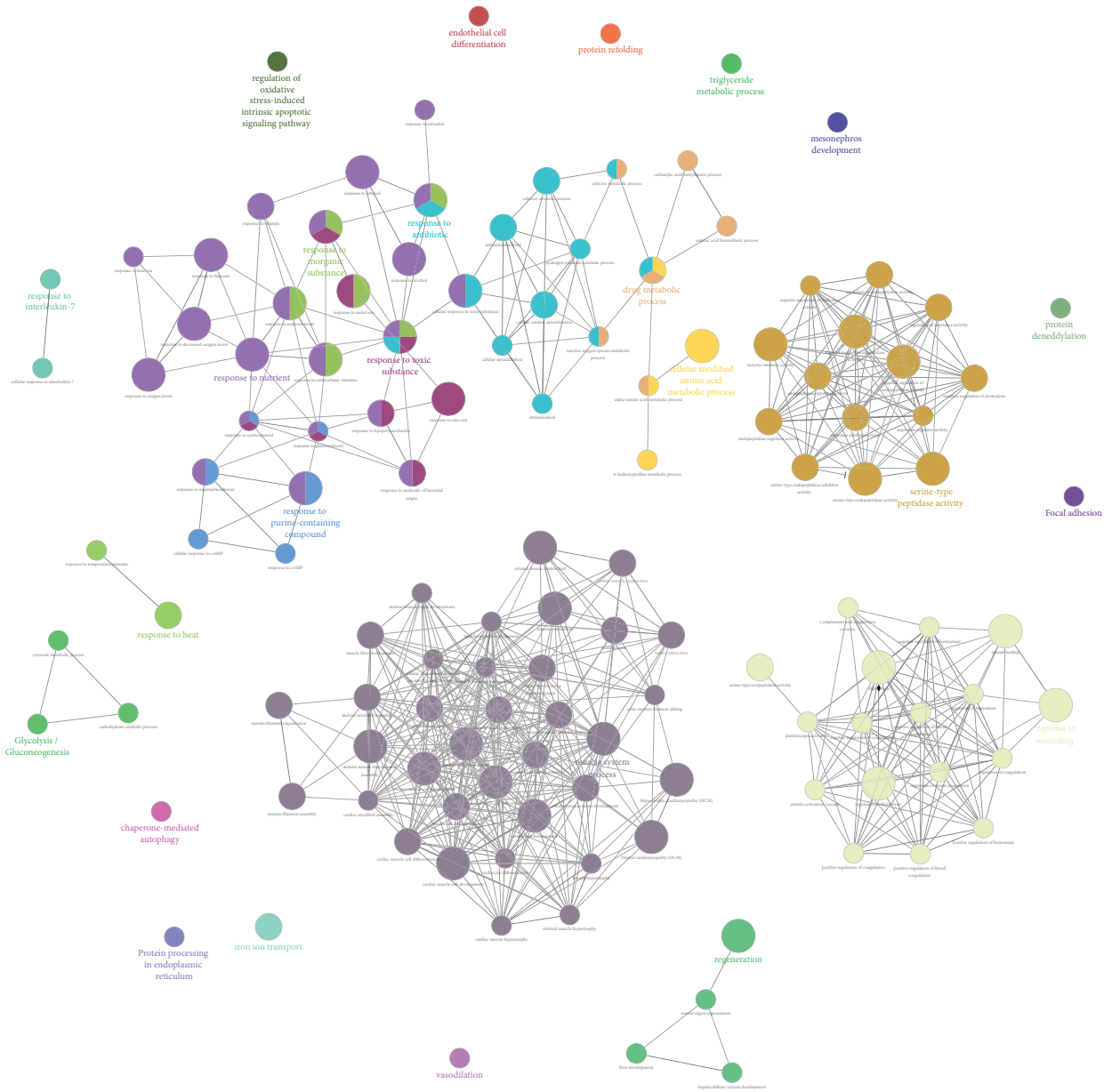

(e)

Figure 6: Continued.

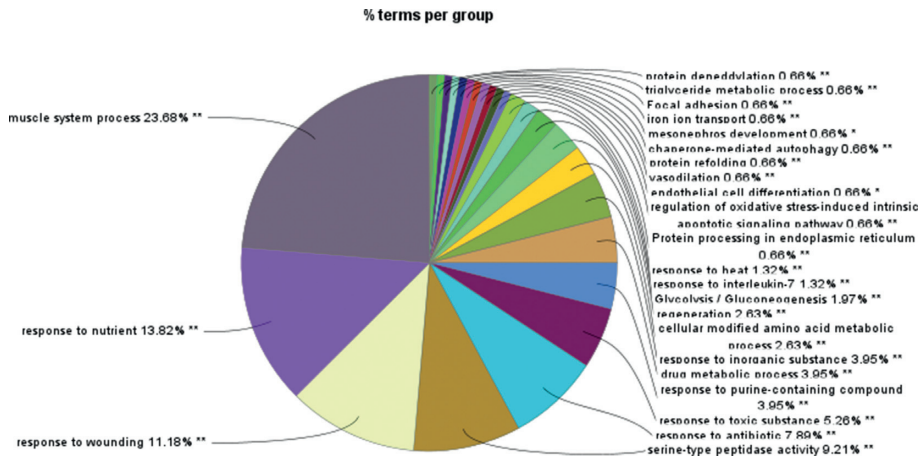

(f)

FIGURE 6: The results of enrichment analysis (a: biological processes; b: cell components; c molecular function; d signaling pathways; *X*-axis stands for fold enrichment. e and f Cluego analysis).

Studies have confirmed that edaravone can protect body tissues by inhibiting the activity of cyclooxygenase (COX, including COX-1, and COX-2). COX-2 is mainly expressed in hippocampal tissue and cortical neurons and can mediate neuronal damage. COX-2 is a key enzyme and rate-limiting enzyme produced by prostaglandin E2 (PGE2) metabolism, and it can also promote the production of nitric oxide (NO), while PGE2 and NO can participate in various pathological processes, such as inflammation, oxidative stress, and apoptosis. Current clinical and basic research shows that edaravone, which has an antioxidant effect, may become a new type of drug for the treatment of CI. This study established the CI rat model and used serum proteomics to determine the serum markers for edaravone to interfere with CI. 153 differentially expressed proteins include Rps6, Spp2, Lgals1, Pros1, Aldh9a1, Fcn2, Serpinf1, Asl, Agt, Cat, Ckm, Pfkfb1, Fbp1, Aldh1l1, Irak2, Gk, Mat1a, Pah, Tf, Adh1, Bhmt, Cps1, Prss1, LOC103691744, Tpm1, and Myh1. Recent studies have shown that ribosomal protein S6 (rpS6), extracellular signal-regulated mitogen-activated protein (MAP) kinase p44/42 (p44/42MAPK), and ribosomal protein S6 kinase (S6K) are significantly reduced in the brains of hibernating squirrels and rats. Therefore, we believe that the downregulation of rpS6 signal transduction may be an important reason for the increased cell tolerance to cerebral ischemia observed during hibernation numbness and after ischemic preconditioning, by inhibiting protein synthesis and/or energy expenditure [24]. Qu et al. showed that galectin-1 (Gal-1) can regulate the proliferation of a variety of cells and play an important role after nervous system injury. Galectin-1 can reduce astrocyte damage and improve the recovery of rats with focal cerebral ischemia [25]. Ishibashi S. et al. also found that galectin-1 regulates neurogenesis in the subventricular zone and promotes functional recovery after stroke [26]. Agt is the gene encoding angiotensinogen, and current studies have shown that its polymorphism is closely related to stroke, especially cerebral small vessel disease [27–29]. Current research shows that Catalase (CAT) has important physiological functions in oxidative stress. CAT can quickly remove the toxic substances produced by cell metabolism, so as to protect sulfhydrylase and membrane protein and detoxify together with glutathione peroxidase (GSHPx). It plays an important protective role against cerebral ischemia in CI patients [30, 31]. Aldh1l1 is mainly related to the proliferation of astrocytes after CI [32]. Interleukin-1 receptor-associated kinases (IRAKs) are mainly related to inflammation and cell apoptosis after cerebral ischemia and reperfusion [33].

The enrichment analysis of these 153 differentially expressed proteins involved a total of 12 signal pathways, 84 biological processes, 41 cell components, and 29 molecular functions. The biological process is mainly in platelet activation and aggregation (GO:0002576~platelet degranulation, GO:0070527~platelet aggregation), oxidative stress (GO:0098869~cellular oxidant detoxification; GO:0006986~response to unfolded protein; GO:0042542~response to hydrogen peroxide; GO:0000302~response to reactive oxygen species; GO:0090201~negative regulation of release of cytochrome c from mitochondria; GO:0042744~hydrogen peroxide catabolic process; GO:0045454~cell redox homeostasis), intercellular adhesion (GO:0098609~cell-cell adhesion), glycolysis and gluconeogenesis (GO:0061621~canonical glycolysis; GO:0006094~gluconeogenesis), iron metabolism (GO:0033572~transferrin transport; GO:0071281~cellular response to iron ion), hypoxia (GO:0001666~response to hypoxia), inflammatory chemokines and their mediated signal transduction (GO:0050729~positive regulation of inflammatory response; GO:0051092~positive regulation of NF-kappaB transcription factor activity; GO:0032602~chemokine production) reaction, coagulation (GO:0030194~positive regulation of blood coagulation; GO:0007597~blood coagulation, intrinsic pathway), apoptosis (GO:0043066~negative regulation of apoptotic process; GO:1902175~ regulation of oxidative stress-induced intrinsic apoptotic signaling pathway), fibrinolysis system (GO:

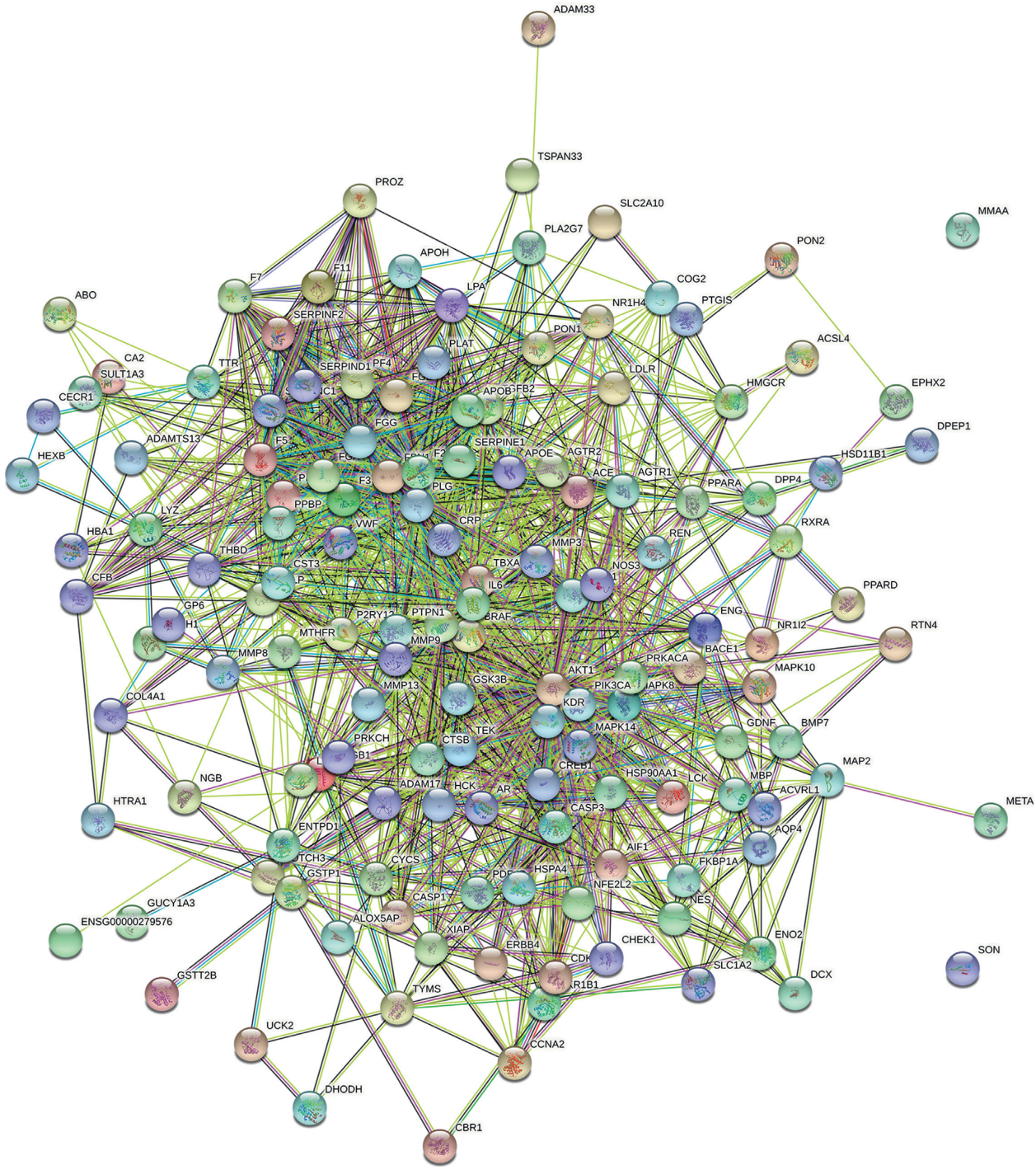

Figure 7: Edaravone-CI PPI network.

0042730~fibrinolysis; GO:0051919~positive regulation of fibrinolysis); angiogenesis (GO:0016525~negative regulation of angiogenesis) endoplasmic reticulum stress (GO: 0034976~response to endoplasmic reticulum stress), and energy metabolism (GO:0046034~ATP metabolic process; GO:0045040~protein import into mitochondrial outer membrane). These biological modules play an important role in the acute pathological process of cerebral infarction.

The molecular functions also focused on oxidative stress (GO:0016209~antioxidant activity; GO:0004029~aldehyde dehydrogenase (NAD) activity; GO: 0016620~oxidoreductase activity, acting on the aldehyde or oxo group of donors, NAD or NADP as acceptor), calcium ion binding (GO:0005509~calcium ion binding; GO: 0098641~cadherin binding involved in cell-cell adhesion), energy metabolism (GO:0005524~ATP binding),

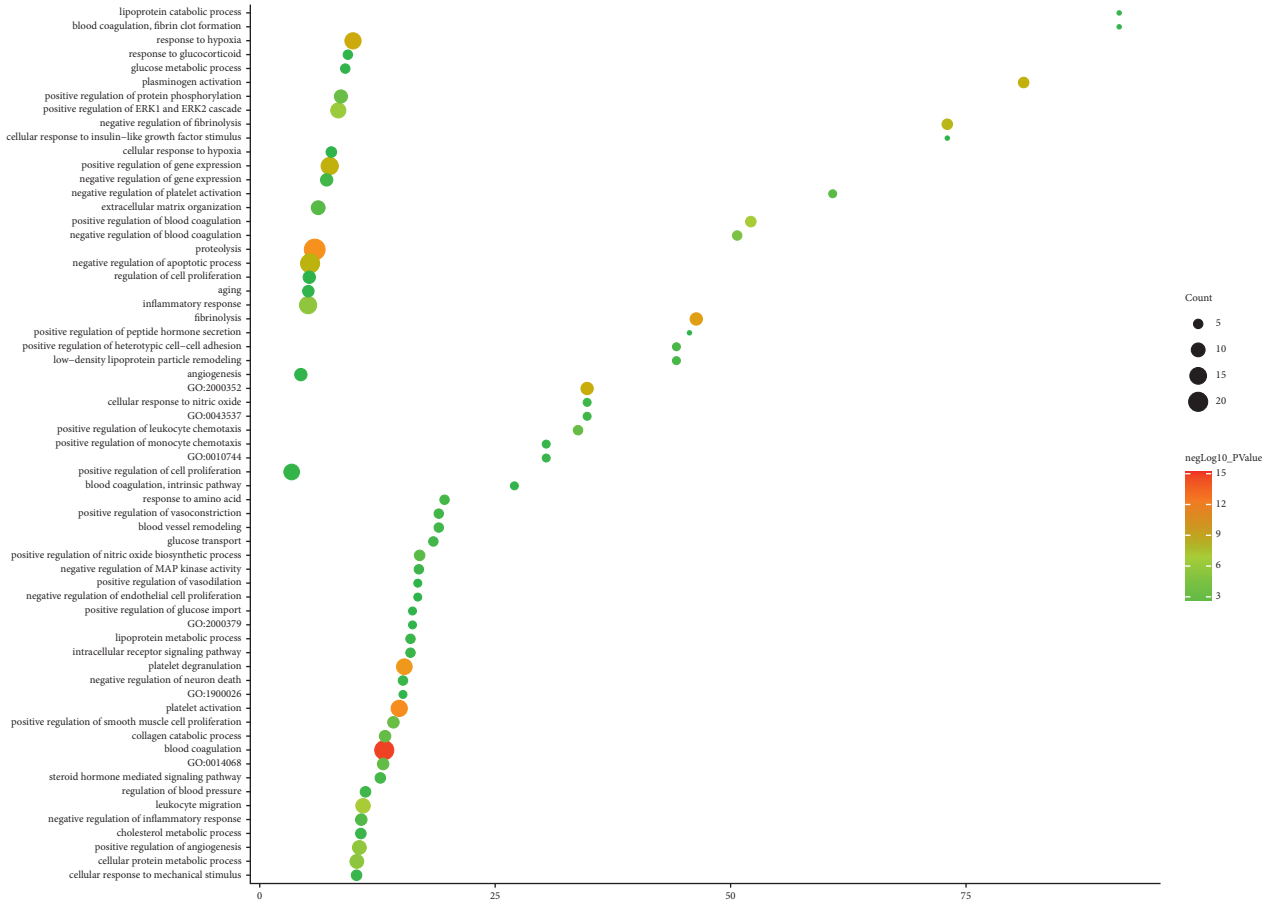

(a)

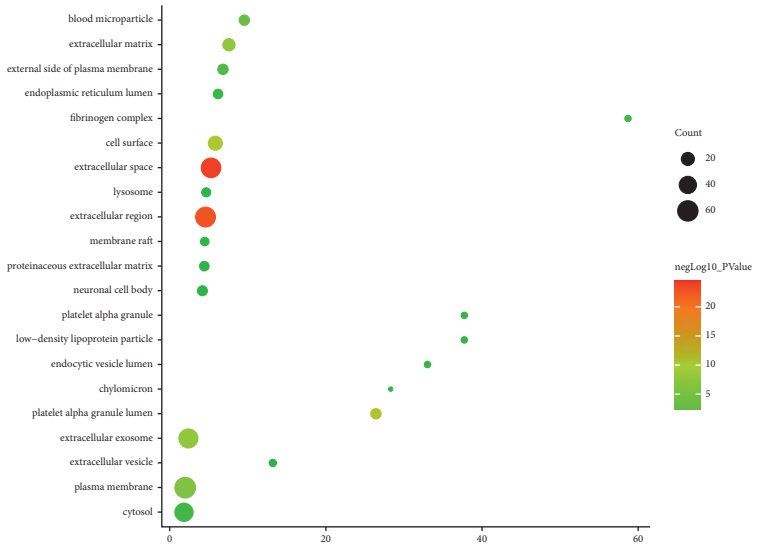

(b)

Figure 8: Continued.

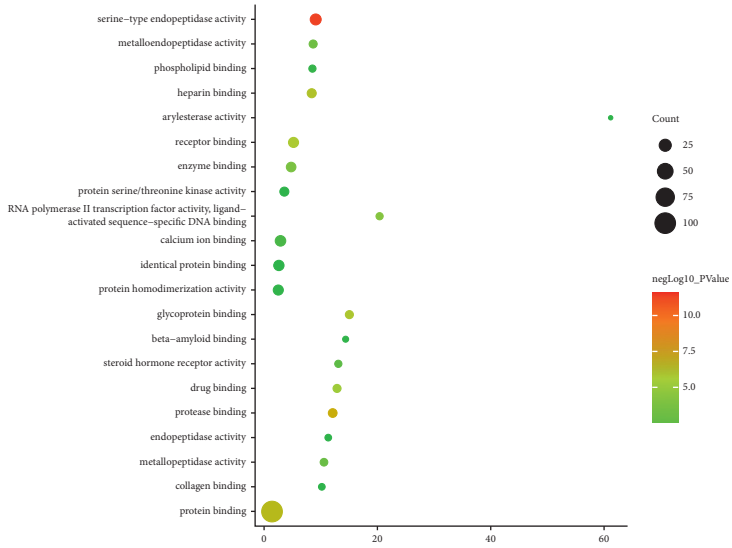

(c)

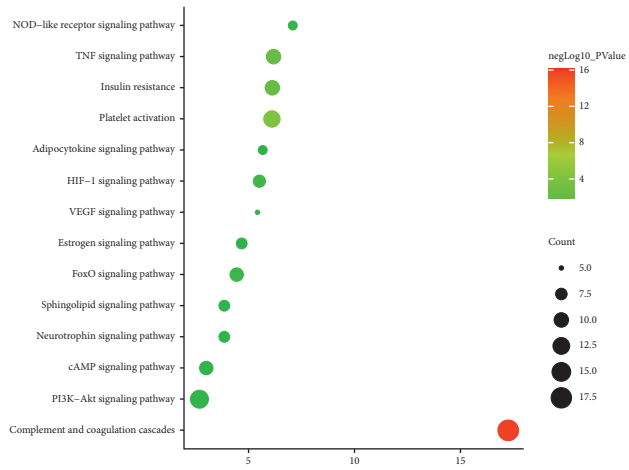

(d)

Figure 8: Continued.

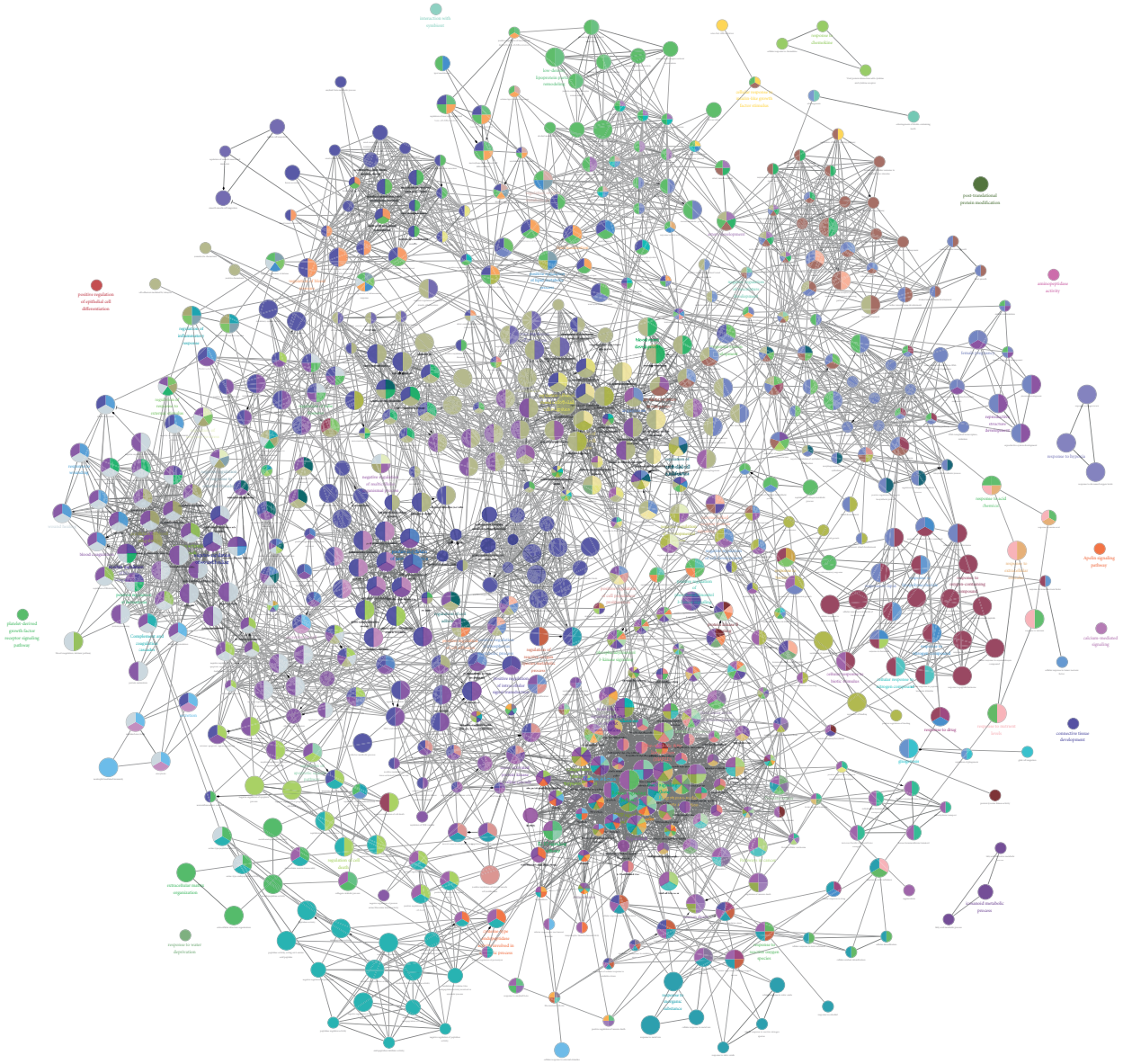

(e)

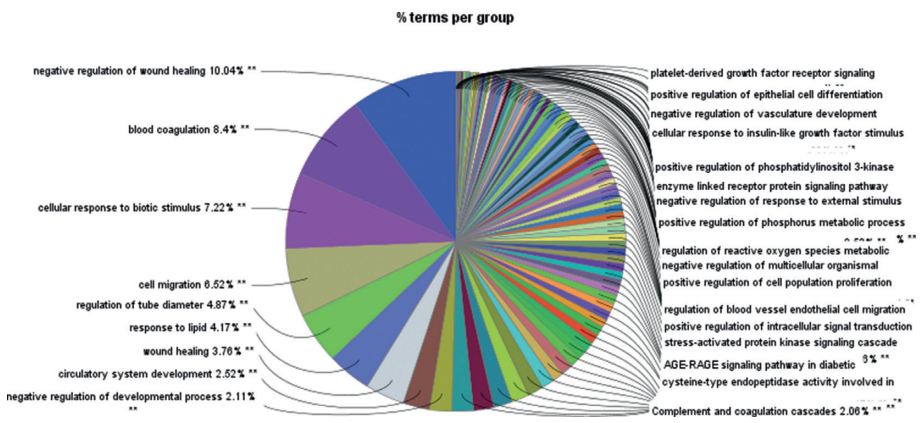

(f)

Figure 8: The results of enrichment analysis (a: biological processes; b: cell components; c: molecular function; d: signaling pathways; *X*-axis stands for fold enrichment. e and f: Cluego analysis).

Table 4: DEPs with higher expression in brain tissue in the CI/CE operation comparison group.

Gene name	Adrenal gland	Brain	Gastrocnemius	Heart	Kidney	Liver	Lung	Spleen	Testis	Thymus
Ctsd	297	167	154	126	258	125	651	195	35	182
Sri	28	45	11	16	68	13	100	146	144	85
Lgals1	311	37	254	156	42	6	274	79	65	161
Crp	20	27	9	8	15	1447	27	19	21	24
Rps6	30	24	18	18	22	24	50	145	29	98

Table 5: DEPs with higher expression in brain tissue in the CI/CN comparison group.

Gene name	Adrenal gland	Brain	Gastrocnemius	Heart	Kidney	Liver	Lung	Spleen	Testis	Thymus
Cst3	279	1558	273	279	240	112	722	495	381	638
Tf	42	447	41	24	43	18878	109	126	127	41
Ppia	183	308	37	54	217	181	207	269	236	413
B2m	685	186	166	558	507	1168	1661	1926	156	1003
Car2	27	183	12	11	250	6	101	293	40	12
Agt	47	96	2	2	13	372	31	6	0.7	51
Prdx6	108	68	28	59	103	79	292	41	46	54
Gpx1	347	52	160	330	635	1326	375	669	27	189
Aldh9a1	62	21	28	30	151	258	46	33	29	41
Cat	146	21	48	46	379	1270	113	81	8	56

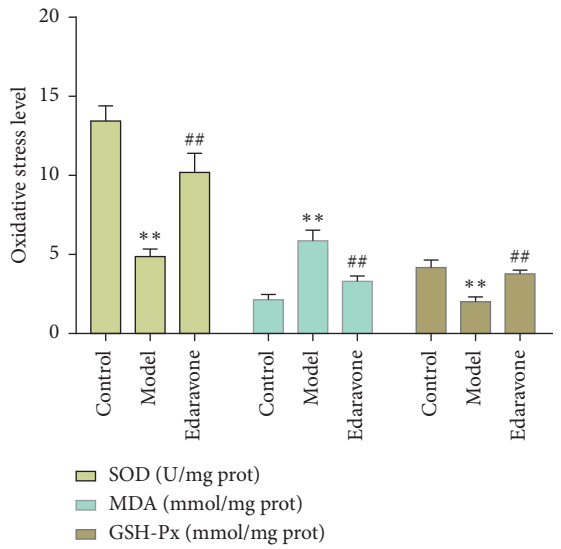

Figure 9: Oxidative stress indicators in brain tissue (**compared with sham operation group, $P < 0.05$; ##compared with model group, $P < 0.05$).

inflammation (GO:0050544~arachidonic acid binding), and other molecular functions. The cellular components focus on exosomes (GO:0070062~extracellular exosome), extracellular space (GO:0005615~extracellular space.; GO: 0031012~extracellular matrix), blood particles (GO: 0072562~blood microparticle), intercellular adhesion (GO: 0005925~focal adhesion; 5913~cell-cell adherens junction), platelet (GO:0031093~platelet alpha granule lumen; GO: 0031089~platelet dense granule lumen), endoplasmic reticulum cavity (GO:0005788), and myelin sheath (GO:0043209).

Oxidative stress is considered to be an important factor leading to cell damage in acute stroke events. During the period of cerebral ischemia and perfusion, especially the reperfusion period, a large number of free radicals are produced, which attack the lipids and proteins of cell membranes [34, 35]. In recent years, studies have found that in addition to directly attacking cell membranes and causing cell oxidative damage, free radicals can also participate in the process of neuronal damage by initiating apoptosis pathways. The free radicals produced after cerebral ischemia can act on mitochondria and change the permeability of mitochondrial pores. The depolarization of the mitochondrial membrane leads to the release of cytochrome c from mitochondria into the cytoplasm, which activates the caspase family to cause

DNA damage and lead to apoptosis [36, 37]. In addition, the reactive oxygen species produced by oxidative stress can also regulate the activity of nuclear transcription factor NF-kB and affect the downstream genes of NF-kB, including iNOs, COX-2, intercellular adhesion molecules, and cytokines [38–41]. They mediate the destruction of blood-brain barrier function and inflammation and play an important role in the signal transduction of apoptosis [42–44]. Therefore, after cerebral infarction and its reperfusion, the overproduction and burst of free radicals play a key role in the programmed death of neurons. Edaravone is an effective antioxidant, which can inhibit the oxidation of NO and increase the production of NO by increasing the expression of eNOS and inhibit the formation of peroxygen during reperfusion to improve or protect vascular blood flow [45]. According to recent reports, in MCAO model mice, edaravone administered within 6 hours of reperfusion can reduce infarct volume and improve neurological deficits. In the early stage of ischemic events, edaravone can inhibit the accumulation of 4-hydroxy-2-nonenal (HNE) modified protein and 8-hydroxydeoxyguanosine (8-OHdG) in the ischemic penumbra. In the later period, it reduces the activation of microglia, the expression of iNOS, and the formation of astrocytes peroxygen [46]. Jiao et al. found that edaravone can reduce the delayed neuronal death of the hippocampus after middle cerebral artery ischemia reperfusion, and its mechanism may be related to scavenging free radicals, resisting inflammation, and inhibiting the activation of astrocytes [47]. In terms of cerebral hemorrhage, edaravone may inhibit the activation of M1 type microglia and the accumulation of proinflammatory factors through the IRE1α/TRAF2 signaling pathway after ER stress, reduce the edema and apoptosis of nerve cells after cerebral hemorrhage in mice, reduce the damage of white matter fiber bundles, and then protect nerve function [48]. In terms of the proliferation and differentiation of neural stem cells, edaravone can promote the proliferation of endogenous neural stem cells and astrocytes in the subventricular area of the ischemic injury side and the cerebral cortex around ischemia and promote the differentiation of endogenous neural stem cells into neurons [49]. Further studies have shown that edaravone promotes neuronal proliferation in acute stroke rats through the Wnt/β-catenin signaling pathway and improves the neurological and cognitive functions of acute stroke rats [50]. In terms of iron metabolism, the effect of edaravone in repairing spinal cord injury in rats is achieved by regulating the xCT/GPX4/ACSL4/5-LOX iron death pathway and rebalancing the homeostasis of lipid oxidation. Further studies have shown that edaravone reduces 5-LOX metabolites to inhibit neuroinflammation, promote neuronal survival after spinal cord injury, and prevent iron death in neuronal cell lines [51]. Compared with previous studies, this study revealed the serum protein profile of edaravone in the treatment of cerebral infarction rats through serum TMT proteomics and discovered the relevant mechanism of edaravone regulating iron metabolism in cerebral infarction, which provides new ideas for the study of edaravone intervention in cerebral infarction and also provides reference information for future research on the mechanism of edaravone intervention in iron metabolism-related diseases.

5. Conclusion

The therapeutic mechanism of edaravone in the treatment of CI may involve platelet activation and aggregation, oxidative stress, intercellular adhesion, glycolysis and gluconeogenesis, iron metabolism, hypoxia, and so on. This study provides new reference for the clinical application of edaravone for CI.

Data Availability

The data that support the findings of this study are openly available in supplementary materials.

Conflicts of Interest

The authors declare no conflicts of interest.

Authors' Contributions

Guozuo Wang, Xiaomei Zeng, Shengqiang Gong, Shanshan Wang, Anqi Ge, Wenlong Liu, and Jinwen Ge are responsible for the study concept and design. Guozuo Wang, Xiaomei Zeng, Qi He, Shengqiang Gong, Shanshan Wang, Anqi Ge, Wenlong Liu, and Jinwen are responsible for the data collection, data analysis, and interpretation of network analysis; Guozuo Wang and Shengqiang Gong are responsible for the data collection, data analysis, and interpretation of experiments. Guozuo Wang drafted the paper; Jinwen Ge supervised the study; all the authors participated in the analysis and interpretation of data and approved the final paper. Guozuo Wang and Xiaomei Zeng should be considered joint first authors.

Acknowledgments

This work was supported by the National Natural Science Foundation of China (no. 81274008), the Key Project of Scientific Research Fund of Hunan Provincial Education Department (no. 19A378), the National Natural Science Foundation of Hunan Province, China (no. 2020JJ4467), and the National Key Research and Development Project of China (no. 2018YFC1704904).

Supplementary Materials

Table S1: edaravone potential targets and CI genes. Table S2: enrichment analysis results of proteomics. Table S3: enrichment analysis results of edaravone-CI PPI network (*Supplementary Materials*)

References

[1] H. Amani, E. Mostafavi, M. R. Alebouyeh et al., "Would colloidal gold nanocarriers present an effective diagnosis or treatment for ischemic stroke?" *International Journal of Nanomedicine*, vol. 14, pp. 8013–8031, 2019.

[2] R. A. Grysiewicz, K. Thomas, and D. K. Pandey, "Epidemiology of ischemic and hemorrhagic stroke: incidence, prevalence, mortality, and risk factors," *Neurologic Clinics*, vol. 26, no. 4, pp. 871–895, 2008.

[3] W. Wang, B. Jiang, H. Sun et al., "Prevalence, incidence, and mortality of stroke in China," *Circulation*, vol. 135, no. 8, pp. 759–771, 2017.

[4] S. Hu, R. Gao, L. Liu et al., "Summary of "Chinese cardiovascular disease report 2018," *Chinese Journal of Circulation*, vol. 34, no. 3, pp. 209–220, 2019, in chinese.

[5] L. Wang, J. Wang, B. Peng, and Y. Xu, "Summary of "China stroke prevention and treatment report 2016"," *Chinese Journal of Cerebrovascular Disease*, vol. 14, no. 04, pp. 217–224, 2017, in chinese.

[6] L. Sun, R. Clarke, R. Clarke et al., "Causal associations of blood lipids with risk of ischemic stroke and intracerebral hemorrhage in Chinese adults," *Nature Medicine*, vol. 25, no. 4, pp. 569–574, 2019.

[7] R. Rodrigo, R. Fernandez-Gajardo, R. Gutierrez et al., "Oxidative stress and pathophysiology of ischemic stroke: novel therapeutic opportunities," *CNS & Neurological Disorder-Drug Targets*, vol. 12, no. 5, pp. 698–714, 2013.

[8] Y.-C. Cheng, J.-M. Sheen, W. L. Hu, and Y.-C. Hung, "Polyphenols and oxidative stress in atherosclerosis-related ischemic heart disease and stroke," *Oxidative Medicine and Cellular Longevity*, vol. 2017, Article ID 8526438, 16 pages, 2017.

[9] S. Orellana-Urzúa, I. Rojas, L. Líbano, and R. Rodrigo, "Pathophysiology of ischemic stroke: role of oxidative stress," *Current Pharmaceutical Design*, vol. 26, no. 34, pp. 4246–4260, 2020.

[10] S. Lorenzano, N. S. Rost, M. Khan et al., "Early molecular oxidative stress biomarkers of ischemic penumbra in acute stroke," *Neurology*, vol. 93, no. 13, pp. e1288–e1298, 2019.

[11] P. Narne, V. Pandey, and P. B. Phanithi, "Interplay between mitochondrial metabolism and oxidative stress in ischemic stroke: an epigenetic connection," *Molecular and Cellular Neuroscience*, vol. 82, pp. 176–194, 2017.

[12] S. Matsumoto, M. Murozono, M. Kanazawa, T. Nara, T. Ozawa, and Y. Watanabe, "Edaravone and cyclosporine A as neuroprotective agents for acute ischemic stroke," *Acute Medicine & Surgery*, vol. 5, no. 3, pp. 213–221, 2018.

[13] S. Wu, E. Sena, K. Egan, M. Macleod, and G. Mead, "Edaravone improves functional and structural outcomes in animal models of focal cerebral ischemia: a systematic review," *International Journal of Stroke*, vol. 9, no. 1, pp. 101–106, 2014.

[14] J. Yang, X. Cui, J. Li, C. Zhang, J. Zhang, and M. Liu, "Edaravone for acute stroke: meta-analyses of data from randomized controlled trials," *Developmental Neurorehabilitation*, vol. 18, no. 5, pp. 330–335, 2015.

[15] Y. Yamamoto, "Plasma marker of tissue oxidative damage and edaravone as a scavenger drug against peroxyl radicals and peroxynitrite," *Journal of Clinical Biochemistry & Nutrition*, vol. 60, no. 1, pp. 49–54, 2017.

[16] M. Frantzi, A. Latosinska, and H. Mischak, "Proteomics in drug development: the dawn of a new era?" *Proteomics-Clinical Applications*, vol. 13, no. 2, Article ID 1800087, 2019.

[17] C. Monti, M. Zilocchi, I. Colugnat, and T. Alberio, "Proteomics turns functional," *Journal of Proteomics*, vol. 198, pp. 36–44, 2019.

[18] E. Z. Longa, P. R. Weinstein, and S. Carlson, "Reversible middle cerebral artery occlusion without craniectomy in rats," *Stroke*, vol. 20, no. 1, p. 84, 1989.

[19] X. Liu, S. Ouyang, B. Yu et al., "PharmMapper server: a web server for potential drug target identification using pharmacophore mapping approach," *Nucleic Acids Research*, vol. 38, pp. W609–W614, 2010.

[20] G. Stelzer, R. Rosen, I. Plaschkes et al., "The GeneCards suite: from gene data mining to disease genome sequence analysis," *CurrProtoc Bioinformatics*, vol. 54, 2016.

[21] A. Hamosh, A. F. Scott, J. S. Amberger, V. A. Bocchini, and C. A. McKusick, "Online Mendelian Inheritance in Man (OMIM), a knowledgebase of human genes and genetic disorders," *Nucleic Acids Research*, vol. 33, pp. D514–D517, 2005.

[22] D. Szklarczyk, A. Franceschini, S. Wyder, K. Forslund, D. Heller, and J. Huerta-Cepas, "STRING v10: protein-protein interaction networks, integrated over the tree of life," *Nucleic Acids Research*, vol. 43, pp. D447–D452, 2015.

[23] D. W. Huang, B. T. Sherman, and R. A. Lempicki, "Systematic and integrative analysis of large gene lists using DAVID bioinformatics resources," *Nature Protocols*, vol. 4, pp. 44–57, 2009.

[24] S. Miyake, H. Wakita, J. D. Bernstock et al., "Hypophosphorylation of ribosomal protein S6 is a molecular mechanism underlying ischemic tolerance induced by either hibernation or preconditioning," *Journal of Neurochemistry*, vol. 135, no. 5, pp. 943–957, 2015.

[25] W. S. Qu, Y. H. Wang, J. F. Ma et al., "Galectin-1 attenuates astrogliosis-associated injuries and improves recovery of rats following focal cerebral ischemia," *Journal of Neurochemistry*, vol. 116, no. 2, pp. 217–226, 2011.

[26] S. Ishibashi, T. Kuroiwa, M. Sakaguchi et al., "Galectin-1 regulates neurogenesis in the subventricular zone and promotes functional recovery after stroke," *Experimental Neurology*, vol. 207, no. 2, pp. 302–313, 2007.

[27] T. Nakase, T. Mizuno, S. Harada et al., "Angiotensinogen gene polymorphism as a risk factor for ischemic stroke," *Journal of Clinical Neuroscience*, vol. 14, no. 10, pp. 943–947, 2007.

[28] S. Wang, R. Zeng, L. Lei, and J. Huang, "Angiotensinogen gene polymorphism and ischemic stroke in East Asians: a meta-analysis," *Neural Regen Research*, vol. 8, no. 13, pp. 1228–1235, 2013.

[29] K. Gormley, S. Bevan, and H. S. Markus, "Polymorphisms in genes of the renin-angiotensin system and cerebral small vessel disease," *Cerebrovascular Diseases*, vol. 23, no. 2-3, pp. 148–155, 2007.

[30] M. Armogida, A. Spalloni, D. Amantea et al., "The protective role of catalase against cerebral ischemia in vitro and in vivo," *International Journal of Immunopathology & Pharmacology*, vol. 24, no. 3, pp. 735–747, 2011.

[31] R. Nisticò, S. Piccirilli, M. L. Cucchiaroni et al., "Neuroprotective effect of hydrogen peroxide on an in vitro model of brain ischaemia," *British Journal of Pharmacology*, vol. 153, no. 5, pp. 1022–1029, 2008.

[32] G. E. Barreto, X. Sun, L. Xu, and R. G. Giffard, "Astrocyte proliferation following stroke in the mouse depends on distance from the infarct," *PLoS One*, vol. 6, no. 11, Article ID e27881, 2011.

[33] Y. F. Yang, Z. Chen, S. L. Hu et al., "Interleukin-1 receptor associated kinases-1/4 inhibition protects against acute hypoxia/ischemia-induced neuronal injury in vivo and in vitro," *Neuroscience*, vol. 196, pp. 25–34, 2011.

[34] P. H. Chan, "Role of oxidants in ischemic brain damage," *Stroke*, vol. 27, no. 6, pp. 1124–1129, 1996.

[35] L. Li, J. Tan, Y. Miao, P. Lei, and Q. Zhang, "ROS and autophagy: interactions and molecular regulatory mechanisms," *Cellular and Molecular Neurobiology*, vol. 35, no. 5, pp. 615–621, 2015.

[36] T. Sugawara, N. Noshita, A. Lewén et al., "Overexpression of copper/zinc superoxide dismutase in transgenic rats protects

vulnerable neurons against ischemic damage by blocking the mitochondrial pathway of caspase activation," *Journal of Neuroscience*, vol. 22, no. 1, pp. 209–217, 2002.

[37] C. Michiels, E. Minet, D. Mottet, and M. Raes, "Regulation of gene expression by oxygen: NF-kappaB and HIF-1, two extremes," *Free Radical Biology and Medicine*, vol. 33, no. 9, pp. 1231–1242, 2002.

[38] C. T. D'Angio and J. N. Finkelstein, "Oxygen regulation of gene expression: a study in opposites," *Molecular Genetics and Metabolism*, vol. 71, no. 1-2, pp. 371–380, Article ID 11001829, 2000.

[39] Y. Ye, T. Jin, X. Zhang et al., "Meisoindigo protects against focal cerebral ischemia-reperfusion injury by inhibiting NLRP3 inflammasome activation and regulating microglia/macrophage polarization via TLR4/NF-κB signaling pathway," *Frontiers in Cellular Neuroscience*, vol. 13, p. 553, 2019.

[40] L. Ruan, F. Li, S. Li et al., "Effect of different exercise intensities on hepatocyte apoptosis in HFD-induced NAFLD in rats: the possible role of endoplasmic reticulum stress through the regulation of the IRE1/JNK and eIF2α/CHOP signal pathways," *Oxidative Medicine and Cellular Longevity*, vol. 2021, Article ID 6378568, 15 pages, 2021.

[41] B. Puig, S. Brenna, and T. Magnus, "Molecular communication of a dying neuron in stroke," *International Journal of Molecular Sciences*, vol. 19, no. 9, Article ID 2834, 2018.

[42] A. M. Pourbagher-Shahri, T. Farkhondeh, M. Talebi, D. M. Kopustinskiene, S. Samarghandian, and J. Bernatoniene, "An overview of NO signaling pathways in aging," *Molecules*, vol. 26, no. 15, p. 4533, 2021.

[43] M. Hedtjärn, A. L. Leverin, K. Eriksson, K. Blomgren, C. Mallard, and H. Hagberg, "Interleukin-18 involvement in hypoxic-ischemic brain injury," *Journal of Neuroscience*, vol. 22, no. 14, pp. 5910–5919, 2002.

[44] G. del Zoppo, I. Ginis, J. M. Hallenbeck, C. Iadecola, X. Wang, and G. Z. Feuerstein, "Inflammation and stroke: putative role for cytokines, adhesion molecules and iNOS in brain response to ischemia," *Brain Pathology*, vol. 10, no. 1, pp. 95–112, 2000.

[45] H. Yoshida, H. Yanai, Y. Namiki, K. Fukatsu-Sasaki, N. Furutani, and N. Tada, "Neuroprotective effects of edaravone: a novel free radical scavenger in cerebrovascular injury," *CNS Drug Reviews*, vol. 12, no. 1, pp. 9–20, 2006.

[46] N. Zhang, M. Kominc-Kobayashi, R. Tanaka, M. Liu, Y. Mizuno, and T. Urabc, "Edaravone reduces early accumulation of oxidative products and sequentialinflammatory responses after transient focal ischemia in mice brain," *Stroke*, vol. 36, pp. 2220–2225, 2005.

[47] L. Jiao, *The Role of Edaravone in Hippocampal Delayed Neuronal Death and Distant Memory Function after Middle Cerebral Artery Ischemia-Reperfusion in Rats and its mechanism*, Huazhong University of Science and Technology, Wuhan, China, 2011.

[48] S. H. Jiang, *Effects of Edaravone on Inflammatory Response and Endoplasmic Reticulum Stress Pathway after Cerebral hemorrhage*, Zunyi Medical University, Zunyi, China, 2020.

[49] X. Y. Liang, Y. Gu, M. Zhao et al., "Edaravone intervenes in the proliferation and differentiation of neural stem cells in rats with permanent cerebral ischemia," *Journal of Anatomy*, vol. 52, no. 3, pp. 370–376, 2021.

[50] F. Wang, Y. Wang, and B. Zhao, "Effects of edaravone based on Wnt/β-catenin signaling pathway on neuronal proliferation in rats with acute stroke," *Journal of Brain and Neurological Disorders*, vol. 29, no. 7, pp. 406–411, 2021.

[51] X. Wang, *Experimental Study on the Regulation of Iron Death by Edaravone to Repair Spinal Cord injury*, Tianjin Medical University, Tianjin, China, 2020.

Hindawi
Evidence-Based Complementary and Alternative Medicine
Volume 2021, Article ID 4835488, 9 pages
https://doi.org/10.1155/2021/4835488

Review Article

A Systematic Review and Meta-Analysis of the Effects of Herbal Medicine Buyang Huanwu Tang in Patients with Poststroke Fatigue

Chul Jin, Seungwon Kwon, Seung-Yeon Cho, Seong-Uk Park, Woo-Sang Jung, Sang-Kwan Moon, Jung-Mi Park, Chang-Nam Ko, and Ki-Ho Cho

Department of Cardiology and Neurology, College of Korean Medicine, Kyung Hee University, Seoul, Republic of Korea

Correspondence should be addressed to Seungwon Kwon; kkokkottung@hanmail.net

Received 28 August 2021; Revised 17 November 2021; Accepted 29 November 2021; Published 14 December 2021

Academic Editor: Thanasekaran Jayakumar

Poststroke fatigue (PSF) is reported to occur in 30%–72% of all patients with stroke. PSF not only is a symptom of stroke but has also been reported to adversely affect the prognosis of patients with stroke. However, no treatment has had a significant effect on PSF. In East Asian countries, several herbal medicines have been used to treat stroke, with Buyang Huanwu Tang (BHT) being the most common. This review aimed to evaluate the efficacy and safety of BHT for PSF. A literature search was conducted on MEDLINE, CENTRAL, Scopus, CiNii, CNKI, OASIS, NDSL, and KTKP databases for randomized controlled trials that evaluated the effects and safety of BHT on PSF. Six studies ($n = 427$) were included. The overall methodological quality of these studies was relatively low. In the adjunctive BHT group, the meta-analysis indicated statistically significant improvements in the Fatigue Severity Scale score (mean difference −1.49, 95% CI [−2.25, −0.73]) and total clinical efficacy rate (risk ratio 0.11, 95% CI [0.03, 0.41]) compared to those in the nonherbal group. Adverse events were only reported in one study, and no serious adverse events occurred. BHT administration might be effective in the treatment of PSF. We were unable to draw definitive conclusions owing to the limitations of the included studies. The trial is registered with CRD42019130178 in PROSPERO.

1. Introduction

Poststroke fatigue (PSF) can be defined as a feeling of early exhaustion with weariness, lack of energy, and aversion to effort that develops during physical or mental activity after a stroke that is usually not ameliorated by rest [1]. PSF has been reported to occur in 30%–72% of all stroke patients [2–5], with a potentially negatively effect on prognosis. In particular, PSF is known to adversely affect activities of daily living in patients with stroke [6]. As a result, patients with PSF show decreased participation in physical activity and rehabilitation treatment [6], resulting in poor neurological recovery, high mortality, and poor quality of life [7, 8]. Most of the recovery after a stroke has been reported to occur in the first 3–6 months after onset [9]. Therefore, patients who require rehabilitation treatment and feel significant fatigue need to be promptly assessed and treated.

Various pharmacological and nonpharmacological interventions have been used to treat PSF [10]. Specifically, fluoxetine and citicoline have been applied as pharmacological interventions, while fatigue education programs and mindfulness-based stress reduction programs have been attempted as nonpharmacological treatments [10]. However, a recent systematic review and meta-analysis suggested that there was insufficient evidence to support the use of any of these interventions to treat PSF [10]. The cause of PSF is multidimensional, including factors related to demographic data (e.g., age, sex, and marital status), neurological and physical deficits, medical comorbidities, smoking status, the use of certain medications, sleep disturbances, pain, prestroke fatigue, depression, anxiety, and cognitive impairment [11]. The pathophysiology of PSF is also unclear, with altered cortical excitability, inflammation, immune response, and genetic factors reported as major

pathophysiological factors associated with PSF [11]. We hypothesize that these complex multidimensional influences on PSF are the main hindrances to the development of effective treatments.

Therefore, in this review, we focused on traditional East Asian herbal medicine. In East Asian countries, herbal medicine has been used to treat stroke. According to the results of a previous systematic review and meta-analysis [12], adjunctive treatment for acute cerebral infarction using herbal medicine is known to help alleviate neurological deficits. Various herbal medicines have been assessed in previous systematic reviews and meta-analyses, with Buyang Huanwu Tang (BHT, Boyang Hwano Tang in Korean, Hoyangkango in Japanese) and its variants being the most common among them [12]. BHT is a prescription that has been used for stroke patients with "Qi deficiency" and "blood stasis," which is a type of pattern identification used in traditional East Asian medicine [13]. Since Qi deficiency is known to be closely related to fatigue symptoms [14, 15], we assumed that BHT could be effective not only for stroke itself but also for PSF.

Although previous studies have assessed the effects of BHT on stroke, no systematic literature review and meta-analysis has been conducted to evaluate the efficacy and safety of BHT for PSF. Therefore, in the present study, we systematically reviewed the clinical effect and safety of BHT on PSF based on the results of published randomized controlled trials (RCTs).

2. Methods

The trial registration number of this systematic review and meta-analysis was CRD42019130178 in PROSPERO. The present study was conducted based on a previously published protocol [16]. We followed the methods of Kwon et al., 2021 [17].

2.1. Database Search. Electronic databases including MEDLINE (via PubMed), the Cochrane Central Register of Controlled Trials (CENTRAL), Scopus, Citation Information by Nii (CiNii), China National Knowledge Infrastructure Database (CNKI), Oriental Medicine Advanced Searching Integrated System (OASIS), National Digital Science Library (NDSL), and Korean Traditional Knowledge Portal (KTKP) were searched up to October 2021. The search strategies were modified based on the characteristics of the individual databases; however, the main keywords used were as follows: "(Buyang Huanwu OR Boyang Hwano OR Hoyangkango) AND (Poststroke fatigue OR PSF OR stroke fatigue OR fatigue after stroke OR [cerebrovascular accident AND fatigue] OR [CVA AND fatigue] OR [stroke AND fatigue])," which were appropriately combined for each database search. The specific search terms used for each database are presented in Appendix 1. There was no language or other publication restrictions in the study selection process.

2.2. Eligibility Criteria. The studies were screened and selected according to the inclusion criteria and subsequently reviewed. Only RCTs and quasi-RCTs investigating BHT for PSF treatment were included; nonrandomized clinical trials, case reports and series, uncontrolled trials, and laboratory (experimental) studies were excluded. Additionally, only patients with PSH who were diagnosed using a qualified clinical diagnostic method (such as the Fatigue Assessment Scale [FAS] and the Fatigue Severity Scale [FSS]) or subjective fatigue symptoms were included; patients with other conditions that could cause fatigue, such as cancer, chronic kidney disease, and liver cirrhosis, were excluded. There were no restrictions based on sex, ethnicity, symptom severity, disease duration, or clinical setting. Only studies that used BHT or modified (herbs added) BHT as experimental interventions were included. There were no limitations on dosage, frequency, duration of treatment, or formulation (e.g., decoctions, extracts, tablets, capsules, and powders). For the control group, only studies that included placebos, a no-treatment group, or conventional Western medicine therapies were included. Studies that used other traditional Chinese medicine therapies (including traditional Korean medicine and Japanese Kampo Medicine), such as those using different types of herbal medicines, acupuncture treatments, or moxibustion treatments, were excluded. Following the electronic search, two independent researchers (SK and CJ) screened and selected the studies according to the eligibility criteria. After any duplicates were removed, the remaining studies were assessed based on their titles and abstracts.

2.3. Outcome Assessment. The primary outcome was the FAS score. For secondary outcomes, we used other parameters such as the FSS score, total clinical efficacy rate (TCER, percentage of patients whose fatigue symptoms improved), and inflammatory cytokine levels. TCER was defined as the sum of the categories identified with the terms "cure," "improved," or "slightly improved." In other words, all categories other than "unchanged" or "worse" were included in the TCER. The number and type of adverse events were also investigated.

2.4. Data Extraction and Quality Assessment of Individual Studies. Two independent reviewers (SK and CJ) who had received training regarding the process and purpose of selection independently reviewed the titles, abstracts, and manuscripts of the studies to determine if they were eligible for inclusion in the analysis. All studies were uploaded to EndNote X7 (Clarivate Analytics). The reasons for excluding studies were recorded and are shown in a Preferred Reporting Items for Systematic Reviews and Meta-Analyses (PRISMA) flow chart (Figure 1). All disagreements were resolved through discussion between the two reviewers. Following this, two review writers (SK and CJ) independently extracted the data and completed a standard data extraction form, which included study information such as the first author, publication year, language, research design, sample size, characteristics of the participants (e.g., age and sex), details of randomization, blinding, interventions, treatment period, outcome measurements, primary outcomes, secondary outcomes, and statistical methods used. If

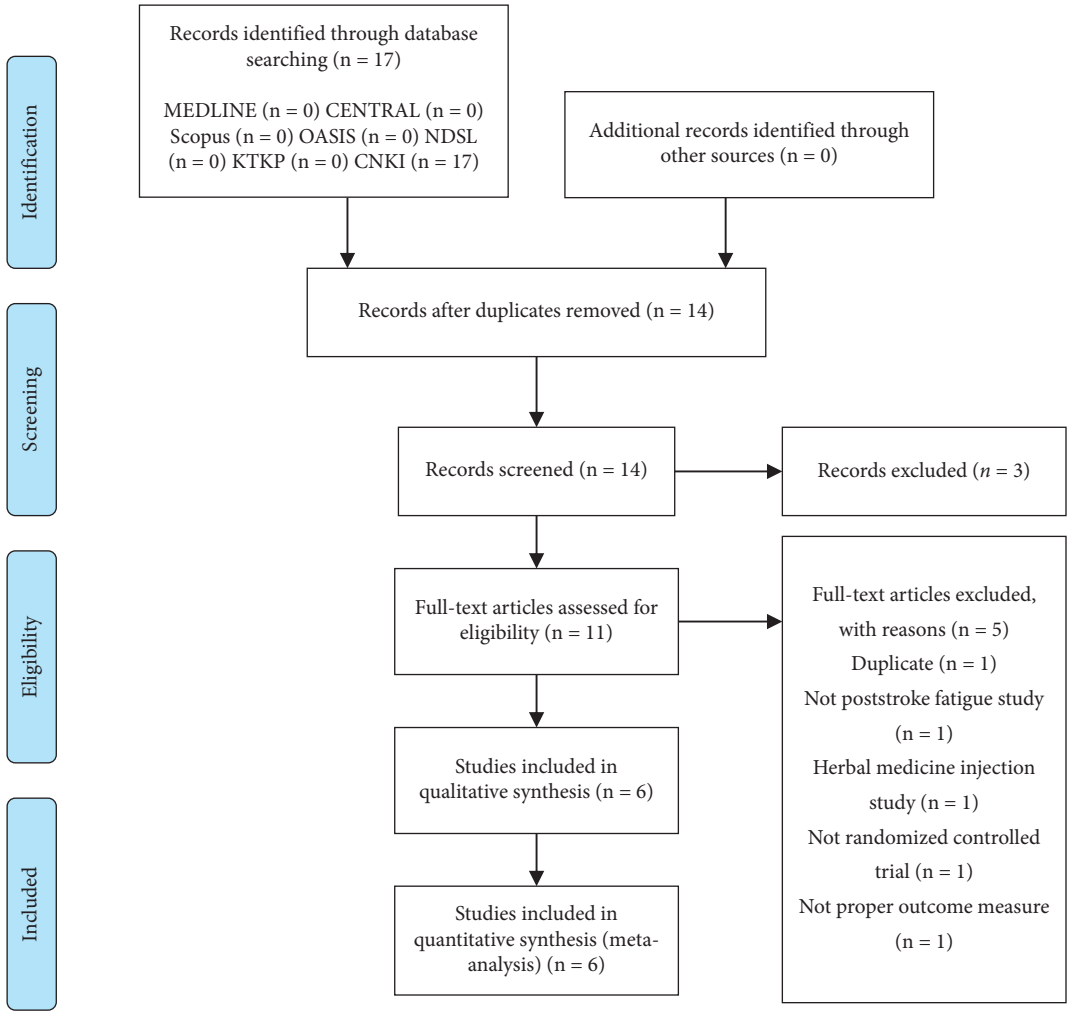

Figure 1: PRISMA flow diagram of study selection.

there were disagreements, another review writer (WSJ) was consulted and assisted in the decision-making.

The quality and risk of bias assessment was performed based on the Cochrane Collaboration tool [18] and was conducted by two independent reviewers (SK and CJ). Any disagreements were resolved by an arbiter (WSJ) who made the final decision. A total of seven domains, including sequence generation, allocation concealment, blinding of participants, blinding of outcome assessors, incomplete outcomes, selective outcome reporting, and other risks of bias, were assessed. Each domain was evaluated as having a high risk of bias (H), low risk of bias (L), or unclear risk of bias (U).

2.5. Synthesis of Data and Meta-Analysis. Dichotomous data, such as the TCER, are presented using the risk ratio (RR) and 95% confidence interval (CI). Continuous data such as the FAS and FSS are presented as the mean difference (MD). A fixed-effect model was used for the meta-analysis when no statistical heterogeneity was found. The statistical heterogeneity of the risk factors among the trials was analyzed using I^2. When I^2 was <50%, it was assumed that no statistical heterogeneity was observed. In addition, the heterogeneity of the study methodologies was evaluated. In cases where the heterogeneity of one study was greater than that of the others, the relevant study was excluded from the analysis. For example, if the specific details of the intervention, such as the duration of treatment and the method used in one study, were clinically different from those of other studies, the study was excluded. The RevMan 5.3.5 software recommended by the Cochrane Collaboration (Oxford, UK) was used for all data analyses (http://tech.cochrane.org/revman/).

3. Result

3.1. Study Selection and Characteristics. Seventeen studies were retrieved by electronic search and included in the first screening stage. Of these, eleven studies were further assessed for eligibility to be included in the meta-analysis by a full reading of the text. Five studies were excluded for the following reasons: duplication ($n = 1$), ineligible participants ($n = 1$), ineligible interventions ($n = 1$), ineligible study design ($n = 1$), and ineligible outcome measurements ($n = 1$) (Figure 1). After reviewing the full text of each study, six

studies (427 patients with PSF) [19–24] were finally included in the systematic review and meta-analysis (Table 1). All the six studies were written in Chinese and conducted in China [19–24].

There were two types of comparisons in the included studies: (1) herbal medicine + conventional therapies (including rehabilitation therapies for stroke) vs. conventional therapies alone (including rehabilitation therapies for stroke) (5 studies) [19, 20, 22–24] and (2) herbal medicine vs. conventional therapies (1 study) [21].

FAS was not evaluated in any of the included studies, TCER was evaluated in one study [20], and FSS was evaluated in five studies [19, 21–24]. The inflammatory cytokine levels of interleukin and tumor necrosis factor-α (TNF-α) were evaluated in one study [22].

The herbal medicines used in the studies were all BHT variants [19–24]. For each study, several herbs were added to the basic composition of BHT. Details regarding these compositions are shown in Table 2.

3.2. Risk of Bias within the Studies. In most studies, the risk of bias was high. Among the seven bias domains, concerns regarding random sequence generation, allocation concealment, blinding of participants, and outcome assessors were present. However, two studies had only low risk of bias in two items (randomization sequence generation and incomplete outcome data) [22, 23]. All studies [19–24] demonstrated a low risk of bias in incomplete outcome data. A summary of the risk of bias assessment is shown in Figure 2.

3.3. Fatigue Severity Scale. Four of the studies [19, 22–24] that compared add-on BHT variants (conventional therapies including rehabilitation therapies for stroke + BHT variant) with a control treatment (conventional therapies including rehabilitation therapies for stroke only) assessed fatigue using the FSS. The meta-analysis showed a significantly lower FSS score in the BHT variant group than in the control group (MD −1.49, 95% CI [−2.25, −0.73]) (Figure 3(a)).

One RCT [21] compared the FSS scores in the BHT variant group with those in the conventional therapy group. In this RCT, the BHT variant group received only the BHT variant, while the control group received only conventional therapy. The BHT variant group showed significantly lower FSS scores than the control group (−1.08, 95% CI [−1.20, −0.96]) (Figure 3(b)).

3.4. Total Clinical Effective Rate. One of the RCTs [20] that compared add-on BHT variants (conventional therapies including rehabilitation therapies for stroke + BHT variant) with a control treatment (conventional therapies including rehabilitation therapies for stroke only) assessed TCER. In this RCT, the BHT variant group showed significantly lower RR than the control group (0.11, 95% CI [0.03, 0.41], $p = 0.002$).

3.5. Inflammatory Cytokine Levels. Only one of the studies [22] that compared add-on BHT variants (conventional therapies including rehabilitation therapies for stroke + BHT variant) with a control treatment (conventional therapies including rehabilitation therapies for stroke only) assessed the inflammatory cytokine levels of interleukin (IL)-1β, IL-6, and TNF-α. Notably, TNF-α levels were significantly lower in the BHT variant group than in the control group (MD −9.20, 95% CI [−18.19, −0.21], $p = 0.011$). However, the IL-1β and IL-6 levels were not significantly different between the two groups (IL-1β, MD −5.40, 95% CI [−11.44, 0.64]; IL-6, MD −5.50, 95% CI [−11.24, 0.24]).

3.6. Safety. Only one study [22] investigated adverse events, and no adverse effects were reported in either group in that study (Table 1).

4. Discussion

4.1. Main Findings. PSF is known to occur in 30%–72% of all stroke patients [2–5], and it has been reported to induce physical deconditioning, which results in reduced self-efficacy in terms of physical performance, poor rehabilitation participation and outcomes, reduced social participation, poor quality of life, functional limitations, and increased mortality [25]. Therefore, an appropriate treatment for PSF is crucial for improving outcomes. However, sufficient evidence for the treatment or prevention of PSF has not been found for several pharmacological agents (e.g., antidepressants) and nonpharmacological approaches (e.g., mindfulness-based stress reduction and fatigue education programs) [10]. Therefore, finding alternative treatment options is essential. The results of the meta-analysis in the present study indicate that the administration of herbal medicine (BHT or BHT variants) might result in significant improvements in PSF in stroke patients. The administration of BHT or BHT variants for PSF was found to significantly reduce the FSS scores and TCER.

4.2. The Mechanism of BHT or BHT Variants on PSF. BHT is known to treat the condition called "blood stasis" in traditional East Asian medicine and is used for the treatment of hemiparesis in patients with stroke [13, 26]. The herbal prescriptions used to treat blood stasis in traditional East Asian medicine have varied. While BHT is one of the treatment options, it is different from other herbal prescriptions for blood stasis treatment in that it has mainly been used for blood stasis with Qi deficiency [13]. Qi deficiency, a type of pattern identification that has been used in clinical practice in traditional East Asian medicine, is known to be closely associated with fatigue symptoms. A previous study has suggested that Qi deficiency is associated with fatigue in patients with breast cancer [14]. In addition, according to the standardized predictive models for traditional Korean medical diagnostic pattern identification in stroke subjects previously developed by this study team, the likelihood of a Qi deficiency diagnosis was significantly increased when a patient had symptoms such as pale complexion, faint low voice, reversal cold of the extremities, and fatigue [15]. Therefore, we assumed that BHT, which has

Table 1: Characteristics of the included studies.

Study (first author, year)	Subjects (herbal/control)	Stroke type (ischemic/hemorrhagic)	Interventions		Main outcomes (herbal/control)	Duration of outcome assessment (weeks)	Adverse events (herbal/control)
			Herbal medicines	Control group			
Song, 2011	70 (35/35)	53/17	Conventional therapies + rehabilitation therapies for stroke + BHT variant 1 4 weeks	Conventional therapies + rehabilitation therapies for stroke 4 weeks	FSS 3.15 ± 1.71/4.09 ± 1.86 IL-1β (23/19) 21.3 ± 9.5/26.7 ± 10.3 (pg/ml) IL-6 (23/19) 16.2 ± 8.3/21.7 ± 9.2 (pg/ml) TNF-α (23/19) 20.6 ± 14.3/29.8 ± 15.2 (pg/ml)	4	0/0
Liang, 2016	92 (46/46)	57/35	Conventional therapies + rehabilitation therapies for stroke + BHT variant 2 4 weeks	Conventional therapies + rehabilitation therapies for stroke 4 weeks	FSS 3.39 ± 0.73/5.33 ± 5.45	4	Unreported
Xu, 2018	62 (31/31)	Unreported	Conventional therapies + rehabilitation therapies for stroke + BHT variant 3 4 weeks	Conventional therapies + rehabilitation therapies for stroke 4 weeks	TCER 29/31 (93.55%)/19/31 (61.29%)	4	Unreported
Yin, 2020	80 (40/40)	Unreported	Conventional therapies + rehabilitation therapies for stroke + BHT variant 4 4 weeks	Conventional therapies + rehabilitation therapies for stroke 4 weeks	FSS 3.27 ± 0.81/5.41 ± 0.56	4	Unreported
Duan, 2021	60 (30/30)	Unreported	Conventional therapies + rehabilitation therapies for stroke + BHT variant 5 4 weeks	Conventional therapies + rehabilitation therapies for stroke 4 weeks	FSS 2.73 ± 0.23/3.81 ± 0.24	4	Unreported
Ye, 2018	63 (33/30)	Unreported	BHT variant 5 4 weeks	Conventional therapies for stroke 4 weeks	FSS 2.73 ± 0.24/3.81 ± 0.24	4	Unreported

BHT: Buyang Huanwu Tang; FSS: Fatigue Severity Scale; TCER: total clinical efficacy rate.

Table 2: Herbal medicines and treatment details.

Study (first author, year, type of BHT)	Components of the herbal medicines (g/day)
Song, 2011, BHT variant 1	Astragali radix 60~120 g, Angelicae gigantis radix 10 g, Cnidii rhizoma 15 g, paeoniae radix rubra 15 g, lumbricus 10~15 g, Carthami flos 5 g, persicae semen 10 g, Achyranthis radix 15 g, Atractylodis rhizoma Alba 20 g, Cistanchis herba 20 g, Codonopsis pilosulae radix 15 g, epimedii herba 15 g, glycyrrhizae radix et rhizoma 5 g, pinelliae tuber 10 g, spatholobi Caulis 30 g
Liang, 2016, BHT variant 2	Astragali radix 50 g, Angelicae gigantis radix 10 g, Cnidii rhizoma 10 g, paeoniae radix rubra 15 g, lumbricus 10 g, Carthami flos 10 g, persicae semen 10 g, Atractylodis rhizoma Alba 10 g, bupleuri radix 10 g, glycyrrhizae radix et rhizoma 6 g, menthae herba 3 g, paeoniae radix Alba 10 g, poria sclerotium 10 g, zingiberis rhizoma recens 3 g
Xu, 2018, BHT variant 3	Astragali radix 120 g, Angelicae gigantis radix 12 g, Cnidii rhizoma 10 g, paeoniae radix rubra 15 g, lumbricus 10 g, Carthami flos 10 g, persicae semen 10 g
Yin, 2020 BHT variant 4	Astragali radix 25 g, Angelicae gigantis radix 25 g, Cnidii rhizoma 15 g, paeoniae radix Alba 10 g, lumbricus 10 g, Carthami flos 10 g, persicae semen 10 g, bupleuri radix 15 g, Citri unshius pericarpium 10 g, Atractylodis rhizoma Alba 10 g, poria sclerotium 20 g, Cyperi rhizoma 6 g, scorpio 3 g, zingiberis rhizoma recens 3 pieces
Duan, 2021 Ye, 2018, BHT variant 5	Astragali radix 120 g, Angelicae gigantis radix 10 g, Cnidii rhizoma 10 g, paeoniae radix rubra 15 g, lumbricus 10 g, Carthami flos 10 g, persicae semen 10 g

BHT: Buyang Huanwu Tang.

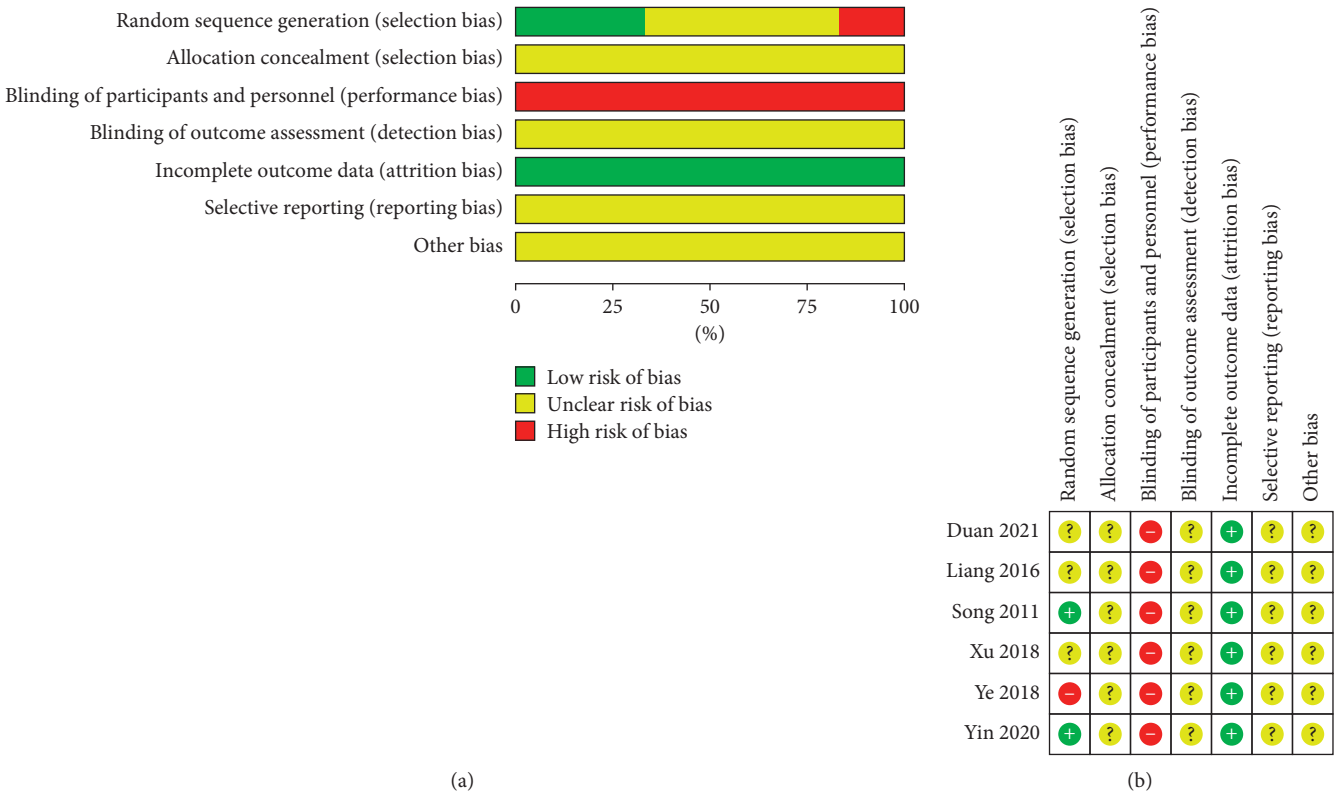

Figure 2: (a) Risk of bias graph: review of the authors' judgments regarding each risk of bias item is presented as percentages across all included studies. (b) Risk of bias summary: review of authors' judgments regarding each risk of bias item for each included study. "+": low risk, "?": unclear risk, and "−": high risk.

been used for Qi deficiency in stroke patients, would be effective for PSF.

This application could also be explained by the pharmacological mechanism of action of BHT. A previous experimental study has suggested that BHT has a neuroprotective effect in cerebral ischemic conditions [27]. The administration of BHT to mice with middle cerebral ischemic/reperfusion injury has been shown to lead to a significant downregulation of the genes involved in inflammation, apoptosis, angiogenesis, and blood coagulation as well as the upregulation of the genes mediating neurogenesis and nervous system development [27]. While the number of studies is not substantial, a link between stroke-induced inflammation and PSF has been suggested in some studies [28]. Therefore, BHT could be effective against PSF through the inhibition of stroke-induced inflammation.

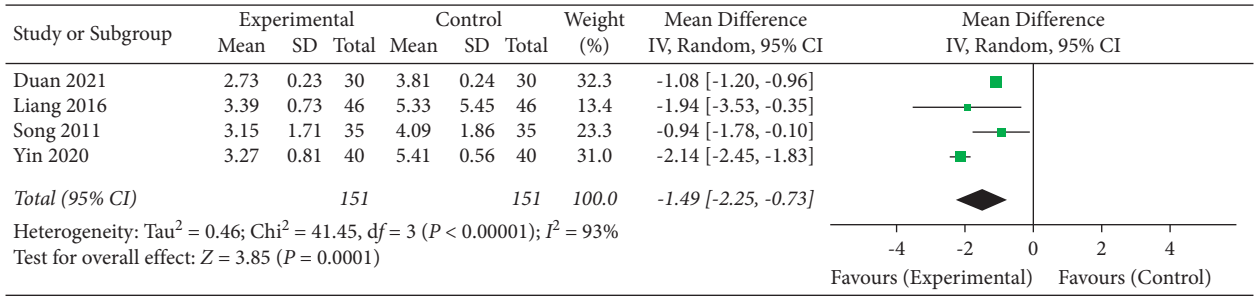

(a)

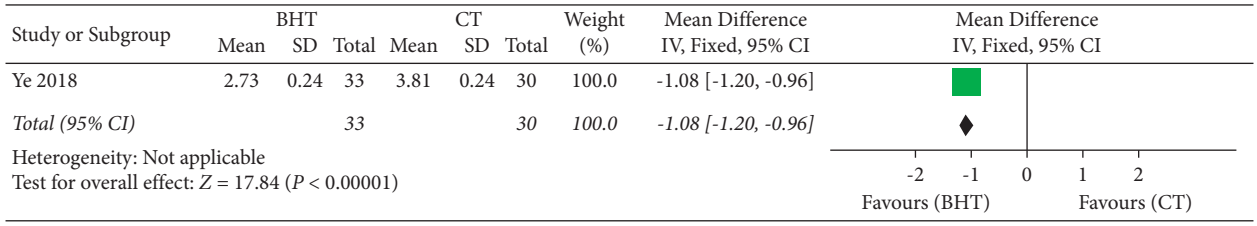

(b)

Figure 3: (a) FSS: Buyang Huanwu Tang + conventional therapies vs. conventional therapies only. (b) FSS: Buyang Huanwu Tang vs. conventional therapies BHT: Buyang Huanwu Tang; CT: conventional therapy; FSS: Fatigue Severity Scale.

4.3. Strengths and Limitations. This study has a number of strengths. First, this is the first systematic review and meta-analysis to evaluate the effects of BHT or its variants on PSF. Second, no restriction on language was applied during the literature search process. Therefore, we were able to review all the relevant studies available. Furthermore, we provided a detailed summary of the BHT or BHT variant compositions used in the studies (Table 2). This information can be utilized by clinicians prescribing BHT to patients with PSF in clinical settings.

However, there are some limitations to the present study. First, all eligible studies exhibited methodological flaws, such as in terms of patient selection, performance, and detection bias. Only two studies had low risk of bias in two items (randomization sequence generation and incomplete outcome data) [22, 23]. Second, detailed information regarding the protocols used in the RCTs was not provided in the included studies. Third, all of the eligible studies, except one [22], did not report adverse events. Fourth, most included studies had different BHT and BHT variant components (Table 2) [19–24]. There are five types of BHT and their variants. Although Astragali Radix, Angelicae Gigantis Radix, Cnidii Rhizoma, Paeoniae Radix Rubra, Lumbricus, Carthami Flos, and Persicae Semen were commonly present in all types of BHT, the specific dosages were all different. In addition, the three types of BHT contain various herbs, in addition to the common herbs mentioned above [19, 22, 23]. Fifth, only 17 studies were found using an electronic search, and only 6 of them could be analyzed. As a result, both the quantity and quality of evidence are insufficient to reach a concrete conclusion. Lastly, all the trials included in this study were conducted in China [19–24]. Therefore, there could be a publication bias given the high rate of studies published in China. A previous study has called attention to the exceptionally high success rate of trials conducted in China compared to those conducted in other regions [29]. Therefore, it is possible that the results of this meta-analysis reflect only the clinical settings in China and may not be applicable to patients in other countries or of other ethnic backgrounds (besides North East Asia). Based on these limitations, we could not draw concrete conclusions from the current literature.

4.4. Comparison with Existing Literature. The present study is the first systematic review and meta-analysis to evaluate the efficacy of the alternative therapeutic options of BHT and BHT variants on PSF. However, several studies have been conducted on conventional pharmacological and non-pharmacological treatments for PSF. Based on these studies, a Cochrane review was first published in 2009 to evaluate the efficacy of pharmacological and nonpharmacological interventions on PSF [30], and an updated version was published in 2015 [10]. However, both studies failed to find significant improvements using either pharmacological approaches, such as the antidepressant fluoxetine, or non-pharmacological approaches, such as education programs.

The present systematic review showed that the administration of BHT and BHT variants might be effective in treating PSF. Additionally, the results of this study showed that BHT could be a new therapeutic option for patients with PSF. However, it is difficult to draw definitive conclusions regarding the efficacy and safety of BHT owing to the limitations of the included studies.

4.5. Implications for Research. First, to provide a higher level of evidence, the heterogeneity of the interventions used in future studies should be reduced. Specific details regarding the BHT compositions used in the eligible RCTs were all different. Therefore, it is necessary to standardize the

composition of BHT for future clinical trials. Second, the risk of bias should be minimized as much as possible. Above all, specific information about allocation concealment and blinding of participants, investigators, and statisticians should be provided. It is also essential to use a placebo in the control group. If the patients, evaluators, and statisticians are not blinded, this could influence the results. However, making a placebo for herbal medicines tends to be difficult due to their unique color, taste, and flavor [31]. Therefore, establishing a process for making an effective placebo should be the focus of future research. Finally, future studies should provide detailed information regarding their study protocols, such as protocol registration numbers.

5. Conclusions

In conclusion, we could suggest the administration of BHT and BHT variants to treat patients with PSF might reduce their clinical symptoms and inflammatory cytokine levels. However, the quality of the studies reviewed was generally low, and there was insufficient data to draw concrete conclusions regarding the efficacy and safety of BHT and BHT variants in patients with PSF. Therefore, further studies are required to confirm these findings.

Data Availability

The data used to support the findings of this study are included within the article.

Conflicts of Interest

The authors declare no conflicts of interest.

Acknowledgments

This research was supported by the First Research in Lifetime Program through the National Research Foundation of Korea (NRF) funded by the Ministry of Education (MOE) (NRF-2018R1C1B5086119).

Supplementary Materials

Appendix 1: specific search terms used for each database. (*Supplementary Materials*)

References

[1] F. Staub and J. Bogousslavsky, "Fatigue after stroke: a major but neglected issue," *Cerebrovascular Diseases*, vol. 12, no. 2, pp. 75–81, 2001.

[2] V. L. Feigin, S. Barker-Collo, V. Parag et al., "Prevalence and predictors of 6-month fatigue in patients with ischemic stroke: a population-based stroke incidence study in Auckland, New Zealand, 2002-2003," *Stroke*, vol. 43, no. 10, pp. 2604–2609, 2012.

[3] V. Vuletić, Z. Lezaić, and S. Morović, "Post-stroke fatigue," *Acta Clinica Croatica*, vol. 50, no. 3, pp. 341–344, 2011.

[4] F. Colle, I. Bonan, M.-C. Gellez Leman, N. Bradai, and A. Yelnik, "Fatigue après accident vasculaire cérébral," *Annales de Readaptation et de Medecine Physique*, vol. 49, no. 6, 2006.

[5] S. Choi-Kwon and J. S. Kim, "Poststroke fatigue: an emerging, critical issue in stroke medicine," *International Journal of Stroke*, vol. 6, no. 4, pp. 328–336, 2011.

[6] S. Choi-Kwon, S. W. Han, S. U. Kwon, and J. S. Kim, "Poststroke fatigue: characteristics and related factors," *Cerebrovascular Diseases*, vol. 19, no. 2, pp. 84–90, 2005.

[7] E.-L. Glader, B. Stegmayr, and K. Asplund, "Poststroke fatigue," *Stroke*, vol. 33, no. 5, pp. 1327–1333, 2002.

[8] H. Naess, L. Lunde, and J. Brogger, "The effects of fatigue, pain, and depression on quality of life in ischemic stroke patients: the Bergen stroke study," *Vascular Health and Risk Management*, vol. 8, pp. 407–413, 2012.

[9] C. E. Skilbeck, D. T. Wade, R. L. Hewer, and V. A. Wood, "Recovery after stroke," *Journal of Neurology, Neurosurgery & Psychiatry*, vol. 46, no. 1, pp. 5–8, 1983.

[10] S. Wu, M. A. Kutlubaev, H. Y. Chun et al., "Interventions for post-stroke fatigue," *Cochrane Database of Systematic Reviews*, vol. 2015, no. 7, Article ID Cd007030, 2015.

[11] J. L. Hinkle, K. J. Becker, J. S. Kim et al., "Poststroke fatigue: emerging evidence and approaches to management: a scientific statement for healthcare professionals from the American heart association," *Stroke*, vol. 48, no. 7, pp. e159–e170, 2017.

[12] C.-h. Han, M. Kim, S.-Y. Cho et al., "Adjunctive herbal medicine treatment for patients with acute ischemic stroke: a systematic review and meta-analysis," *Complementary Therapies in Clinical Practice*, vol. 33, pp. 124–137, 2018.

[13] R. L. Wei, H. J. Teng, B. Yin et al., "A systematic review and meta-analysis of buyang huanwu decoction in animal model of focal cerebral ischemia," *Evidence-based Complementary and Alternative Medicine: eCAM*, vol. 2013, Article ID 138484, 2013.

[14] T.-J. Chien, Y.-L. Song, C.-P. Lin, and C.-H. Hsu, "The correlation of traditional Chinese medicine deficiency syndromes, cancer related fatigue, and quality of life in breast cancer patients," *Journal of Traditional and Complementary Medicine*, vol. 2, no. 3, pp. 204–210, 2012.

[15] W.-S. Jung, S.-Y. Cho, S.-U. Park et al., "Development of standardized predictive models for traditional Korean medical diagnostic pattern identification in stroke subjects: a hospital-based multi-center trial," *Journal of Korean Medicine*, vol. 40, no. 4, pp. 49–60, 2019.

[16] C. Jin, S.-Y. Cho, S.-U. Park et al., "Buyang huanwu Tang (Boyang Hwano Tang) for the treatment of post-stroke fatigue," *Medicine (Baltimore)*, vol. 98, no. 37, p. e17116, 2019.

[17] S. Kwon, C. Jin, M. Chung et al., "Herbal medicine treatment for patients with chronic subdural hematoma: a systematic review and meta-analysis," *Complementary Therapies in Clinical Practice*, vol. 43, p. 101307, 2021.

[18] J. P. T. Higgins, D. G. Altman, P. C. Gotzsche et al., "The cochrane collaboration's tool for assessing risk of bias in randomised trials," *BMJ*, vol. 343, no. oct18 2, p. d5928, 2011.

[19] Y. Liang, W. Gong, Y. Su, and C. Li, "Observation on the effect of buyang huanwu decoction and xiaoyao powder in adjuvant treatment of post-stroke fatigue," *People Military Surgery*, vol. 59, no. 2, pp. 169-170, 2016, in Chinese.

[20] Y. Xu, "Clinical observation on modified buyang huanwu decoction in the treatment of fatigue after stroke," *Journal of Practical Traditional Chinese Medicine*, vol. 9, pp. 1087-1088, 2018, in Chinese.

[21] C. Ye, Z. Chen, L. Wang et al., "Application of Buyang Huanwu decoction in the treatment of post-stroke fatigue

patients in the community," *China Modern Doctor*, vol. 56, no. 31, pp. 116–119, 2018, in Chinese.

[22] X. J. Song, "Effect of the Combination of Jiawei Buyang Huanwu Decoction and Rehabilitation Training on the Serum Proinflammatory Cytokines in Patients with Post Stroke Fatigue," Guangzhou University of Traditional Chinese Medicine, Guangzhou, China, 2011.

[23] Y. Yin, "Clinical observation of chaihu shugan powder and buyang huanwu decoction combined with western medicine in treating fatigue after stroke," *China's Naturopathy*.vol. 28, no. 10, pp. 63–65, 2020, in Chinese.

[24] D. Duan, "Clinical analysis of buyang huanwu decoction in treating fatigue patients after stroke in community," *Journal of Mathematical Medicine*, vol. 34, no. 5, pp. 708–710, 2021, in Chinese.

[25] M. Nadarajah and H.-T. Goh, "Post-stroke fatigue: a review on prevalence, correlates, measurement, and management," *Topics in Stroke Rehabilitation*, vol. 22, no. 3, pp. 208–220, 2015.

[26] H.-Q. Li, J.-J. Wei, W. Xia et al., "Promoting blood circulation for removing blood stasis therapy for acute intracerebral hemorrhage: a systematic review and meta-analysis," *Acta Pharmacologica Sinica*, vol. 36, no. 6, pp. 659–675, 2015.

[27] H.-W. Wang, K.-T. Liou, Y.-H. Wang et al., "Deciphering the neuroprotective mechanisms of Bu-yang Huan-Wu decoction by an integrative neurofunctional and genomic approach in ischemic stroke mice," *Journal of Ethnopharmacology*, vol. 138, no. 1, pp. 22–33, 2011.

[28] H. Wen, K. B. Weymann, L. Wood, and Q. M. Wang, "Inflammatory signaling in post-stroke fatigue and depression," *European Neurology*, vol. 80, no. 3-4, pp. 138–148, 2018.

[29] A. Vickers, N. Goyal, R. Harland, and R. Rees, "Do certain countries produce only positive results? a systematic review of controlled trials," *Controlled Clinical Trials*, vol. 19, no. 2, pp. 159–166, 1998.

[30] E. McGeough, A. Pollock, L. N. Smith et al., "Interventions for post-stroke fatigue," *Cochrane Database of Systematic Reviews*, vol. 3, p. Cd007030, 2009.

[31] X. Zhang, R. Tian, C. Zhao, X. Tang, A. Lu, and Z. Bian, "Placebo design in WHO-registered trials of Chinese herbal medicine need improvements," *BMC Complementary and Alternative Medicine*, vol. 19, no. 1, p. 299, 2019.

Hindawi
Evidence-Based Complementary and Alternative Medicine
Volume 2021, Article ID 5319584, 11 pages
https://doi.org/10.1155/2021/5319584

Research Article

Auraptene, a Monoterpene Coumarin, Inhibits LTA-Induced Inflammatory Mediators via Modulating NF-κB/MAPKs Signaling Pathways

Chih-Hsuan Hsia,[1,2] **Thanasekaran Jayakumar**,[1] **Wan-Jung Lu**,[3,4,5] **Joen-Rong Sheu**,[1] **Chih-Wei Hsia**,[1] **Periyakali Saravana Bhavan**,[6] **Manjunath Manubolu**,[7] **Wei-Chieh Huang**,[1] **and Yi Chang**[8,9]

[1]*Graduate Institute of Medical Sciences, College of Medicine, Taipei Medical University, Taipei 110, Taiwan*
[2]*Translational Medicine Center, Shin Kong Wu Ho-Su Memorial Hospital, Taipei 111, Taiwan*
[3]*Department of Pharmacology, School of Medicine, College of Medicine, Taipei Medical University, Taipei 110, Taiwan*
[4]*Department of Medical Research, Taipei Medical University Hospital, Taipei 110, Taiwan*
[5]*Graduate Institute of Metabolism and Obesity Sciences, College of Nutrition, Taipei Medical University, Taipei 110, Taiwan*
[6]*Department of Zoology, Bharathiar University, Coimbatore 641046, Tamil Nadu, India*
[7]*Department of Evolution, Ecology and Organismal Biology, Ohio State University, Columbus, OH 43212, USA*
[8]*School of Medicine, Fu Jen Catholic University, New Taipei City 242, Taiwan*
[9]*Department of Anesthesiology, Shin Kong Wu Ho-Su Memorial Hospital, Taipei 111, Taiwan*

Correspondence should be addressed to Yi Chang; m004003@ms.skh.org.tw

Received 10 June 2021; Accepted 1 November 2021; Published 16 November 2021

Academic Editor: Weicheng Hu

Objective. Oxidative stress-mediated inflammatory events involve in the progress of several diseases such as asthma, cancers, and multiple sclerosis. Auraptene (AU), a natural prenyloxycoumarin, possesses numerous pharmacological activities. Here, the anti-inflammatory effects of AU were investigated in lipoteichoic acid- (LTA-) induced macrophage cells (RAW 264.7). *Methods*. The expression of cyclooxygenase (COX-2), tumor necrosis factor (TNF-α), interleukin-1β (IL-1β), and inducible nitric oxide synthase (iNOS) and the phosphorylation of extracellular signal-regulated kinase (ERK) 1/2, p38 MAPK, c-Jun N-terminal kinase (JNK), heme oxygenase (HO-1), p65, and IκBα were all identified by western blotting assay. The level of nitric oxide (NO) was measured by spectrometer analysis. The nuclear translocation of p65 nuclear factor kappa B (NF-κB) was assessed by the confocal microscopic staining method. Native polyacrylamide gel electrophoresis was performed to perceive the activity of antioxidant enzyme catalase (CAT). *Results*. AU expressively reduced NO production and COX-2, TNF-α, IL-1 β, and iNOS expression in LTA-stimulated cells. AU at higher concentration (10 μM) inhibited ERK and JNK, but not p38 phosphorylation induced by LTA. Moreover, AU blocked IκB and p65 phosphorylation, and p65 nuclear translocation. However, AU pretreatment was not effective on antioxidant HO-1 expression, CAT activity, and reduced glutathione (GSH, a nonenzymatic antioxidant), in LTA-induced RAW 264.7 cells. *Conclusion*. The findings of this study advocate that AU shows anti-inflammatory effects via reducing NF-κB/MAPKs signaling pathways.

1. Introduction

Various chemicals and pathogens considered as harmful stimuli produce inflammation, which is a protective response of our body. Inflammation can be classified as acute and chronic, which induces pain and tissue injuries. Rapid onset and short duration of action can be noticed in the acute form, which is facilitated by the excretion of numerous cytokines including interleukin-1 (IL-1), IL-6, IL-11, IL-8, and tumor necrosis factor-alpha (TNF-α)

[1, 2]. Nevertheless, in chronic inflammation, persistence of the inflammatory reactions could induce the migration of lymphocytes and macrophages to the damaged tissues [3]. Chronic inflammatory responses have been associated with the progression of various diseases such as asthma, arthritis, and neurodegenerative disorders [4]. Studies have established the involvement of several mediators including prostaglandin E2 (PGE2) in inflammatory events. Various symptoms including bone metabolism, wound healing, kidney function, blood vessel, and the immune responses have been associated with PGE2 secretion [5]. Cyclooxygenase (COX-2) protein can be expressed in response to physical, chemical, and biological stimulation [6]. The production of PGE2 can be augmented by COX-2, which denotes a central step in the events of inflammation.

Oxidative stress is known to be induced by elevated reactive oxygen species (ROS) and nitric oxide (NO) or reduced antioxidant enzymes catalase (CAT) and superoxide dismutase (SOD) and nonenzymatic glutathione (GSH) [7, 8]. Studies have indicated that oxidative stress plays a major role in the progress of inflammatory diseases [9]. The major component of Gram-positive bacteria, lipoteichoic acid (LTA), induces pathogenesis of sepsis [10] and lung injury by producing inflammatory reactions [11]. Therefore, examining the mechanisms that control LTA-stimulated cell activation is important for the analysis and treatment of lung inflammatory diseases. This bacterial component stimulates the release of IL-1β, IL-6, and TNF-α [12]. LTA induces TNF-α and IL-6 expressions by inducing the phosphorylation of ERK1/2 in macrophages, and it also activates nuclear translocation of nuclear factor- (NF-) κB from the cytoplasm [13]. It has been proposed that various plant-based natural components have reported to have anti-inflammatory effects through suppressing inflammation-associated mediators and enhancing antioxidant defense molecules.

Auraptene, a geranyloxyl moiety of C-7 (7-geranyloxycoumarin), is a promising and most rich natural prenyloxycoumarin compound [14]. Plants of the Rutaceae family are the highest source of auraptene, and it is also the most general component of citrus fruits. Hence, citrus species are the major natural source of auraptene [14]. Several exciting pharmacological activities have been reported for this bioactive phytochemical such as antioxidant [15], anti-inflammatory [16], antimicrobial [17], antigenotoxic [18], neuroprotective [19], and immunomodulatory properties [20]. Murakami et al. [16] had well discussed the effect of auraptene in inflammation-mediated carcinogenesis. A study specified that dietary supplementation of auraptene in mice diminishes pulmonary metastasis of B16BL6 melanoma cells and prevents the growth of metastatic tumors in the lungs via inducing apoptosis [21]. In addition, auraptene showed promising effects of wound healing through inhibiting the secretion of inflammatory mediators in vitro, including IL-6 and IL-8 [22]. Hence, this study aimed to assess the anti-inflammatory mechanism of auraptene against LTA-stimulation in RAW 264.7 cells.

2. Materials and Methods

2.1. Materials. RAW 264.7 cells were obtained from the American Type Culture Collection (ATCC, Manassas, VA, USA, TIB-71). Auraptene (AU, >98%, Figure 1(a)) was purchased from ChemFaces Biochem, Wuhan, Hubei, China. Sigma (St Louis, MO, USA) supplied potassium ferricyanide, ferric chloride, and dimethyl sulfoxide (DMSO). Santa Cruz Biotechnology (Dallas, TX, USA) supplied anti-iNOS and COX-2 polyclonal antibodies (pAb). We purchased antibodies against TNF-α, phospho-p38 MAPK Thr180/Tyr182, phospho-c-JNK (Thr183/Tyr185), phospho-p44/p42 ERK (Thr202/Tyr204), phospho-IκBα Ser32/36, and phospho-NF-κB p65 (Ser536) pAbs from Cell Signaling (Beverly, MA, USA). Anti-IL-1β and anti-HO-1 pAbs were purchased from BioVision (Milpitas, CA, USA) and Enzo (Farmingdale, New York, USA), respectively. The antibody against α-tubulin was purchased from NeoMarkers (Fremont, CA, USA). AU was dissolved in 0.1% DMSO.

2.2. Cell Viability and Morphology of RAW Cells. RAW 264.7 cells were cultivated in Dulbecco's Modified Eagle's Medium (DMEM) at 37°C under 5% CO_2 and 95% air. At a concentration of 1×10^5 cells/well, they were pretreated with AU (5–20 μM) for 24 h. The 3-(4,5-dimethylthiazol-2-yl)-2,5-diphenyl-2H-tetrazolium bromide (MTT) assay was used to measure cell viability in which 5 mg/mL of MTT working solution was added to the culture medium. The formation of crystals was digested by suing 300 μl of DMSO. The formula of absorbance of treated cells/absorbance of control cells $\times$ 100% is used to measure the cell viability index.

2.3. Measurement of NO Production. To estimate the level of NO, AU at 5 and 10 μM was added to cells with or without LTA (5 μg/ml) for 24 h in the medium. Briefly, a 100 μl equal volume of culture suspension and Griess reagent was mixed and incubated for 10 min. NO levels were estimated by quantifying nitrite levels by an MRX absorbance reader with the optical density at 550 nm.

2.4. Immunoblotting Assay. The equal amount (50 μg) of proteins from 6×10^5 cells were run on 12% sodium dodecyl sulphate-polyacrylamide gel electrophoresis (SDS-PAGE) gels. The separated proteins were transferred to polyvinylidene difluoride (PVDF) membranes and then blocked using 5% skim milk for 40 min. After blocking, the membrane was titrated with different primary antibodies of targeted proteins for 2 h and consequently incubated with anti-rabbit IgG or sheep anti-mouse IgG for 1 h. The intensity of protein bands was measured by using the Biolight Windows Application, V2000.01 (Bio-Profil, Vilber Lourmat, France) software.

2.5. Confocal Microscopy Assay. Cells were seeded at 5×10^4/well, cultured on cover slips, and treated by AU (10 μM) for 30 min and then triggered by LTA (5 μg/ml) for 1 h. Coverslips were successively fixed with 4%

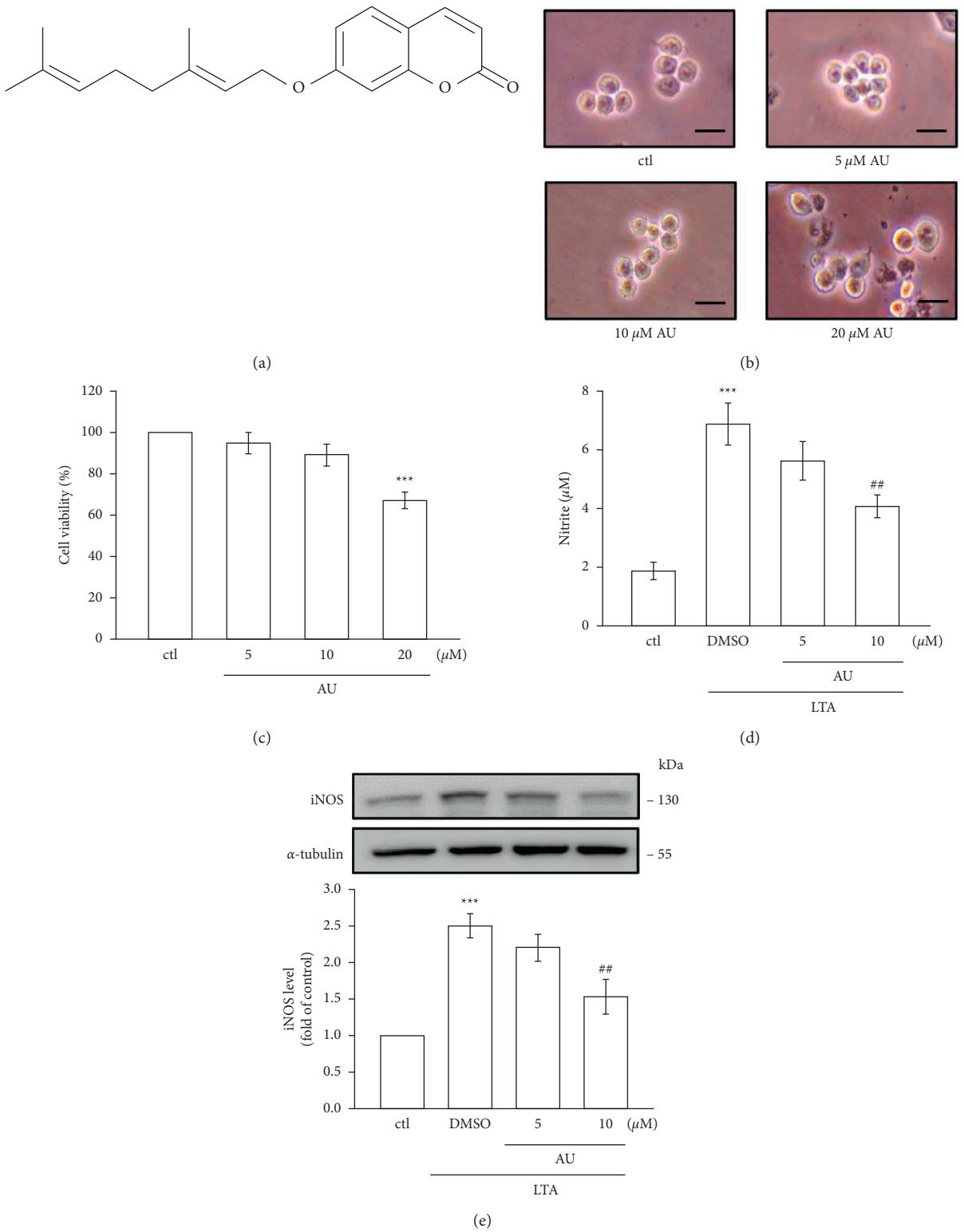

Figure 1: Chemical structure of auraptene (AU) and the effects of AU on morphology and cell viability and on LTA-induced NO production and iNOS expression in RAW 264.7 cells. (a) Chemical structure of AU. (b), (c) Cells were pretreated with AU (5, 10, or 20 μM) for 24. Cell viabilities were determined by the MTT assay. Scale bar = 25 μm. (d), (e) Cells were untreated or pretreated with AU (5 and 10 μM) for 30 min prior to stimulation with LTA (5 μg/ml) for 24 h. Control cells were not treated with LTA or AU. NO was measured using the Griess reaction assay. iNOS expression was detected using western blotting assay. The values shown are the means ± S.E.M. of four independent experiments. $^{***}P < 0.001$ vs. the control cells; $^{\#\#}P < 0.01$ vs. LTA-stimulated cells.

paraformaldehyde for 10 min at 37°C, double washed using PBS, incubated with 0.1% Triton X-100 for 10 min, and then, blocked with 5% BSA for 1 h. Besides, the primary p65 antibody was added over the coverslips at 4°C overnight, and then, secondary goat anti-rabbit IgG antibody was incubated for 1 h at 37°C. 4,6-Diamidino-2 phenylindole (DAPI) was used to stain nuclei in cells. The location of nuclear translocation of p65 was spotted by using the Leica TCS SP5 confocal spectral microscope imaging system (Mannheim, Germany).

2.6. Detection of Antioxidant Enzyme Catalase (CAT). According to the method defined by Woodbury et al. [23], a native polyacrylamide gel electrophoresis (NATIVE-PAGE) was run to spot the relative banding patterns of antioxidant enzyme catalase (CAT). To this analysis, unlike normal SDS-PAGE, the running buffers and protein samples did not heat and omit SDS. The equal amounts of 50 μg proteins were run in 8% PAGE.

2.7. Statistical Analysis. The results are presented as mean ± standard error (S. E. M). The statistical difference among the groups was determined using one-way analysis of variance (ANOVA). Statistical alterations were detected significant. The P value of the Student–Newman–Keuls test was regarded as $P < 0.05$.

3. Results

3.1. AU Did Not Affect the Viability and Morphology of RAW 264.7 Cells. Cell morphology and viability were studied to evaluate the toxic effect of AU in RAW 264.7 cells. Among the tested concentrations of 5, 10, and 20 μM AU in RAW cells for 24 h, 5 and 10 μM did not affect cell morphology as well as viability (Figures 1(b) and 1(c)), respectively. However, AU at 20 μM significantly affected the morphology and viability of RAW cells. Thus, AU at feasible concentrations of 5 and 10 μM were used for the subsequent investigation.

3.2. LTA-Induced NO Production and iNOS Were Inhibited by AU. Griess reaction was applied to measure the level of NO production in AU pretreated LTA-induced RAW 264.7 cells. Systemic inflammatory events have been reported to induce a proinflammatory mediator NO [24]. A rate-limiting enzyme, inducible nitric oxide synthase (iNOS), regulates the production of NO [25]. To examine if AU inhibits NO production via the modulation of iNOS expression, the expression of iNOS was detected as shown in Figure 1(e). Figures 1(d) and 1(e) show that, at a high concentration of 10 μM, AU significantly inhibited the LTA-induced production of NO and its enzyme iNOS expression (control: 1 ± 0, DMSO: 2.5 ± 0.2, 5 μM: 2.2 ± 0.2, 10 μM: 1.5 ± 0.2) in RAW 264.7 cells. This result apprehends that the inhibition of iNOS expression by AU may be involved in the inhibition of LTA-induced NO production.

3.3. AU Inhibited LTA-Induced IL-1β, TNF-α, and COX-2 Expressions. LTA stimulated the levels of COX-2 (2.1 ± 0.3, $P < 0.01$), IL-1β (3.1 ± 0.3, $P < 0.001$), and TNF-α (3.3 ± 0.4, $P < 0.001$) dramatically compared to the nonstimulated control RAW cells (Figures 2(a)–2(d)). In contrast, AU at 5 and 10 μM distinctly alleviated COX-2 (5 μM: 1.5 ± 0.2, 10 μM: 1.1 ± 0.2), IL-1β (5 μM: 1.9 ± 0.3, 10 μM: 0.7 ± 0.1), and TNF-α (5 μM: 1.7 ± 0.3, 10 μM: 0.9 ± 0.2) induced by LTA. Moreover, AU more prominently inhibited IL-1β and TNF-α (Figures 2(c) and 2(d)).

3.4. AU Inhibits ERK1/2 and JNK1/2, But Not p38 MAPK Phosphorylation. We examined the effect of AU on LTA-induced mitogen-activated protein kinases (MAPKs), since several studies have shown that these molecules actively involve on inflammation-related events. Figure 3 shows the elevated phosphorylation of ERK1/2 (3.1 ± 0.5), JNK1/2 (3.2 ± 0.3), and p38 MAPK (3.2 ± 0.3) in LTA-induced RAW cells compared to control cells. However, AU at a higher concentration of 10 μM significantly diminished the LTA-induced phosphorylation of JNK1/2 (1.9 ± 0.2), and it concentration-dependently inhibited the ERK1/2 phosphorylation (5 μM: 1.8 ± 0.4, 10 μM: 1.4 ± 0.2); however, it is not effective on p38 (5 μM: 2.9 ± 0.4, 10 μM: 2.8 ± 0.2). These outcomes designated that AU reveals its inhibitory effects in LTA-induced inflammatory events in RAW 264.7 cells via suppressing ERK1/2 and JNK1/2 signaling cascade.

3.5. LTA-Induced NF-κB Signaling Pathway Was Inhibited by AU. NF-κB, a major transcription factor, is constantly inducing proinflammatory mediators and cytokines. This transcription factor translocates to the nucleus once it activates and binds with target DNA and then controls the activation of numerous inflammatory cytokines [25]. Here, the inhibitory effect of AU on NF-κB signaling pathways was examined by investigating the phosphorylations of IκBα and p65 and also the nuclear translocation of p65 in LTA-induced RAW cells. The results showed that AU reduced LTA-induced IκBα (DMSO: 4.0 ± 0.7, 5 μM: 2.5 ± 0.5, and 10 μM: 1.4 ± 0.3) and p65 phosphorylation (DMSO: 3.5 ± 0.3, 5 μM: 2.7 ± 0.2, and 10 μM: 1.9 ± 0.2) (Figures 4(a) and 4(b)) and withdrew the nuclear translocation of p65 (Figure 4(c)). These results demonstrate that AU's anti-inflammatory effect in LTA-induced cells may probably be via inhibiting the NF-κB signaling pathway.

3.6. AU Enhances Antioxidant Defense Molecules. Oxidative stress occurs by the elevated levels of reactive oxygen species (ROS) and NO or reduced levels of antioxidant defense molecules, such as reduced glutathione (GSH), catalase (CAT), and superoxide dismutase (SOD) [7]. Numerous studies have established that oxidative stress could induce the progress of inflammatory diseases [26]. LTA stimulation in RAW cells has been demonstrated to decrease in the expression of HO-1 (1.7 ± 0.3), antioxidant enzyme catalase, and the nonenzymatic GSH (Figures 5(a)–5(c)). AU pretreatment was not effective on LTA-stimulated

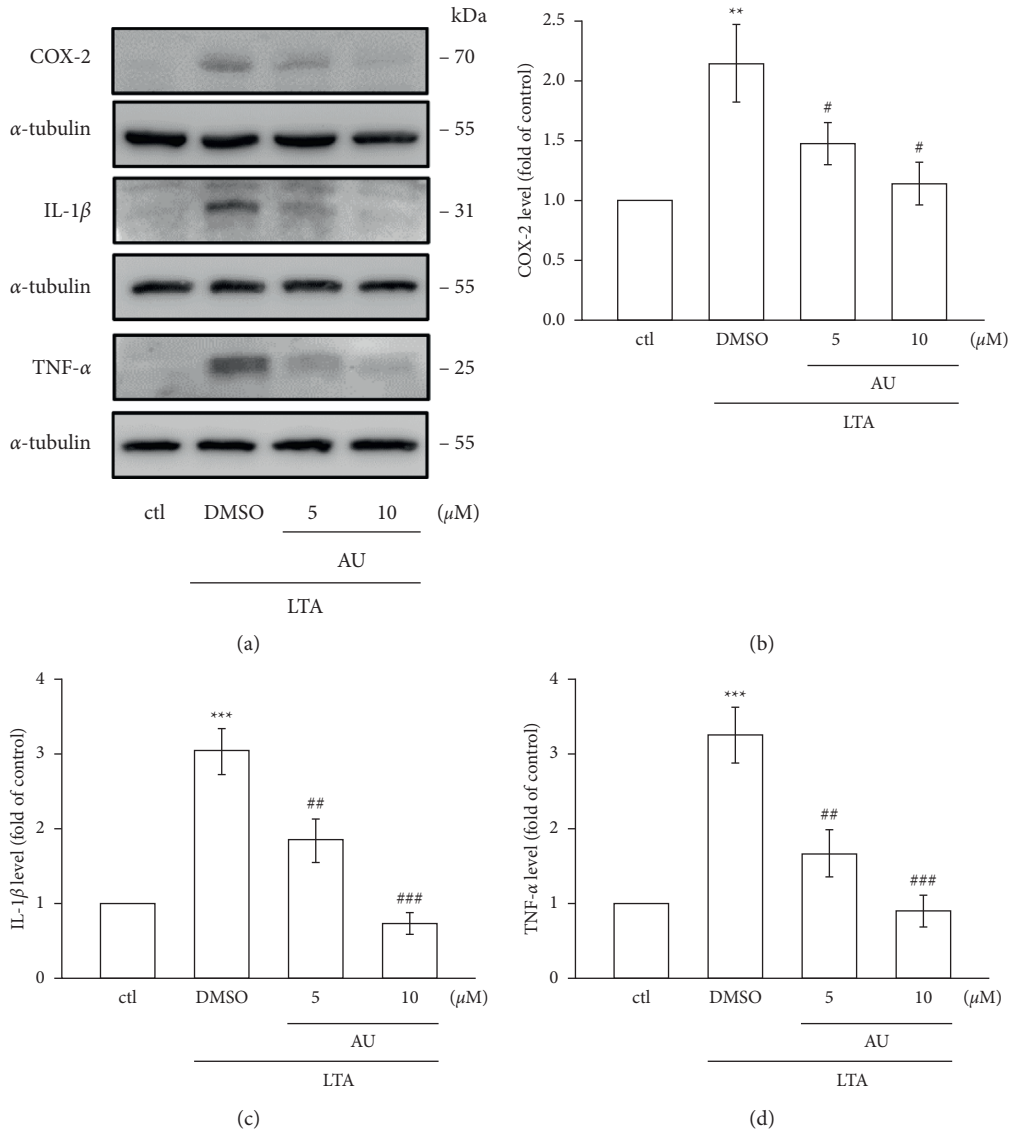

Figure 2: Effects of AU on the LTA-induced expression COX-2, IL-1β, and TNF-α in RAW 264.7 macrophages. (a)–(d) Cells were untreated or pretreated with AU (5 and 10 μM) for 30 min and then stimulated with LTA (5 μg/ml) for 24 h. COX-2, IL-1β, and TNF-α were detected as described in Section 2. The values shown are the means ± S.E.M. of four independent experiments. $^{**}P < 0.01$ and $^{***}P < 0.001$ vs. the control cells; $^{\#}P < 0.05$, $^{\#\#}P < 0.01$, and $^{\#\#\#}P < 0.001$ vs. LTA-stimulated cells.

reduction of HO-1 (5 μM: 2.4 ± 0.4, 10 μM: 2.3 ± 0.3), CAT, and GSH in RAW cells. These results indicate that the antioxidant defense systems could not play a role in AU-mediated anti-inflammatory effects in LTA-stimulated RAW cells.

4. Discussion

Auraptene (AU), a natural prenyloxycoumarin, is mostly present in citrus fruits. Auraptene (AU) possesses numerous pharmacological properties such as anticancer, antibacterial, antioxidant, and antiinflammatory [27]. Here, we found that auraptene (5 and 10 μM) did not display cytotoxicity in both control and LTA-stimulated RAW cells. Hence, the ideal concentrations of 5 and 10 μM of auraptene were used in this study. A study exposed that auraptene at concentrations of 5–40 μM had no cytotoxicity on murine lymphocytes [28]. Together, as revealed in the present study, anti-inflammatory and antioxidative effects of auraptene are not through its cytotoxicity. Moreover, this study found that anti-inflammatory effects of AU was facilitated via preventing the production of NO and its enzyme iNOS expression. Auraptene also inhibited the LTA-induced protein expression of IL-1β and TNF-α by inhibiting the mitogen activated protein kinases (MAPKs)/NF-κB pathways.

As it is established, proinflammatory cytokines and mediators such as NO, IL-1β, IL-6, and TNF-α play a major role in the inflammatory process. Chronic inflammation has been reported to cause several diseases such as cancers, arthritis, and cardiovascular diseases [29]. A recent study

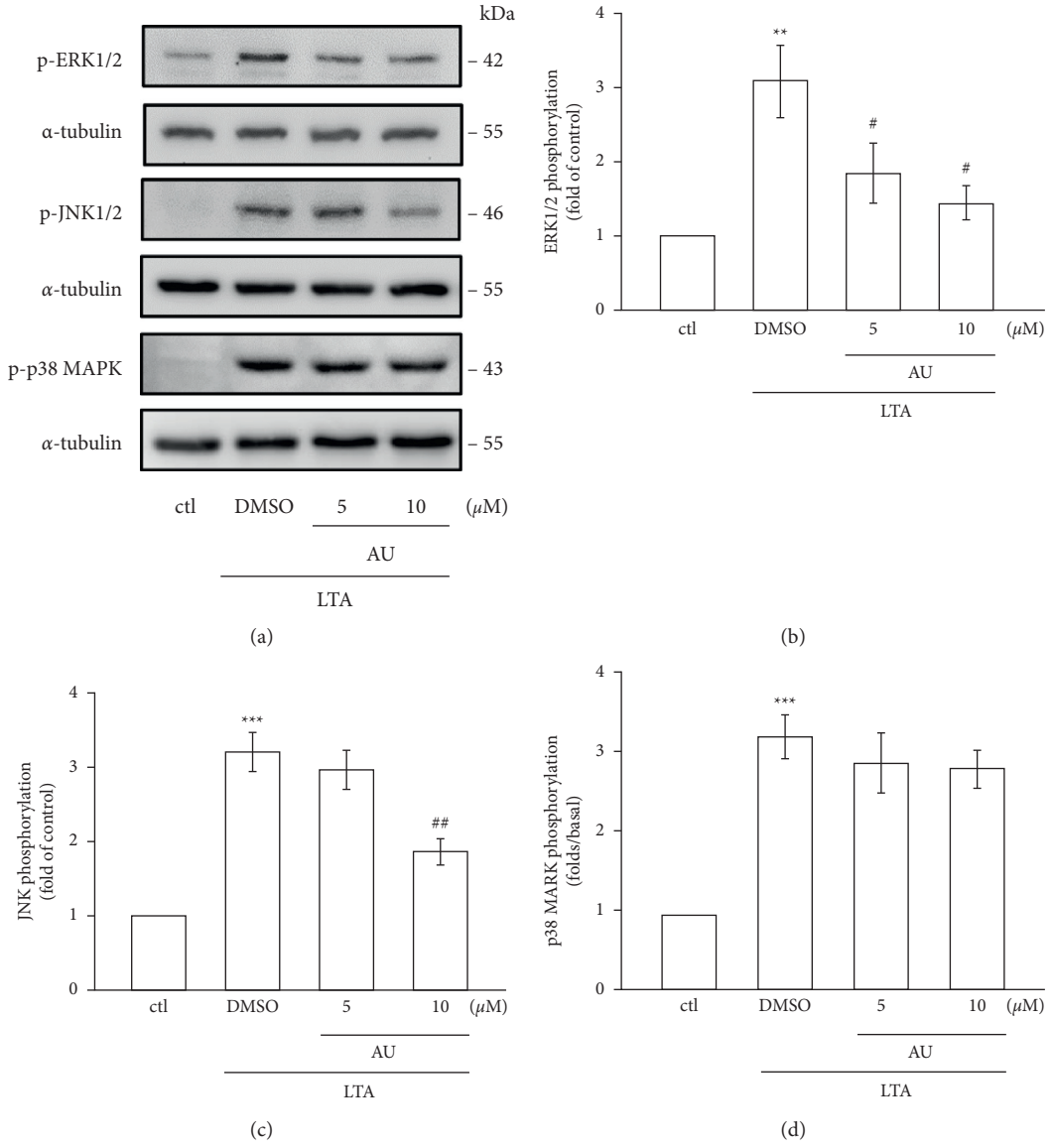

Figure 3: Effects of AU in LTA-induced phosphorylation of MAPKs in RAW 264.7 macrophages. (a) Cells were untreated or pretreated with AU (5 and 10 μM) for 30 min and were then stimulated with LTA (5 μg/ml) for 1 h. The specific pERK, pJNK, and p38 MAPK antibodies were used to detect these proteins. α-Tubulin was used as the internal control. (b)–(d) The statistical values shown are the means ± S.E.M. of four independent experiments. $^{**}P < 0.01$ and $^{***}P < 0.001$ vs. the control cells; $^{\#}P < 0.05$ and $^{\#\#}P < 0.01$ vs. LTA-stimulated cells.

specified that AU at 10–90 μM reduced the levels of IL-6 and TNF-α in phytohemagglutinin- (PHA-) stimulated human lymphocytes [30]. A previous study from these authors has also established that AU alleviates IL-4, IL-10, and interferon (IFN-γ) levels [29]. NO plays a role in the pathogenesis of several inflammatory disorders, and its production in activated macrophages via the rate-limiting enzyme iNOS induces several acute and chronic inflammatory conditions [31]. COX-2 is reported to be overexpressed during the course of LPS-induced inflammatory reaction [32]. Studies have described that the overexpression of iNOS and COX-2 stimulates the activation of NO and PGE_2 in activated macrophages, respectively. Overproduction of such inflammatory mediators can result in chronic inflammatory diseases [33]. Here, we found that AU expressively and without causing cytotoxicity inhibits the level of NO in LTA-stimulated RAW 264.7 cells. The AU's inhibitory effect on LTA-induced NO production appears to involve the reduction of iNOS expression. Moreover, AU dramatically inhibited the LTA-induced expression of iNOS, COX-2, TNF-α, and IL-1β. Okuyama et al. [34] showed that AU suppressed the LPS-induced expression of COX-2, IL-1β, and TNF-α in astrocytes isolated from the cerebral cortex of ICR mice. Niu et al. found an inhibitory mechanism for AU via IL-2, IFN-γ, and IL-4 in lymphocytes isolated from C57BL/6 mice [28]. These results are consistent with our results and evident of the anti-inflammatory properties of AU.

The induction of inflammatory mediators involves the activation of multiple signal transduction pathways,

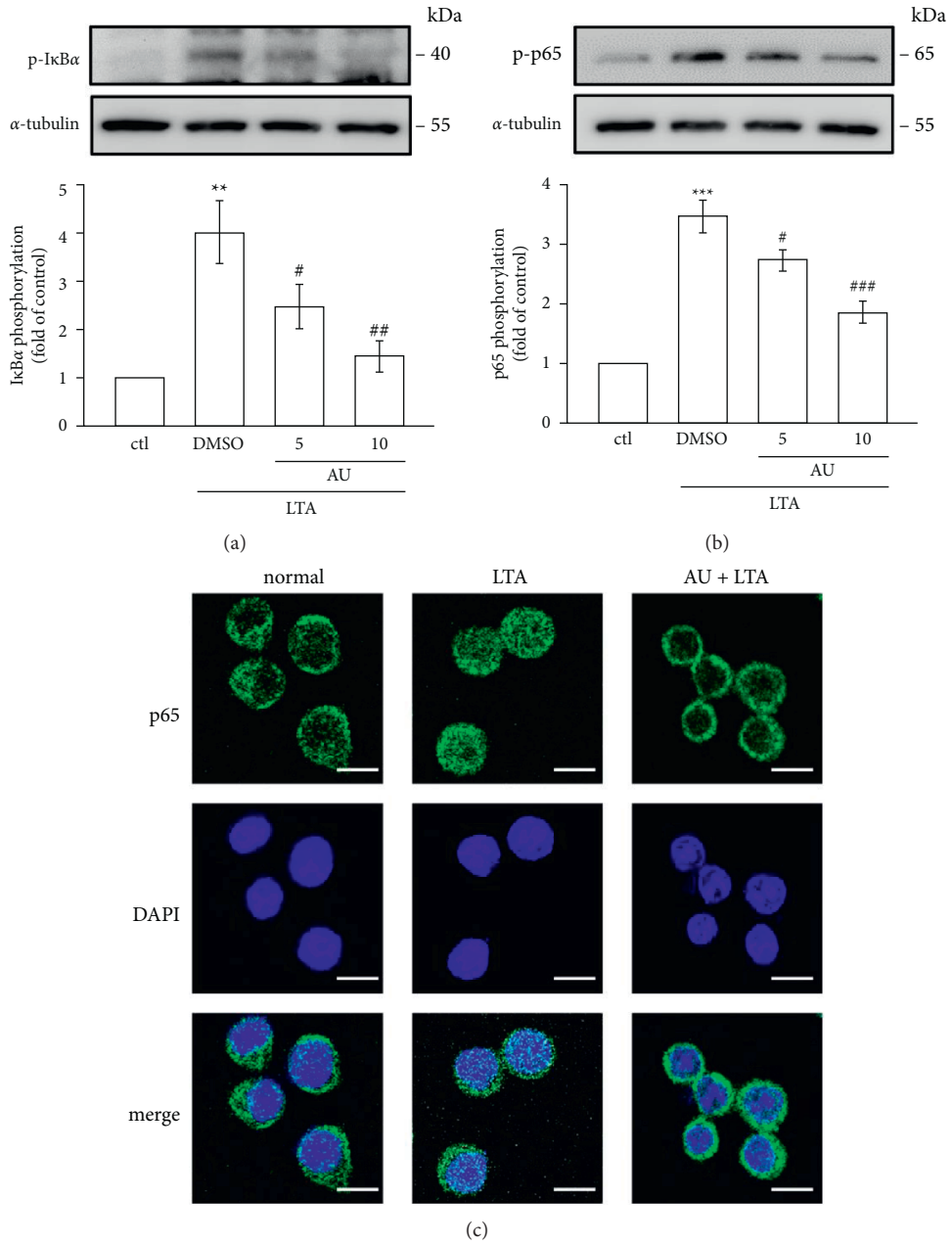

Figure 4: AU controls the NF-κB signaling pathway induced by LTA in RAW 264.7 macrophages. Cells were pretreated with AU (5 and 10 μM) for 30 min and were then stimulated with LTA (5 μg/ml) for 1 h. The phosphorylation of (a) IκBα and (b) p65 in LTA-induced RAW cells was detected as described in Section 2. (c) PTE inhibited LTA-induced p65 nuclear translocation. The values shown are the means ± S.E.M. of four independent experiments. $^{**} < 0.01$ and $^{***} < 0.001$ vs. the control cells; $^{\#}P < 0.05$, $^{\#\#}P < 0.01$, and $^{\#\#\#}P < 0.001$ vs. LTA-stimulated cells.

including mitogen-activated protein kinases (MAPKs) such as p38, ERK, and JNK [35]. It is reported that blocking p38, ERK, and JNK MAPK pathways could decrease iNOS and COX-2 expression and TNF-α and IL-1β production in macrophage inflammation [36]. The MAPK/NF-κB signaling pathway was conveyed to play a vital role in the expression of TNF-α, IL-6, IL-1β, and COX-2 in many cell types [37]. Therefore, we examined the effect of AU on MAPK/NF-κB pathway activation. Niu et al. found esculin significantly inhibited the activation of the MAPK pathway in LPS-induced peritoneal macrophages [38]. Guo et al. found both degradation and phosphorylation of IκBα and activation of NF-κB p65 stimulated by LPS are significantly controlled by imperatorin in RAW 264.7 macrophages [39]. Our recent study found that pterostilbene, a natural substance of blueberry and an analog of resveratrol, significantly inhibited the NF-κB signaling pathway and ERK phosphorylation in RAW 264.7 cells [40]. Thus, it is proposed that coumarin derivatives may inhibit the MAPK/NF-κB signaling pathway in LPS-induced inflammatory reaction.

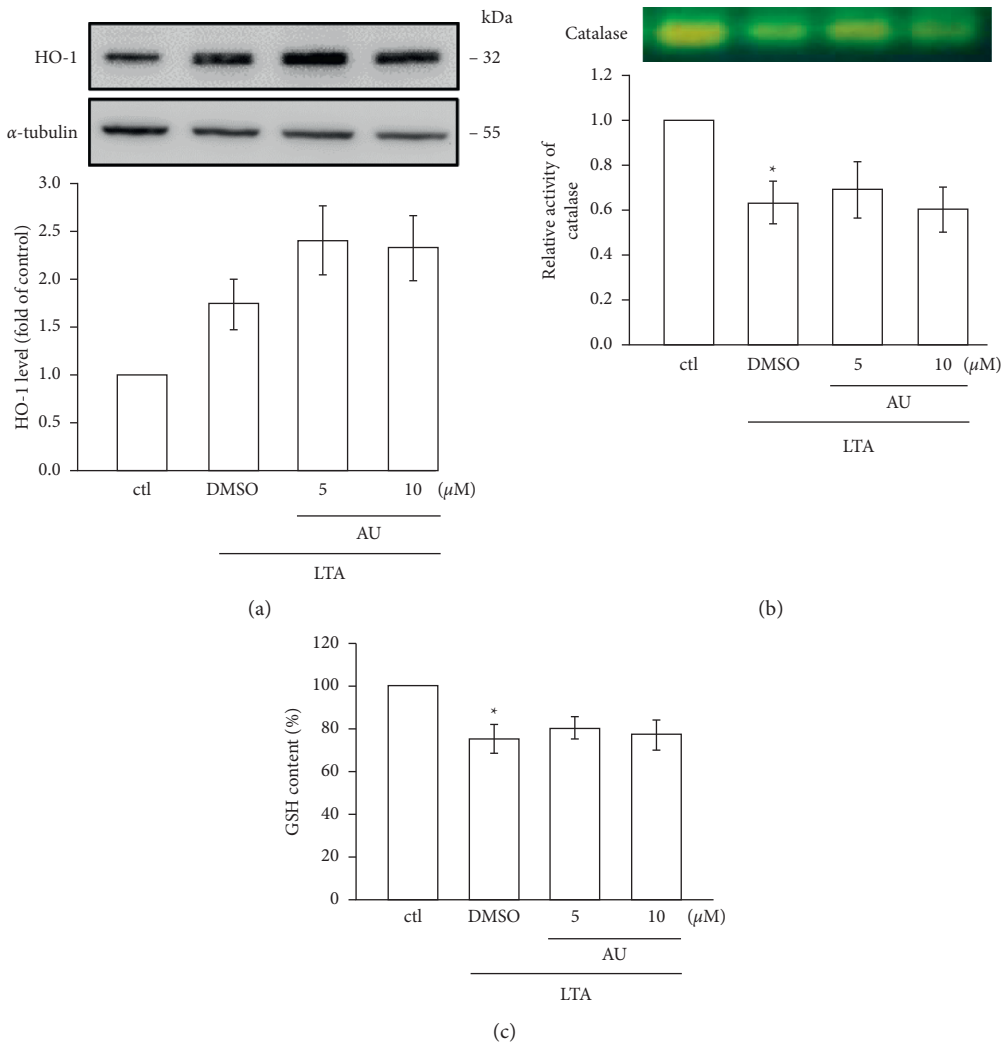

Figure 5: AU enhances antioxidant defense molecules in LTA-stimulated RAW cells. Cells were untreated or pretreated with AU (5 and 10 μM) for 30 min followed by LTA (5 μg/ml) for 24 h. The expression of HO-1 (a), catalase (CAT) activity (b), and glutathione (GSH) content (c) in LTA-induced RAW cells was determined using western blotting, native polyacrylamide gel electrophoresis (NATIVE-PAGE), and spectrophotometric analyses, respectively. The values shown are the means ± S.E.M. of four independent experiments. $^{*}P < 0.05$ vs. the control cells.

The results of this study consistently showed that AU strongly reversed the LTA-induced phosphorylation of JNK and ERK and the nuclear translocation of the p65 subunit. The induction of NF-κB is controlled by IκB kinase (IKK) complex activation, and IKK phosphorylates IκBα and initiates ubiquitin-dependent IκBα degradation [41]. This process could lead NF-κB translocation to the nucleus, where it attaches to the promoter regions of the target gene and brings proinflammatory mediators such as iNOS, COX-2, TNF-α, and IL-6 [42]. The phosphorylation of IκB and p65 can be induced by LTA, and it also can induce p65 translocation from the cytoplasm to nuclei [13]. LTA binds with toll-like receptor (TLR2), which in turn activates NF-κB and consequently translocated to nuclei from the cytoplasm [43]. Hence, these outcomes may propose that AU decreases LTA-induced inflammatory events in RAW cells via inhibiting the activation of JNK/ERK and NF-κB pathways.

Activated oxygen (O_2^*) radicals are metabolized to H_2O and successively converted to H_2O_2 by superoxide dismutase enzymes (SOD) and then to H_2O by glutathione peroxidase or to H_2O_2 and O_2 by catalases (CAT) [44]. A previous study found that irisin, a molecule secreted from skeletal muscle in response to physical exercise, plays a regulatory role in an immune system activity and can protect the cell from free-radical-induced cellular oxidative damage by the activation of antioxidative mechanisms [45]. Furthermore, a rise in HO-1 expression was identified to exert both antioxidant and anti-inflammatory effects [44]. HO-1 plays an important role in the protection of oxidative stress in chronic disease [46]. Furthermore, HO-1 has been reported to inhibit various inflammatory responses to exhibit its cellular protective role. Several antioxidants can induce HO-1 expression to cope oxidative damage, and thus, compounds that can activate HO-1 expression may be favorable in the

treatment of oxidative damage. A natural anti-inflammatory compound curcumin was found to increase the activity of CAT to protect RAW cells from LPS-induced ROS damages [47]. Reduction of reduced glutation (GSH) had reported to lead the progress of several diseases, as GSH inhibits oxidative stress-induced cell damage [48]. Therefore, we examined whether AU can involve the downstream mechanism via interaction with HO-1 to its antioxidative action. However, AU did not augment HO-1, CAT, and GSH, which postulates that antioxidant mechanisms may not associate to AU's anti-inflammatory role in LTA-induced RAW cells.

5. Conclusions

This study shows the anti-inflammatory effects of auraptene via diminishing iNOS, COX-2, IL-1β, and TNF-α expression in LTA-induced RAW 264.7 macrophages. The inhibitory property of AU is mediating at least in part via inhibiting NF-κB, along with the MAPK (JNK and ERK) pathway. Moreover, this study also found that AU's anti-inflammatory role was not depending on antioxidant mechanisms, as AU was not effective in HO-1, CAT, and GSH in the LTA-induced inflammatory RAW 264.7 cells.

Data Availability

Data can be obtained from the corresponding author on reasonable request.

Conflicts of Interest

The authors declare no conflicts of interest.

Authors' Contributions

Chih-Hsuan Hsia, Thanasekaran Jayakumar, Wan-Jung Lu, and Joen-Rong Sheu authors are contributed equally in this work. CHH, TJ, and JRS designed work and wrote the paper. WJL, CWH, and CHH carried out the experiments. CHH, PSB, and WJL performed data analyses. WCH, MM, and YC provided interpretation. All authors approved for the final submission.

Acknowledgments

This study was funded by grants from the Ministry of Science and Technology of Taiwan (MOST 107-2320-B-038-035-MY2 and MOST108-2320-B-038-031-MY3), Taipei Medical University (DP2-107-21121-N-02), Shin Kong Wu Ho-Su Memorial Hospital-Taipei Medical University (SKH-TMU-107-04), and Shin Kong Wu Ho-Su Memorial Hospital (2019SKHADR032 and 2021SKHAND005).

References

[1] P. P. Tak and G. S. Firestein, "NF-κB: a key role in inflammatory diseases," *Journal of Clinical Investigation*, vol. 107, no. 1, pp. 7–11, 2001.

[2] V. R. Askari, V. Baradaran Rahimi, S. A. Tabatabaee, and R. Shafiee-Nick, "Combination of Imipramine, a sphingomyelinase inhibitor, and β-caryophyllene improve their therapeutic effects on experimental autoimmune encephalomyelitis (EAE)," *International Immunopharmacology*, vol. 77, Article ID 105923, 2019.

[3] P. Fu, A. A. Birukova, J. Xing et al., "Amifostine reduces lung vascular permeability via suppression of inflammatory signalling," *European Respiratory Journal*, vol. 33, no. 3, pp. 612–624, 2009.

[4] V. R. Askari and R. Shafiee-Nick, "The protective effects of β-caryophyllene on LPS-induced primary microglia M1/M2 imbalance: a mechanistic evaluation," *Life Sciences*, vol. 219, no. 15, pp. 40–73, 2019.

[5] C.-j. Huang and M.-C. Wu, "Differential effects of foods traditionally regarded as "heating" and "cooling" on prostaglandin E2 production by a macrophage cell line," *Journal of Biomedical Science*, vol. 9, no. 6, pp. 596–606, 2002.

[6] A. Murakami, T. Shigemori, and H. Ohigashi, "Zingiberaceous and citrus constituents, 1′-acetoxychavicol acetate, zerumbone, auraptene, and nobiletin, suppress lipopolysaccharide-induced cyclooxygenase-2 expression in RAW264.7 murine macrophages through different modes of action," *Journal of Nutrition*, vol. 135, no. 12, pp. 2987s–2992s, 2005.

[7] A. Rahal, A. Kumar, V. Singh et al., "Oxidative stress, prooxidants, and antioxidants: the interplay," *BioMed Research International*, vol. 2014, Article ID 761264, 19 pages, 2014.

[8] V. Baradaran Rahim, M. T. Khammar, H. Rakhshandeh, A. Samzadeh-Kermani, A. Hosseini, and V. R. Askari, "Crocin protects cardiomyocytes against LPS-Induced inflammation," *Pharmacological Reports*, vol. 71, no. 6, pp. 1228–1234, 2019.

[9] M. Khosravi, A. Poursaleh, G. Ghasempour, S. Farhad, and M. Najafi, "The effects of oxidative stress on the development of atherosclerosis," *Biological Chemistry*, vol. 400, no. 6, pp. 711–732, 2019.

[10] J. E. Wang, M. K. Dahle, M. McDonald, S. J. Foster, A. O. Aasen, and C. Thiemermann, "Peptidoglycan and lipoteichoic acid in gram-positive bacterial sepsis: receptors, signal transduction, biological effects, and synergism," *Shock*, vol. 20, no. 5, pp. 402–414, 2003.

[11] J. C. Leemans, M. Heikens, K. P. M. van Kessel, S. Florquin, and T. van der Poll, "Lipoteichoic acid and peptidoglycan from Staphylococcus aureus synergistically induce neutrophil influx into the lungs of mice," *Clinical and Vaccine Immunology*, vol. 10, no. 5, pp. 950–953, 2003.

[12] E. M. Greenfield, M. A. Beidelschies, J. M. Tatro, V. M. Goldberg, and A. G. Hise, "Bacterial pathogen-associated molecular patterns stimulate biological activity of orthopaedic wear particles by activating cognate Toll-like receptors," *Journal of Biological Chemistry*, vol. 285, no. 42, pp. 32378–32384, 2010.

[13] H.-C. Chang, K.-H. Lin, Y.-T. Tai, J.-T. Chen, and R.-M. Chen, "Lipoteichoic acid-induced TNF-α and IL-6 gene expressions and oxidative stress production IN macrophages are suppressed BY ketamine through downregulating toll-like receptor 2-MEDIATED activation OF ERK1/2 and NFκB," *Shock*, vol. 33, no. 5, pp. 485–492, 2010.

[14] F. Epifano, S. Genovese, and M. Curini, "Auraptene: phytochemical and pharmacological properties," in *Phytochemistry Research Progressed*, T. Matsumoto, Ed., pp. 145–162, Nova Science Publishers Inc., New York, NY, USA, 2008.

[15] M. Prince, Y. Li, A. Childers, K. Itoh, M. Yamamoto, and H. E. Kleiner, "Comparison of citrus coumarins on carcinogen-detoxifying enzymes in Nrf2 knockout mice," *Toxicology Letters*, vol. 185, no. 3, pp. 180–186, 2009.

[16] A. Murakami, Y. Nakamura, and T. Tanaka, "Suppression by citrus auraptene of phorbol ester- and endotoxin-induced inflammatory responses: role of attenuation of leukocyte activation," *Carcinogenesis*, vol. 21, no. 10, pp. 1843–1850, 2000.

[17] K. Takeda, H. Utsunomiya, S. Kakiuchi et al., "Citrus auraptene reduces Helicobacter pylori colonization of glandular stomach lesions in Mongolian gerbils," *Journal of Oleo Science*, vol. 56, no. 5, pp. 253–260, 2007.

[18] F. Soltani, F. Mosaffa, M. Iranshahi et al., "Auraptene from Ferula szowitsiana protects human peripheral lymphocytes against oxidative stress," *Phytotherapy Research*, vol. 24, no. 1, pp. 85–89, 2010.

[19] F. Epifano, G. Molinaro, S. Genovese, R. T. Ngomba, F. Nicoletti, and M. Curini, "Neuroprotective effect of prenyloxycoumarins from edible vegetables," *Neuroscience Letters*, vol. 443, no. 2, pp. 57–60, 2008.

[20] T. Tanaka, H. Sugiura, and R. Inaba, "Immunomodulatory action of citrus auraptene on macrophage functions and cytokine production of lymphocytes in female BALB/c mice," *Carcinogenesis*, vol. 20, no. 8, pp. 1471–1476, 1999.

[21] T. Tanaka, H. Kohno, and M. Murakami, "Suppressing effects of dietary supplementation of the organoselenium 1,4-henylenebis(methylene)selenocyanate and the Citrus antioxidant auraptene on lung metastasis of melanoma cells in mice," *Cancer Research*, vol. 14, pp. 3713–3716, 2000.

[22] V. D. La, L. Zhao, F. Epifano, S. Genovese, and D. Grenier, "Anti-inflammatory and wound healing potential of citrus auraptene," *Journal of Medicinal Food*, vol. 16, no. 10, pp. 961–964, 2013.

[23] W. Woodbury, A. K. Stahmann, and M. A. Stahman, "An improved procedure using ferricyanide for detecting catalase isozymes," *Analytical Biochemistry*, vol. 44, no. 1, pp. 301–305, 1971.

[24] J. N. Sharma, A. Al-Omran, and S. S. Parvathy, "Role of nitric oxide in inflammatory diseases," *Inflammopharmacology*, vol. 15, no. 6, pp. 252–259, 2007.

[25] X. Li and G. R. Stark, "NF-κB-dependent signaling pathways," *Experimental Hematology*, vol. 30, no. 4, pp. 285–296, 2002.

[26] A. Singh, R. Kukreti, L. Saso, and S. Kukreti, "Oxidative stress: a key modulator in neurodegenerative diseases," *Molecules*, vol. 24, no. 8, p. 1583, 2019.

[27] S. Genovese and F. Epifano, "Auraptene: a natural biologically active compound with multiple targets," *Current Drug Targets*, vol. 12, no. 3, pp. 381–386, 2011.

[28] X. Niu, Z. Huang, L. Zhang, X. Ren, and J. Wang, "Auraptene has the inhibitory property on murine T lymphocyte activation," *European Journal of Pharmacology*, vol. 750, pp. 8–13, 2015.

[29] V. R. Askari, V. Baradaran Rahimi, S. A. Rezaee, and M. H. Boskabady, "Auraptene regulates Th 1/Th 2/T Reg balances, NF-κB nuclear localization and nitric oxide production in normal and Th 2 provoked situations in human isolated lymphocytes," *Phytomedicine*, vol. 43, pp. 1–10, 2018.

[30] V. R. Askari, V. B. Rahimi, and R. Zargarani, "Anti-oxidant and anti-inflammatory effects of auraptene on phytohemagglutinin (PHA)-induced inflammation in human lymphocytes," *Pharmacological Reports*, vol. 73, pp. 54–162, 2021.

[31] F. Aktan, "iNOS-mediated nitric oxide production and its regulation," *Life Sciences*, vol. 75, no. 6, pp. 639–653, 2004.

[32] J. K. Lee, B. C. Sayers, K.-S. Chun et al., "Multi-walled carbon nanotubes induce COX-2 and iNOS expression via MAP kinase-dependent and -independent mechanisms in mouse RAW264.7 macrophages," *Particle and Fibre Toxicology*, vol. 9, no. 1, p. 14, 2012.

[33] F. Zhao, L. Chen, C. Bi, M. Zhang, W. Jiao, and X. Yao, "In vitro anti-inflammatory effect of picrasmalignan A by the inhibition of iNOS and COX-2 expression in LPS-activated macrophage RAW 264.7 cells," *Molecular Medicine Reports*, vol. 8, no. 5, pp. 1575–1579, 2013.

[34] S. Okuyama, M. Morita, M. Kaji et al., "Auraptene acts as an anti-inflammatory agent in the mouse brain," *Molecules*, vol. 20, no. 11, pp. 20230–20239, 2015.

[35] S. H. Kim, C. J. Smith, and L. J. Van Eldik, "Importance of MAPK pathways for microglial pro-inflammatory cytokine IL-1β production," *Neurobiology of Aging*, vol. 25, no. 4, pp. 431–439, 2004.

[36] G. Pearson, F. Robinson, T. Beers Gibson et al., "Mitogen-activated protein (MAP) kinase pathways: regulation and physiological functions," *Endocrine Reviews*, vol. 22, no. 2, pp. 153–183, 2001.

[37] O. A. Olajide, M. A. Aderogba, and B. L. Fiebich, "Mechanisms of anti-inflammatory property of Anacardium occidentale stem bark: inhibition of NF-κB and MAPK signalling in the microglia," *Journal of Ethnopharmacology*, vol. 145, no. 1, pp. 42–49, 2013.

[38] X. Niu, Y. Wang, W. Li et al., "Esculin exhibited anti-inflammatory activities in vivo and regulated TNF-α and IL-6 production in LPS-stimulated mouse peritoneal macrophages in vitro through MAPK pathway," *International Immunopharmacology*, vol. 29, no. 2, pp. 779–786, 2015.

[39] W. Guo, J. Sun, L. Jiang et al., "Imperatorin attenuates LPS-induced inflammation by suppressing NF-κB and MAPKs activation in RAW 264.7 macrophages," *Inflammation*, vol. 35, no. 6, pp. 1764–1772, 2012.

[40] T. Jayakumar, M. P. Wu, and J. R. Sheu, "Involvement of antioxidant defenses and NF-κB/ERK signaling in anti-inflammatory effects of pterostilbene, a natural analogue of resveratrol," *Applied Sciences*, vol. 11, pp. 1–12, 2021.

[41] A. Oeckinghaus and S. Ghosh, "The NF-kappaB family of transcription factors and its regulation," *Cold Spring Harbor Perspectives in Biology*, vol. 1, no. 4, Article ID a000034, 2009.

[42] T. Liu, L. Zhang, D. Joo, and S. C. Sun, "NF-κB signaling in inflammation," *Signal transduction and targeted therapy*, vol. 2, Article ID 17023, 2017.

[43] C.-Y. Chuang, T.-L. Chen, and R.-M. Chen, "Molecular mechanisms of lipopolysaccharide-caused induction of surfactant protein-A gene expression in human alveolar epithelial A549 cells," *Toxicology Letters*, vol. 191, no. 2-3, pp. 132–139, 2009.

[44] B. Usluoğullari, C. A. Usluogullari, F. Balkan, and M. Orkmez, "Role of serum levels of irisin and oxidative stress markers in pregnant women with and without gestational diabetes," *Gynecological Endocrinology: The Official Journal of the International Society of Gynecological Endocrinology*, vol. 33, no. 5, pp. 405–407, 2017.

[45] A. I. Mazur-Bialy, K. Kozlowska, and E. Pochec, "Myokine irisin-induced protection against oxidative stress *in vitro*. Involvement of heme oxygenase-1 and antioxidazing enzymes superoxide dismutase-2 and glutathione peroxidase," *Journal of Physiology and Pharmacology*, vol. 69, no. 1, pp. 117–125, 2018.

[46] B. G. Park, C. I. Yoo, H. T. Kim, C. H. Kwon, and Y. K. Kim, "Role of mitogen-activated protein kinases in hydrogen peroxide-induced cell death in osteoblastic cells," *Toxicology*, vol. 215, no. 1-2, pp. 115–125, 2005.

[47] X. Lin, D. Bai, Z. Wei et al., "Curcumin attenuates oxidative stress in RAW264.7 cells by increasing the activity of antioxidant enzymes and activating the Nrf2-Keap1 pathway," *PLoS One*, vol. 14, no. 5, Article ID e0216711, 2019.

[48] M. Deponte, "The incomplete glutathione puzzle: just guessing at numbers and figures?" *Antioxidants and Redox Signaling*, vol. 27, no. 15, pp. 1130–1161, 2017.

Hindawi
Evidence-Based Complementary and Alternative Medicine
Volume 2021, Article ID 1021127, 7 pages
https://doi.org/10.1155/2021/1021127

Research Article

Analysis of Influencing Factors of Compliance with Non-Vitamin K Antagonist Oral Anticoagulant in Patients with Nonvalvular Atrial Fibrillation and Correlation with the Severity of Ischemic Stroke

Li Zhu, Xiaodan Zhang, and Jing Yang

Clinical Nursing Teaching and Research Section, The Second Xiangya Hospital of Central South University, Changsha, Hunan 410011, China

Correspondence should be addressed to Jing Yang; yangj3637@csu.edu.cn

Received 15 August 2021; Revised 15 September 2021; Accepted 4 October 2021; Published 19 October 2021

Academic Editor: Thanasekaran Jayakumar

Nonvalvular atrial fibrillation (NVAF) is associated with an increased risk of stroke and thrombus, and anticoagulant therapy is a key link in the prevention of stroke. At present, the anticoagulation rate of atrial fibrillation in China is low, and there are many factors affecting the adherence of patients with atrial fibrillation to anticoagulation. Non-vitamin K antagonist oral anticoagulants (NOACs) are anticoagulant with high application value due to their high safety and low risk of intracranial hemorrhage, stroke, and death. However, the compliance of NOACs is poor, and the current situation of anticoagulants in China is not optimistic. In this study, a total of 156 patients with NVAF who received NOAC anticoagulation therapy in our hospital from January 2018 to January 2019 were retrospectively analyzed. The results showed that education background, place of residence, number of complications, CHA2DS2-VASc score, and HAS-BLED score were independent influencing factors for NOACS compliance of NVAF patients. Also, the Pearson correlation analysis showed that there was a negative correlation ($r = -0.465$, $P < 0.001$) between NOAC compliance and severity of ischemic stroke in patients with NVAF. Therefore, clinical supervision and management of patients with NVAF after NOACs should be strengthened to improve the compliance of patients with NVAF after NOACs, reduce the damage of ischemic stroke, and improve their prognosis.

1. Introduction

Atrial fibrillation (AF) is an atrial rhythm with ineffective contractions and chaotic excitement caused by disorders of the heart's electrical system [1]. This is the most common persistent arrhythmia in clinical practice. Ischemic stroke is one of the most dangerous complications of AF. Epidemiological statistics show that the prevalence of AF in our country is 0.8%, and the incidence of subsequent ischemic stroke is up to 5%. [2]. Also, the annual incidence of ischemic stroke in patients with nonvalvular atrial fibrillation (NVAF) is 3–5 times that of patients with non-AF [2]. The non-vitamin K antagonist oral anticoagulants (NOACs) can effectively reduce the stroke risk of NVAF patients by 60%~70% [3].

However, in the actual application of anticoagulation therapy, under the influence of individualized differences in dosages, cross reactions between medicines and foods, insufficient clinical anticoagulation therapy, and patients' lack of awareness of the necessity of anticoagulation, the overall treatment rate and medication compliance of NOAC anticoagulation in NVAF patients are not high [4, 5]. It largely increases the risk of ischemic stroke in patients with NVAF in China, and the severity of stroke and its recurrence rate are also affected [6]. Based on this, this research discusses the influencing factors of NOAC anticoagulation compliance in NVAF patients and their correlation with the severity of ischemic stroke. It is expected to provide relevant references for the improvement of compliance with NOAC anticoagulation therapy and the

management of safety and effectiveness in clinical NVAF patients.

2. Materials and Methods

2.1. General Information. 156 patients with NVAF who received NOAC anticoagulation therapy in our hospital from January 2018 to January 2019 were retrospectively analyzed. There were 87 males and 69 females, with an average age of (59.87 ± 11.64) years.

2.2. Inclusion Criteria. (i) All patients met the diagnostic criteria for NVAF in the 2017ACC Expert Consensus on Perioperative Anticoagulation Management Decisions in Patients with Nonvalvular Atrial Fibrillation [6]; (ii) the diagnostic criteria for patients with ischemic stroke were referred to the Chinese Guidelines for the Diagnosis and Treatment of Acute Ischemic Stroke (2018 edition); and (iii) patients who met the CHA2DS2-VASc (Including congestive heart failure/left ventricular dysfunction, hypertension, age ≥ 75 years, diabetes, history of stroke/TIA/thromboembolism, vascular disease, and female) and HAS-BLED (including hypertension, abnormal renal and liver function, stroke, bleeding, labile INRS, elderly, drugs, or alcohol) scoring criteria for NOACs anticoagulation [7].

2.3. Exclusion Criteria. (i) Accompanied by other diseases such as valvular disease and thromboembolic disease that require anticoagulation; (ii) pregnant and/or lactating women; (iii) patients with previous bleeding history; (iv) with other serious complications or important organ diseases; (v) patients with mental or consciousness disorders and communication difficulties; and (vi) patients who have joined other studies or received other anticoagulation therapy in recent 3 months.

2.4. Method

2.4.1. Collecting the Baseline Information. All patients were followed up for 2 years, with an interval of 2 months in the first 6 months, an interval of 3 months in the next 6 months, and an interval of 4 months in the second year. Hospital review was the main method of follow-up.

The electronic medical records were used to collect baseline data on all patients, including gender, age, diploma, occupation, marriage, smoking history, drinking history, number of complications, number of drugs used for complications, CHA2DS2-VASc score, and HAS-BLED score. Also, personal health follow-up records were established according to the collected data.

2.4.2. Survey of Compliance. Design of the medication compliance questionnaire: patient compliance was measured by the following four questions: (i) Can you take your medication as often as your doctor requires? (ii) Can you take the medication in the amount required by the doctor? (iii) Are you able to take your medication at the time and in the manner required by your doctor? (vi) Can you take your medication for a long period of time as required by your doctor? (v) Can you take your medication regularly according to your doctor's requirements? The options are "not at all," "occasionally," "basically," and "completely," respectively, 0~3 points.

The total score ranges from 0 to 12 points. If the score is 12, the medication adherence is good. If the score is <12, the medication adherence is poor. In this study, the Cronbach's α coefficient of the questionnaire was 0.867, indicating good reliability.

2.4.3. Investigation of Clinical End Points. At the last follow-up, the number of ischemic stroke, hemorrhagic events, and death cases in the good compliance group and poor compliance group was counted.

2.4.4. Survey of Ischemic Stroke Severity. The severity of stroke in all patients with ischemic stroke was assessed using the NIH Stroke Scale (NIHSS) [8]. The full score of the NIHSS scale was 42; a score of 0-1 was classified as normal, 1~4 as mild stroke/minor stroke, 5–15 as moderate stroke, 16–20 as moderate severe stroke, and 21~42 as severe stroke.

2.5. Statistical Methods. All data were processed with SPSS 22.0 statistical software, and GraghPad prism 8 was used to make statistical graphs. Measurement data are expressed as mean ± standard deviation ($\overline{x} \pm s$), an independent-sample t-test is used for comparison between groups, count data are expressed as [n (%)], and the chi-square (χ^2) test is performed. Factors significant in univariate analysis were subjected to multiple logistic regression model analysis. Correlation analysis was performed by Pearson correlation analysis. The difference is statistically significant when $P < 0.05$.

3. Results

3.1. Baseline Data and Compliance Scores of Follow-Up Patients. A total of 156 patients were followed up, and there were 8 cases of lost contact and 2 cases of death due to various reasons during the follow-up period. The actual number of effective cases during the follow-up period was 146, and the effective rate was 93.6%. The compliance score of 146 patients was (10.5 ± 1.4) points, among which 59 patients (40.4%) were in the good compliance group and 87 patients (59.6%) were in the poor compliance group (Table 1).

3.2. Univariate Analysis of Influencing Compliance with NOACs. Univariate analysis showed that age, educational background, place of residence, number of complications, CHA2DS2-VASc score, and HA-BLED score were the influencing factors for NOAC compliance of NVAF patients ($P < 0.05$) (Table 2).

Table 1: Baseline information and the compliance scores of 146 follow-up patients (n, $\overline{x} \pm s$).

Clinical information	Baseline information situation
Gender	85 males (58.2%), 61 females (41.8%)
Age	53 patients with age <65 years (36.3%), 93 patients with age ≥65 years (63.7%)
Educational background	46 patients (31.5%) with no educational background/primary school, 58 patients (39.7%) with middle school/high school, and 42 cases (28.8%) with university or above
Place of residence	67 patients (45.9%) in rural areas and 79 patients (54.1%) in cities and towns
Marriage situation	69 patients were unmarried/widowed (47.3%), and 77 patients were married (52.7%)
Smoking history	51 patients (34.9%) had smoking history, 95 patients (65.1%) had no smoking history
Drinking history	56 patients (38.4%) had a history of drinking alcohol, 90 patients (61.6%) had no history of drinking alcohol.
Number of complications	0~6 (2.9 ± 1.6) species
Number of concomitant medications	0~8 (4.1 ± 2.1) species
CHA_2DS_2-VASc score	45 patients (30.8%) with scores <2/3 (male/female) and 101 patients (69.2%) with scores ≥2/3 (male/female)
HAS-BLED score	77 patients (52.7%) with score <3 and 69 patients (47.3%) with score ≥3
Compliance	(10.5 ± 1.4) points, good compliance in 59 patients (40.4%), poor compliance in 87 patients (59.6%)

Table 2: Univariate analysis of influencing compliance with NOACs (n, %, $\overline{x} \pm s$).

Clinical information	Good compliance group ($n = 59$)	Poor compliance group ($n = 87$)	χ^2/t	P
Gender				
Male	35 (59.3)	50 (57.5)	0.050	0.824
Female	24 (40.7)	37 (42.5)		
Age				
<65 years	41 (69.5)	40 (75.5)	7.870	0.001
≥65 years	18 (30.5)	47 (72.3)		
Educational background				
No educational background/primary school	28 (47.5)	18 (20.7)	16.350	≤0.001
Middle school/high school	18 (30.5)	40 (46.0)		
University or above	9 (15.3)	33 (37.9)		
Place of residence				
Rural area	49 (83.1)	18 (20.7)	55.062	≤0.001
Cities and towns	10 (16.9)	69 (79.3)		
Marriage situation				
Unmarried/widowed	36 (61.0)	33 (37.93)	7.518	0.006
Married	23 (29.87)	54 (70.13)		
Smoking history				
Yes	25 (42.4)	26 (29.9)	2.412	0.120
No	34 (57.6)	61 (70.1)		
Drinking history				
Yes	18 (30.5)	33 (37.9)	0.852	0.356
No	41 (69.5)	54 (62.1)		
Number of complications	2.6 ± 1.4	3.1 ± 0.9	2.627	0.012
Number of concomitant medications	4.3 ± 2.1	4.6 ± 2.2	0.823	0.412
CHA_2DS_2-VASc score				
<2/3 (male/female)	40 (67.80)	5 (5.75)	63.484	≤0.001
≥2/3 (male/female)	19 (32.20)	82 (94.25)		
HAS-BLED score				
<3 score	51 (86.44)	16 (18.39)	49.313	≤0.001
≥3 score	8 (13.56)	51 (58.62)		

3.3. Multivariate Analysis of Influencing Compliance with NOACs. The compliance was taken as the dependent variable, and the factors with significant differences in Table 2 were taken as independent variables into the logistic regression model. The assignments of the dependent variables and independent variables are shown in Table 3.

Education background, place of residence, number of complications, CHA2DS2-VASc score, and HAS-BLED

Table 3: Variable assignment for multivariate analysis of influencing compliance with NOACs.

Variable	The assignment
Dependent variable	
Compliance	0 = good, 1 = poor
Independent variables	
Age	<60 years = 0, ≥60 years = 1
Marriage situation	Married = 0, unmarried/widowed = 1
Educational background	University or above = 0, middle school/high school = 1, no educational background/primary school = 2
Place of residence	Cities and towns = 0, rural area = 1
Number of complications	Enter the actual value
CHA_2DS_2-VASc score	≥2/3 (male/female) = 0, <2/3 (male/female) = 1
HAS-BLED score	≥3 score = 0, <3 score = 1

score were independent influencing factors for oral NOACs compliance of NVAF patients (Table 4).

3.4. Comparison Scores of Clinical End Points between the Two Groups. The incidence of ischemic stroke in the good compliance group (5.1%) was lower than that in the poor compliance group (71.2%), and the difference was significant ($P < 0.05$). But, there was no significant difference in the incidence of hemorrhagic events between the two groups ($P > 0.05$). Among the patients who died, 2 patients in the poor compliance group died of stroke, while the remaining patients died of nonthromboembolism and hemorrhagic events (Table 5).

3.5. Correlation between NOAC Compliance and Severity of Ischemic Stroke. The types of stroke that occurred in the 3 patients in the good adherence group were all minor/minor stroke, and the types of stroke that occurred in the 12 patients in the poor adherence group were all moderate and major stroke (Table 6).

Pearson correlation analysis showed that there was a negative correlation ($r = -0.791$, $P < 0.001$) between NOAC compliance and severity of ischemic stroke in patients with NVAF (Figure 1).

4. Discussion

As a member of the cardiovascular epidemic in the 21st century, NVAF has become a major public health problem threatening the safety of citizens [9]. It occurs mainly in the middle-aged and elderly people with organic heart disease, and the prevalence was increased with age. The most serious complication after NVAF is thromboembolic events such as stroke [10]. According to statistics, about 13~26% of ischemic strokes are directly associated with NVAF. Also, in patients of advanced age >80 years, AF is more a high-risk influential cause of concurrent ischemic stroke [11].

At present, NOACs are an approved treatment for thromboembolic disease in multiple clinical indications [12]. However, the investigation showed that the drug intake rate of patients with NVAF in China was extremely low, and the high prevalence of stroke and low rate of anticoagulant therapy have become the new features of atrial fibrillation patients in China [13].

With the wide application of the risk stratification and scoring tools for atrial fibrillation thrombosis and bleeding, such as CHA2DS2-VASc and HAS-BLED, clinical practice HAS-BLED found that it is of certain value to identify the risk of ischemic stroke and hemorrhagic transformation in NVAF patients before NOACs. It is not only beneficial to the correction of adverse events of NOACs but also enhances the confidence of clinical use of NOACs to a certain extent. In our study, 156 patients with NVAF who received NOACs in our institution were followed up for 2 years. The results showed that 87 patients (59.59%) were in the poor compliance.

Multiple logistic regression analysis was further used to confirm that education background, place of residence, number of complications, CHA2DS2-VASc score, and HA-BLED score were independent influencing factors for NOAC compliance of NVAF patients. The reasons include many aspects. First of all, in terms of educational background, patients with higher educational level have a higher understanding of NOACs and the individualized medication, so their subjective initiative of anticoagulation is also greater [14]. Secondly, compared with rural areas where communication and medical equipment are not well established, urban residents may have more advantages in regular monitoring, physician-patient interactions, and the popularization of relevant knowledge [15]. Thirdly, in terms of the number of complications, most patients with NVAF are complicated with basic diseases such as three highs, cardiovascular and cerebrovascular diseases, and liver and kidney diseases, which had higher variable in individuals, and a large impact on the blood concentration after treatment, and some patients may stop taking drugs or change medicines halfway, leading to a high probability of stopping medication or changing medication midway. At last, in terms of CHA2DS2-VASc and HAS-BLED score, patients with CHA2DS2-VASc score ≥2/3 (male/female) and HAS-BLED score ≥3 may be more aware of taking medicine due to the fear of discovering hemorrhagic conversion events under the crisis of high stroke risk [16].

In our study, the incidence of ischemic stroke in the good compliance group was lower than that in the poor compliance group, and the stroke degree of the 3 patients in the good compliance group was lower than that of the 12 patients in the poor compliance group. Moreover, Pearson correlation analysis showed that the compliance of NOACs

Table 4: Multivariate analysis of influencing compliance with NOACs.

Factors	β	SE	Wald	P	OR (95% CI)
Age ≥ 60 years	0.943	1.117	4.297	0.174	3.116 (0.561~1.209)
Unmarried/widowed	1.165	2.545	4.436	0.098	1.765 (0.361~1.935)
Educational background					
No educational background/primary school	5.112	1.628	9.817	0.007	166.861 (6.796~4094.401)
Middle school/high school	3.290	1.432	5.254	0.027	26.983 (1.610~451.128)
Place of residence					
Rural area	1.566	0.742	4.579	0.041	1.342 (0.571~0.478)
Number of complications	0.928	0.454	4.136	0.047	2.538 (1.030~6.244)
CHA_2DS_2-VASc score					
<2/3 (male/female)	2.211	0.982	5.004	0.029	0.106 (0.012~0.756)
HAS-BLED score					
≥3 score	2.786	1.247	5.132	0.028	12.431 (0.964~38.657)

Table 5: Comparison of clinical end points between the two groups (n, %).

Group	Ischemic stroke	Hemorrhagic events
Good compliance group ($n = 59$)	3 (5.1)	6 (10.2)
Poor compliance group ($n = 87$)	15 (17.2)	10 (11.5)
χ^2	4.807	0.063
P	0.028	0.801

Table 6: The compliance scores and NIHSS score of 15 patients with ischemic stroke (cases, points).

Group	Number	Compliance scores	NIHSS score
Good compliance group ($n = 3$)	7	12.0	3
	26	12.0	4
	69	12.0	2
Poor compliance group ($n = 12$)	4	9.3	31
	11	4.8	6
	28	10.5	22
	43	10.8	8
	47	11.0	15
	61	10.5	9
	70	10	23
	77	9.7	14
	85	4	19
	94	6.3	17
	97	5.5	24
	109	6.7	21

Note: a score of 0-1 was classified as normal, 1–4 as mild stroke/minor stroke, 5–15 as moderate stroke, 16–20 as moderate severe stroke, and 21–42 as severe stroke.

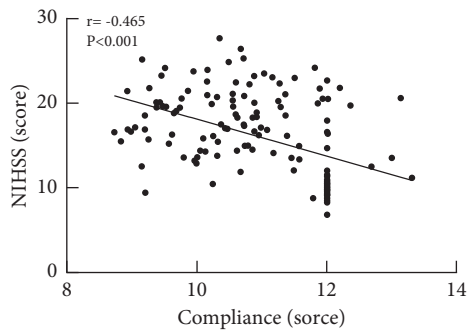

Figure 1: Correlation between NOAC compliance and severity of ischemic stroke. There was a negative correlation ($r = -0.465$, $P < 0.001$) between NOAC compliance and severity of ischemic stroke in patients with NVAF.

in NVAF patients was negatively correlated with the severity of ischemic stroke [17]. These indicate that active and effective treatment with NOACs is an independent protective factor for effectively reducing the severity of ischemic stroke [18].

Some studies have pointed out the risk of bleeding rises accordingly when NOACs benefit [19]. In addition, due to differences in race, genetics, weight, and dietary structure, the hemorrhagic events in Chinese patients will increase. However, in practice, the benefits of NOAC therapy far outweigh the risks provided that the relevant guidelines are strictly followed, indications are properly mastered, embolism and bleeding risks are dynamically assessed, and coagulation function is closely monitored [20].

Notably, there was no significant difference in the incidence of hemorrhagic events between the good compliance group and the poor compliance group in our study. Possible reasons for this were the limited sample size and wide variation in age distribution in our study, and the sample subjects were not limited to elderly patients as in previous studies, which may have an impact on the results [21].

In conclusion, a variety of factors lead to the poor adherence of NOACs in NVAF patients. Therefore, clinical supervision and management of patients with NVAF after NOACs should be strengthened to improve the compliance of patients with NVAF after NOACs, reduce damage of ischemic stroke, and improve their prognosis.

Data Availability

The data used and analyzed during the current study are available from all the authors.

Conflicts of Interest

The authors declare no conflicts of interest.

Acknowledgments

This work was supported by the Clinical Nursing Research Fund Project of The Second Xiangya Hospital of Central South University for 2020 (2020-HLKY-48).

References

[1] Y. Ingrasciotta, S. Crisafulli, V. Pizzimenti et al., "Pharmacokinetics of new oral anticoagulants: implications for use in routine care," *Expert Opinion on Drug Metabolism & Toxicology*, vol. 14, no. 10, pp. 1057–1069, 2018.

[2] A. Corsini, N. Ferri, M. Proietti, and G. Boriani, "Edoxaban and the issue of drug-drug interactions: from pharmacology to clinical practice," *Drugs*, vol. 80, no. 11, pp. 1065–1083, 2020.

[3] S. Kohsaka, J. Katada, K. Saito et al., "Safety and effectiveness of non-vitamin K oral anticoagulants versus warfarin in real-world patients with non-valvular atrial fibrillation: a retrospective analysis of contemporary Japanese administrative claims data," *Open Heart*, vol. 7, Article ID e001232, 2020.

[4] S. Deitelzweig, A. Keshishian, X. Li et al., "Comparisons between oral anticoagulants among older nonvalvular atrial fibrillation patients," *Journal of the American Geriatrics Society*, vol. 67, no. 8, pp. 1662–1671, 2019.

[5] O. Y. Bang, Y. K. On, M. Y. Lee et al., "The risk of stroke/systemic embolism and major bleeding in Asian patients with non-valvular atrial fibrillation treated with non-vitamin K oral anticoagulants compared to warfarin: results from a real-world data analysis," *PLoS One*, vol. 15, Article ID e0242922, 2020.

[6] J. Steffel, P. Verhamme, T. S. Potpara et al., "The 2018 European heart rhythm association practical guide on the use of non-vitamin K antagonist oral anticoagulants in patients with atrial fibrillation," *European Heart Journal*, vol. 39, no. 16, pp. 1330–1393, 2018.

[7] G. Y. H. Lip, A. Keshishian, X. Li et al., "Effectiveness and safety of oral anticoagulants among nonvalvular atrial fibrillation patients," *Stroke*, vol. 49, no. 12, pp. 2933–2944, 2018.

[8] S.-R. Lee, E.-K. Choi, S. Kwon et al., "Effectiveness and safety of contemporary oral anticoagulants among Asians with nonvalvular atrial fibrillation," *Stroke*, vol. 50, no. 8, pp. 2245–2249, 2019.

[9] Y. H. Chan, L. C. See, H. T. Tu et al., "Efficacy and safety of apixaban, dabigatran, rivaroxaban, and warfarin in asians with nonvalvular atrial fibrillation," *Journal of the American Heart Association*, vol. 7, 2018.

[10] G. Y. H. Lip, A. V. Keshishian, A. L. Kang et al., "Oral anticoagulants for nonvalvular atrial fibrillation in frail elderly patients: insights from the ARISTOPHANES study," *Journal of Internal Medicine*, vol. 289, no. 1, pp. 42–52, 2021.

[11] P. Priyanka, J. T. Kupec, M. Krafft, N. A. Shah, and G. J. Reynolds, "Newer oral anticoagulants in the treatment of acute portal vein thrombosis in patients with and without cirrhosis," *International Journal of Hepatology*, vol. 2018, Article ID 8432781, 9 pages, 2018.

[12] A. A. Dalia, A. Kuo, M. Vanneman, J. Crowley, A. Elhassan, and Y. Lai, "Anesthesiologists guide to the 2019 AHA/ACC/HRS focused update for the management of patients with atrial fibrillation," *Journal of Cardiothoracic and Vascular Anesthesia*, vol. 34, no. 7, pp. 1925–1932, 2020.

[13] C. Godino, F. Melillo, B. Bellini et al., "Percutaneous left atrial appendage closure versus non-vitamin K oral anticoagulants in patients with non-valvular atrial fibrillation and high bleeding risk," *EuroIntervention*, vol. 15, no. 17, pp. 1548–1554, 2020.

[14] W. S. Aronow and T. A. Shamliyan, "Comparative clinical outcomes of edoxaban in adults with nonvalvular atrial fibrillation," *American Journal of Therapeutics*, vol. 27, no. 3, pp. e270–e285, 2020.

[15] Z. Cen, Q. Meng, and K. Cui, "New oral anticoagulants for nonvalvular atrial fibrillation with stable coronary artery disease: a meta-analysis," *Pacing and Clinical Electrophysiology*, vol. 43, no. 11, pp. 1393–1400, 2020.

[16] G. Simonyi, A. Paksy, R. Várnai, and M. Medvegy, "[Real-world adherence to oral anticoagulants in atrial fibrillation]," *Orvosi Hetilap*, vol. 161, no. 20, pp. 839–845, 2020.

[17] S. V. Emren, M. Zoghi, R. Berilgen et al., "Safety of once-or twice-daily dosing of non-vitamin K antagonist oral anticoagulants (NOACs) in patients with nonvalvular atrial fibrillation: a NOAC-TR study," *Bosnian Journal of Basic Medical Sciences*, vol. 18, pp. 185–190, 2018.

[18] D. Pol, C. Curtis, S. Ramkumar, and L. Bittinger, "NOACs now mainstream for the use of anticoagulation in non-valvular atrial fibrillation in Australia," *Heart Lung & Circulation*, vol. 28, no. 4, pp. e40–e42, 2019.

[19] A. Tufano, M. Galderisi, L. Esposito et al., "Anticancer drug-related nonvalvular atrial fibrillation: challenges in management and antithrombotic strategies," *Seminars in Thrombosis and Hemostasis*, vol. 44, pp. 388–396, 2018.

[20] A. M. Alshehri, "Stroke in atrial fibrillation: review of risk stratification and preventive therapy," *Journal of Family & Community Medicine*, vol. 26, pp. 92–97, 2019.

[21] R. Pisters, A. Elvan, H. J. G. M. Crijns, and M. E. W. Hemels, "Optimal long-term antithrombotic management of atrial fibrillation: life cycle management," *Netherlands Heart Journal*, vol. 26, no. 6, pp. 311–320, 2018.

Hindawi
Evidence-Based Complementary and Alternative Medicine
Volume 2021, Article ID 8219141, 8 pages
https://doi.org/10.1155/2021/8219141

Research Article

Tournefortia sarmentosa Inhibits the Hydrogen Peroxide-Induced Death of H9c2 Cardiomyocytes

Chih-Jen Liu,[1] Lu-Kai Wang,[2] Chan-Yen Kuo,[3] Mao-Liang Chen,[3] I-Shiang Tzeng,[3] and Fu-Ming Tsai[3]

[1]*Division of Cardiology, Department of Internal Medicine, Taipei Tzu Chi Hospital, The Buddhist Tzu Chi Medical Foundation, New Taipei City 231, Taiwan*
[2]*Radiation Biology Core Laboratory, Institute for Radiological Research, Chang Gung University/Chang Gung Memorial Hospital, Linkou, Taoyuan 333, Taiwan*
[3]*Department of Research, Taipei Tzu Chi Hospital, The Buddhist Tzu Chi Medical Foundation, New Taipei City 231, Taiwan*

Correspondence should be addressed to Fu-Ming Tsai; afu2215@gmail.com

Received 5 July 2021; Revised 29 July 2021; Accepted 18 August 2021; Published 26 August 2021

Academic Editor: Thanasekaran Jayakumar

Tournefortia sarmentosa is a traditional Chinese medicine used to reduce tissue swelling, to exert the antioxidant effect, and to detoxify tissue. *T. sarmentosa* is also used to promote development in children and treat heart dysfunction. However, many of the mechanisms underlying the effects of *T. sarmentosa* in the treatment of disease remain unexplored. In this study, we investigated the antioxidant effect of *T. sarmentosa* on rat H9c2 cardiomyocytes treated with hydrogen peroxide (H_2O_2). *T. sarmentosa* reduced the cell death induced by H_2O_2. *T. sarmentosa* inhibited H_2O_2-induced changes in cell morphology, activation of cell death-related caspases, and production of reactive oxygen species. In addition, we further analyzed the potential active components of *T. sarmentosa* and found that the compounds present in the *T. sarmentosa* extract, including caffeic acid, rosmarinic acid, salvianolic acid A, and salvianolic acid B, exert effects similar to those of the *T. sarmentosa* extract in inhibiting H_2O_2-induced H9c2 cell death. Therefore, according to the results of this study, the ability of the *T. sarmentosa* extract to treat heart disease may be related to its antioxidant activity and its ability to reduce the cellular damage caused by free radicals.

1. Introduction

Oxidative stress caused by free radicals is associated with many cardiovascular diseases, including ischemic heart disease, atherosclerosis, hypertension, and cardiomyopathies [1–4]. Free radicals are generated in the human body during the process of energy production. When the body suffers from inflammation, such as inflammation elicited by infection or injury, many free radicals are produced to remove foreign substances [5]. However, if the host does not have a sufficient protective mechanism to remove excess free radicals after infection, these free radicals will cause cell damage (including lipid peroxidation of the cell membrane and DNA damage) [6, 7]. In addition, environmental factors such as ultraviolet radiation, chemical drugs, and even excessive pressure result in a substantial increase in the production of free radicals in the body [8]. When cardiac muscle cells are attacked by free radicals, the free radicals-induced injury can damage nuclear DNA and lead to permanent DNA damage. The lipids in the cell membrane can be oxidized, altering cell membrane fluidity, preventing nutrients from entering the cell, and eventually causing necrosis. Free radicals attack the side chains of amino acids, causing proteins to lose their function and disrupting the normal functions of cells [5].

Several antioxidant enzymes in the human body, such as superoxide dismutase, glutathione peroxidase, or catalase, counteract free radicals. These enzymes quickly convert the free radicals produced by the body into less toxic or nontoxic substances through redox reactions [9, 10]. However, when the activity of such antioxidant enzymes is insufficient due to insufficient intake of cofactors (superoxide dismutase

requires metal ions, such as Cu^{2+} or Zn^{2+}) or differences in genetic background, cells are unable to avoid free radicals attack and subsequent damage [11]. When a tissue is damaged and dies, it can be restored by the proliferation of stem cells present in the tissue in order to maintain the normal operation of the organ or tissue. However, the existence of cardiac stem cells remains controversial [12]. Therefore, methods to prevent cardiomyocyte damage by free radicals or to reduce cells damage caused by the oxidative pressure generated by free radicals are important topics at present.

Tournefortia sarmentosa is often mentioned in reports that evaluate its antioxidant activity in Chinese medicine [13, 14]. *T. sarmentosa* also exerts the effects of relieving wind, detoxifying, reducing swelling, treating aching muscles and bones, and promoting childhood development [15–17]. In addition to being used as a specific therapeutic drug in traditional Chinese medicine, *T. sarmentosa* has recently been promoted as a health food. However, although several studies have investigated the antioxidant effect of *T. sarmentosa*, researchers have not determined whether *T. sarmentosa* protects cardiomyocytes from oxidative stress. In this study, we investigated the protective effect of *T. sarmentosa* on hydrogen peroxide- (H_2O_2-) induced myocardial cell death. In addition to the protective effect of *T. sarmentosa* on cardiomyocytes, we also analyzed the potential active components of *T. sarmentosa* that protect against cardiomyocyte death.

2. Materials and Methods

2.1. Preparation of an Aqueous Extract of T. sarmentosa and Reagents. The preparation of the aqueous extract of *T. sarmentosa* was described in a previous study [14]. The various components of the *T. sarmentosa* extract, including caffeic acid, rosmarinic acid, salvianolic acid A, and salvianolic acid B, were purchased from Sigma-Aldrich (St. Louis, MO, USA).

2.2. Cell Culture. Rat H9c2 (2-1) cardiomyocytes were purchased from Bioresource Collection and Research Center (Hsinchu city, Taiwan). The cells were cultured in 90% Dulbecco's modified Eagle's medium (DMEM) containing 4 mM L-glutamine, 1.5 g/L sodium bicarbonate, 4.5 g/L glucose, and 10% fetal bovine serum at 37°C in a 5% carbon dioxide environment. During cell culture, mycoplasma contamination was regularly evaluated, and mycoplasma contamination was not detected.

2.3. Detection of Cell Viability and Cell Death. WST-1 reagent (Roche Diagnostics, Mannheim, Germany) and a cytotoxicity detection kit (Roche Diagnostics) were used to measure cell viability and cell death, respectively [18]. H9c2 cells were plated in a 6-well plate in triplicate at a density of 10^5 cells/well and cultured overnight. The medium was replaced with serum-free DMEM, and various doses of *T. sarmentosa* or 100 μm solutions of the components present in *T. sarmentosa* were added and incubated for another 24 h. After incubation with WST-1 for 3 h and 100 μM H_2O_2 for another 1 h, the supernatants were collected, and the absorbance values were measured at 450 nm and 650 nm using a multifunctional microplate instrument (Infinite F200, Tecan, Durham, NC, USA). Alternatively, cells growing in the serum-free medium were cultured with various concentrations of *T. sarmentosa* or 100 μm solutions of the components present in *T. sarmentosa* for 24 h, followed by incubation with 100 μM H_2O_2 for 1 h. The samples were then centrifuged, and the supernatant of each sample was collected. The amounts of lactate dehydrogenase present in the supernatants were detected with a cytotoxicity detection kit.

2.4. Western Blotting. H9c2 cells were plated in a 10 cm dish at a density of 10^6 cells/dish and cultured overnight. After the cells were cultured in the serum-free medium supplemented with various doses of *T. sarmentosa* or 100 μm components present in *T. sarmentosa* for 24 h, the cells were treated with 100 μM H_2O_2 for 1 h, and the cell extracts were collected with mammalian protein extraction buffer (GE Healthcare Bio-Sciences, MJ, USA). The expression of protein in each sample was analyzed using Western blotting, as described in the previous literature [19]. Caspase-8, caspase-9, and caspase-3 antibodies were purchased from Cell Signaling Technology Inc. (Beverly, MA, USA). The actin antibody was purchased from Sigma-Aldrich.

2.5. Reactive Oxygen Species (ROS) Measurement. Dihydrorhodamine 123 (DHR123) dye was used to detect ROS levels in cells as previously described [14]. Briefly, H9c2 cells were plated in a 10 cm dish at a density of 10^6 cells/dish and cultured overnight. After the cells were cultured in serum-free medium supplemented with various doses of *T. sarmentosa* or 100 μm components present in *T. sarmentosa* for 24 h, the cells were treated with 100 μM H_2O_2 and 2.5 μM DHR123 for 1 h. The cells were then trypsinized and passed through a 30 μm filter, and the ROS contents in the cells were analyzed with a flow cytometer (FACScan, Becton Dickinson, Franklin Lakes, NJ, USA).

2.6. Statistical Analysis. The experimental data are presented as the average value ± SD of triplicate samples from each independent biological sample. Statistical analysis was analyzed using Student's t-test, and p values less than 0.05 were considered significant.

3. Results

3.1. T. sarmentosa Prevented the H_2O_2-Induced Death of H9c2 Cardiomyocytes. H9c2 cells were selected as the experimental material and treated with 100 μM H_2O_2 for one hour to induce cell death as described in a previously published study in order to determine whether ROS caused cardiomyocyte death [20]. As shown in Figures 1(a) and 1(b), H_2O_2 significantly reduced the cell survival rate and increased the number of dead H9c2 cells. However, when the cells were treated with increasing doses of *T. sarmentosa*, the

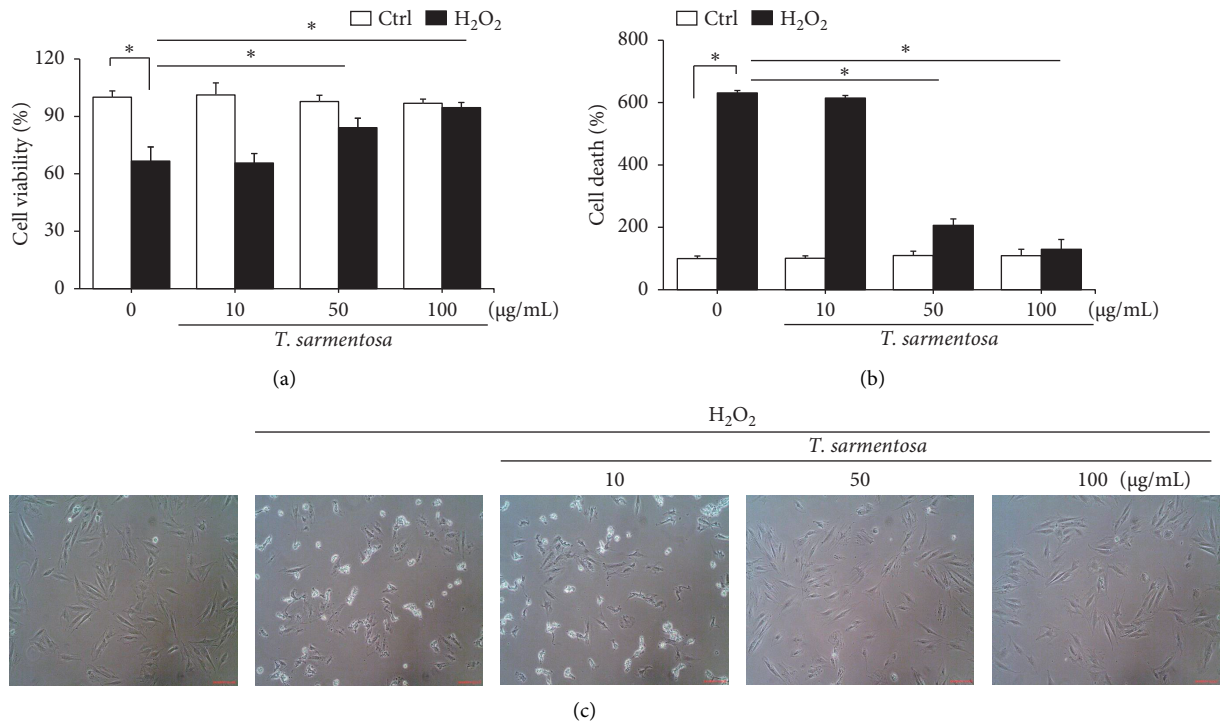

Figure 1: *T. sarmentosa* extract inhibiting H_2O_2-induced H9c2 cell death. H9c2 cells are treated with different doses of the *T. sarmentosa* extract for 24 h and then treated with 100 μM H_2O_2 for 1 h. Cell viability (a) and cell death (b) are detected using WST-1 reagent or by measuring the amount of LDH release, respectively. Cell morphology observed under a light microscope at 40x magnification (c). $^*P < 0.05$ for comparisons between two groups.

H_2O_2-induced decrease in the cell survival rate and increase in the cell death rate were significantly inhibited (Figures 1(a) and 1(b)). When the cells were treated with different doses of *T. sarmentosa* alone, no significant changes in cell survival or cell death were observed, suggesting that *T. sarmentosa* is not cytotoxic to H9c2 cells. In addition, the morphology of the cells was observed directly under a microscope. When the cells were treated with H_2O_2, the spindle-like morphology of the cells was not maintained, and the cells detached. When the cells were pretreated with *T. sarmentosa*, especially at a high dose of 50–100 μg/mL, the cell morphology recovered noticeably. Based on these results, *T. sarmentosa* inhibited the changes in cell morphology and cell death induced by H_2O_2 (Figure 1(c)).

3.2. T. sarmentosa Reduced the Levels of Apoptosis-Related Caspases and Increased the Production of ROS Induced by H_2O_2. Since *T. sarmentosa* inhibited the H_2O_2-induced death of H9c2 cells, we further explored whether *T. sarmentosa* altered the H_2O_2-induced activation of cell death-related signal transduction pathways. In the cells treated with different doses of *T. sarmentosa*, no caspase-8, caspase-9, or caspase-3 expression was detected. However, when the cells were treated with H_2O_2, the levels of caspase-8, caspase-9, and caspase-3 significantly increased. When the cells were pretreated with high doses of 50–100 μg/mL *T. sarmentosa*, the H_2O_2-induced increases in the levels of the death-related caspases mentioned above were significantly reduced (Figure 2(a)).

Cell death caused by H_2O_2 is closely related to ROS production. Therefore, we further verified whether the inhibition of H_2O_2-induced cell death by *T. sarmentosa* is related to ROS production. As shown in Figure 2(b), H_2O_2 significantly increased the intracellular ROS levels, and the H_2O_2-induced increase in the intracellular ROS content was significantly decreased by treatment with increasing doses of *T. sarmentosa*.

3.3. All the Compounds Present in the T. sarmentosa Extract Inhibited H_2O_2-Induced H9c2 Cell Death. We selected several compounds present in the *T. sarmentosa* extract that are commercially available to further explore the components of *T. sarmentosa* that effectively inhibit H_2O_2-induced H9c2 cell death [21]. As shown in Figures 3(a) and 3(b), caffeic acid, rosmarinic acid, salvianolic acid A, and salvianolic acid B exhibited effects similar to those of *T. sarmentosa*, as they significantly reversed the H_2O_2-induced decrease in the H9c2 cell survival rate and increase in the cell death rate.

3.4. All Compounds Present in the T. sarmentosa Extract Decreased the H_2O_2-Induced Increases in the Levels of Apoptosis-Related Caspases and Production of ROS. We further analyzed whether the compounds present in the *T. sarmentosa* extract also altered the H_2O_2-induced expression of caspases and production of ROS. H_2O_2 induced the expression of caspases, and except for caffeic acid, which had only a slight effect on the expression of caspase-3, the

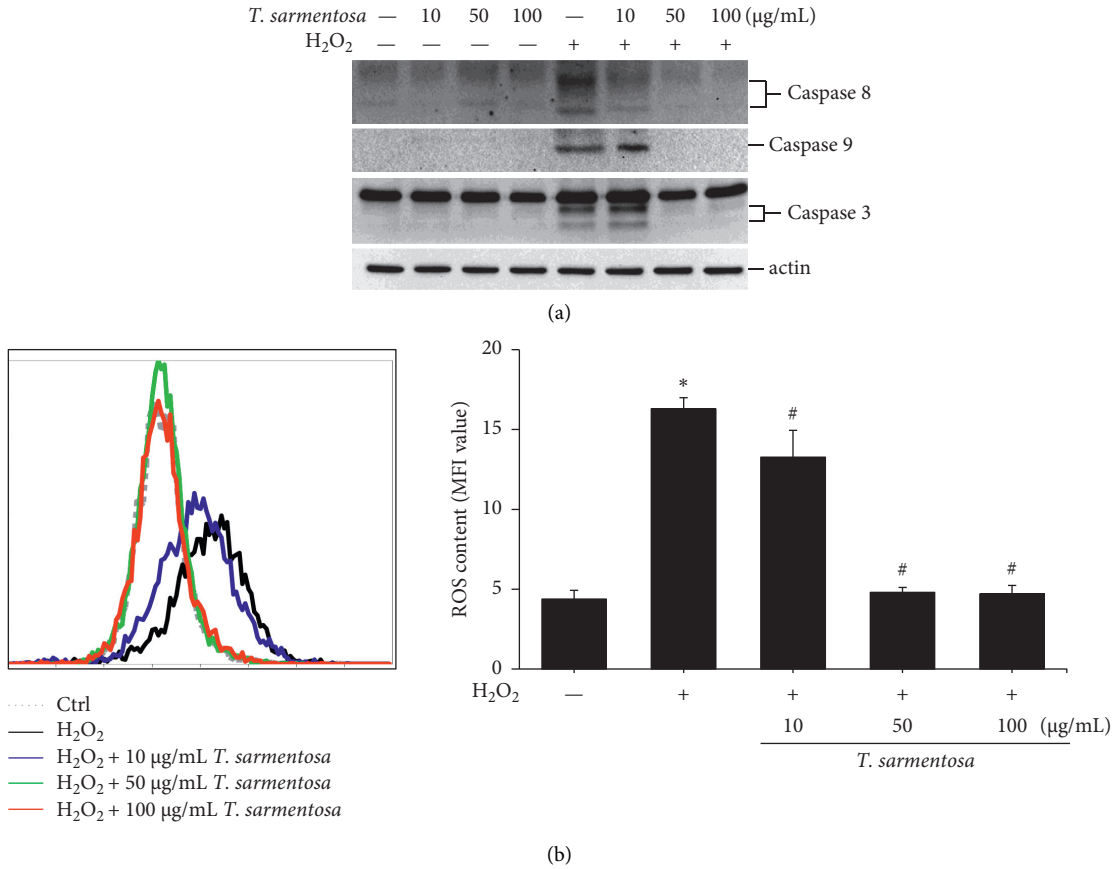

FIGURE 2: *T. sarmentosa* extract inhibiting the H_2O_2-induced expression of cell death-related caspases and production of ROS. H9c2 cells are treated with different doses of the *T. sarmentosa* extract for 24 h and then treated with 100 μM H_2O_2 for 1 h. The levels of cell death-related caspases are analyzed using Western blotting (a). ROS production is detected by staining the cells with the DHR123 dye and analyzed using flow cytometry (b).

H_2O_2-induced expression of caspase-8, caspase-9, and caspase-3 was inhibited by all the compounds found in *T. sarmentosa* extract (Figure 4(a)). In addition, we also analyzed the effects of these compounds on the H_2O_2-induced intracellular ROS production. As shown in Figure 4(b), all the compounds present in the *T. sarmentosa* extract significantly inhibited the H_2O_2-induced ROS production.

4. Discussion

T. sarmentosa is widely distributed and is found in Taiwan, Vietnam, Malaysia, the Philippines, Indonesia, and many other regions. *T. sarmentosa* is also widely used as a medicinal material. For example, the stems and leaves are mashed and taken orally with wine to promote blood circulation and treat old and new injuries. The medical efficacy of this plant extract has consistently been reported; however, few studies have explored its potential efficacy because the use of traditional Chinese medicine is not often investigated in many scientific studies.

In this study, we confirmed the antioxidant effect of *T. sarmentosa* on cardiomyocytes, but it only inhibited H_2O_2-induced cell death at higher doses. Although *T. sarmentosa* extract has been used as a traditional Chinese medicine in humans for years, no studies have reported its concentration in human blood after consumption; thus, researchers have not determined whether the dose exerts a cardioprotective antioxidant effect. However, *T. sarmentosa* was orally administered at doses of 2,000 mg/kg bodyweight in in vivo studies and at doses of 10–100 mg/mL in cell-based experiments [15]. Therefore, the concentration of the *T. sarmentosa* extract tested in this study should be within a reasonable range. Magnolol is the most popular Chinese medicine used to protect the myocardium and possesses antioxidant activity. The oral dose of *Magnolia officinalis* extract in live animals ranges from 0.48 to 2.5 g/kg/day [22, 23], which was not significantly different from the *T. sarmentosa* dose. In addition, the half-life of magnolol in vivo and the organs to which the drug is distributed after injection have been reported in a review [24]. Therefore, compared with magnolol, the cardioprotective effects of *T. sarmentosa* still need to be verified in additional experiments.

The efficacy of *T. sarmentosa* is related to its individual components. The individual compounds present in the *T. sarmentosa* extract used in this study, including caffeic acid, rosmarinic acid, and salvianolic acid, have a benzene

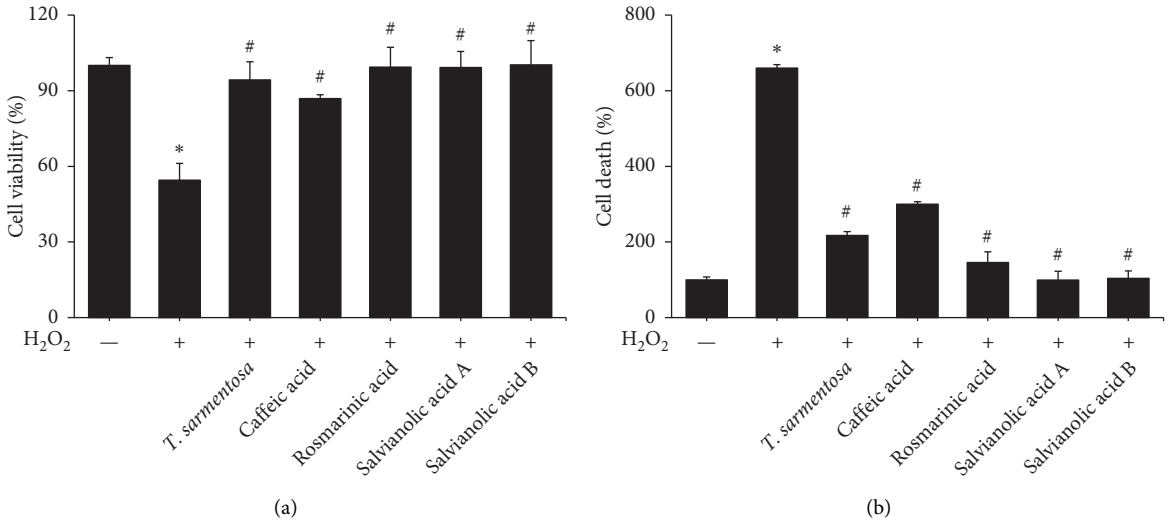

FIGURE 3: The compounds present in the *T. sarmentosa* extract inhibiting H_2O_2-induced H9c2 cell death. H9c2 cells are treated with 100 μm solutions of the indicated compounds present in the *T. sarmentosa* extract for 24 h and then treated with 100 μM H_2O_2 for 1 h. Cell viability (a) and cell death (b) are detected using the WST-1 reagent or by measuring the amount of LDH release, respectively. $^*P < 0.05$ compared with the control group. $^\#P < 0.05$ compared with the control group treated with H_2O_2.

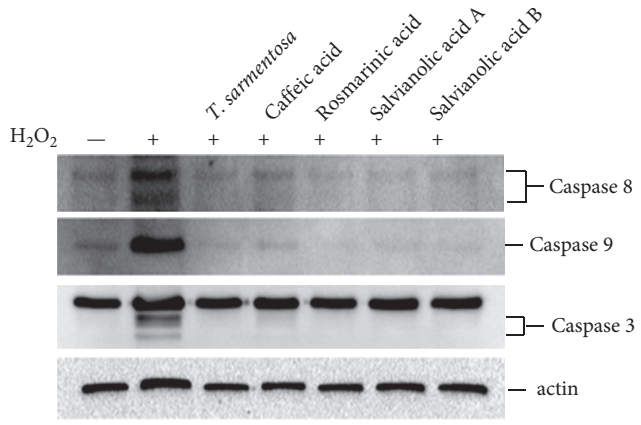

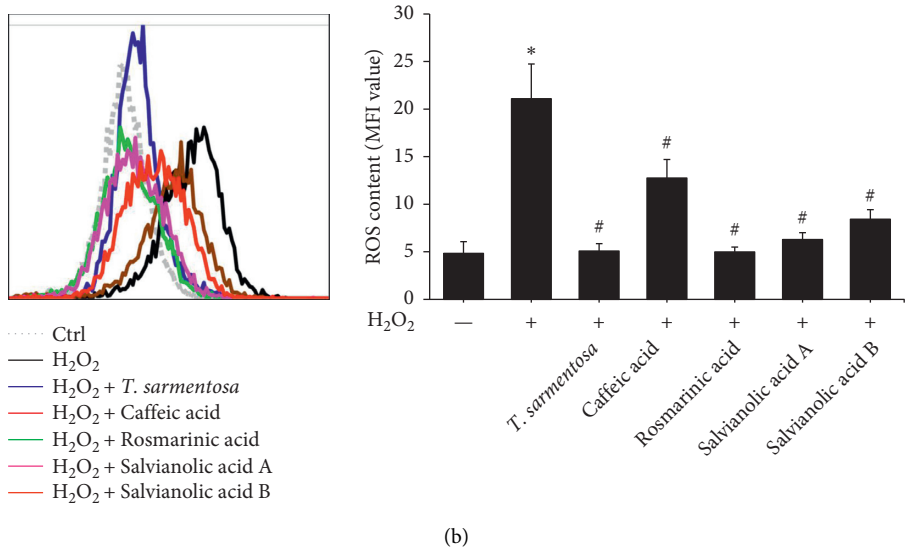

FIGURE 4: *T. sarmentosa* extract inhibiting the H_2O_2-induced expression of cell death-related caspases and production of ROS. H9c2 cells treated with 100 μM solutions of the indicated compounds present in the *T. sarmentosa* extract for 24 h and then treated with 100 μM H_2O_2 for 1 h; the level of cell death-related caspases is analyzed by Western blotting (a). The production of ROS is measured with the DHR123 dye and analyzed by flow cytometry (b). $^*P < 0.05$ compared with the control group. $^\#P < 0.05$ compared with the control group treated with H_2O_2.

ring structure, which has antioxidant properties [25]. In addition, the various compounds present in *T. sarmentosa* mentioned above have been reported to possess antioxidant properties [26–32]. Although different plants exert effects similar to those of traditional Chinese medicines, many differences in their internal components have been noted, and these differences also result in their different medicinal purposes. For example, many components of *T. sarmentosa* are similar to those of *Salvia officinalis* [33], but significant differences were observed after a further analysis of the components [34]; thus, the two plants have different therapeutic purposes. *Salvia officinalis* is mainly used for relieving anxiety, while *T. sarmentosa* is mainly used for detoxification and to exert the antioxidant effect.

Many studies have reviewed the antioxidant, anti-inflammatory, and antiangiogenic properties of caffeic acid that exert important antiatherosclerotic effects and protect tissues from the ischemia/reperfusion injury and cell dysfunction caused by different physical and chemical agents [35, 36]. Rosmarinic acid has been shown to protect against inflammation and myocardial cell apoptosis during myocardial ischemia/reperfusion injury by activating peroxisome proliferator-activated receptor γ and inhibiting the production of inflammatory cytokines, such as IL-6, TNF-α, and C-reactive protein [37]. In addition, rosmarinic acid has been shown to improve cardiac dysfunction and mitochondrial damage in mice with diabetic cardiomyopathy by activating the SIRT1/PGC-1α signaling pathway [38]. The pathway by which salvianolic acid A exerts its protective effects was similar to that of rosmarinic acid. Arsenic trioxide induced the production of ROS and decreased the expression level of PGC-1α in cardiomyocytes. The addition of salvianolic acid A could restore the above phenomena to reduce cardiac mitochondrial damage and improve the cardiotoxicity induced by arsenic trioxide [39]. The protective potential of compounds found in the *T. sarmentosa* extract is closely related to the benzene ring structure of these compounds.

In addition to traditional Chinese medicine, coenzyme Q10 (CoQ10) is widely used in the market as a health food. CoQ10 is a coenzyme that is indispensable in the human body. CoQ10 exists in cells and is mainly distributed in the heart, kidneys, liver, and muscles. CoQ10 functions to stimulate mitochondrial energy production. In addition, CoQ10 functions as an antioxidant in the mitochondria, is involved in the energy production process, and reduces free radicals. Damage to mitochondria maintains the integrity and stability of cells, slows the oxidation of bad cholesterol, delays aging, and activates the immune system [40]. The effective dose of CoQ10 for the prevention of cardiovascular disease is approximately 100–300 mg [41–43]. However, due to the regulatory limitations of many local laws and regulations, high doses of CoQ10 are not available to many people, and thus, its efficacy is controversial. From the perspective of the structures of the compounds, CoQ10 and *T. sarmentosa* extracts contain similar antioxidant components that have benzene ring structures and unsaturated hydrocarbon chains, indicating the potential use of *T. sarmentosa* as a health food for heart protection.

5. Conclusions

In summary, the *T. sarmentosa* extract and several compounds present in the *T. sarmentosa* extract inhibit the H_2O_2-induced death of H9c2 cardiomyocytes. Furthermore, the *T. sarmentosa* extract and several of its compounds inhibit the H_2O_2-induced expression of cell death-related caspases and production of ROS. Therefore, the *T. sarmentosa* extract may have potential for use as a cardioprotective health food.

Data Availability

The data used to support the results of this study are included within the article.

Conflicts of Interest

The authors declare that they have no conflicts of interest.

Acknowledgments

This study was supported by a grant (TCRD-TPE-110-13) from the Taipei Tzu Chi Hospital through the Buddhist Tzu Chi Medical Foundation, Taipei, Taiwan. The authors thank the Core Laboratory of the Buddhist Tzu Chi General Hospital for providing support.

References

[1] R. D'Oria, R. Schipani, A. Leonardini et al., "The role of oxidative stress in cardiac disease: from physiological response to injury factor," *Oxidative Medicine and Cellular Longevity*, vol. 2020, Article ID 5732956, 29 pages, 2020.

[2] R. R. Campos, "Oxidative stress in the brain and arterial hypertension," *Hypertension Research*, vol. 32, no. 12, pp. 1047-1048, 2009.

[3] D. Romero-Alvira, E. Roche, and L. Placer, "Cardiomyopathies and oxidative stress," *Medical Hypotheses*, vol. 47, no. 2, pp. 137–144, 1996.

[4] N. S. Dhalla, R. M. Temsah, and T. Netticadan, "Role of oxidative stress in cardiovascular diseases," *Journal of Hypertension*, vol. 18, no. 6, pp. 655–673, 2000.

[5] E. Cadenas and K. J. Davies, "Mitochondrial free radical generation, oxidative stress, and aging," *Free Radical Biology & Medicine*, vol. 29, no. 3-4, pp. 222–230, 2000.

[6] M. Lagouge and N. G. Larsson, "The role of mitochondrial DNA mutations and free radicals in disease and ageing," *Journal of Internal Medicine*, vol. 273, no. 6, pp. 529–543, 2013.

[7] U.-E.-A. Warraich, F. Hussain, and H. U. R. Kayani, "Aging—oxidative stress, antioxidants and computational modeling," *Heliyon*, vol. 6, no. 5, Article ID e04107, 2020.

[8] A. Phaniendra, D. B. Jestadi, and L. Periyasamy, "Free radicals: properties, sources, targets, and their implication in various diseases," *Indian Journal of Clinical Biochemistry*, vol. 30, no. 1, pp. 11–26, 2015.

[9] E. Pigeolet, P. Corbisier, A. Houbion et al., "Glutathione peroxidase, superoxide dismutase, and catalase inactivation by peroxides and oxygen derived free radicals," *Mechanism of Ageing and Development*, vol. 51, no. 3, pp. 283–297, 1990.

[10] O. I. Aruoma and B. Halliwell, "Action of hypochlorous acid on the antioxidant protective enzymes superoxide dismutase,

catalase and glutathione peroxidase," *Biochemical Journal*, vol. 248, no. 3, pp. 973–976, 1987.

[11] P. Mondola, S. Damiano, A. Sasso, and M. Santillo, "The Cu, Zn superoxide dismutase: not only a dismutase enzyme," *Frontiers in Physiology*, vol. 7, p. 594, 2016.

[12] K. Kretzschmar, Y. Post, M. Bannier-Hélaouët et al., "Profiling proliferative cells and their progeny in damaged murine hearts," *Proceedings of the National Academy of Sciences*, vol. 115, no. 52, pp. E12245–E12254, 2018.

[13] Y.-L. Lin, Y.-Y. Chang, Y.-H. Kuo, and M.-S. Shiao, "Anti-lipid-peroxidative principles from Tournefortia sarmentosa," *Journal of Natural Products*, vol. 65, no. 5, pp. 745–747, 2002.

[14] M.-L. Chen, S. Wu, T.-C. Tsai, L.-K. Wang, W.-M. Chou, and F.-M. Tsai, "Effect of aqueous extract of Tournefortia sarmentosa on the regulation of macrophage immune response," *International Immunopharmacology*, vol. 17, no. 4, pp. 1002–1008, 2013.

[15] C.-Y. Teng, Y.-L. Lai, H.-I. Huang, W.-H. Hsu, C.-C. Yang, and W.-H. Kuo, "Tournefortia sarmentosaextract attenuates acetaminophen-induced hepatotoxicity," *Pharmaceutical Biology*, vol. 50, no. 3, pp. 291–396, 2012.

[16] L. K. Wang, F. M. Tsai, S. Wu et al., "Aqueous extract of tournefortia sarmentosa stem inhibits ADP-induced platelet aggregation," *Indian Journal of Pharmaceutical Sciences*, vol. 80, no. 1, pp. 126–134, 2018.

[17] C. Lans, "Comparison of plants used for skin and stomach problems in trinidad and tobago with Asian ethnomedicine," *Journal of Ethnobiology and Ethnomedicine*, vol. 3, no. 1, p. 12, 2007.

[18] C.-C. Wu, R.-Y. Shyu, C.-H. Wang et al., "Involvement of the prostaglandin D2 signal pathway in retinoid-inducible gene 1 (RIG1)-mediated suppression of cell invasion in testis cancer cells," *Biochimica et Biophysica Acta (BBA)—Molecular Cell Research*, vol. 1823, no. 12, pp. 2227–2236, 2012.

[19] C. C. Wang, L. K. Wang, M. L. Chen, C. Y. Kuo, F. M. Tsai, and C. H. Wang, "Triterpenes in the ethanol extract of poria cocos induce dermal papilla cell proliferation," *International Journal of Pharmacology*, vol. 16, no. 1, pp. 1–9, 2020.

[20] H. Chang, C. Li, K. Huo et al., "Luteolin prevents H_2O_2-induced apoptosis in H9C2 cells through modulating Akt-P53/mdm2 signaling pathway," *BioMed Research International*, vol. 2016, Article ID 5125836, 9 pages, 2016.

[21] Y.-L. Lin, Y.-L. Tsai, Y.-H. Kuo, Y.-H. Liu, and M.-S. Shiao, "Phenolic compounds from tournefortia sarmentosa," *Journal of Natural Products*, vol. 62, no. 11, pp. 1500–1503, 1999.

[22] N. Li, Y. Song, W. Zhang et al., "Evaluation of the in vitro and in vivo genotoxicity of magnolia bark extract," *Regulatory Toxicology and Pharmacology*, vol. 49, no. 3, pp. 154–159, 2007.

[23] Z. Liu, X. Zhang, W. Cui et al., "Evaluation of short-term and subchronic toxicity of magnolia bark extract in rats," *Regulatory Toxicology and Pharmacology*, vol. 49, no. 3, pp. 160–171, 2007.

[24] J. Ho and C.-Y. Hong, "Cardiovascular protection of magnolol: cell-type specificity and dose-related effects," *Journal of Biomedical Science*, vol. 19, no. 1, p. 70, 2012.

[25] J. Chen, J. Yang, L. Ma, J. Li, N. Shahzad, and C. K. Kim, "Structure-antioxidant activity relationship of methoxy, phenolic hydroxyl, and carboxylic acid groups of phenolic acids," *Scientific Reports*, vol. 10, no. 1, p. 2611, 2020.

[26] K. M. M. Espíndola, R. G. Ferreira, L. E. M. Narvaez et al., "Chemical and pharmacological aspects of caffeic acid and its activity in hepatocarcinoma," *Frontiers in Oncology*, vol. 9, p. 541, 2019.

[27] I. Gülçin, "Antioxidant activity of caffeic acid (3,4-dihydroxycinnamic acid)," *Toxicology*, vol. 217, no. 2-3, pp. 213–220, 2006.

[28] T. C. Genaro-Mattos, Â. Q. Maurício, D. Rettori, A. Alonso, and M. Hermes-Lima, "Antioxidant activity of caffeic acid against iron-induced free radical generation-a chemical approach," *PLoS One*, vol. 10, no. 6, Article ID e0129963, 2015.

[29] A. G. Adomako-Bonsu, S. L. Chan, M. Pratten, and J. R. Fry, "Antioxidant activity of rosmarinic acid and its principal metabolites in chemical and cellular systems: importance of physico-chemical characteristics," *Toxicology in Vitro*, vol. 40, pp. 248–255, 2017.

[30] R. Taguchi, K. Hatayama, T. Takahashi et al., "Structure-activity relations of rosmarinic acid derivatives for the amyloid β aggregation inhibition and antioxidant properties," *European Journal of Medicinal Chemistry*, vol. 138, pp. 1066–1075, 2017.

[31] H. Xu, Y. Li, X. Che, H. Tian, H. Fan, and K. Liu, "Metabolism of salvianolic acid A and antioxidant activities of its methylated metabolites," *Drug Metabolism and Disposition*, vol. 42, no. 2, pp. 274–281, 2014.

[32] L. Ma, L. Tang, and Q. Yi, "Salvianolic acids: potential source of natural drugs for the treatment of fibrosis disease and cancer," *Frontiers in Pharmacology*, vol. 10, p. 97, 2019.

[33] W. Bors, C. Michel, K. Stettmaier, Y. Lu, and L. Y. Foo, "Antioxidant mechanisms of polyphenolic caffeic acid oligomers, constituents of salvia officinalis," *Biological Research*, vol. 37, no. 2, pp. 301–311, 2004.

[34] C. M. Uritu, C. T. Mihai, G. D. Stanciu et al., "Medicinal plants of the family lamiaceae in pain therapy: a review," *Pain Research & Management*, vol. 2018, Article ID 7801543, 44 pages, 2018.

[35] H. Silva and N. M. F. Lopes, "Cardiovascular effects of caffeic acid and its derivatives: a comprehensive review," *Frontiers in Physiology*, vol. 11, Article ID 595516, 2020.

[36] H. Parlakpinar, E. Sahna, A. Acet, B. Mizrak, and A. Polat, "Protective effect of caffeic acid phenethyl ester (CAPE) on myocardial ischemia-reperfusion-induced apoptotic cell death," *Toxicology*, vol. 209, no. 1, pp. 1–14, 2005.

[37] J. Han, D. Wang, L. Ye et al., "Rosmarinic acid protects against inflammation and cardiomyocyte apoptosis during myocardial ischemia/reperfusion injury by activating peroxisome proliferator-activated receptor gamma," *Frontiers in Pharmacology*, vol. 8, p. 456, 2017.

[38] J. Diao, H. Zhao, P. You et al., "Rosmarinic acid ameliorated cardiac dysfunction and mitochondrial injury in diabetic cardiomyopathy mice via activation of the SIRT1/PGC-1α pathway," *Biochemical and Biophysical Research Communications*, vol. 546, pp. 29–34, 2021.

[39] J.-Y. Zhang, M. Wang, R.-Y. Wang et al., "Salvianolic acid A ameliorates arsenic trioxide-induced cardiotoxicity through decreasing cardiac mitochondrial injury and promotes its anticancer activity," *Frontiers in Pharmacology*, vol. 9, p. 487, 2018.

[40] V. I. Zozina, S. Covantev, O. A. Goroshko, L. M. Krasnykh, and V. G. Kukes, "Coenzyme Q10 in cardiovascular and metabolic diseases: current state of the problem," *Current Cardiology Reviews*, vol. 14, no. 3, pp. 164–174, 2018.

[41] S. A. Mortensen, F. Rosenfeldt, A. Kumar et al., "The effect of coenzyme Q10 on morbidity and mortality in chronic heart failure: results from Q-SYMBIO: a randomized double-blind trial," *Journal of the American College of Cardiology: Heart Failure*, vol. 2, no. 6, pp. 641–649, 2014.

[42] A. E. Ghule, C. P. Kulkarni, S. L. Bodhankar, and V. A. Pandit, "Effect of pretreatment with coenzyme Q10 on isoproterenol-induced cardiotoxicity and cardiac hypertrophy in rats," *Current Therapeutic Research*, vol. 70, no. 6, pp. 460–471, 2009.

[43] B.-J. Lee, Y.-F. Tseng, C.-H. Yen, and P.-T. Lin, "Effects of coenzyme Q10 supplementation (300 mg/day) on antioxidation and anti-inflammation in coronary artery disease patients during statins therapy: a randomized, placebo-controlled trial," *Nutrition Journal*, vol. 12, no. 1, p. 142, 2013.

Hindawi
Evidence-Based Complementary and Alternative Medicine
Volume 2021, Article ID 5644171, 15 pages
https://doi.org/10.1155/2021/5644171

Research Article

Efficacy and Safety of Resveratrol Supplements on Blood Lipid and Blood Glucose Control in Patients with Type 2 Diabetes: A Systematic Review and Meta-Analysis of Randomized Controlled Trials

Tianqing Zhang,[1] Qi He,[2] Yao Liu,[1] Zhenrong Chen,[1] and Hengjing Hu[1,3]

[1]*The First Affiliated Hospital, Department of Cardiovascular Medicine, Hengyang Medical School, University of South China, Hengyang, Hunan Province, China*
[2]*People's Hospital of Ningxiang City, Ningxiang City, Hunan Province, China*
[3]*Institute of Cardiovascular Disease and Key Lab for Arteriosclerology of Hunan Province, University of South China, Hengyang, Hunan, China*

Correspondence should be addressed to Hengjing Hu; bestmanhhj123@163.com

Received 3 June 2021; Accepted 19 July 2021; Published 25 August 2021

Academic Editor: Thanasekaran Jayakumar

Background. Diabetes is a major public health concern. Resveratrol has shown great beneficial effects on hyperglycemia and insulin resistance and as an antioxidant. *Methods*. We searched the Chinese and English databases (such as CNKI, PubMed, and Embase) and extracted data from randomized controlled trials (RCTs). Then, RevMan 5.3 was used for bias risk assessment and meta-analysis. The primary outcome indicators include insulin-resistance-related indicators and blood-lipid-related indicators. This systematic review and meta-analysis was registered in PROSPERO (CRD42018089521). *Results*. Fifteen RCTs involving 896 patients were included. For insulin-resistance-related indicators, the summary results showed that, compared with the control group, homeostasis model assessment for insulin resistance (HOMA-IR) in the resveratrol group is lower (WMD: −0.99; 95% CI −1.61, −0.38; $P = 0.002$). For blood-lipid-related indicators, the total cholesterol (TC) and triglyceride (TG) in the resveratrol group is of no statistical significance (for TC, WMD: −7.11; 95% CI −16.28, 2.06; $P = 0.13$; for TG, WMD: −2.15; 95% CI −5.52, 1.22; $P = 0.21$). For adverse events, the summary results showed that there was no statistical difference in the incidence of adverse events between the resveratrol and control groups (WMD: 2; 95% CI 0.44, 9.03; $P = 0.37$). *Conclusion*. Based on the current evidence, resveratrol may improve insulin resistance, lower fasting blood glucose and insulin levels, and improve oxidative stress in patients with type 2 diabetes mellitus.

1. Introduction

Diabetes is a serious metabolic disease that affects about 5% of the world's people. Epidemiological data show that the number of people with diabetes is expected to increase dramatically to 592 million by 2035 [1]. 12% of global health expenditure is spent annually on diabetes and its complications [2]. Diabetes is divided into different types: type 1 and type 2 diabetes account for more than 90% of all cases. Metabolic abnormalities and serious complications caused by type 2 diabetes have profound effects on the life and quality of life of patients, such as microvascular (retinopathy, nephropathy), large blood vessels and peripheral vascular disease [3, 4], and increased risk of cancer [5, 6]. Type 2 diabetes mellitus (T2DM) is characterized by insulin resistance and hyperglycemia [7]. The treatment drugs for T2DM include insulin, alpha glucosidase inhibitors, dipeptidyl peptidase 4 inhibitors, incretin analogues, biguanides, insulin secretagogues, insulin sensitizers, and intestinal lipase inhibitors [8, 9]. However, the currently used therapies are accompanied by side effects, such as hypoglycemia, gastrointestinal problems, and weight gain [8]. Therefore, new drugs and natural compounds are constantly being tested to better prevent and treat diabetes [10].

In the alternative treatment strategy for diabetes treatment, resveratrol, a naturally occurring polyphenolic compound, mainly derived from the rhizome of the main natural source of *Polygonum cuspidatum*. Studies have shown that resveratrol has shown great beneficial effects on hyperglycemia, insulin resistance, and antioxidant [11, 12]. Clinical trials have shown that resveratrol has potential benefits for patients with T2DM, and relevant systematic reviews and reviews have also made relevant comments. However, some results contradict the evidence for the beneficial effects of resveratrol in the treatment of T2DM [13, 14]. This may be due to the limitation of sample size and treatment duration masking clear changes in clinical practice [12–14]. Meanwhile, the most recent meta-analysis search deadline was in June 2017, and a large number of RCTs appeared in the following period [15–20]. Therefore, we conduct a new systematic review and meta-analysis on this topic to evaluate the effects of resveratrol supplements on blood sugar, blood lipids, oxidative stress, safety, and other aspects of T2DM.

2. Materials and Methods

2.1. Protocol. This systematic review and meta-analysis were conducted strictly in accordance with the protocol (CRD42018089521) and PRISMA 2020 guidelines (see Supplementary Materials).

2.2. Inclusion and Exclusion Criteria

2.2.1. Participants. Participants are patients with T2DM diagnosed through recognized standards, regardless of age, gender, and nationality. Records need to mention clear diagnostic criteria for RA, with a balanced baseline and comparability.

2.2.2. Intervention. The intervention in experiments group was resveratrol supplements with no limits on the type, dose, frequency, and so on. The intervention in control group was western medicine, blanks, or placebo.

2.2.3. Outcomes. The primary outcomes are as follows: homeostasis model assessment for insulin resistance (HOMA-IR), total cholesterol (TC), triglyceride (TG). The Secondary outcomes are as follows: HbA1c, low density lipoprotein cholesterol (LDL-C), high density lipoprotein cholesterol (HDL-C), fasting glucose, fasting insulin, and MDA.

2.2.4. Study Type. This study is a randomized controlled trial (RCT), with no limits on the manner by which randomization has been achieved, blinding, or language of publication.

2.2.5. Exclusion Criteria. The exclusion criteria are as follows: (1) not T2DM patients; (2) the participant is not human; (3) nonoriginal research literature; (4) non-RCT.

2.3. Search Strategy. The English databases (Web of Science, EMBASE, PubMed, and Medline Complete) and Chinese databases (China National Knowledge Infrastructure Databases (CNKI), Chinese Biomedical Database (CBM), Chinese Science and Technology Periodical Database (VIP), and Wan Fang Database) were searched. The search time period is from the establishment of the database to 16th of February, 2020. In addition, the Cochrane Library (until Issue 2, 2020) and clinical trial registration database (ClinicalTrials) were also searched. The search strategy for PubMed is presented in Table S1, as an example.

2.4. Literature Screening and Study Quality Assessment. Literature screening and study quality assessment were performed according to the Cochrane system evaluation method. First, the reviewers read the title and abstract for a preliminary screening and then screened them based on the full text. If there is a disagreement, it is resolved through discussion with all researchers. The lack of information would be supplemented by contacting the author through a letter or by imputation [21].

The quality of the literature was evaluated using the Cochrane bias risk assessment tool provided by the Cochrane Collaboration [22], and the following were evaluated: (1) whether the random method is correct; (2) whether the allocation is hidden; (3) blind method; (4) data bias; (5) selective reporting bias; (6) other biases. The evaluation was first conducted independently by two researchers. If there is a disagreement, it is resolved through discussion with all researchers.

2.5. Statistical Analysis. The RevMan version 5.3 statistical software provided by Cochrane Collaboration was used for analysis [23]. When the heterogeneity of RCTs was small ($P > 0.1$, $I^2 < 50\%$), the fixed-effects model was used for meta-analysis. If there is statistical heterogeneity ($P < 0.1$, $I^2 > 50\%$), the reviewers would first look for the source of heterogeneity. If the heterogeneity between the RCTs was statistical rather than clinical heterogeneity, the random-effects model would be used for meta-analysis. If the heterogeneity was too large or the data source cannot be found, a descriptive analysis would be performed. For continuous variables, the weighted mean difference (WMD) was used as the effect analysis statistic, and the interval is estimated using a 95% confidence interval (95% CI). If the difference in the value of the outcome exceeds 10 times or the unit of measurement is different, the standard MD (SMD) was used. For dichotomous variable, the risk ratio (RR) was used as the effect analysis statistic with 95% CI.

2.6. Sensitivity Analysis. STATA 15.0 was utilized for sensitivity analysis. The outcomes that met the following conditions were all subjected to sensitivity analysis: (1) random-effects model is used; (2) the results of the fixed-effects model are inconsistent with the results of the random-effects model (whether it is a subgroup result or a summary result).

3. Results

3.1. Results of the Search and Description of Included Trials. A total of 616 articles were retrieved through the database: 590 articles were excluded by reading titles and abstracts, and eight articles were excluded by reading the full text. Finally, 18 articles met the inclusion criteria [15–19, 24–36] (Figure 1). Three studies are by Bo et al. [16, 29, 30], two studies are by Imamura et al. [17], and two studies are by Abdollahi et al. [33, 34], and they were merged. Study characteristics are presented in Table 1.

3.2. Risk of Bias Assessments. The summary and graph of risk of bias are shown in Figure 2.

3.2.1. Random Sequence Generation and Allocation Concealment. Five RCTs [15, 17, 26, 27, 36] did not describe the method of generating random sequences and were rated as unclear risk of bias. Other RCTs describe the random sequence generation methods and are assessed as low risk of bias.

Six RCTs [15, 17, 26, 27, 35, 36] did not describe the allocation concealment method and were rated as having an unclear risk of bias. The other RCTs utilized the capsules in the same shape, size, and color to contain curcumin and placebo; hence, they were considered to have allocation concealment and rated as having low risks of bias.

3.2.2. Blinding. Three RCTs [28, 35, 36] did not specify whether blinding was used and therefore were assessed as high risk of bias. The other RCTs claimed to use blinding, but Goh et al. [25], Brasnyó et al. [26], Bashmakov et al. [27], Zare Javid et al. [15], and Imamura et al. [17] did not describe the implementation process for both researchers and participants. They were rated as unclear risk of bias. The other RCTs described blinding of participants, so the blinding of participants and personnel (performance bias) was rated as low risk of bias.

3.2.3. Incomplete Outcome Data and Selective Reporting. Six RCTs [17, 18, 25, 31, 32, 35] were assessed as unclear risk of bias because of missing data and did not describe whether to use intend-to-treat analysis. The incomplete outcome data of the other RCTs are rated as low risk of bias because the number of missing people and the reasons for the missing between groups is balanced. All RCTs reported study's prespecified outcomes that are of interest in the review; their risks of bias were low.

3.2.4. Other Potential Bias. There were other sources of bias in all RCTs; therefore, the risks of other bias were low.

3.3. Primary Outcomes

3.3.1. Homeostasis Model Assessment for Insulin Resistance. Ten RCTs reported the changes in HOMA-IR, and there was a large statistical heterogeneity among the studies ($P < 0.00001$, $I^2 = 83\%$), so the random-effects model was used. The HOMA-IR of the resveratrol group was significantly lower than that of the control group, and the difference was statistically significant (WMD = −0.99; 95% CI (−1.61, −0.38); $P = 0.002$; random-effect model) (Figure 3).

3.3.2. Total Cholesterol. Ten RCTs reported the changes in TC, and there was a large statistical heterogeneity among the studies ($P < 0.00001$, $I^2 = 86\%$), so the random-effects model was used. The results showed that there was no statistical difference in TC between the resveratrol and control groups (WMD = −7.11; 95% CI (−16.28, 2.06); $P = 0.13$; random-effect model) (Figure 4).

3.3.3. Triglyceride. Eleven RCTs reported the changes in TG, and the statistical heterogeneity among the studies was low ($P = 0.12$, $I^2 = 34\%$), so the fixed-effects model was used. The results showed that there was no statistical difference in TG between the resveratrol and control groups (WMD = −2.15; 95% CI (−5.52, 1.22); $P = 0.21$; fixed-effect model) (Figure 5).

3.4. Secondary Outcomes

3.4.1. Glycosylated Hemoglobin. Eleven RCTs reported the changes in HbA1c, and there was a large statistical heterogeneity among the studies ($P < 0.00001$, $I^2 = 95\%$), so the random-effects model was used. The HbA1c of the resveratrol group was significantly lower than that of the control group, and the difference was statistically significant (WMD = −0.45; 95% CI (−0.73, −0.16); $P = 0.002$; random-effect model) (Figure 6).

3.4.2. Fasting Glucose and Fasting Insulin. Fourteen RCTs reported the changes in fasting glucose, and there was a large statistical heterogeneity among the studies ($P < 0.00001$, $I^2 = 85\%$), so the random-effects model was used. The fasting glucose of the resveratrol group was significantly lower than that of the control group, and the difference was statistically significant (WMD = −19.61; 95% CI (−26.02, −13.20); $P < 0.00001$; random-effect model) (Figure 7).

Thirteen RCTs reported the changes in fasting insulin, and there was a large statistical heterogeneity among the studies ($P < 0.00001$, $I^2 = 90\%$), so the random-effects model was used. The fasting insulin of the resveratrol group was significantly lower than that of the control group, and the difference was statistically significant (SMD = −0.67; 95% CI (1.21, −0.14); $P = 0.01$; random-effect model) (Figure 8).

3.4.3. LDL-C and HDL-C. Ten RCTs reported the changes in LDL-C, and there was a large statistical heterogeneity among the studies ($P < 0.00001$, $I^2 = 93\%$), so the random-effects model was used. The results showed that there was no statistical difference in LDL-C between the resveratrol and control groups (WMD = −6.84; 95% CI (−16.60, 2.92); $P = 0.17$; random-effect model) (Figure 9).

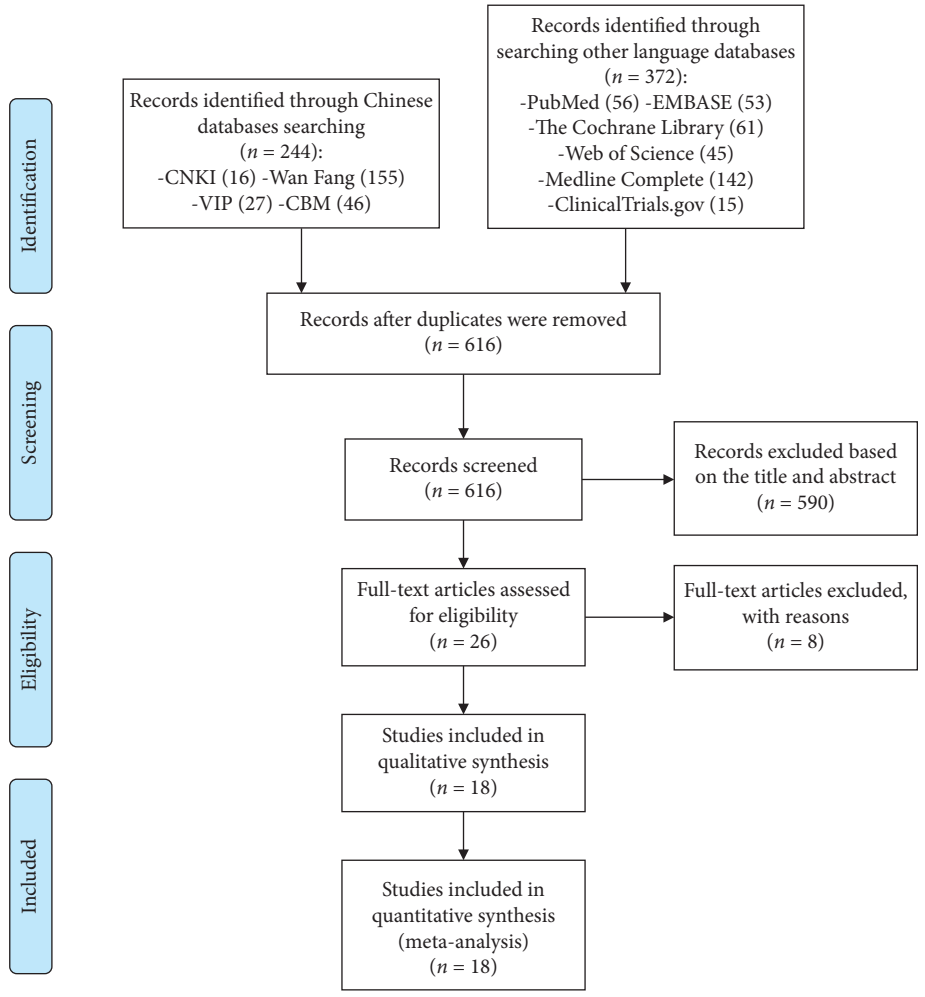

Figure 1: Flow diagram of searching and article selection.

Table 1: The characteristics of the included studies.

Study	Country	Sample size (female/male)		Intervention		Relevant outcomes	Mean age (years)		Duration
		Trial group	Control group	Trial group	Control group		Trial group	Control group	
Movahed et al. [23]	Iran	33 (16/17)	31 (17/16)	Resveratrol 500 mg, bid	Microcellulose (placebo) 500 mg, bid	HOMA-IR, HbA1c, fasting blood glucose, fasting insulin, TC, TG, HDL-C, LDL-C	52.45 ± 6.18	51.81 ± 6.99	1.5 months

Table 1: Continued.

Study	Country	Sample size (female/male)		Intervention		Relevant outcomes	Mean age (years)		Duration
		Trial group	Control group	Trial group	Control group		Trial group	Control group	
Goh et al. [24]	Singapore	5 (0/5)	5 (0/5)	Resveratrol 500 mg, qd, initially, increased by 500 mg per day every 3 days, to a maximum dose of 3000 mg per day (1000 mg, tid)	Placebo 500 mg, qd, initially, increased by 500 mg per day every 3 days, to a maximum dose of 3000 mg per day (1000 mg, tid)	HbA1c, fasting blood glucose, fasting insulin, TC, TG, HDL-C, LDL-C, adverse events	55.8 ± 7.3	56.8 ± 5.3	3 months
Brasnyó et al. [25]	Hungary	10 (0/10)	9 (0/9)	Resveratrol 5 mg, bid	Placebo, bid	HOMA-IR	57.79 ± 7.9	52.5 ± 11.1	1 month
Bashmakov et al. [26]	Egypt	14 (6/8)	10 (3/10)	Resveratrol 50 mg, bid	Placebo, bid	Fasting blood glucose, fasting insulin, TC, HDL-C, LDL-C	54.0 ± 10.1	59.8 ± 6.6	2 months
Bhatt et al. [27]	India	28 (20/9)	29 (16/12)	Resveratrol 250 mg, qd, with oral hypoglycemic agents such as glibenclamide and/or metformin	Oral hypoglycemic agents such as glibenclamide and/or metformin	HbA1c, fasting blood glucose, TC, TG, HDL-C, LDL-C	56.67 ± 8.91	57.75 ± 8.71	3 months
Zare Javid et al. [15]	Iran	21 (18/4)	22 (16/5)	Resveratrol 240 mg, bid	Starch (placebo) 240 mg, bid	HOMA-IR, fasting blood glucose, fasting insulin, TG	49.1 ± 7.4	50.9 ± 8.9	1 month
Bo et al. [16, 28, 29]	Italy	130 (51/79)	62 (15/47)	Resveratrol 500 mg, qd, or 40 mg, qd	Placebo, qd	HOMA-IR, HbA1c, fasting blood glucose, fasting insulin, TC, TG, HDL-C, LDL-C	64.95 ± 8.08	65.4 ± 8.8	6 months
Imamura et al. [17]	Japan	25 (10/15)	25 (14/11)	Resveratrol 100 mg, qd	Placebo, qd	HbA1c, fasting blood glucose, fasting insulin, TC, TG, HDL-C, adverse events	57.4 ± 10.6	58.2 ± 10.1	3 months

Table 1: Continued.

Study	Country	Sample size (female/male)		Intervention		Relevant outcomes	Mean age (years)		Duration
		Trial group	Control group	Trial group	Control group		Trial group	Control group	
Sattarinezhad et al. [18]	Iran	30 (16/14)	30 (17/13)	Resveratrol 500 mg, qd + losartan 12.5 mg, qd	Placebo 500 mg, qd + losartan 12.5 mg, qd	HOMA-IR, HbA1c, fasting blood glucose, fasting insulin, adverse events	56.8 ± 9.7	55.7 ± 10.8	3 months
Khodabandehloo et al. [19]	Iran	25 (12/13)	20 (10/10)	Resveratrol 400 mg, bid	Microcellulose (placebo) 400 mg, bid	HOMA-IR, HbA1c, fasting blood glucose, fasting insulin, TC, TG, HDL-C, LDL-C, adverse events	56.48 ± 6.72	61.10 ± 5.61	2 months
Seyyedebrahimi et al. [30]	Iran	23 (12/11)	23 (13/10)	Resveratrol 400 mg, bid	Microcellulose (placebo) 400 mg, bid	HOMA-IR, HbA1c, fasting blood glucose, fasting insulin, TC, TG, HDL-C, LDL-C, MDA, adverse events	54.96 ± 6.37	58.72 ± 6.06	2 months
Hoseini et al. [31]	Iran	28 (unknown/ unknown)	28 (unknown/ unknown)	Resveratrol 500 mg, qd	Placebo, qd	HOMA-IR, fasting blood glucose, fasting insulin, TG, TC, HDL-C, LDL-C, MDA, TAC, adverse events	61.0 ± 8.6	63.3 ± 10.1	1 month

Table 1: Continued.

Study	Country	Sample size (female/male)		Intervention		Relevant outcomes	Mean age (years)		Duration
		Trial group	Control group	Trial group	Control group		Trial group	Control group	
Abdollahi et al. [32, 33]	Iran	35 (15/20)	36 (16/20))	Resveratrol 500 mg, bid	Placebo, bid	HOMA-IR, HbA1c, fasting blood glucose, fasting insulin, TG, TC, HDL-C, LDL-C, adverse events	50.14 ± 7.38	50.06 ± 7.69	2 months
Zhang et al. [34]	China	48 (24/24)	48 (23/25)	Resveratrol 300 mg, bid	Blank	HbA1c, fasting blood glucose, fasting insulin, TG, TC, HDL-C, LDL-C	50.9 ± 9.7	52.3 ± 11.2	3 months
Ying et al. [35]	China	32 (12/20)	31 (11/20)	Resveratrol 500 mg, bid	Blank	HbA1c, fasting blood glucose, fasting insulin	64.94 ± 1.36	64.95 ± 1.35	2 months

HOMA-IR: homeostasis model assessment for insulin resistance; TC: total cholesterol; TG: triglyceride; LDL-C: low density lipoprotein cholesterol; HDL-C: high density lipoprotein cholesterol.

Eleven RCTs reported the changes in HDL-C, and there was a large statistical heterogeneity among the studies ($P < 0.0001$, $I^2 = 72\%$), so the random-effects model was used. The results showed that there was no statistical difference in HDL-C between the resveratrol and control groups (WMD = 1.38; 95% CI (−0.43, 3.18); $P = 0.13$; random-effect model) (Figure 10).

3.4.4. Oxidative-Stress-Related Indicators. Two RCTs reported the changes in MDA, and the statistical heterogeneity among the studies was low ($P = 0.55$, $I^2 = 0\%$), so the fixed-effects model was used. The results showed that there was no statistical difference in MDA between the resveratrol and control groups (WMD = −0.05; 95% CI (−0.33, 0.23); $P = 0.71$; fixed-effect model) (Figure 11).

3.5. Adverse Events. Two RCTs reported the adverse events, and the statistical heterogeneity among the studies was low ($P = 0.51$, $I^2 = 0\%$), so the fixed-effects model was used. The results showed that there was no statistical difference of adverse events between the resveratrol and control groups (RR = 2; 95% CI (0.44, 9.03); $P = 0.37$; fixed-effect model)] (Figure 12).

3.6. Sensitivity Analysis Results. Sensitivity analyses were performed for five outcomes: TC and LDL-C. (1) In the outcome "TC," no matter which study was removed, the results were not significantly changed, suggesting that the heterogeneity may not come from RCT (Figure 13(a)). (2) In the outcome "LDL-C," after we omitted the study of Zhang et al. [35], we found that the estimate of the result moved out of the lower limit of 95% CI (Figure 13(b)). This indicates that the study of Zhang et al. [35] may be the source of heterogeneity of LDL-C outcomes.

4. Discussion

This systematic review and meta-analysis included 15 RCTs involving 896 patients. This research showed that resveratrol may improve HOMA-IR and reduce HbA1c, fasting blood sugar, and fasting insulin levels, indicating that resveratrol may reduce insulin resistance, thereby lowering blood sugar and insulin levels. Although the results found in the current research are meaningful, they should be interpreted with caution due to the high heterogeneity of these results and small number of participants involved. This study did not show the positive effects of resveratrol on blood lipid levels and oxidative stress levels but showed that they have a trend of improvement. In the future, more RCTs may be needed to

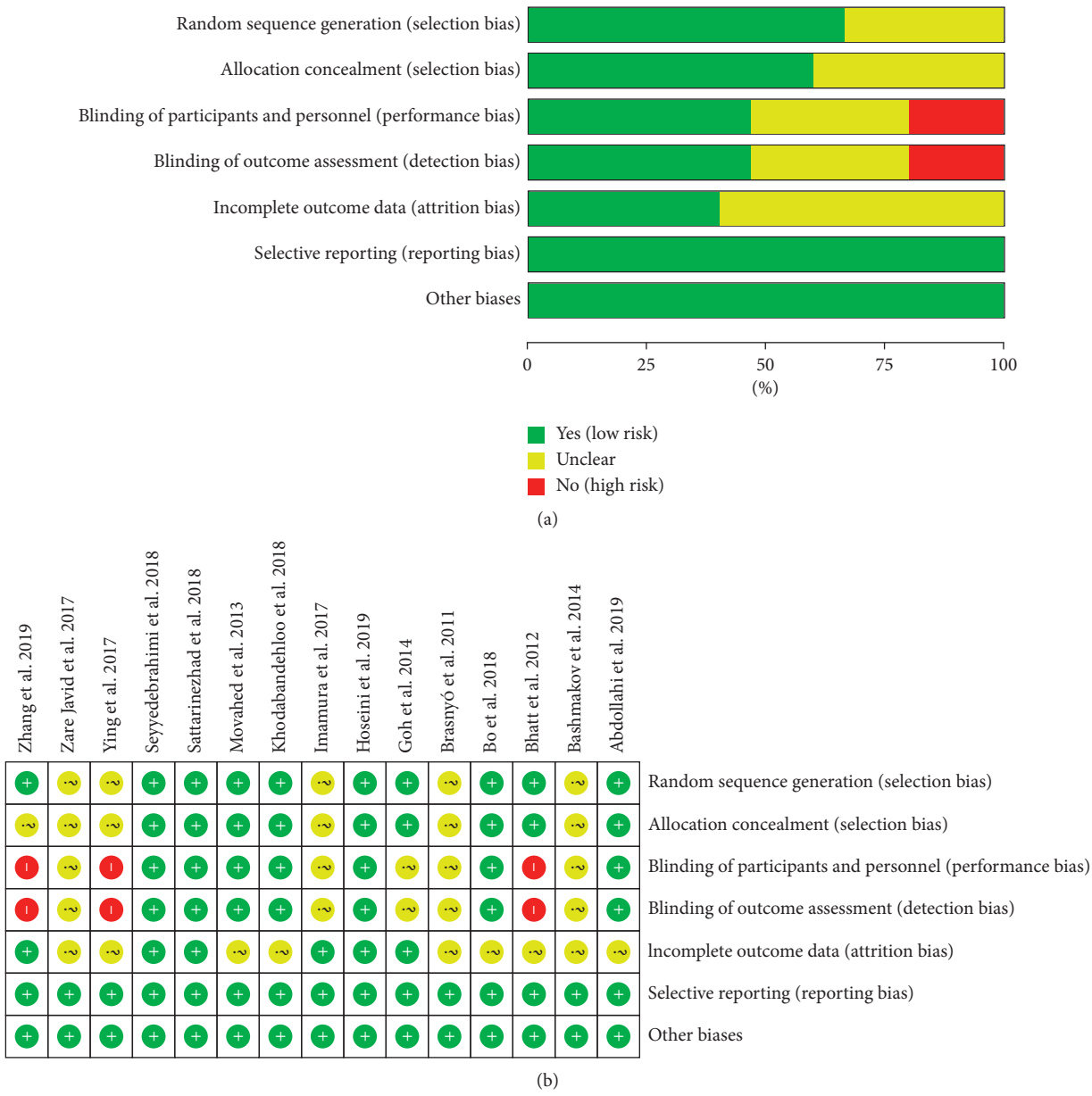

Figure 2: The risk of bias assessment. (a) The risk of bias graph; (b) the risk of bias table.

confirm or modify the effects of resveratrol on blood lipids and oxidative stress indicators in patients with T2DM. Only two RCTs reported adverse events, and the meta-analysis results showed that there was no statistically significant difference in adverse events between the control and resveratrol groups. Due to the insufficient number of RCTs, this result is doubtful. It can only be inferred based on the existing evidence that resveratrol may be a safe therapy for the treatment of T2DM. More RCTs are needed in the future to report on the safety of resveratrol.

Resveratrol, as a type of polyphenolic phytoalexin, has good antioxidant properties. It is produced by plants under the action of exogenous stimuli, such as ultraviolet light irradiation, mechanical damage or fungal infection [37–41]. A large number of in vitro and in vivo tests have shown that resveratrol can effectively prevent hypertension through antioxidant effects [42], cardiovascular diseases [43], non-alcoholic fatty liver [44], metabolic syndrome [45], aging [46], cancer [47], and immunological diseases [48], through its antioxidant effect, and has a good application prospect. Based on this, the research on the safety of resveratrol is meaningful. Williams et al. [49] showed that resveratrol is not irritating to the skin and eyes, and the micronucleus test in vivo proved that resveratrol has no genetic toxicity. After a 90-day subchronic toxicity test, it was found that resveratrol did not cause any adverse effects on the body and did not have reproductive toxicity at the maximum dose of 700 mg/(kg·d). This preliminarily proves that resveratrol is nontoxic and safe. Hebbar et al. [50] administered resveratrol to CD rats at 0.3, 1.0, and 3.0 g/(kg·d). They found that, at 0.3 g/

Study or subgroup	Resveratrol Mean	SD	Total	Control Mean	SD	Total	Weight (%)	Mean difference IV, random, 95% CI
Movahed et al. 2013	−2.69	2.79	33	0.22	1.5	31	8.6	−2.91 [−4.00, −1.82]
Goh et al. 2014	0.228	0.549	5	0.136	0.196	5	10.8	0.09 [−0.42, 0.60]
Brasnyó et al. 2011	−1.52	1.18	10	0.04	1.4	9	8.2	−1.56 [−2.73, −0.39]
Zare Javid et al. 2017	−0.56	1.26	21	−0.15	1.48	22	9.7	−0.41 [−1.23, 0.41]
Bo et al. 2018a	−4.33	1.8	65	−4.06	1.59	31	10.1	−0.27 [−0.98, 0.44]
Bo et al. 2018b	−6.15	1.8	65	−4.06	1.59	31	10.1	−2.09 [−2.80, −1.38]
Sattarinezhad et al. 2018	−1	3	30	1.6	1.9	30	7.8	−2.60 [−3.87, −1.33]
Khodabandehloo et al. 2018	−1.64	2.58	25	−0.36	1.03	20	8.5	−1.28 [−2.39, −0.17]
Seyyedebrahimi et al. 2018	−1.18	2	23	−1.58	3.08	23	6.9	0.40[−1.10, 1.90]
Hoseini et al. 2019	−0.6	1.87	28	−0.2	2.5	28	8.3	−0.40 [−1.56, 0.76]
Abdollahi et al. 2019	−0.36	0.83	35	−0.1	1.18	36	11.0	−0.26 [−0.73, 0.21]
Total (95% CI)			*340*			*266*	*100.0*	*−0.99 [−1.61, −0.38]*

Heterogeneity: tau^2 = 0.83; chi^2 = 59.01, df = 10 (P < 0.00001); I^2 = 83%
Test for overall effect: Z = 3.17 (P = 0.002)

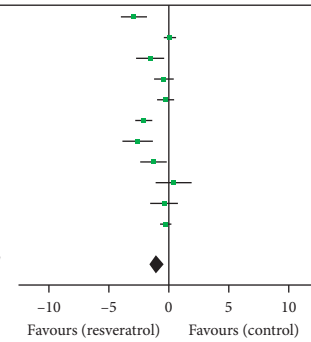

Risk of bias legend
(A) Random sequence generation (selection bias)
(B) Allocation concealment (selection bias)
(C) Blinding of participants and personnel (performance bias)
(D) Blinding of outcome assessment (detection bias)
(E) Incomplete outcome data (attrition bias)
(F) Selective reporting (reporting bias)
(G) Other biases

Figure 3: Homeostasis model assessment for insulin resistance (HOMA-IR).

Study or subgroup	Resveratrol Mean	SD	Total	Control Mean	SD	Total	Weight (%)	Mean difference IV, random, 95% CI
Movahed et al. 2013	−11.33	35.24	33	6.69	40.68	31	8.0	−18.02 [−36.72, 0.68]
Bashmakov et al. 2014	17.29	23.84	14	32.6	39.58	10	5.8	−15.31 [−42.84, 12.22]
Bhatt et al. 2012	−14.32	5.31	28	6.9	0.31	29	11.9	−21.22 [−23.19, −19.25]
Bo et al. 2018a	1.57	24.22	65	−6.95	28.86	31	10.0	8.52 [−3.22, 20.26]
Bo et al. 2018b	1.14	24.22	65	−6.95	28.86	31	10.0	8.09 [−3.65, 19.83]
Imamura et al. 2017	2.7	24.2	25	1.7	38.6	25	8.2	1.00 [−16.86, 18.86]
Seyyedebrahimi et al. 2018	−12.34	32.49	23	−1.11	25.12	23	8.5	−11.23 [−28.01, 5.55]
Zhang et al. 2019	−44.39	36.44	48	−19.3	30.12	48	9.5	−25.09 [−38.46, −11.72]
Abdollahi et al. 2019	1.57	25.34	35	1.94	18.21	36	10.4	−0.37 [−10.66, 9.92]
Khodabandehloo et al. 2018	−8.36	30.24	25	−7.15	27.15	20	8.5	−1.21 [−18.01, 15.59]
Hoseini et al. 2019	−5.8	29.01	28	−0.1	25.13	28	9.3	−5.70 [−19.92, 8.52]
Total (95% CI)			*389*			*312*	*100.0*	*−7.11 [−16.28, 2.06]*

Heterogeneity: tau^2 = 183.44; chi^2 = 72.74, df = 10 (P < 0.00001); I^2 = 86%
Test for overall effect: Z = 1.52 (P = 0.13)

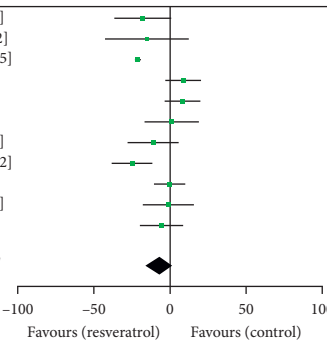

Risk of bias legend
(A) Random sequence generation (selection bias)
(B) Allocation concealment (selection bias)
(C) Blinding of participants and personnel (performance bias)
(D) Blinding of outcome assessment (detection bias)
(E) Incomplete outcome data (attrition bias)
(F) Selective reporting (reporting bias)
(G) Other biases

Figure 4: Total cholesterol.

Study or subgroup	Resveratrol Mean	SD	Total	Control Mean	SD	Total	Weight (%)	Mean difference IV, fixed, 95% CI
Movahed et al. 2013	−17.81	39.87	33	−11.56	36.71	31	3.2	−6.25 [−25.01, 12.51]
Goh et al. 2014	32.76	66.41	5	−1.77	43.39	5	0.2	34.53 [−35.00, 104.06]
Bhatt et al. 2012	0.75	9.59	28	2.8	2.96	29	82.6	−2.05 [−5.76, 1.66]
Zare Javid et al. 2017	−12	65.56	21	9.3	67.71	22	0.7	−21.30 [−61.13, 18.53]
Bo et al. 2018a	23.78	48.53	65	3.68	44.13	31	3.0	20.10 [0.59, 39.61]
Bo et al. 2018b	−8.76	48.53	65	3.68	44.13	31	3.0	−12.44 [−31.95, 7.07]
Imamura et al. 2017	3.4	47.2	25	−2.4	75.4	25	0.9	5.80 [−29.07, 40.67]
Zhang et al. 2019	−69.44	121.25	48	−3.472	129.77	48	0.5	−65.97 [−116.21, −15.73]
Khodabandehloo et al. 2018	−1.92	67.19	25	−19.44	49.02	20	1.0	17.52 [−16.47, 51.51]
Abdollahi et al. 2019	−0.54	55.99	35	2.05	34.98	36	2.4	−2.59 [−24.38, 19.20]
Hoseini et al. 2019	−7.4	60.51	28	2.4	57.2	28	1.2	−9.80 [−40.64, 21.04]
Seyyedebrahimi et al. 2018	−9.95	62.57	23	2.88	38.63	23	1.3	−12.83 [−42.88, 17.22]
Total (95% CI)			*401*			*329*	*100.0*	*−2.15 [−5.52, 1.22]*

Heterogeneity: chi^2 = 16.62, df = 11 (P = 0.12); I^2 = 34%
Test for overall effect: Z = 1.25 (P = 0.21)

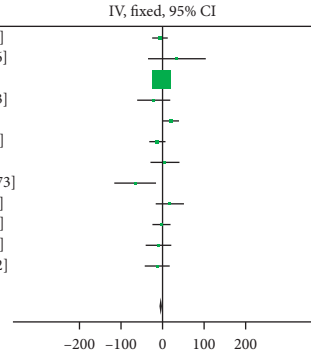

Risk of bias legend
(A) Random sequence generation (selection bias)
(B) Allocation concealment (selection bias)
(C) Blinding of participants and personnel (performance bias)
(D) Blinding of outcome assessment (detection bias)
(E) Incomplete outcome data (attrition bias)
(F) Selective reporting (reporting bias)
(G) Other biases

Figure 5: Triglyceride.

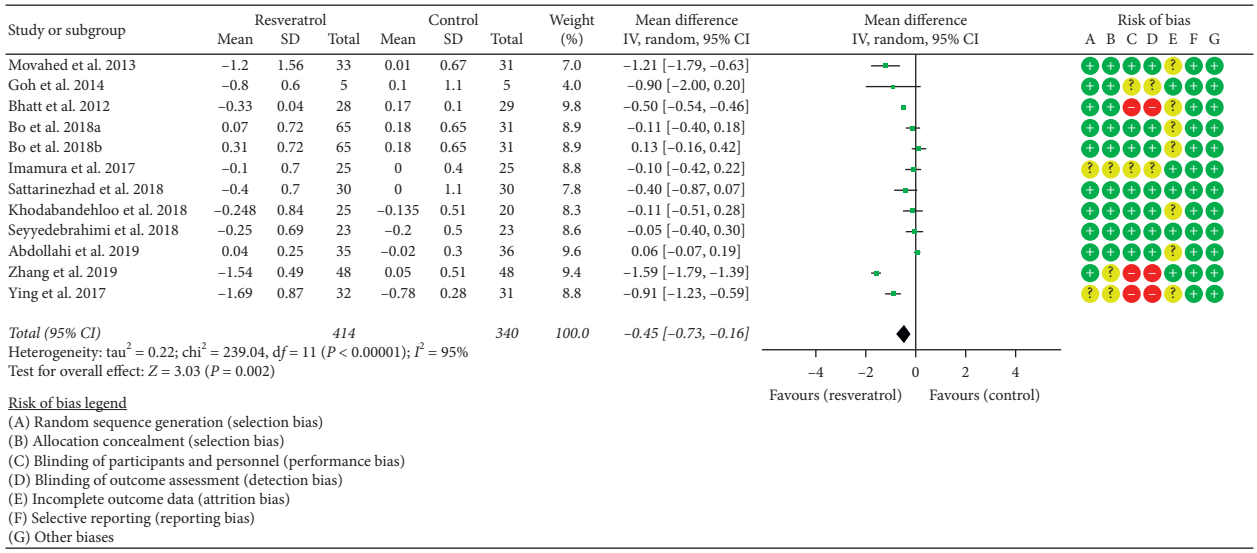

Figure 6: Glycosylated hemoglobin.

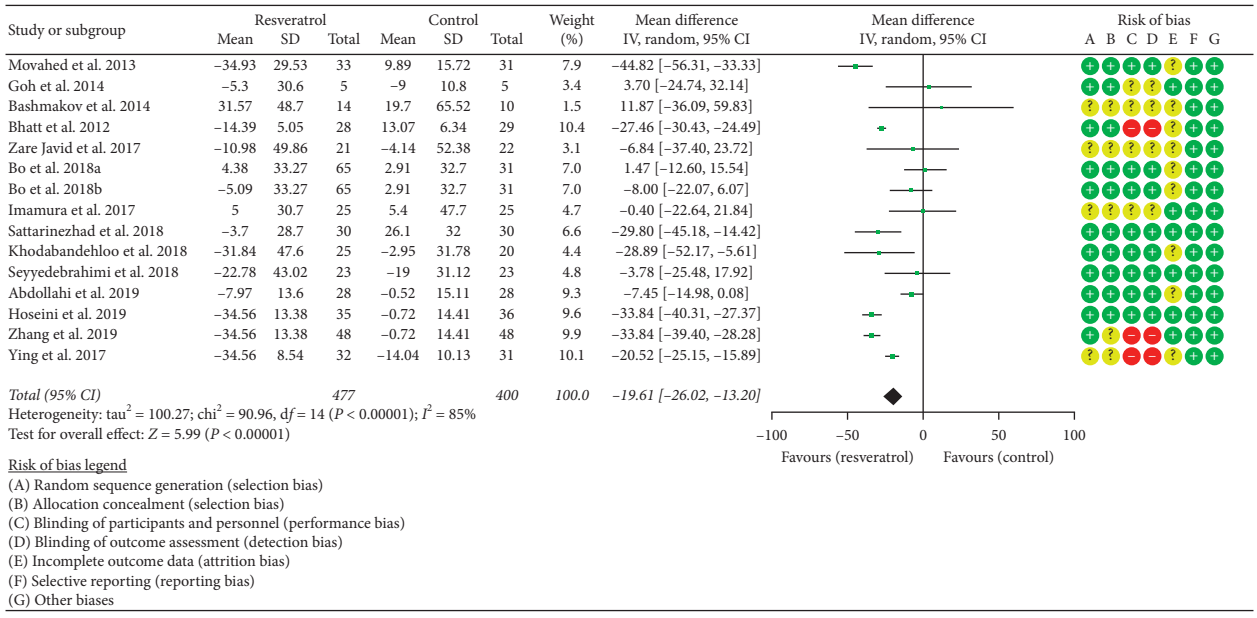

Figure 7: Fasting blood glucose.

(kg·d), the rats showed no adverse reactions. However, at 1.0 and 3.0 g/(kg·d), female and male rats experienced different degrees of dehydration, dyspnea, kidney toxicity, and increased serum liver enzymes. It shows that resveratrol has certain toxicity at high doses. In order to determine the safe dose range of resveratrol, Johnson et al. [51] also studied the subchronic oral toxicity of resveratrol. The results showed that when the dose was increased to 1 000 mg/(kg·d), resveratrol showed certain toxicity; it showed that the no-observed-adverse-effect levels (NOAELs) of resveratrol in rats and dogs are 200 mg/(kg·d) and 600 mg/(kg·d), respectively. Since the content of resveratrol in plants or foods is lower than NOAEL, it can be considered that normal consumption of foods rich in resveratrol can not only give full play to its physiological activities but also be safe. In clinical trials, a randomized, double-blind, placebo-controlled clinical trial found that, at a clinical dose of 150 mg/day, no effect of resveratrol supplementation on cardiometabolic risk parameters was observed. It suggests that resveratrol supplements are well tolerated and safe [52]. Federica et al. found that high daily doses (≥300 mg/day) of resveratrol can promote cardiovascular health. Resveratrol is well tolerated, and no serious adverse events occurred in most eligible trials [53]. This study also showed that the adverse events of the resveratrol group were the same as those of the control group, and no serious adverse events occurred, which suggested that resveratrol has good safety.

Most of the results, such as HOMA-IR, TC, TG, and LDL-C, have large heterogeneity, so this study used sensitivity analysis to find the source of heterogeneity. Sensitivity

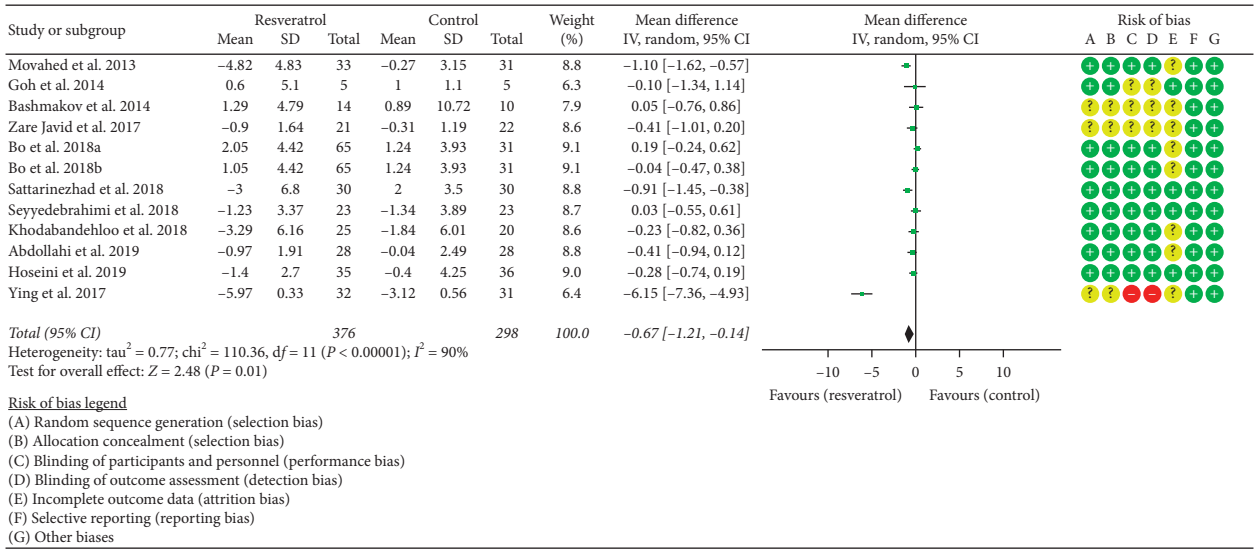

Figure 8: Fasting insulin.

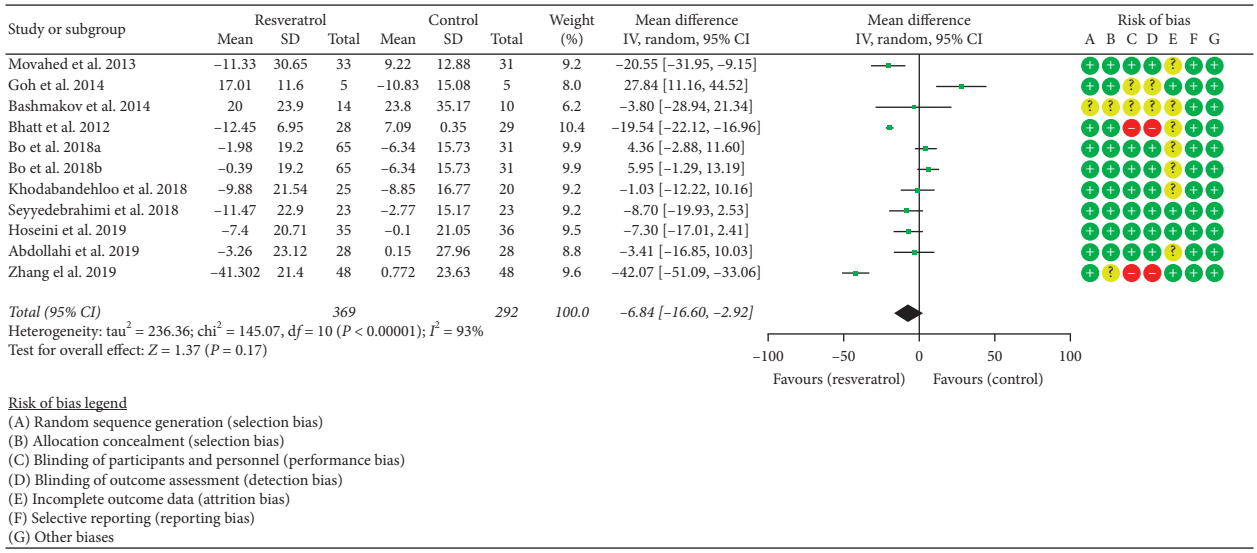

Figure 9: LDL-C.

analyses were performed for TC and LDL-C. For outcome "LDL-C," the study of Zhang et al. [35] may be the source of heterogeneity. Compared with other studies, the blinding method of Zhang et al. [35] was assessed as a high risk of bias, and allocation concealment was assessed as an unknown risk of bias. This suggests that the heterogeneity may be due to the low quality of RCTs, and failure to apply blinding may lead to biased results. In addition to the possible sources of heterogeneity found by sensitivity analysis, heterogeneity may also come from ethnic differences, regional differences, gender differences, and so on: (1) most of the RCTs are from Iran, and a few are from China, Japan, Egypt, Singapore, Hungary, and Italy (see Table 1); there are differences between races in these countries, and this may cause different sensitivities to resveratrol. (2) The gender composition ratio of RCTs is different. The participants in the studies of Goh et al. [25] and Brasnyó et al. [26] were all male, while the gender ratio in the study of Hoseini et al. [32] is not clear. Males and females having different sensitivities to drugs may lead to heterogeneity. (3) The dosage, preparation type, and usage of resveratrol in RCTs are different. The difference between the dosage and type of preparation may affect the efficacy of the drug, which may be the source of heterogeneity.

This meta-analysis is similar to the works of Zhu et al. [13] and Liu et al. [14] in that both have shown that resveratrol can improve HOMA-IR, fasting blood glucose, and HbA1c insulin levels. The differences are as follows. (1) *Research Process.* This research was registered with PROSPERO in advance, and it was analyzed strictly according to the protocol and PRISMA-guidelines. The inclusion and exclusion criteria were more stringent. (2) *Literature Quality*

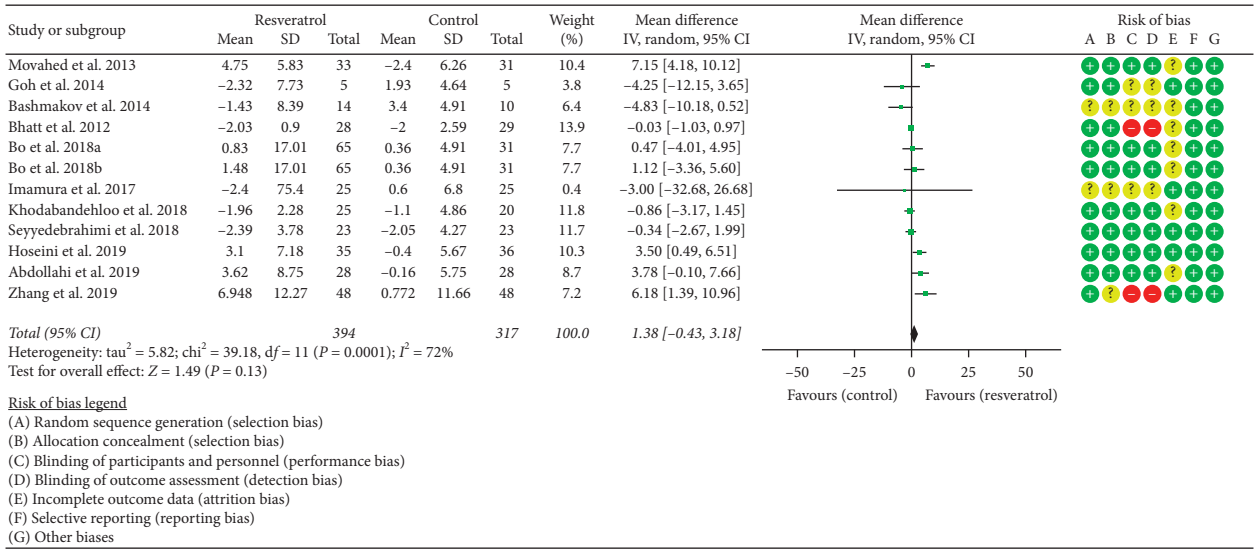

Figure 10: HDL-C.

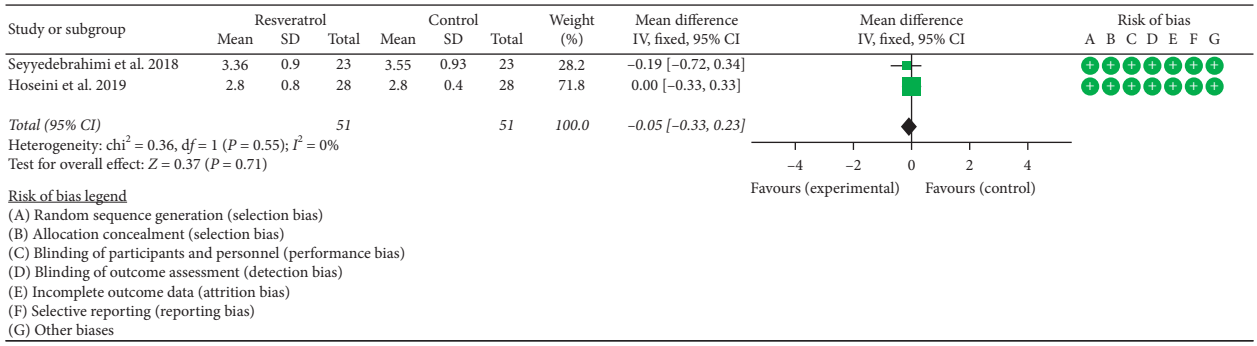

Figure 11: MDA.

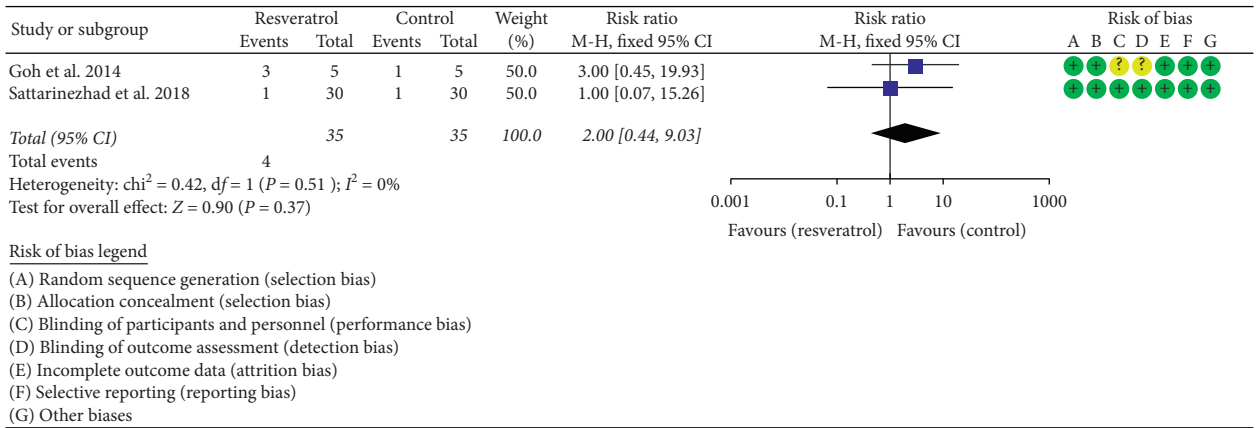

Figure 12: Adverse events.

Assessment. Cochrane bias risk assessment tool is used to evaluate the literature quality. (3) *Included Literature.* Liu et al. [14] only evaluated RCTs of types 1 and 2 diabetes, while Zhu et al. [13] only evaluated nine RCTs. This study evaluated 15 diabetes-related RCTs; 10 of them [15–19, 29–36] are published after 2016, which showed more stable results.

The advantage of this study is that the systematic review and meta-analysis include all available RCTs for clinical problems. The study is the latest systematic review and meta-

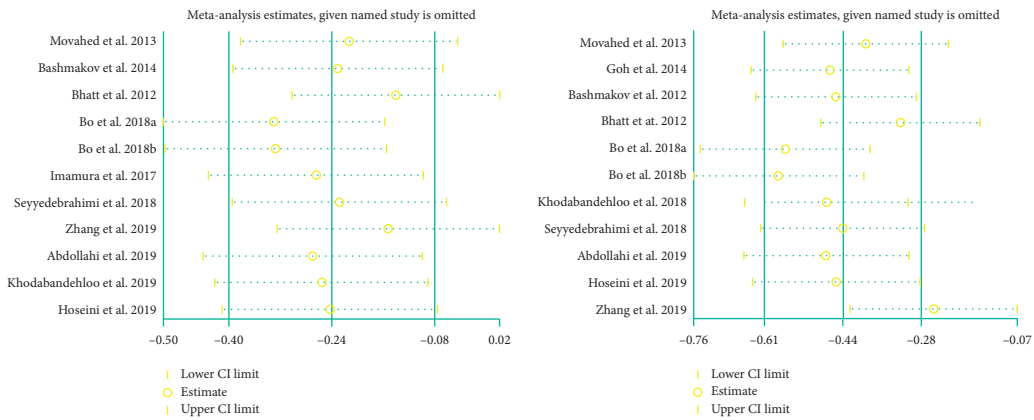

Figure 13: Sensitivity analysis results: (a) TC; (b) LDL-C.

analysis on this topic, and it is conducted in strict accordance with the guidelines and protocol. In addition, this study included a wider range of populations, including Iran, China, Japan, Egypt, Singapore, Hungary, and Italy, which promoted the applicability of the conclusions. The limitations of this study are as follows: (1) some RCTs are of low quality because they did not describe specific random sequence generation methods, allocation concealment methods, or blind methods, which lead to a decrease in the reliability of the results, and the results should be treated with caution in clinical practice. For example, five RCTs [15, 17, 26, 27, 36] did not describe the method of generating random sequences; six RCTs [15, 17, 26, 27, 35, 36] did not describe the allocation concealment method; three RCTs [28, 35, 36] did not specify whether blinding; six RCTs [17, 18, 25, 31, 32, 35] did not describe whether to use intend-to-treat analysis. (2) Some RCTs involve few participants (lower than 50), which may lead to changes in clinical efficacy indicators that cannot be detected. Goh et al. [25] included only 10 participants; Brasnyó et al. [26], 19 participants; Bashmakov et al. [27], 24 participants; Zare Javid et al. [15], 43 participants; Khodabandehloo et al. [19], 45 participants; Seyyedebrahimi et al. [31], 46 participants. (3) The different resveratrol preparations used by RCTs may affect the accuracy of the results. For example, the dose and usage of resveratrol in the study of Brasnyó et al. [26] was 5 mg, bid; in the study of Bashmakov et al. [27], 50 mg, bid; in the study of Movahed et al. [24], 500 mg, bid. The dosage of resveratrol in each RCT was different. (4) The heterogeneity of most outcomes, such as HOMA-IR, TC, TG, and LDL-C, was high. The high heterogeneity may reduce the applicability of the results. Therefore, high-quality research is needed to determine or modify the results of this research.

5. Conclusion

Resveratrol may improve insulin resistance, lower fasting blood glucose and insulin levels, and improve oxidative stress in patients with T2DM. However, due to the generally low quality of research and high heterogeneity among RCTs, the results should be interpreted with caution.

Data Availability

All data generated or analyzed during this study are included within the article.

Disclosure

Tianqing Zhang and Qi He are the co-first authors. Hengjing Hu is the corresponding author.

Conflicts of Interest

The authors declare that there are no conflicts of interest.

Authors' Contributions

Tianqing Zhang, Qi He, and Hengjing Hu are responsible for the study concept and design. Tianqing Zhang, Qi He, Yao Liu, Zhenrong Chen, and Hengjing Hu are responsible for the literature search. Tianqing Zhang, Qi He, Yao Liu, Zhenrong Chen, and Hengjing Hu are responsible for data analysis and interpretation. Tianqing Zhang and Qi He drafted the paper. Hengjing Hu supervised the study. All authors participated in the analysis and interpretation of data and approved the final paper.

Acknowledgments

This work was supported by grants from the National Natural Science Foundation of China (grant no. 81700306), Natural Science Foundation of Hunan Province (grant no. 2018JJ3469), and China Postdoctoral Science Foundation (grant no. 2017M622588). Thanks are due to Kailin Yang for his guidance on the systematic review and meta-analysis.

Supplementary Materials

The "PRISMA 2020 checklist" is a standardized checklist that ensures that systematic reviews and meta-analyses are implemented according to this standard. Table S1: search strategies for PubMed. (*Supplementary Materials*)

References

[1] P. Saeedi, I. Petersohn, P. Salpea et al., "Global and regional diabetes prevalence estimates for 2019 and projections for 2030 and 2045: results from the international diabetes federation diabetes atlas, 9th edition," *Diabetes Research and Clinical Practice*, vol. 157, Article ID 107843, 2019.

[2] GBD 2015 Mortality and Causes of Death Collaborators, "Global, regional, and national life expectancy, all-cause mortality, and cause-specific mortality for 249 causes of death, 1980–2015: a systematic analysis for the global burden of disease study 2015," *Lancet*, vol. 388, pp. 1459–1544, 2016.

[3] J. M. Forbes and M. E. Cooper, "Mechanisms of diabetic complications," *Physiological Reviews*, vol. 93, no. 1, pp. 137–188, 2013.

[4] M. Stolar, "Glycemic control and complications in type 2 diabetes mellitus," *The American Journal of Medicine*, vol. 123, pp. S3–11, 2010.

[5] D. Wu, D. Hu, H. Chen et al., "Glucose-regulated phosphorylation of TET2 by AMPK reveals a pathway linking diabetes to cancer," *Nature*, vol. 559, no. 7715, pp. 637–641, 2018.

[6] R. M. Carrillo-Larco, J. Pearson-Stuttard, A. Bernabe-Ortiz, and E. W. Gregg, "The andean latin-American burden of diabetes attributable to high body mass index: a comparative risk assessment," *Diabetes Research and Clinical Practice*, vol. 160, Article ID 107978, 2020.

[7] A. J. Vegas, O. Veiseh, M. Gürtler et al., "Long-term glycemic control using polymer-encapsulated human stem cell-derived beta cells in immune-competent mice," *Nature Medicine*, vol. 22, no. 3, pp. 306–311, 2016.

[8] A. Y. Y. Cheng and I. G. Fantus, "Oral antihyperglycemic therapy for type 2 diabetes mellitus," *Canadian Medical Association Journal*, vol. 172, no. 2, pp. 213–226, 2005.

[9] G. Nicholson and G. M. Hall, "Diabetes mellitus: new drugs for a new epidemic," *British Journal of Anaesthesia*, vol. 107, no. 1, pp. 65–73, 2011.

[10] E. J. Verspohl, "Novel pharmacological approaches to the treatment of type 2 diabetes," *Pharmacological Reviews*, vol. 64, no. 2, pp. 188–237, 2012.

[11] T. Szkudelski and K. Szkudelska, "Resveratrol and diabetes: from animal to human studies," *Biochimica et Biophysica Acta (BBA)—Molecular Basis of Disease*, vol. 1852, no. 6, pp. 1145–1154, 2015.

[12] E. Öztürk, A. K. K. Arslan, M. B. Yerer, and A. Bishayee, "Resveratrol and diabetes: a critical review of clinical studies," *Biomedicine & Pharmacotherapy*, vol. 95, pp. 230–234, 2017.

[13] X. Zhu, C. Wu, S. Qiu, X. Yuan, and L. Li, "Effects of resveratrol on glucose control and insulin sensitivity in subjects with type 2 diabetes: systematic review and meta-analysis," *Nutrition & Metabolism*, vol. 14, no. 1, p. 60, 2017.

[14] K. Liu, R. Zhou, B. Wang, and M.-T. Mi, "Effect of resveratrol on glucose control and insulin sensitivity: a meta-analysis of 11 randomized controlled trials," *The American Journal of Clinical Nutrition*, vol. 99, no. 6, pp. 1510–1519, 2014.

[15] A. Zare Javid, R. Hormoznejad, H. A. Yousefimanesh et al., "The impact of resveratrol supplementation on blood glucose, insulin, insulin resistance, triglyceride, and periodontal markers in type 2 diabetic patients with chronic periodontitis," *Phytotherapy Research*, vol. 31, no. 1, pp. 108–114, 2017.

[16] S. Bo, V. Ponzo, A. Evangelista et al., "Effects of 6 months of resveratrol versus placebo on pentraxin 3 in patients with type 2 diabetes mellitus: a double-blind randomized controlled trial," *Acta Diabetologica*, vol. 54, no. 5, pp. 499–507, 2017.

[17] H. Imamura, T. Yamaguchi, D. Nagayama, A. Saiki, K. Shirai, and I. Tatsuno, "Resveratrol ameliorates arterial stiffness assessed by cardio-ankle vascular index in patients with type 2 diabetes mellitus," *International Heart Journal*, vol. 58, no. 4, pp. 577–583, 2017.

[18] A. Sattarinezhad, J. Roozbeh, B. Shirazi Yeganeh, G. R. Omrani, and M. Shams, "Resveratrol reduces albuminuria in diabetic nephropathy: a randomized double-blind placebo-controlled clinical trial," *Diabetes & Metabolism*, vol. 45, no. 1, pp. 53–59, 2019.

[19] H. Khodabandehloo, S. Seyyedebrahimi, E. N. Esfahani, F. Razi, and R. Meshkani, "Resveratrol supplementation decreases blood glucose without changing the circulating $CD14^+$ $CD16^+$ monocytes and inflammatory cytokines in patients with type 2 diabetes: a randomized, double-blind, placebo-controlled study," *Nutrition Research*, vol. 54, pp. 40–51, 2018.

[20] M. de Ligt, Y. M. H. Bruls, J. Hansen et al., "Resveratrol improves ex vivo mitochondrial function but does not affect insulin sensitivity or brown adipose tissue in first degree relatives of patients with type 2 diabetes," *Molecular Metabolism*, vol. 12, pp. 39–47, 2018.

[21] J. J. Deeks, J. P. Higgins, and D. G. Altman, "Chapter 16: special topics in statistics," in *Cochrane Handbook for Systematic Reviews of Interventions*, J. P. Higgins and S. Green, Eds., The Cochrane Collaboration, London, UK, 2020.

[22] J. J. Deeks, J. P. Higgins, and D. G. Altman, Edited by J. P. Higgins, Ed., "Chapter 8: assessing risk of bias in included studies," in *Cochrane Handbook or Systematic Reviews of Interventions Version 6.1.0*, S. Green, Ed., The Cochrane Collaboration, London, UK, 2020.

[23] J. J. Deeks, J. P. Higgins, and D. G. Altman, "Chapter 9: analyzing data and undertaking meta-analyses," in *Cochrane Handbook for Systematic Reviews of Interventions*, J. P. Higgins and S. Green, Eds., The Cochrane Collaboration, London, UK, 2020.

[24] A. Movahed, I. Nabipour, X. Lieben Louis et al., "Antihyperglycemic effects of short term resveratrol supplementation in type 2 diabetic patients," *Evidence-based Complementary and Alternative Medicine: ECAM*, vol. 2013, Article ID 851267, 11 pages, 2013.

[25] K. P. Goh, H. Y. Lee, D. P. Lau, W. Supaat, Y. H. Chan, and A. F. Y. Koh, "Effects of resveratrol in patients with type 2 diabetes mellitus on skeletal muscle SIRT1 expression and energy expenditure," *International Journal of Sport Nutrition and Exercise Metabolism*, vol. 24, no. 1, pp. 2–13, 2014.

[26] P. Brasnyó, G. A. Molnár, M. Mohás et al., "Resveratrol improves insulin sensitivity, reduces oxidative stress and activates the Akt pathway in type 2 diabetic patients," *British Journal of Nutrition*, vol. 106, no. 3, pp. 383–389, 2011.

[27] Y. K. Bashmakov, S. H. Assaad-Khalil, M. Abou Seif et al., "Resveratrol promotes foot ulcer size reduction in type 2 diabetes patients," *ISRN Endocrinology*, vol. 2014, Article ID 816307, 8 pages, 2014.

[28] J. K. Bhatt, S. Thomas, and M. J. Nanjan, "Resveratrol supplementation improves glycemic control in type 2 diabetes mellitus," *Nutrition Research*, vol. 32, no. 7, pp. 537–541, 2012.

[29] S. Bo, V. Ponzo, G. Ciccone et al., "Six months of resveratrol supplementation has no measurable effect in type 2 diabetic patients. a randomized, double blind, placebo-controlled trial," *Pharmacological Research*, vol. 111, pp. 896–905, 2016.

[30] S. Bo, R. Gambino, V. Ponzo et al., "Effects of resveratrol on bone health in type 2 diabetic patients. a double-blind randomized-controlled trial," *Nutrition & Diabetes*, vol. 8, no. 1, p. 51, 2018.

[31] S. Seyyedebrahimi, H. Khodabandehloo, E. Nasli Esfahani, and R. Meshkani, "The effects of resveratrol on markers of oxidative stress in patients with type 2 diabetes: a randomized, double-blind, placebo-controlled clinical trial," *Acta Diabetologica*, vol. 55, no. 4, pp. 341–353, 2018.

[32] A. Hoseini, G. Namazi, A. Farrokhian et al., "The effects of resveratrol on metabolic status in patients with type 2 diabetes mellitus and coronary heart disease," *Food & Function*, vol. 10, no. 9, pp. 6042–6051, 2019.

[33] S. Abdollahi, A. Salehi-Abargouei, O. Toupchian et al., "The effect of resveratrol supplementation on cardio-metabolic risk factors in patients with type 2 diabetes: a randomized, double-blind controlled trial," *Phytotherapy Research*, vol. 33, no. 12, pp. 3153–3162, 2019.

[34] M. Tabatabaie, S. Abdollahi, A. Salehi-Abargouei et al., "The effect of resveratrol supplementation on serum levels of asymmetric de-methyl-arginine and paraoxonase 1 activity in patients with type 2 diabetes: a randomized, double-blind controlled trial," *Phytotherapy Research*, vol. 34, no. 8, pp. 2023–2031, 2020.

[35] H. Zhang, A. Li, H. Xiao, D. Wang, and L. Zhang, "Effects of resveratrol on blood glucose, blood lipids and hemorheology in patients with type 2 diabetes," *Modern Journal of Integrated Traditional Chinese and Western Medicine*, vol. 28, no. 17, pp. 1888–1891, 2019.

[36] J. Ying, J. Li, and S. Yu, "The value of resveratrol soft capsules in the treatment of early retinopathy and its effect on blood glucose in diabetic patients," *China Modern Doctor*, vol. 55, no. 6, pp. 4–7, 2017.

[37] T. H. Sanders, R. W. Mc Michael Jr, and K. W. Hendrix, "Occurrence of resveratrol in edible peanuts," *Journal of Agricultural and Food Chemistry*, vol. 48, no. 4, pp. 1243–1246, 2000.

[38] M. Shakibaei, K. B. Harikumar, and B. B. Aggarwal, "Resveratrol addiction: to die or not to die," *Molecular Nutrition & Food Research*, vol. 53, no. 1, pp. 115–128, 2009.

[39] M.-E. García-Pérez, M. Royer, G. Herbette, Y. Desjardins, R. Pouliot, and T. Stevanovic, "Picea mariana bark: a new source of trans-resveratrol and other bioactive polyphenols," *Food Chemistry*, vol. 135, no. 3, pp. 1173–1182, 2012.

[40] L. Nemcova, J. Zima, J. Barek, and D. Janovská, "Detemination of resveratrol in grains, hulls and leaves of common and tartary buckwheat by HPLC with electrochemical detection at carbon paste electrode," *Food Chemistry*, vol. 126, no. 1, pp. 374–378, 2011.

[41] A. Betelli, A. A. Bertelli, A. Gozzini, and L. Giovannini, "Plasma and tisue resveratrol concentrations and pharmacological activity," *Drugs Under Experimental and Dinical Research*, vol. 24, no. 3, pp. 133–138, 1998.

[42] S. Fogacci, F. Fogacci, and A. F. G. Cicero, "Nutraceuticals and hypertensive disorders in pregnancy: the available clinical evidence," *Nutrients*, vol. 12, no. 2, p. 378, 2020.

[43] C. Borghi, K. Tsioufis, E. Agabiti-Rosei et al., "Nutraceuticals and blood pressure control: a European society of hypertension position document," *Journal of Hypertension*, vol. 38, no. 5, pp. 799–812, 2020.

[44] F. Fogacci, M. Banach, and A. F. G. Cicero, "Resveratrol effect on patients with non-alcoholic fatty liver disease: a matter of dose and treatment length," *Diabetes, Obesity and Metabolism*, vol. 20, no. 7, pp. 1798-1799, 2018.

[45] C. R. Sirtori, A. Arnoldi, and A. F. G. Cicero, "Nutraceuticals for blood pressure control," *Annals of Medicine*, vol. 47, no. 6, pp. 447–456, 2015.

[46] M. Sadria and A. T. Layton, "Aging affects circadian clock and metabolism and modulates timing of medication," *iScience*, vol. 24, no. 4, Article ID 102245, 2021.

[47] M. D. van Die, S. G. Williams, J. Emery et al., "A placebo-controlled double-blinded randomized pilot study of combination phytotherapy in biochemically recurrent prostate cancer," *The Prostate*, vol. 77, no. 7, pp. 765–775, 2017.

[48] J. L. Espinoza, L. Q. Trung, P. T. Inaoka et al., "The repeated administration of resveratrol has measurable effects on circulating T-cell subsets in humans," *Oxidative Medicine and Cellular Longevity*, vol. 2017, Article ID 6781872, 10 pages, 2017.

[49] L. D. Williams, G. A. Burdock, J. A. Edwards, M. Beck, and J. Bausch, "Safety studies conducted on high-purity trans-resveratrol in experimental animals," *Food and Chemical Toxicology*, vol. 47, no. 9, pp. 2170–2182, 2009.

[50] V. Hebbar, G. Shen, R. Hu et al., "Toxicogenomics of resveratrol in rat liver," *Life Sciences*, vol. 76, no. 20, pp. 2299–2314, 2005.

[51] W. D. Johnson, R. L. Morrissey, A. L. Usborne et al., "Subchronic oral toxicity and cardiovascular safety pharmacology studies of resveratrol, a naturally occurring polyphenol with cancer preventive activity," *Food and Chemical Toxicology*, vol. 49, no. 12, pp. 3319–3327, 2011.

[52] K. Kantartzis, L. Fritsche, M. Bombrich et al., "Effects of resveratrol supplementation on liver fat content in overweight and insulin-resistant subjects: a randomized, double-blind, placebo-controlled clinical trial," *Diabetes, Obesity and Metabolism*, vol. 20, no. 7, pp. 1793–1797, 2018.

[53] F. Fogacci, G. Tocci, V. Presta, A. Fratter, C. Borghi, and A. F. G. Cicero, "Effect of resveratrol on blood pressure: a systematic review and meta-analysis of randomized, controlled, clinical trials," *Critical Reviews in Food Science and Nutrition*, vol. 59, no. 10, pp. 1605–1618, 2019.

Hindawi
Evidence-Based Complementary and Alternative Medicine
Volume 2021, Article ID 9980429, 13 pages
https://doi.org/10.1155/2021/9980429

Research Article

New Therapeutic Insight into the Effect of Ma Huang Tang on Blood Pressure and Renal Dysfunction in the L-NAME-Induced Hypertension

Mi Hyeon Hong,[1,2] Hye Yoom Kim,[1,2] Youn Jae Jang,[1,2] Se Won Na,[1,2] Byung Hyuk Han,[1,2] Jung Joo Yoon,[1,2] Chang Seob Seo,[3] Ho Sub Lee,[1,2] Yun Jung Lee,[1,2] and Dae Gill Kang[1,2]

[1]*Hanbang Cardio-Renal Syndrome Research Center, Wonkwang University, 460 Iksan-daero, Iksan, Jeonbuk 54538, Republic of Korea*
[2]*College of Korean Medicine and Professional Graduate School of Korean Medicine, Wonkwang University, 460 Iksan-daero, Iksan, Jeonbuk 54538, Republic of Korea*
[3]*Herbal Medicine Research Division, Korea Institute of Oriental Medicine, 1672 Yuseong-daero, Yuseong-gu, Daejeon 34054, Republic of Korea*

Correspondence should be addressed to Yun Jung Lee; shrons@wku.ac.kr and Dae Gill Kang; dgkang@wku.ac.kr

Received 29 March 2021; Revised 29 June 2021; Accepted 3 July 2021; Published 14 July 2021

Academic Editor: Thanasekaran Jayakumar

In this study, we evaluated the effect of a traditional herbal formula, Ma Huang Tang (MHT), on blood pressure and vasodilation in a rat model of N^G-nitro-L-arginine methylester- (L-NAME-) induced hypertension. We found that MHT-induced vascular relaxation in a dose-dependent manner in rat aortas pretreated with phenylephrine. However, pretreatment of endothelium-intact aortic rings with L-NAME, an inhibitor of nitric oxide synthesis (NOS), or 1H-[1, 2, 4]-oxadiazole-[4, 3-α]-quinoxalin-1-one (ODQ), an inhibitor of soluble guanylyl cyclase, significantly abolished vascular relaxation induced by MHT. MHT also increased the production of guanosine 3′,5′-cyclic monophosphate (cGMP) in the aortic rings pretreated with L-NAME or ODQ. To examine the *in vivo* effects of MHT, Sprague Dawley rats were treated with 40 mg/kg/day L-NAME for 3 weeks, followed by administration of 50 or 100 mg/kg/day MHT for 2 weeks. MHT was found to significantly normalize systolic blood pressure and decreased intima-media thickness in aortic sections of rats treated with L-NAME compared to that of rats treated with L-NAME alone. MHT also restored the L-NAME-induced decrease in vasorelaxation response to acetylcholine and endothelial nitric oxide synthase (eNOS) and endothelin-1 (ET-1) expression. Furthermore, MHT promoted the recovery of renal function, as indicated by osmolality, blood urea nitrogen (BUN) levels, and creatinine clearance. These results suggest that MHT-induced relaxation in the thoracic aorta is associated with activation of the nitric oxide/cGMP pathway. Furthermore, it provides new therapeutic insights into the regulation of blood pressure and renal function in hypertensive patients.

1. Introduction

Hypertension is a major cause of cardiovascular diseases, such as heart failure, stroke, and myocardial infarction [1]. Adding to this, 10% mortality due to hypertension is caused as a result of renal dysfunction and failure. Systemic arterial hypertension is closely related to vascular endothelial cell dysfunction [2]. Endothelial cells are stimulated by releasing endothelium-dependent vasodilators or endothelium-derived relaxing factors. Nitric oxide (NO), which is generated in endothelial cells, activates soluble guanylyl cyclase (sGC) and increases the production of intracellular guanosine 3′,5′-cyclic monophosphate (cGMP) [3], which induces vascular relaxation. The impairment of the NO-cGMP pathway induces hypercholesterolemia, diabetes, and hypertension because of a decline in vascular relaxation [4, 5]. Nonmediated vascular relaxation is essential for the maintenance of vascular function. NO is also an important

regulator of blood pressure, regional blood flow, vascular smooth muscle proliferation, platelet aggregation, and leukocyte adhesion [6]. Vascular activity regulation by the NO pathway is altered in various models of hypertension [7]. Of them, in this study, we used the N^G-nitro-L-arginine methylester (L-NAME) model to study the *in vivo* vascular response after chemical inhibition of endothelial NOS (eNOS) production.

Ma Huang Tang (MHT), mentioned in the Treatise on Febrile Disease of Zhang Zhongjing, has been used for thousands of years to treat many diseases, such as exogenous wind-cold, cough, and asthma [8]. MHT is a formulation derived from Ephedra (*Ephedra sinica*), Cinnamomi Ramulus (*Cinnamomum cassia*), Armeniacae Semen (*Prunus armeniaca*), and Glycyrrhizae Radix et Rhizoma Praeparata Cum Melle (*Glycyrrhiza uralensis*). Modern pharmacological research has shown that MHT exhibits therapeutic effects against inflammation, allergy, asthma, and hyperglycemia [8, 9] and is used to treat bronchitis, asthma, respiratory infection, hypertension, acute glomerulonephritis, and chronic renal failure [10]. However, the therapeutic effect of MHT on hypertension has not been investigated. Therefore, in this present study, we investigated the mechanism of MHT-induced vascular relaxation in rat aorta and its effect on blood pressure and renal function in rats with L-NAME-induced hypertension.

2. Experimental Methods

2.1. High-Performance Liquid Chromatography (HPLC) Analysis of MHT. HPLC analysis of the seven characteristic constituents in MHT was performed using a Shimadzu Prominence LC-20A series HPLC system (Kyoto, Japan) coupled with a photodiode array detector and LabSolutions software (Version 5.54 SP3, Shimadzu, Kyoto, Japan). A Waters Sun Fire C_{18} analytical column (250 × 4.6 mm, 5 μm; Milford, MA, USA) as the stationary phase, maintained at 40°C, was used for the separation of the main components. The mobile phases consisted of 0.1% (v/v) trifluoroacetic acid in distilled water (A) and acetonitrile (B). The elution gradient used for chromatographic separation was as follows: 10%–60% B for 30 min, 60%–100% B for 30–40 min, 100% B for 40–45 min, 100%–10% B for 45–50 min, and 10% B for 50–60 min. The flow rate was set to 1.0 mL/min, and the injection volume was 10 μL.

2.2. L-NAME Induction of Hypertension in Rats. Male Sprague-Dawley rats weighing 180–200 g were acclimatized for 7 days under a 12 h light-dark cycle. After which, the rats were randomly divided into five experimental groups: (1) control ($n = 8$); (2) L-NAME (40 mg/kg/day, $n = 8$); (3) L-NAME + Olmetec® (OMT, angiotensin-II receptor type II blocker, 10 mg/kg/day, per os (p.o.)); (4) L-NAME + MHT (50 mg/kg/day, p.o.); and (5) L-NAME + MHT (100 mg/kg/day, p.o.). All L-NAME groups were administered L-NAME in drinking water for 5 weeks. Each group composed of 8 rats and all L-NAME-induced hypertensive groups were administered L-NAME in the drinking water for 5 weeks. After 3 weeks treated with L-NAME, MHT or OMT was injected by oral administration daily to L-NAME-induced hypertensive rats for 2 weeks.

2.3. Measurement of Blood Pressure. Systolic blood pressure (SBP) and body weight were assessed weekly by tail-cuff plethysmography (MK2000; Muromachi Kikai, Tokyo, Japan) in a quiet and warm room. At least seven determinations were carried out for every cycle of measurement and an average of five cycles of measurement was used for final comparisons. In this study, rats with SBP > 160 mmHg were used.

2.4. Preparation of Aortic Rings. Animal procedures were performed in strict accordance with the National Institute of Health Guidelines for the Care and Use of Laboratory Animals. Animal procedures were approved by the Institutional Animal Care and Utilization Committee of Wonkwang University. Male Sprague Dawley rats (250–300 g) were purchased from Korean Experimental Animals Co. (Wanju, Korea). The thoracic aorta was separated rapidly from these rats, and the fat was removed from aortic tissue in ice-cold Krebs' solution (pH 7.4) containing 118.0 mM NaCl, 1.1 $MgSO_4$, 4.7 KCl, 1.2 KH_2PO_4, 25.0 $NaHCO_3$, 10.0 glucose, and 1.5 $CaCl_2$. The thoracic aorta was cut into rings, approximately 3 mm in width, and the endothelial layer in some aortic rings was removed by rubbing. The relaxation response in the aortic rings with and without the endothelium, precontracted with phenylephrine (PE, 1 μM), upon acetylcholine (Ach, 1 μM) was measured.

2.5. Measurement of cGMP Levels in Rat Aorta. Rat aortic rings were incubated for 60 min in flasks containing 5 mL of Krebs solution placed in a shaking water bath at constant temperature (37°C), 95% O_2, and 5% CO_2. This was followed by incubation with 3-isobutyl-1-methylxanthine (IBMX, 1 μM) and PE (1 μM) for 5 mins. After the aortic rings were incubated with MHT in the presence and absence of modulators for 4 min, the reactions were stopped by freezing the tissues in liquefied N_2. The tissues were homogenized with 0.1 M HCl and centrifuged at 13000 rpm for 15 min. The protein concentration was determined by Bradford assay using bovine serum albumin (BSA) as the standard. The cGMP level was measured by an equilibrated radioimmunoassay, as described previously [11], and results have been expressed as nanomoles of cGMP per milligram of protein (nmol/ml/mg protein).

2.6. Hematoxylin-Eosin (H&E) Staining of Aorta. The thoracic aorta tissues were fixed in 10% (v/v) formalin. Fixed tissue samples were dehydrated and embedded in paraffin and then placed on a poly-L-lysine-coated slide (Fisher Scientific, Pittsburgh, PA, USA). Thin sections (4 μM) of the aortic tissue were stained with H&E stain for histopathological analysis. The length of intima-to-media was determined using AxioVision 4 imaging/archiving software (AxioVision 4, Carl Zeiss, Germany).

2.7. Immunohistochemical (IHC) Analysis of the Aorta. Paraffin-embedded sections were immunostained using Invitrogen's Histostain® Plus Broad Spectrum kit (Novex®, CA, USA). The slides were immersed in 3% hydrogen peroxide for 10 min at room temperature and incubated with primary antibodies against eNOS (1 : 200, Santa Cruz, CA, USA) and ET-1 (1 : 200, Santa Cruz, CA, USA) in humidified chambers overnight at 4°C. All slides were then incubated with a biotinylated secondary antibody for 2 h at room temperature. Peroxidase activity was visualized using 3,3′-diaminobenzidine (Novex®, CA) substrate-chromogen system and counterstained with hematoxylin (Zymed, CA, USA). ImageJ (NIH, Bethesda, MD, USA) was used to quantify protein expression.

2.8. Measurement of Plasma Biomarker. Blood samples were collected in test tubes containing ethylenediaminetetraacetic acid and centrifuged at 990 × g for 20 min at 4°C. Plasma samples were frozen at −70°C until further use. Plasma levels of albumin, BUN, and creatinine were measured using a commercial kit (Arkray Inc., Kyoto, Japan).

2.9. Measurement of Osmolality and Urinary Albumin. Rats from each group were maintained in separate metabolic cages during the experimental period, allowing for the quantitation of urine volume and water intake. Urine samples were collected on a day in the last week of the experimental period to determine osmolality and urine albumin levels. Osmolality was measured using an advanced cryomatic osmometer (Advanced Instruments, Norwood, MS).

2.10. Western Blot Analysis. Thoracic tissue homogenates (40 μg of protein) were separated by 10% sodium dodecyl-polyacrylamide gel electrophoresis and transferred to a nitrocellulose membrane paper. Blots were then blocked with 5% BSA in Tris-buffered saline for 1 h and incubated with the appropriate primary antibody at dilutions recommended by the supplier. The membrane was then washed and incubated with the appropriate horseradish peroxidase-conjugated secondary antibody for 1 h. The bands were visualized using enhanced chemiluminescence (Amersham, Buckinghamshire, UK). Protein expression levels were determined by analyzing the signal intensity using a ChemiDoc image analyzer (Bio-Rad, Hercules, CA, USA).

2.11. Statistical Analysis. The multiple experimental groups were compared using repeated-measures analysis of variance followed by Bonferroni's multiple-comparison test. Two-group comparisons were performed using Student's unpaired t-test. Statistical significance was defined as $p < 0.05$. The results are presented as mean ± standard error of mean.

3. Results

3.1. HPLC Analysis of MHT. HPLC was used to simultaneously detect the seven characteristic components of MHT. Each compound in the MHT was identified based on the retention time and UV spectra of the reference standard. Seven components, namely, ephedrine HCl, liquiritin apioside, liquiritin, coumarin, cinnamic acid, cinnamaldehyde, and glycyrrhizin, were eluted at 9.24, 13.94, 14.20, 20.30, 22.82, 25.50, and 26.31 min, respectively, and their concentrations in MHT measured using an optimized analytical assay were 2.68, 1.08, 0.74, 0.12, 0.09, 0.21, 0.36, and 1.60 mg/freeze-dried g, respectively (Figure 1).

3.2. MHT-Induced Vasodilation and cGMP Production. In endothelium-intact thoracic aorta rings, MHT induced vascular relaxation in a dose-dependent manner. However, MHT-induced vasodilation was blocked in the endothelium-removed thoracic aorta (Figure 2(a)). MHT-induced vasodilation was inhibited in vascular tissue treated with wortmannin, which is a nonselective PI3K inhibitor, compared to untreated vascular tissue. MHT-induced vasodilation was completely abolished by pretreatment with 100 μM L-NAME (Figure 2(b)). We used ODQ, a sGC inhibitor, to understand the mechanism of MHT-induced vasodilation. Pretreatment of vascular tissues with 10 μM ODQ completely abolished MHT-induced vascular relaxant response of the thoracic aorta (Figure 2(c)). We found that MHT treatment resulted in an increase in cGMP production compared to that of the control. However, pretreatment with L-NAME, ODQ, or wortmannin in vascular tissues completely blocked the MHT-induced increases in cGMP production. When MHT was administered to aortic tissues pretreated with L-NAME, ODQ, or wortmannin, there was a significant increase in cGMP production (Figure 2(d)).

3.3. MHT Decreased SBP in L-NAME-Induced Hypertensive Rats. The mean SBP of L-NAME treated rats was 198 ± 8.9 mmHg. Hypertensive rats in the MHT treatment group exhibited significantly lower SBP than those that were treated with L-NAME alone (Figure 3).

3.4. MHT Restored Vascular Function in L-NAME-Induced Hypertensive Rats. Vasodilatory responses to ACh were significantly impaired in the L-NAME-induced hypertensive rats compared to that in the control group. However, the responses evoked by Ach were rescued by MHT treatment in a dose-dependent manner compared with that in the L-NAME hypertensive rats (Figure 4(a)). The cGMP level in the aorta of L-NAME rats was lower than that in control rats, but there was no significant. cGMP production in the MHT and OMT groups treated in L-NAME hypertensive rats was increased compared with that in the L-NAME group and control group (Figure 4(b)).

3.5. MHT Regulated Expression of Vascular Factors in L-NAME Hypertensive Rats. Morphological staining showed that the L-NAME group had an increased thickness of intimal endothelial and medial layers compared to that of the control group. However, treatment with MHT in L-NAME hypertensive rats resulted in markedly decreased thickness

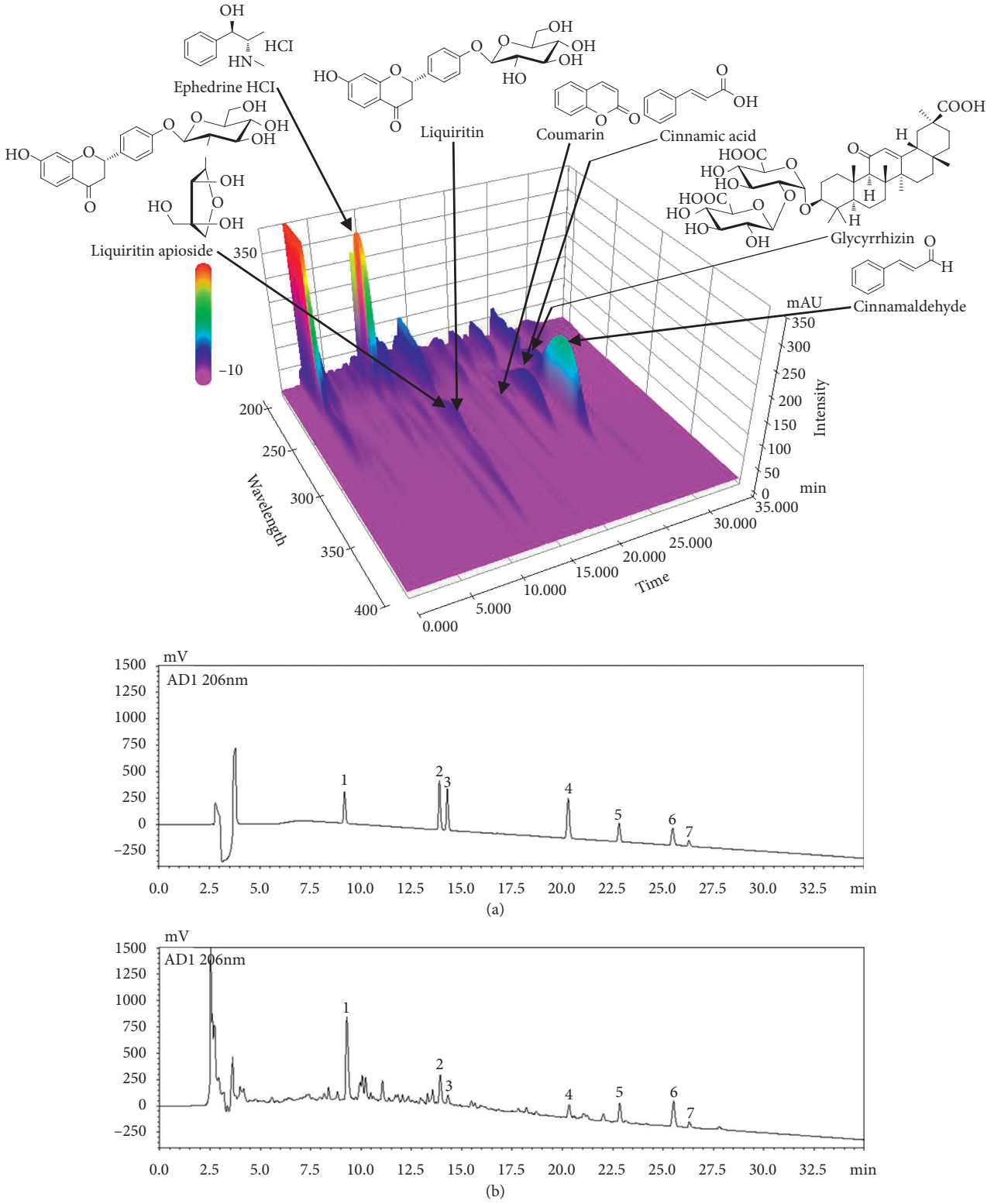

Figure 1: Representative HPLC chromatograms of standard solution (a) and Ma Hwang Tang decoction (b) measured at UV wavelength 206 nm. Ephedrine HCl (1), liquiritin apioside (2), liquiritin (3), coumarin (4), cinnamic acid (5), cinnamaldehyde (6), and glycyrrhizin (7).

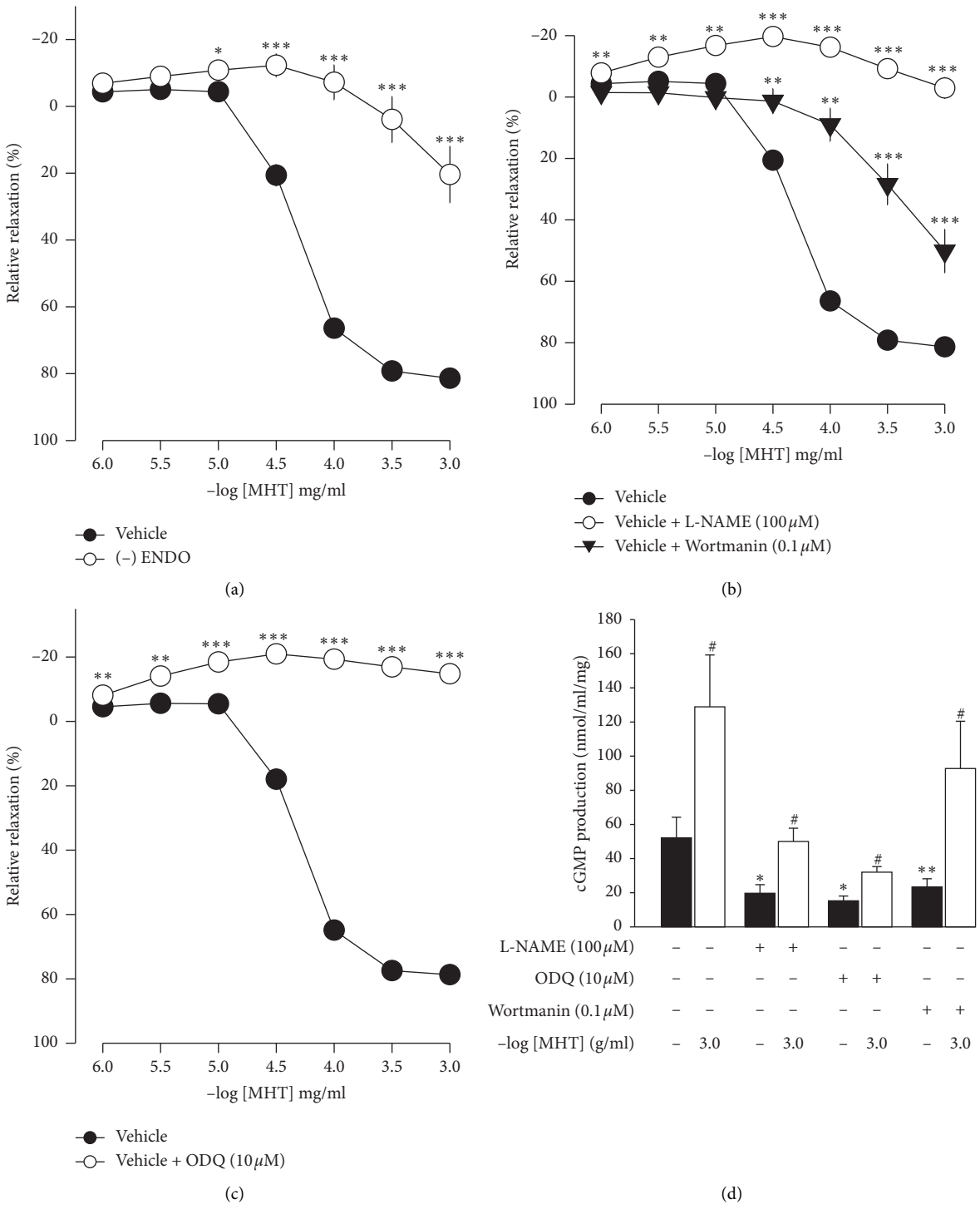

Figure 2: Effect of MHT on vasodilation and cGMP production. Presented vascular relaxation response to MHT in aorta with endothelium or without (a) Presence of L-NAME (100 μM) or wortmannin (0.1 μM) (b). Presence of ODQ (10 μM) (c). The cGMP production response to MHT with L-NAME (100 μM), ODQ (10 μM), or wortmannin (0.1 μM). MHT, Ma Huang Tang; cGMP: guanosine 3′,5′-cyclic monophosphate; L-NAME: N^G-nitro-L-arginine methylester; and ODQ: 1H-[1,2,4]-oxadiazolo-[4,3-α]-quinoxalin-1-one. Values are expressed as mean ± S.E. ($n = 5$ per group). $^*p < 0.05$, $^{**}p < 0.01$, and $^{***}p < 0.001$ versus vehicle: $\#p < 0.05$ versus L-NAME, ODQ, or wortmannin.

of intimal endothelial and medial layers (Figures 5(a) and 5(b)). As shown in Figure 5(c), eNOS expression was suppressed in the aortic tissue of the L-NAME group compared to that in the control group. However, treatment with MHT (50 or 100 mg/kg/day) restored eNOS expression in the L-NAME group (Figures 5(c) and 5(d)). In contrast, aortic ET-1 expression was increased in the L-NAME hypertensive group and MHT treatment groups in L-NAME

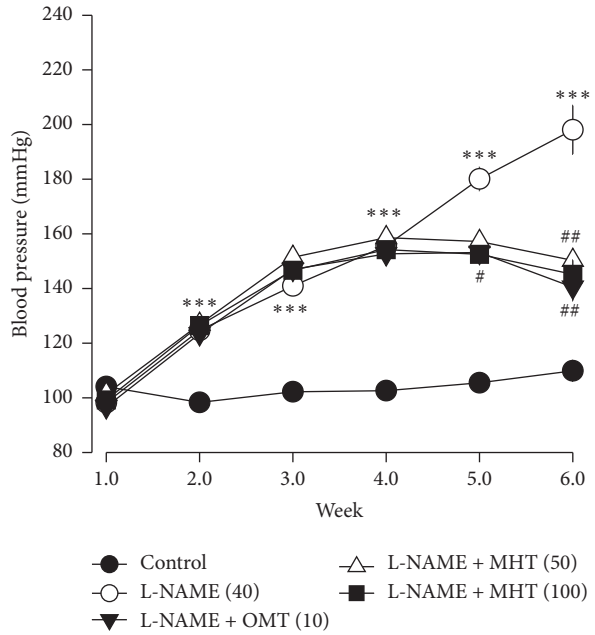

Figure 3: Effect of MHT on blood pressure. Presented systolic blood pressure measured by tail-cuff method (mmHg). MHT: Ma Huang Tang; OMT: Olmetec. Values are expressed as mean ± S.E. ($n = 8$ per group). $^{***}p < 0.01$ versus control: $^{\#}p < 0.05$, $^{\#\#}p < 0.01$ versus L-NAME.

hypertensive rats lowered this compared to that in the L-NAME group (Figures 5(e) and 5(f)). To demonstrate the effect of MHT on blood vessels, thoracic tissues derived from the experimental rats were subjected to western blotting. In the L-NAME group, phospho-Akt1/2/3 and phospho-eNOS expression decreased compared with that of the control, and treatment with MHT rescued this alteration in the expression of phosphorylated Akt/1/2/3 and eNOS (Figure 6).

3.6. MHT Ameliorated Renal Dysfunction in L-NAME-Induced Hypertensive Rats. The plasma levels of BUN and creatinine were remarkably upregulated in the L-NAME group compared with those in the control group. However, the levels of BUN and creatinine in serum were downregulated and albumin was upregulated in the MHT and OMT treatment groups compared to those in the only L-NAME treatment group (Table 1). There was no significant difference in water intake and urine volume between the L-NAME and control groups. MHT treated in L-NAME-induced hypertensive rats also had no effect on water intake and urine volume compared to that in the L-NAME group. The level of osmolality was lower in the L-NAME-induced hypertension group than that in the control group. However, the MHT-treated group in L-NAME-induced hypertensive rats showed a significantly increased osmolality compared to that in the L-NAME group (Table 2). Urinary albumin levels were higher in the L-NAME group than those in the control group. MHT treatment significantly lowered the urinary albumin level in L-NAME-treated rats compared to that in rats treated with L-NAME alone (Table 2).

4. Discussion

MHT has long been used in Korean traditional medicine for the treatment of various diseases and has been previously reported to exhibit protective effects against cough and asthma [8, 9]. However, little is known about the mechanisms that underlie the pharmacological activity of MHT in ethnomedicine. Ephedrine is the most abundant alkaloid found in MHT and has a chemical structure comparable to that of amphetamines, ephedrine. It works directly or indirectly by stimulating the alpha adrenergic and beta adrenergic receptors and trace amine-associated receptors [12, 13]. This receptor activation by ephedrine has been reported extensively and is probably involved in the severe cardiovascular side effects of the Ma Huang decoction (MHD). Interestingly, the contractile response triggered by MHT is much higher than that of a combination of MHT and other components in the MHD. This confirms that the interplay of the various components in the MHD may mitigate the side effects of the MHD [10]. Thus, this study attempted to determine whether MHT, not MHD, would have a beneficial effect on blood pressure-associated hypertension.

Vascular endothelium is known to produce NO, which is an important regulator of vascular tone. NO diffuses out of the endothelium and a fraction of it enters the underlying vascular smooth muscle cells, where it binds to and activates sGC in vascular smooth muscle cells and catalyzes the generation of cGMP, a second messenger, leading to vasorelaxation [14]. We found that MHT did not induce vascular relaxation in endothelium-removed rat thoracic aortic rings, and L-NAME and ODQ significantly inhibited MHT-induced vascular relaxation in endothelium-intact aortic rings. Furthermore, MHT increased cGMP production in aortic smooth muscle, but pretreatment with ODQ and L-NAME blocked MHT-induced increase in cGMP production. These results suggest that MHT induces endothelium-dependent activation of the NO-cGMP pathway and vascular relaxation.

High SBP is a major risk factor for heart disease, stroke, coronary heart disease, and kidney disease [15]. Pharmacologic treatment for hypertension is effective; however, long-term pharmacological therapy can have adverse effects [16]. On the other hand, herbal medicines are known to have few side effects, but further studies are needed to demonstrate the effect of oriental medicine on hypertension. Therefore, in this study, we investigated the effect of MHT on ameliorating symptoms of hypertension in rats treated with L-NAME. Recently, many investigators have reported that intravenous administration of L-NAME has been associated with dose-dependent increases in SBP [17, 18].

The present study showed that treatment with 50 or 100 mg/kg/day MHT lowered blood pressure in L-NAME-induced hypertensive rats. Endothelial function is an important regulator of vascular relaxation. Hypertension induces endothelial dysfunction, which is key to the pathogenesis of coronary heart disease and also increases the risk of developing it. [19]. ACh induced a concentration-dependent dilation of the aorta in control rats. ACh binds to

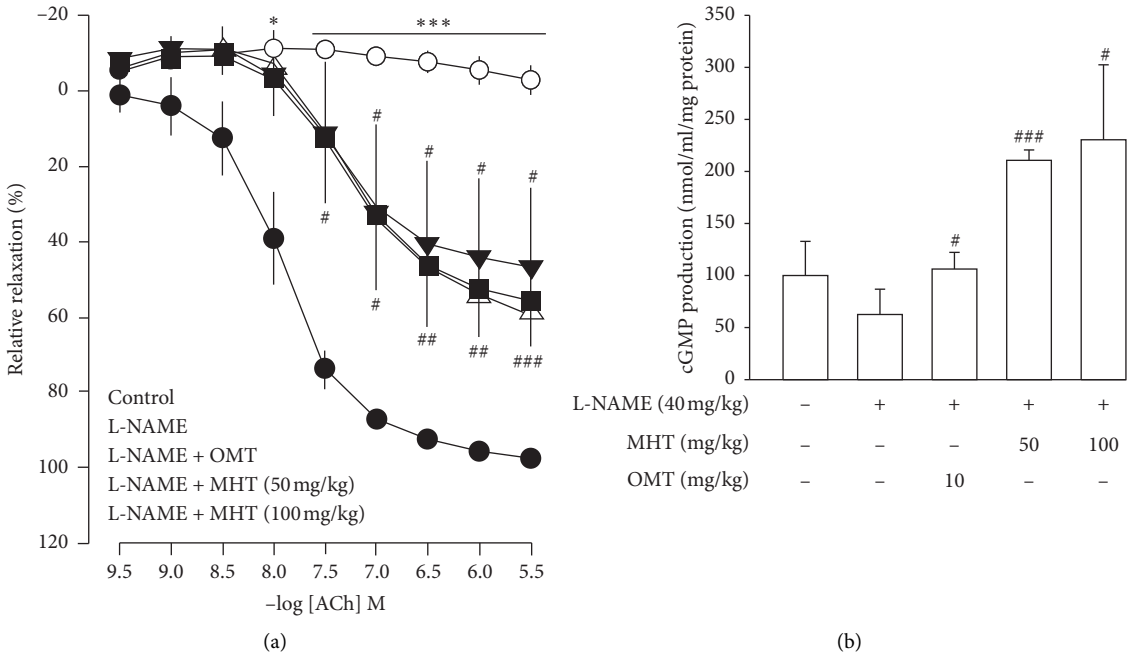

Figure 4: Effect of MHT on vascular relaxation and cGMP level in L-NAME model. (a) Vascular relaxation response to acetylcholine (Ach) in thoracic aorta of L-NAME model. (b) The cGMP production level in the thoracic aorta of control and L-NAME groups. MHT: Ma Huang Tang; cGMP: guanosine 3′,5′-cyclic monophosphate; OMT: Olmetec. Values are expressed as mean ± S.E. ($n = 3$ per group). $^{*}p < 0.05$, $^{***}p < 0.001$ vs. control: $^{\#}p < 0.05$, $^{\#\#}p < 0.01$, $^{\#\#\#}p < 0.001$ vs. L-NAME.

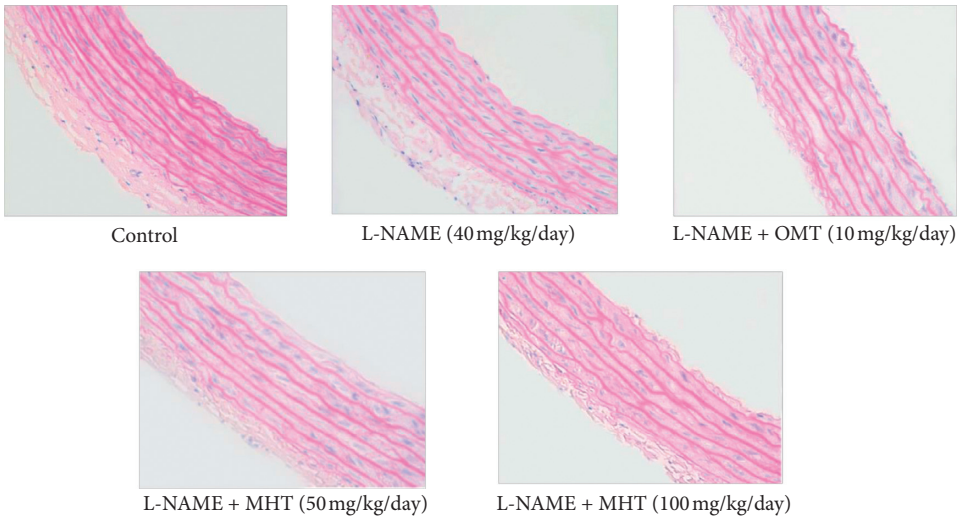

Figure 5: Continued.

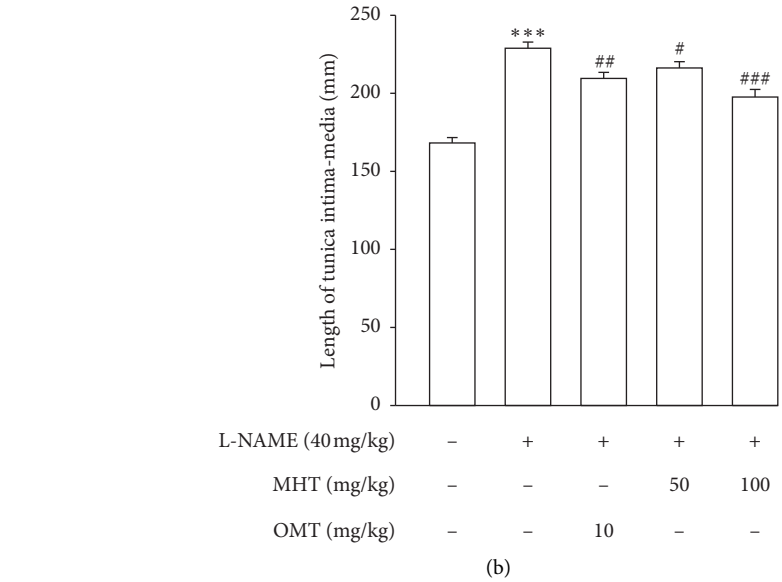

(b)

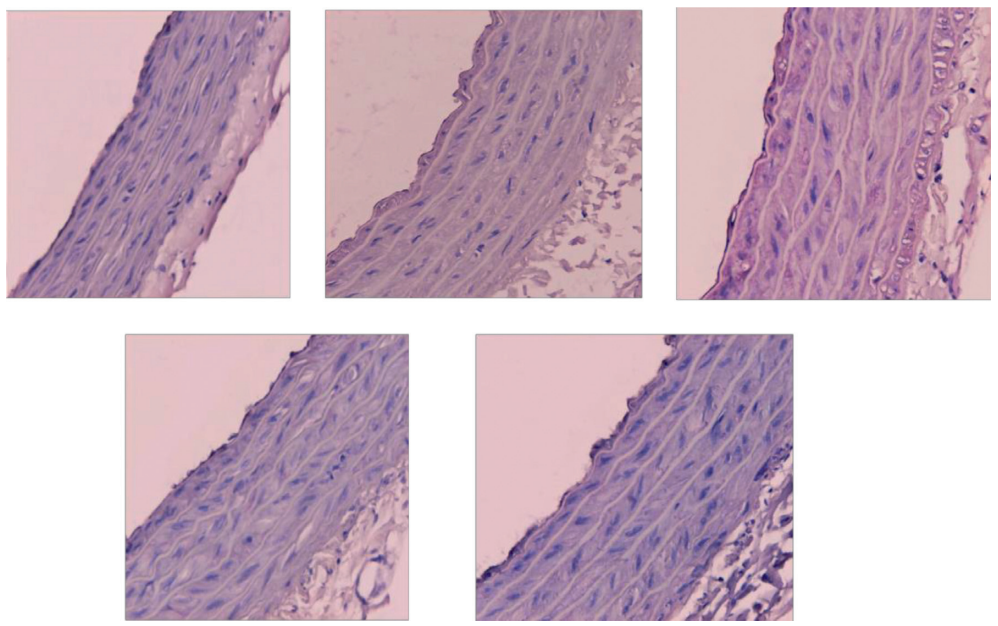

(c)

Figure 5: Continued.

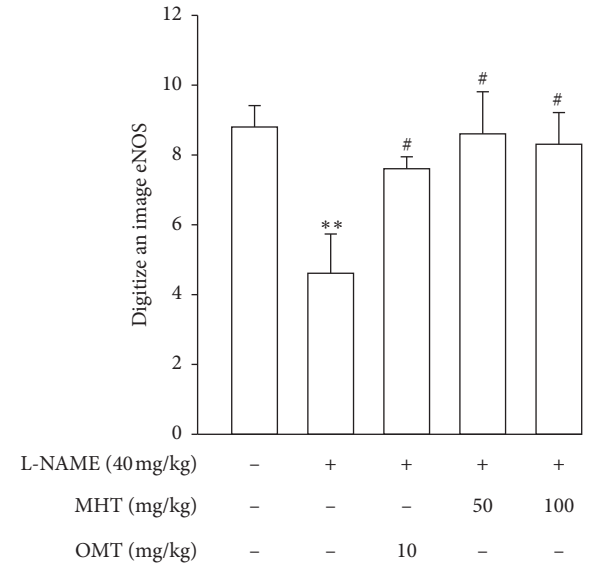

(d)

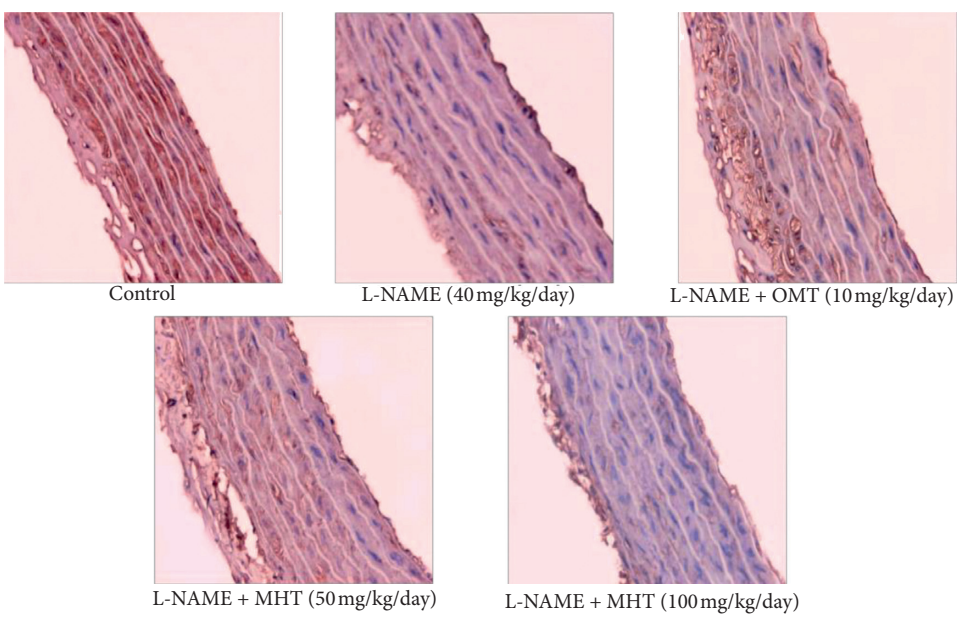

(e)

Figure 5: Continued.

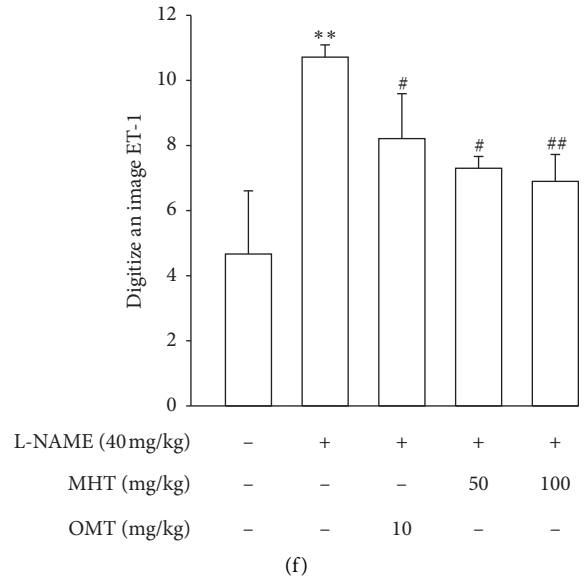

Figure 5: Effect of MHT on aorta morphology, eNOS, and ET-1 immunoreactivity in aortic tissues. (a) Representative microscopic photographs in aorta of control and L-NAME groups were stained with hematoxylin and eosin. (b) Numerical value of the length of tunica intima-media in aorta of L-NAME model. (c) eNOS immunoreactivity in thoracic aorta of L-NAME-induced hypertensive rats. (d) Digitization of eNOS expression. (e) ET-1 immunoreactivity in thoracic aorta of L-NAME-induced hypertensive rats. (f) Digitization of ET-1 expression. MHT: Ma Huang Tang; eNOS: endothelial nitric oxide synthase; ET-1: endothelin-1; OMT: Olmetec. Values are expressed as mean ± S.E. ($n = 3$ per group). $^{**}p < 0.01$, $^{***}p < 0.001$ versus control: $^{\#}p < 0.05$, $^{\#\#}p < 0.01$, and $^{\#\#\#}p < 0.001$ versus L-NAME.

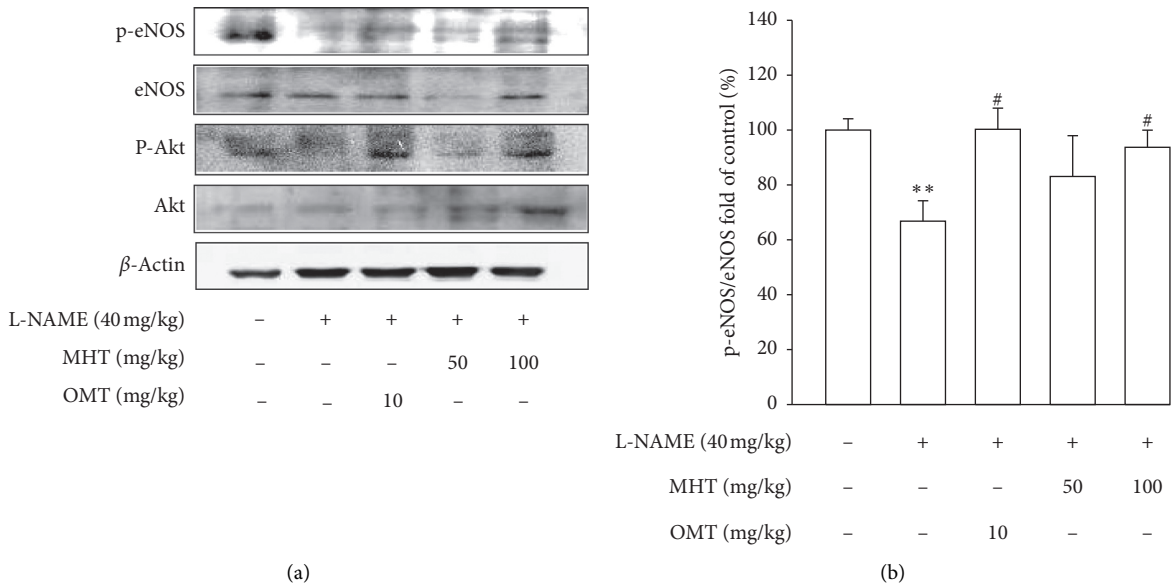

Figure 6: Continued.

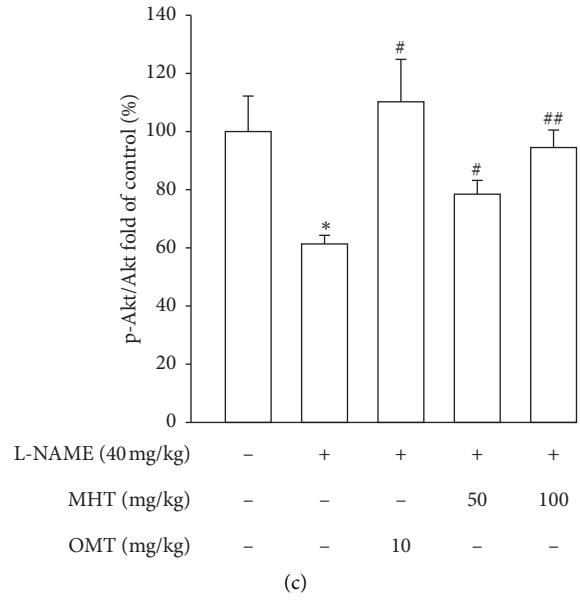

Figure 6: Effect of MHT on the expression of eNOS and Akt phosphorylation by western blot analysis. MHT: Ma Huang Tang; eNOS: endothelial nitric oxide synthase; and OMT: Olmetec. Values are expressed as mean ± S.E. ($n = 3$ per group). $^{*}p < 0.05$, $^{**}p < 0.01$ versus control: $^{\#}p < 0.05$, $^{\#\#}p < 0.01$ versus L-NAME.

Table 1: Effect of MHT on the BUN, albumin, and creatinine in the serum of L-NAME-induced hypertensive rats.

	Cont.	L-NAME	OMT 10 (mg/kg/day)	MHT 50 (mg/kg/day)	MHT 100 (mg/kg/day)
Albumin (g/dl)	3.4 ± 0.05	$3.02 \pm 0.12^{**}$	$3.78 \pm 0.1^{\#\#\#}$	$3.4 \pm 0.1^{\#\#}$	$3.55 \pm 0.1^{\#\#}$
BUN (mg/dl)	14.7 ± 0.9	$51 \pm 13.0^{**}$	$22.9 \pm 0.42^{\#\#}$	$21 \pm 1.4^{\#\#\#}$	$20.3 \pm 1.6^{\#\#}$
Creatinine (mg/dl)	0.7 ± 0.05	$1.21 \pm 0.2^{***}$	1.15 ± 0.14	$0.8 \pm 0.1^{\#\#\#}$	$0.77 \pm 0.1^{\#\#\#}$

Serum albumin, BUN, and creatinine were measured by using kits as described in the methods. Cont.: control; MHT: Ma Huang Tang; and OMT: Olmetec. The data of values shows mean ± S.E. ($n = 8$ per group). $^{**}p < 0.01$, $^{***}p < 0.001$ versus control; $^{\#\#}p < 0.01$, $^{\#\#\#}p < 0.001$ versus L-NAME.

specific endothelial receptors and causes the activation of endothelial NO synthesis, resulting in NO release [20]. Vasodilation in response to ACh stimulation was significantly inhibited in L-NAME hypertensive rats compared to that in normotensive MHT-treated L-NAME hypertensive rats. Treatment with OMT, an ACE inhibitor, also significantly improved vasodilation responses in L-NAME-induced hypertensive rats. NO produced by endothelial cells promotes vascular relaxation by activating guanylate cyclase and increasing cGMP production in vascular smooth muscle [21]. The aortic levels of cGMP were decreased in the L-NAME hypertensive group compared with that in the control group; however, cGMP production in the thoracic aorta was restored after treatment with MHT. Thus, our results demonstrate that MHT-induced vascular dilation is related to decreased blood pressure in L-NAME-induced hypertensive rats.

Several studies have shown that lowering blood pressure and endothelial function are associated with an increase in eNOS reactivity, which in turn increases NO production and vasodilation [22, 23]. Immunohistochemical staining analysis showed that eNOS was weakly expressed in the thoracic aorta of the L-NAME hypertensive group, but this expression was markedly increased in the MHT group. On the other hand, the expression of ET-1 was lower in the MHT group than that in the L-NAME hypertensive group. ET-1 is a potent endothelium-derived vasoconstrictor that causes a prolonged increase in vascular tone [24]. It has also been identified as an important vasoactive substance associated with pathophysiological conditions such as hypertension, ischemic heart disease, and congestive heart failure [25, 26]. These results suggest that MHT ameliorates ACh-induced vascular relaxation by improving the eNOS/cGMP pathway in the L-NAME hypertensive animal model (Figure 7).

There have been many reports suggesting that BUN and creatinine clearance levels are generally considered as prognostic markers of renal function. Moreover, systemic development of hypertension and renal vasoconstriction has been observed upon chronic blockade of endogenous NO synthesis; that is, chronically NO-blocked rats developed proteinuria and glomerular sclerotic injury [27, 28]. Hence, urinary albumin, BUN, and creatinine clearance levels were determined to evaluate the effect of MHT. In this study, BUN and creatinine clearance increased significantly in L-NAME hypertensive rats, whereas MHT suppressed the upregulation of BUN and creatinine clearance. Moreover, osmolality is upregulated by MHT compared to that in L-NAME hypertensive rats. These results suggest that MHT ameliorates renal dysfunction in L-NAME-induced hypertension rat model. Additional experiments including

Table 2: Effect of MHT on the body weight, water intake, urine volume, and osmolality in urine of L-NAME-induced hypertension rats.

	Cont.	L-NAME	OMT 10 (mg/kg/day)	MHT 50 (mg/kg/day)	MHT 100 (mg/kg/day)
Water intake (ml/day)	22.4 ± 1.3	20.9 ± 4.4	25.3 ± 3.9	18.06 ± 9.4	23.7 ± 5.0
Urine volume (g/23 h)	32.9 ± 1.0	42.4 ± 5.9	32.9 ± 2.5	32.2 ± 0.4	35.7 ± 2.2
Osmolality (mOsm/kg H_2O)	2262.7 ± 110	795 ± 79.9***	1932.6 ± 82.3###	1510.5 ± 19.5##	1720.8 ± 94.6###
Albumin (g/dl)	0.473 ± 0.01	0.60 ± 0.05*	0.56 ± 0.06	0.433 ± 0.07#	0.269 ± 0.02###

Water intake and urine samples were acquired for 1 day at last week of experiment. Cont.: control; MHT: Ma Huang Tang; and OMT: Olmetec. The data of values shows mean ± S.E.($n = 4$ per group). $^{*}p < 0.05$; $^{**}p < 0.001$ versus control; $^{\#}p < 0.05$, $^{\#\#}p < 0.01$, and $^{\#\#\#}p < 0.001$ versus L-NAME.

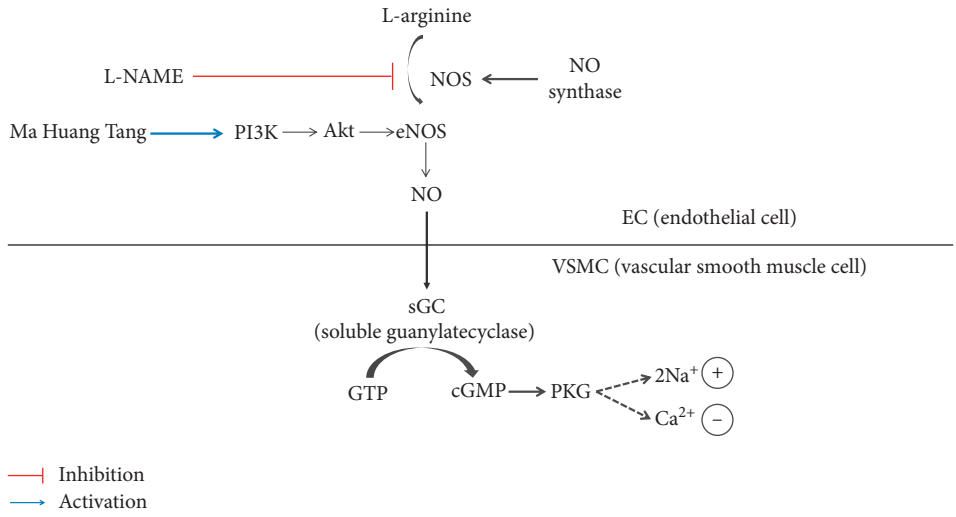

Figure 7: Summary of MHT action in L-NAME-induced hypertensive rats. L-NAME inhibited NO production; therefore, Akt, eNOS, and cGMP activation was decreased. Meanwhile, MHT activated PI3K/Akt/eNOS signaling; as a result, cGMP production was increased. MHT: Ma Huang Tang; eNOS: endothelial nitric oxide synthase; cGMP: guanosine 3′,5′-cyclic monophosphate; and OMT: Olmetec.

preclinical and clinical study are required to demonstrate the safety and LD50 value of MHT in hypertension.

5. Conclusions

This study provides evidence for the therapeutic role of MHT in suppressing blood pressure and renal dysfunction in rats with L-NAME-induced hypertension, via the activation of the vascular NO/cGMP system. Furthermore, our results indicate that MHT may play an important role in the regulation of blood pressure and renal function in experimental hypertensive model.

Data Availability

The data used to support the findings of this study are included within the article.

Conflicts of Interest

The authors report no conflicts of interest regarding the publication of this paper.

Acknowledgments

This study was supported by the National Research Foundation of Korea (NRF) funded by the Korean Government (MSIP) (nos. 2017R1A5A2015805 and 2019R1A2C1085650).

References

[1] P. M. Kearney, M. Whelton, K. Reynolds, P. Muntner, P. K. Whelton, and J. He, "Global burden of hypertension: analysis of worldwide data," *The Lancet*, vol. 365, no. 9455, pp. 217–223, 2005.

[2] X. Nie, Y. Dai, J. Tan et al., "α-Solanine reverses pulmonary vascular remodeling and vascular angiogenesis in experimental pulmonary artery hypertension," *Journal of Hypertension*, vol. 35, no. 12, pp. 2419–2435, 2017.

[3] R. Rahimian, L. Chan, A. Goel, D. Poburko, and C. van Breemen, "Estrogen modulation of endothelium-derived relaxing factors by human endothelial cells," *Biochemical and Biophysical Research Communications*, vol. 322, no. 2, pp. 373–379, 2004.

[4] R. K. Daniel, B. Kevin, M. Carol, W. Rebecca, L. L. Jennifer, and J. Alan, "Impaired brachial artery endothelium-dependent and –independent vasodilation in men with erectile dysfunction and no other clinical cardiovascular disease," *Journal of the American College of Cardiology*, vol. 43, pp. 179–184, 2004.

[5] R. Thoonen, P. Y. Sips, K. D. Bloch, and E. S. Buys, "Pathophysiology of hypertension in the absence of nitric oxide/cyclic GMP signaling," *Current Hypertension Reports*, vol. 15, no. 1, pp. 47–58, 2013.

[6] F. Portaluppi, Y. Touitou, and M. H. Smolensky, "Ethical and methodological standards for laboratory and medical biological rhythm research," *Chronobiology International*, vol. 25, pp. 999–1016, 2018.

[7] W. C. Ling, D. D. Murugan, Y. S. Lau, P. M. Vanhoutte, and M. R. Mustafa, "Sodium nitrite exerts an antihypertensive effect and improves endothelial function through activation of eNOS in the SHR," *Scientific Reports*, vol. 6, no. 1, Article ID 33048, 2016.

[8] X. Yang, W. B. Peng, and X. Q. Yue, "Syndrome differentiation and treatment of Taiyang disease in Shanghan Lun," *Journal of Chinese Integrative Medicine*, vol. 7, no. 2, pp. 171–174, 2009.

[9] C.-H. Ma, Z.-Q. Ma, Q. Fu, and S.-P. Ma, "Ma Huang Tang ameliorates asthma though modulation of Th1/Th2 cytokines and inhibition of Th17 cells in ovalbumin-sensitized mice," *Chinese Journal of Natural Medicines*, vol. 12, no. 5, pp. 361–366, 2014.

[10] M. Zhang, P. Schiffers, G. Janssen, M. Vrolijk, P. Vangrieken, and G. R. M. M. Haenen, "The cardiovascular side effects of Ma Huang due to its use in isolation in the Western world," *European Journal of Integrative Medicine*, vol. 18, pp. 18–22, 2018.

[11] S. Z. Kim, S. H. Kim, J. K. Park, G. Y. Koh, and K. W. Cho, "Presence and biological activity of C-type natriuretic peptide-dependent guanylate cyclase-coupled receptor in the penile corpus cavernosum," *Journal of Urology*, vol. 159, no. 5, pp. 1741–1746, 1998.

[12] K. M. Blechman, S. B. Karch, and B. G. Stephens, "Demographic, pathologic, and toxicological profiles of 127 decedents testing positive for ephedrine alkaloids," *Forensic Science International*, vol. 139, no. 1, pp. 61–69, 2004.

[13] J.-J. Jia, X.-S. Zeng, Y. Li, S. Ma, and J. Bai, "Ephedrine induced thioredoxin-1 expression through β-adrenergic receptor/cyclic AMP/protein kinase A/dopamine- and cyclic AMP-regulated phosphoprotein signaling pathway," *Cellular Signalling*, vol. 25, no. 5, pp. 1194–1201, 2013.

[14] E. J. Tsai and D. A. Kass, "Cyclic GMP signaling in cardiovascular pathophysiology and therapeutics," *Pharmacology and Therapeutics*, vol. 122, no. 3, pp. 216–238, 2009.

[15] E. O. Gosmanova, M. K. Mikkelsen, M. Z. Molnar et al., "Association of systolic blood pressure variability with mortality, coronary heart disease, stroke, and renal disease," *Journal of the American College of Cardiology*, vol. 68, no. 13, pp. 1375–1386, 2016.

[16] M. F. Tiberio, E. S. Roland, G. Tomasz, and H. M. Franz, "Salt and hypertension : is salt dietary reduction worth the effort?" *The American Journal of Medicine*, vol. 125, pp. 433–439, 2012.

[17] R. F. Abdel-Rahman, A. F. Hessin, M. Abdelbaset, H. A. Ogaly, R. M. Abd-Elsalam, and S. M. Hassan, "Antihypertensive effects of roselle-olive combination in L-NAME-induced hypertensive rats," *Oxidative Medicine and Cellular Longevity*, vol. 2017, Article ID 9460653, 24 pages, 2017.

[18] S. M. Greish, Z. Abdel-Hady, S. S. Mohammed et al., "Protective potential of curcumin in L-NAME-induced hypertensive rat model: AT1R, mitochondrial DNA synergy," *International Journal of Physiology, Pathophysiology and Pharmacology*, vol. 12, pp. 134–146, 2020.

[19] K. Dharmashankar and M. E. Widlansky, "Vascular endothelial function and hypertension: insights and directions," *Current Hypertension Reports*, vol. 12, no. 6, pp. 448–455, 2010.

[20] C. Wilson, M. D. Lee, and J. G. McCarron, "Acetylcholine released by endothelial cells facilitates flow-mediated dilatation," *The Journal of Physiology*, vol. 594, no. 24, pp. 7267–7307, 2016.

[21] A. Sandoo, J. J. C. S. Veldhuijzen van Zanten, G. S. Metsios, D. Carroll, and G. D. Kitas, "The endothelium and its role in regulating vascular tone," *The Open Cardiovascular Medicine Journal*, vol. 4, no. 1, pp. 302–312, 2010.

[22] M. F. Mahmoud, M. El-Nagar, and H. M. El-Bassossy, "Anti-inflammatory effect of atorvastatin on vascular reactivity and insulin resistance in fructose fed rats," *Archives of Pharmacal Research*, vol. 35, no. 1, pp. 155–162, 2012.

[23] D. H. Endemann and E. L. Schiffrin, "Nitric oxide, oxidative excess, and vascular complications of diabetes mellitus," *Current Hypertension Reports*, vol. 6, no. 2, pp. 85–89, 2004.

[24] S. K. Nishiyama, J. Zhao, D. W. Wray, and R. S. Richardson, "Vascular function and endothelin-1: tipping the balance between vasodilation and vasoconstriction," *Journal of Applied Physiology*, vol. 122, no. 2, pp. 354–360, 2017.

[25] N. Sud and S. M. Black, "Endothelin-1 impairs nitric oxide signaling in endothelial cells through a protein kinase Cδ-dependent activation of STAT3 and decreased endothelial nitric oxide synthase expression," *DNA and Cell Biology*, vol. 28, no. 11, pp. 543–553, 2009.

[26] B. A. Maron, Y.-Y. Zhang, K. White et al., "Aldosterone inactivates the endothelin-B receptor via a cysteinyl thiol redox switch to decrease pulmonary endothelial nitric oxide levels and modulate pulmonary arterial hypertension," *Circulation*, vol. 126, no. 8, pp. 963–974, 2012.

[27] J.-J. Boffa, Y. Lu, S. Placier, A. Stefanski, J.-C. Dussaule, and C. Chatziantoniou, "Regression of renal vascular and glomerular fibrosis: role of angiotensin II receptor antagonism and matrix metalloproteinases," *Journal of the American Society of Nephrology*, vol. 14, no. 5, pp. 1132–1144, 2003.

[28] J. F. Ndisang and R. Chibbar, "Heme oxygenase improves renal function by potentiating podocyte-associated proteins in N -Nitro-L-Arginine-Methyl ester (L-NAME)-Induced hypertension," *American Journal of Hypertension*, vol. 28, no. 7, pp. 930–942, 2015.

Hindawi
Evidence-Based Complementary and Alternative Medicine
Volume 2021, Article ID 9945277, 8 pages
https://doi.org/10.1155/2021/9945277

Research Article

Acupuncture Attenuates Blood Pressure via Inducing the Expression of nNOS

Lu Wang, Na-Na Yang, Guang-Xia Shi, Li-Qiong Wang, Qian-Qian Li, Jing-Wen Yang, and Cun-Zhi Liu

International Acupuncture and Moxibustion Innovation Institute, School of Acupuncture-Moxibustion and Tuina, Beijing University of Chinese Medicine, Beijing 100029, China

Correspondence should be addressed to Jing-Wen Yang; yangjw0626@126.com

Received 22 March 2021; Accepted 4 June 2021; Published 19 June 2021

Academic Editor: Thanasekaran Jayakumar

Background. Sympathetic activation leads to elevated blood pressure. Neuronal nitric oxide synthase (nNOS) inhibits sympathetic nervous system activity, thereby decreasing blood pressure (BP). nNOS is highly expressed in the arcuate nucleus (ARC) and ventrolateral periaqueductal gray (vlPAG), which play essential roles in the regulation of the cardiovascular and sympathetic nervous systems. *Objective*. This study was designed to verify the hypothesis that acupuncture exerts an antihypertensive effect via increasing the expression of nNOS in ARC and vlPAG of spontaneously hypertensive (SHR) rats. *Methods*. Rats without anesthesia were subject to daily acupuncture for 2 weeks. BP was monitored by the tail-cuff method. nNOS expressions in the ARC and vlPAG were detected by western blot and immunofluorescence. BP was measured after 7-Nitroindazole (7-NI), a specific nNOS inhibitor, was microinjected into ARC or vlPAG in SHR rats treated with acupuncture. *Results*. Acupuncture for 14 days significantly attenuated BP, and the Taichong (LR3) acupoint was superior to Zusanli (ST36) and Fengchi (GB20) in lowering BP. In addition, acupuncture at Taichong (LR3) induced an increase of nNOS expression in ARC and vlPAG, whereas microinjection of 7-NI into ARC or vlPAG reversed the antihypertensive effect of acupuncture. *Conclusions*. This study indicates that acupuncture at Taichong (LR3) induces a better antihypertensive effect than at Zusanli (ST36) or at Fengchi (GB20) in SHR rats, and enhancement of nNOS in ARC and vlPAG probably contributes to the antihypertensive effect of acupuncture.

1. Introduction

High blood pressure (BP) is the leading modifiable risk factor for mortality, accounting for nearly 1 in 5 deaths worldwide [1, 2]. Hypertension control remains a challenge. There has been an increasing interest in the Western countries in exploring alternative medicinal treatments and in considering new therapies like acupuncture for a number of chronic ailments including cardiovascular diseases. Accumulating clinical trials showed that acupuncture was probably to lower BP in hypertension patients. Acupuncture treatment could be beneficial for ameliorating the circadian rhythm of BP and might reduce BP in prehypertension and stage I hypertension [3, 4]. In addition, in the home health care hypertension population, antihypertensive drugs plus acupuncture could be more useful in lowering BP and in modulating autonomic nervous system activity than drugs alone [5]. However, the potential mechanisms of the effect of acupuncture on hypertension have not been well studied, hindering its application as a therapeutic option in the Western world.

Sympathetic activation represents a hallmark of the essential hypertensive state [6]. Our previous articles observed that acupuncture could influence BP by regulating the sympathetic nervous system. Beta-adrenergic receptors are involved in the modulation of acupuncture on renal sympathetic nerve activity and BP [7]. Moreover, acupuncture was involved in regulating reactive oxygen species and mitogen-activated protein kinases derived from NADPH oxidase in rostral ventrolateral medulla (RVLM), reducing sympathetic outflow and lowering the rise of BP [8]. Recently, acupuncture was reported to modulate

sympathoexcitatory reflex responses and inhibit BP elevated through activation of a long-loop hypothalamic-midbrain-medullary pathway [9]. This pathway involves the arcuate nucleus (ARC), ventrolateral periaqueductal gray (vlPAG), and RVLM. ARC receives convergent input from the stimulation of a number of acupoints and provides excitatory projections to the vlPAG, which, in turn, inhibits premotor cardiovascular sympathoexcitatory RVLM neurons to modulate sympathoexcitatory reflexes evoked by visceral afferent stimulation [10, 11]. Besides, activating the mutual excitatory projection between the ARC and vlPAG contributes to prolonging acupuncture-cardiovascular regulation [12].

It has been established that neuronal nitric oxide synthase (nNOS) plays an important role in the regulation of sympathetic nervous system activity (SNA). Through both upregulating sympathoinhibitory gamma-aminobutyric acid activity and downregulating sympathoexcitatory activity induced by angiotensin II and glutamate, nNOS can inhibit the abnormal excitation of the sympathetic nervous system [13]. Of note, nNOS has a sympathoinhibitory effect in hypertension. A nNOS inhibitor could enhance the tonic sympathetic discharges and increase BP in rats [14]. Introducing a dominant negative construct for nNOS into the brain of hypertensive rats could upregulate BP by activating sympathoexcitation [15]. Furthermore, nNOS signal is regarded as an essential regulator for controlling cardiovascular function in ARC, vlPAG, and RVLM [16–19]. Our previous study had demonstrated that the antihypertensive effect of acupuncture might be associated with the regulation of the expression of nNOS in RVLM [8]. However, the role of nNOS in ARC and vlPAG in acupuncture on spontaneously hypertensive rats is not clear. Moreover, Taichong (LR3), Zusanli (ST36), and Fengchi (GB20) are the most commonly used acupoints for the treatment of hypertension clinically [20–22], but which acupoint is the most effective remains unknown. Therefore, the present study was conducted to identify the optimal points for the acupuncture treatment of hypertension and to preliminarily test the hypothesis that the antihypertensive effect of acupuncture is related, in part, to the increase of nNOS expression in ARC and vlPAG.

2. Methods

2.1. Animals. Nine-week-old male SHR rats (210–230 g) and body weight-matched Wistar Kyoto rats (WKY) were obtained from the Beijing Vital River Laboratory Animals Co. Ltd. (Beijing, China). They were housed at a controlled ambient temperature of 22–25°C with 55 ± 5% relative humidity and a 12 h light/dark cycle (lights on at 8:00 AM). The animals were given food and water ad libitum for 1 week and were acclimatized to handling by the researchers and BP-measuring conditions for 1 week prior to acupuncture treatments. All experimental procedures were carried out according to the requirements of the Provisions and General Recommendations of Chinese Experimental Animal. The protocol was approved by the Committee of Ethics on Animal Experiments at China Academy of Chinese Medical Sciences.

2.2. Experiment Design

2.2.1. Experiment I. To evaluate the effect of acupuncture on BP, we randomly divided the 30 SHR rats into 5 groups: SHR-LR3 (SHR rats treated with acupuncture at Taichong (LR3)), SHR-ST36 (SHR rats treated with acupuncture at Zusanli (ST36)), SHR-GB20 (SHR rats treated with acupuncture at Fengchi (GB20)), SHR-SA (SHR rats treated with acupuncture at nonacupoint), and SHR-Cont (SHR rats without treatment). Body weight-matched 6 WKY rats with normal BP (WKY group) were used as a comparison control group. Systolic blood pressure (SBP) and diastolic blood pressure (DBP) were monitored daily after acupuncture.

2.2.2. Experiment II. To evaluate the effect of acupuncture on the expressions of nNOS in ARC and vlPAG, we randomly assigned 24 rats into 4 groups: WKY, SHR-Cont, SHR-LR3, and SHR-SA ($n = 6$ per group). The protein expressions of nNOS were measured by western blot and the mean fluorescence intensity of nNOS-positive neurons were detected by immunofluorescence.

2.2.3. Experiment III. To examine whether nNOS is involved in the mechanism of acupuncture's antihypertensive effect, we allocated the SHR rats treated with acupuncture at Taichong (LR3) into 4 groups: ARC-7-Nitroindazole (7-NI) (SHR rats microinjected with 7-NI into ARC), ARC-dimethyl sulfoxide (DMSO) (SHR rats microinjected with DMSO into ARC), vlPAG-7-NI (SHR rats microinjected with 7-NI into vlPAG), and vlPAG-DMSO (SHR rats microinjected with DMSO into vlPAG). SBP and DBP were evaluated after the specific nNOS inhibitor, 7-NI, was microinjected into ARC or vlPAG in SHR rats ($n = 4$ per group).

2.3. Acupuncture Treatment. The mouse was lightly fixed by hand to minimize stress during acupuncture treatment. Acupuncture stimulation was performed once daily at 8 am to 10 am for a period of 2 weeks (1 day rest after 6 days of treatment) for a total of 12 stimulations without anesthesia. In the SHR-LR3, SHR-ST36, and SHR-GB20 groups, stainless-steel acupuncture needles (Hwato Co., Suzhou, China) 0.20 mm in diameter were inserted bilaterally at Taichong (LR3), Zusanli (ST36), and Fengchi (GB20) with a depth of 3–5 mm, turned at a rate of two spins per second for 30 s and then removed immediately [7]. In the SHR-SA group, needles were placed bilaterally at nonacupuncture points (about 10 mm above the iliac crest), but no stimulation was given [23]. The rats in the SHR-Cont and WKY groups were given the same level catching-grasping stimulus without acupuncture treatment for the same 30 seconds duration. Detailed acupoint locations and manipulations are presented in Figure 1 and Table 1.

2.4. Measurement of BP. SBP and DBP were measured noninvasively by the tail-cuff method every day from 8 am to 10 am using the BP-6A BP-measuring system from Softron Beijing Biotechnology Co. Ltd. (Beijing, China). SBP and

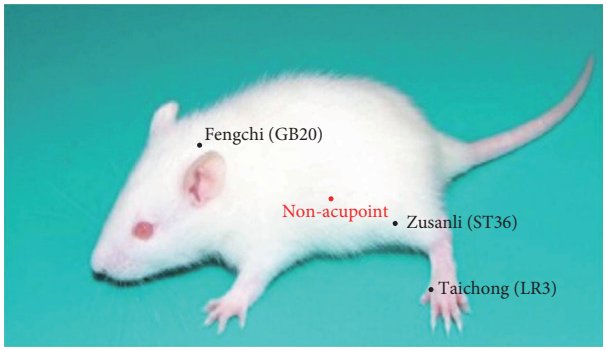

Figure 1: The specific locations of the acupoints and nonacupoints.

DBP were monitored continuously three times a day after a 30 min resting period following acupuncture, and the average value was taken as the experimental results.

2.5. Western Blot. The protein concentrations in the ARC and vlPAG were quantified using a Pierce BCA Protein Assay kit (Thermo Scientific). Protein samples (40 μg) were loaded onto a 6% SDS-PAGE gel for electrophoresis and transblotted to polyvinylidene difluoride membrane (Merck Millipore, US). The membranes were blocked with 5% nonfat dried milk for 1 h and then incubated overnight at 4°C with nNOS antibody (1 : 2000, Abcam) and β-actin (1 : 1000, Bioss). The membranes were incubated with secondary antibodies for 1 h at room temperature and the images were scanned with an imaging system (Bio-Rad, US) and analyzed using Image *J* software.

2.6. Immunofluorescence. After the experimental treatment, rats were sacrificed with an overdose of sodium pentobarbital (100 mg/kg, i.p) and infused intracardially with normal saline followed by 4% paraformaldehyde in PBS. The brain was rapidly removed and placed on dry ice, blocked in the coronal plane, and sectioned at a thickness of 20 μm using a cryostat microtome (Leica CM1850 Heidelberger Strasse, Nussloch, Germany). Free-floating sections were incubated for 24 h in PBS (4°C) containing rabbit anti-nNOS antibody (1 : 5000, Abcam), followed by incubation with a fluorescein-conjugated donkey anti-rabbit IgG secondary antibody (1 : 5000, Invitrogen). Slides were coverslipped using mounting medium (Applygen Technologies Inc.). All images were captured under a fluorescence microscope (BX43, Olympus, Japan) and observed blindly by a second investigator.

2.7. Intra-ARC or vlPAG Microinjection. Anesthetized rats with sodium pentobarbital (40 mg/kg, i.p.) were fixed in a prone position in a stereotaxic frame. A burr hole was made in the bone using the following coordinates relative to the bregma: for ARC injection, 1.8–3.8 mm posterior, 9.8–10.0 mm ventral, and 0.3 mm right and left; for vlPAG injection, 7–8.5 mm posterior, 5.8–6.4 mm ventral, and 0.5 mm right and left. Bilateral microinjection was done 7 days after the operation. The 7-NI was microinjected into the ARC and vlPAG 30 min before acupuncture every day, a total of 12 times. The volumes of 7-NI (5 pmol/100 nl) (Sigma-Aldrich, St. Louis, MO, USA) and DMSO microinjected over one minute into each ARC and vlPAG were 20 and 50 nL, respectively. 7-NI was dissolved in 4% DMSO. The concentrations and doses for microinjection were determined based on several similar studies [11, 24–26]. The actual location of microinjection sites in the area was established after the analysis of serial sections and represented based on the rat brain Atlas of Paxinos and Watson (2007).

2.8. Statistics. All data are expressed as mean ± SD. Statistical analysis was carried out using the two-way repeated ANOVA test when comparing SBP and DBP data obtained from different time points among separate groups. Comparisons of the expressions of nNOS among the four groups were statistically analyzed using one-way ANOVA. IBM SPSS v21.0 was used to perform all the statistical analyses. A value of $P < 0.05$ was considered significant.

3. Results

3.1. Acupuncture Reduces the BP in SHR Rats. SBP and DBP were significantly higher in SHR-Cont than in WKY rats at the beginning of the experiment and remained increased for the period of the study. Acupuncture treatment resulted in significantly reducing SBP and DBP in SHR-LR3, SHR-ST36, and SHR-GB20 rats when compared with SHR-Cont rats. There was no obvious difference in SBP and DBP in the SHR-Cont and SHR-SA rats. Although acupuncture at the acupoints decreased the SBP and DBP, it was still higher than the WKY group during the experiment, which suggested that acupuncture could lower BP but was unable to bring it back to normal. In addition, acupuncture at Taichong (LR3) for 2 weeks showed the best antihypertensive effects on BP compared to the SHR-ST36 and SHR-GB20 groups (Figure 2). Therefore, the subsequent experiments were all carried out with acupuncture at Taichong (LR3).

3.2. Acupuncture Induces Increase of nNOS Expressions in ARC and vlPAG. We then evaluated whether acupuncture treatment attenuated BP in SHR rats via regulating the expression of nNOS in the ARC and vlPAG. As shown in Figure 3, the protein expression and mean fluorescence intensity of nNOS in ARC and vlPAG of the SHR-Cont group were significantly lower than those of the WKY group. Acupuncture at Taichong (LR3) for 2 weeks dramatically increased nNOS levels in both the ARC and vlPAG in SHR rats compared with the SHR-Cont group and SHR-SA group; but no significant differences were found between SHR-Cont group and SHR-SA group.

3.3. The Microinjection of 7-NI Inhibits Antihypertensive Effect of Acupuncture. Given that the antihypertensive effect of acupuncture at Taichong (LR3) may be partly mediated by nNOS, we speculated that a nNOS antagonist 7-NI may reverse the beneficial effect of acupuncture. Compared with

Table 1: Acupuncture acupoints and manipulations.

Points	Anatomical positions	Stimulation parameter	Treatment course
Taichong (LR3)	Between the first and second metatarsal bones on the dorsum of the foot	Needles were stimulated at a rate of two spins per second for 30 sec	Two weeks
Zusanli (ST36)	Two mm lateral to the anterior tubercle of the tibia in the anterior tibial muscle and 5 mm distal to the knee joint lower point	Needles were stimulated at a rate of two spins per second for 30 sec	Two weeks
Fengchi (GB20)	Three mm lateral to the centre of a line joining the two ears at the back of the head	Needles were stimulated at a rate of two spins per second for 30 sec	Two weeks
Nonacupoint	Hypochondrium 10 mm above iliac crest.	Needles were inserted without stimulation for 30 sec	Two weeks

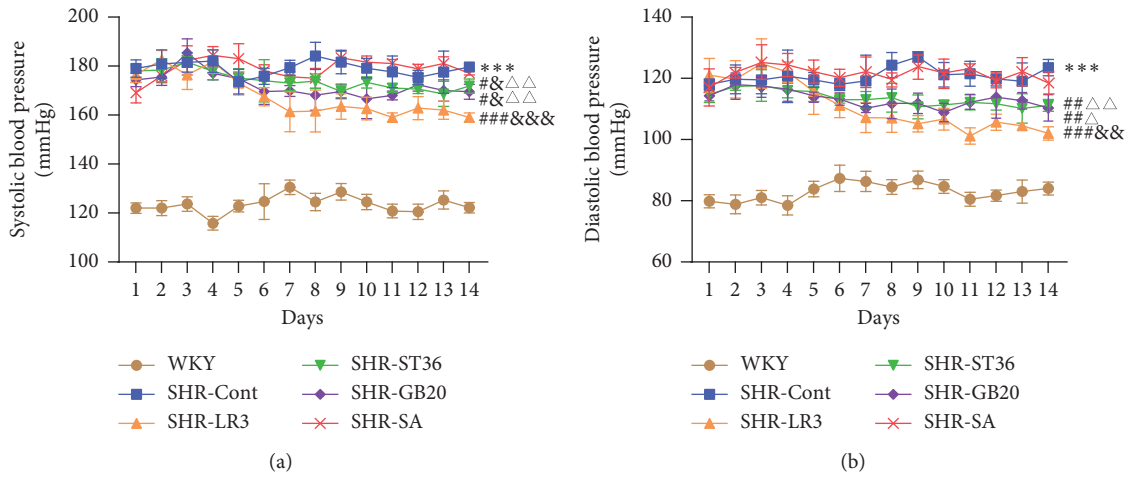

Figure 2: Effect of acupuncture on SBP and DBP as measured by tail-cuff method in all groups. Data are presented as mean ± SD, $n = 6$ in each group. $^{***}P < 0.001$, SHR-Cont vs WKY; $^{\#}P < 0.05$, $^{\#\#}P < 0.01$, $^{\#\#\#}P < 0.001$, SHR-ST36, SHR-GB20, or SHR-LR3 vs SHR-Cont; $^{\&}P < 0.05$, $^{\&\&}P < 0.01$, $^{\&\&\&}P < 0.001$, SHR-ST36, SHR-GB20, or SHR-LR3 vs SHR-SA; $^{\Delta}P < 0.05$, $^{\Delta\Delta}P < 0.01$, SHR-ST36, SHR-GB20 vs SHR-LR3. SHR-Cont: SHR rats without treatment; SHR-SA: SHR rats treated with acupuncture at nonacupoint; SHR-LR3: SHR rats treated with acupuncture at Taichong (LR3); SHR-ST36: SHR rats treated with acupuncture at Zusanli (ST36); SHR-GB20: SHR rats treated with acupuncture at Fengchi (GB20).

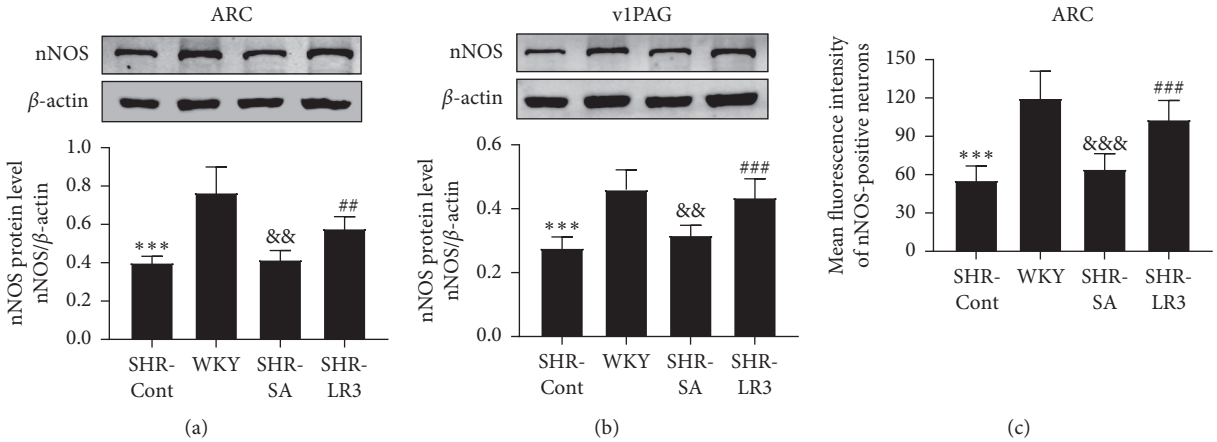

Figure 3: Continued.

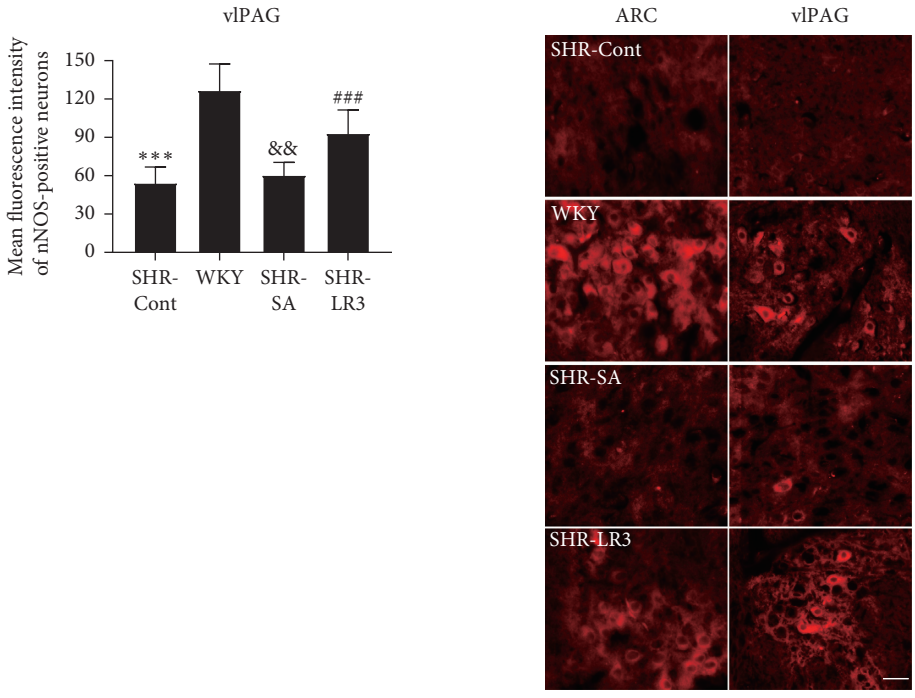

Figure 3: Effect of acupuncture on nNOS in the ARC and vlPAG as detected by western blot and immunofluorescence. Representative gel images and summary data of nNOS (a) in the ARC and (b) in the vlPAG in SHR-Cont, WKY, SHR-SA, and SHR-LR3 groups. (c, d) Summary data show the mean fluorescence intensity of nNOS-positive neurons in the ARC and vlPAG. (e) Representative images show immunofluorescence of nNOS in the ARC and vlPAG. Data are presented as mean ± SD, $n = 6$ in each group. Scale bar = 50 μm. $^{***}P < 0.001$, SHR-Cont vs WKY; $^{\#\#}P < 0.01$, $^{\#\#\#}P < 0.001$, SHR-Cont vs SHR-LR3; $^{\&\&}P < 0.01$, $^{\&\&\&}P < 0.001$, SHR-LR3 vs SHR-SA. SHR-Cont: SHR rats without treatment; SHR-SA: SHR rats treated with acupuncture at nonacupoint; SHR-LR3: SHR rats treated with acupuncture at Taichong; ARC: arcuate nucleus; vlPAG: ventrolateral periaqueductal gray.

rats treated with DMSO, microinjection of 7-NI into ARC and vlPAG significantly increased the SBP and DBP although all rats were treated with acupuncture at Taichong (LR3) for two weeks. The findings suggest that the antihypertensive effect of acupuncture at Taichong (LR3) may be related to the increase of nNOS in ARC and vlPAG (Figure 4).

4. Discussion

In the present study, we show that acupuncture improved BP in SHR rats as compared with SHR rats without treatment. Acupuncture at the Taichong (LR3) had a better antihypertensive effect in comparison to the Zusanli (ST36) and Fengchi (GB20) acupoints. Nonacupoint treatment of SHR rats did not have an antihypertensive effect, which means acupuncture exerts a point-specific effect on regulating BP. In addition, acupuncture at Taichong (LR3) enhanced the expression of nNOS in ARC and vlPAG, whereas microinjections of a nNOS inhibitor reversed the antihypertensive effect of acupuncture.

Our study investigated the effect of different acupoints on BP level. Taichong (LR3), Zusanli (ST36), and Fengchi (GB20) have been reported to be useful to decrease BP according to previous research [8, 27]. Zusanli (ST36) is one of the most commonly used acupoints in research studying the mechanisms of acupuncture, evaluating modulation of the digestive system, cardiovascular system, immune system, and nervous system [28]. Early studies regarding hypertension generally selected Zusanli (ST36) to explore the antihypertensive mechanism of acupuncture and demonstrated that acupuncture improved elevated BP through activation of neurotransmitter systems [10, 29]. The Fengchi (GB20) acupoint is also recommended in the treatment of hypertension. It was [30] discovered that acupuncture at Fengchi (GB20) was effective in primary hypertension, probably related to the decrease of the peripheral vascular resistance due to improvements of microcirculatory state.

In this study, we observed that the antihypertensive effect of Taichong (LR3) is better than Zusanli (ST36) and Fengchi (GB20) in SHR rats. This outcome is in accordance with clinical experience that Taichong (LR3) is the most commonly applied acupoint to treat hypertension in China. Furthermore, according to traditional acupuncture theory, the basis of acupuncture knowledge is rooted in the meridian system. Acupoints are categorized as specific points and subspecific points (also regarded as ordinary points) in keeping with their relevance for different indications. The subspecific acupoints refer to a relative concept that ordinary acupoint showed less specificity in function by comparison to specific acupoint, but considerably more than nonacupoint [31]. Based on acupuncture knowledge,

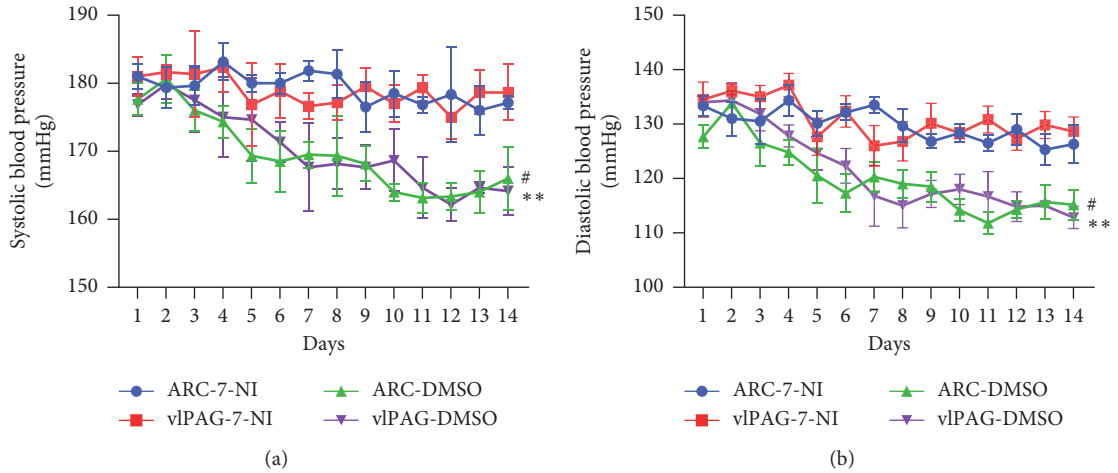

FIGURE 4: Influence of 7-NI on the antihypertensive effect of acupuncture. Data are presented as mean ± SD, $n = 4$ in each group. $^{\#}P < 0.05$, ARC-7-NI vs ARC-DMSO; $^{**}P < 0.01$, vlPAG-7-NI vs vlPAG-DMSO. ARC-7-NI: SHR rats microinjected with 7-NI into ARC; ARC-DMSO: SHR rats microinjected with DMSO into ARC; vlPAG-7-NI: SHR rats microinjected with 7-NI into vlPAG; vlPAG-DMSO: SHR rats microinjected with DMSO into vlPAG.

hypertension is mainly associated with abnormal activity of the liver meridian. Taichong (LR3), the specific acupoint of the liver meridian, affects the liver and regulates qi and is an important acupoint for lowering BP. Consequently, we selected specific acupoint (Taichong (LR3)), on the liver meridian compared with subspecific acupoints to stomach (Zusanli (ST36)) and the gallbladder (Fengchi (GB20)) meridians to treat hypertension. We observed that the antihypertensive effect of Taichong (LR3) is most effective, although SHR rats treated by acupuncture at Taichong (LR3), Zusanli (ST36), and Fengchi (GB20) also had decreased SBP and DBP. Similar to these results, Li et al. [32] reported that Taichong (LR3) acupuncture improves hypertension through a mechanism involving altered brain activation in SHR rats. Zheng et al. [33] demonstrated that acupuncture at Taichong (LR3) decreased SBP in hypertensive participants, which might be closely correlated with functional connectivity changes in the frontal lobe, cerebellum, and insula. Together with mild changes produced by acupuncture at nonacupoints, we also suggest that acupuncture has a point-specific effect. Consequently, in this study, we only explored the antihypertensive mechanism of acupuncture at Taichong (LR3) in SHR rats.

It is well accepted that enhanced SNA is closely related to the development and maintenance of hypertension [6]. Previous studies observed that sympathetic activation was elevated by the blockade of central nitric oxide (NO) production or reduced by the local application of NO donors in discrete brain nuclei, demonstrating that NO may affect SNA in multiple parts of the brain [34]. As a gaseous neurotransmitter, NO plays an important role in the regulation of sympathetic activity in the central nervous system. Nitric oxide synthase (NOS) is the most important rate limiting factor in the process of NO formation, and it is the key enzyme of NO synthesis, so the detection of NOS in tissue can reflect the formation of NO. There are three NOS isoforms: neuronal NOS (nNOS), endothelial NOS (eNOS), and inducible NOS (iNOS) [35]. NO produced through nNOS can suppress the excitation of central sympathetic nerve [36]. Blockade of nNOS in the brain leads to systemic hypertension [37]. Researchers have shown that acupuncture inhibits elevated BP by regulating the expression of nNOS in many regions of the body in hypertensive rats. Hwang et al. [38] found that acupuncture could attenuate the BP elevation of SHR rats, along with enhancing the activity of NO/NOS in their mesenteric artery. Kim et al. [39] showed that activation of nNOS in stomach and cheek pouch tissues was one of the mechanisms through which acupuncture decreased BP in a two-kidney, one-clip renal hypertension model in hamsters. Chen and Ma [40] indicated that the antihypertensive response to acupuncture was attenuated by bilateral microinjection of nNOS antisense oligos into the gracile nucleus.

Previous studies have suggested that nNOS-positive neurons are widely distributed in ARC and vlPAG, which have been implicated in cardiovascular regulation [41, 42]. ARC stimulation elicits depressor responses which are mediated via inhibition of sympathetic input to the heart [42]. The vlPAG, an important modulator of autonomic nervous system activity, is involved in antihypertensive responses [43]. Additionally, ARC provides excitatory projections to the vlPAG [12]. Researches indicated that acupuncture reduced the sympathoexcitatory cardiovascular reflex response through activation of a long-loop pathway including ARC and vlPAG [9, 10]. In our study, we found that acupuncture enhanced the expression of nNOS in ARC and vlPAG. As a relatively selective inhibitor of nNOS, 7-NI was demonstrated in numerous studies to suppress the level of nNOS in the brain [44, 45]. After microinjecting 7-NI into ARC or vlPAG, we found that the antihypertensive effect of acupuncture was eliminated. These findings indicate that the increase of nNOS in ARC and vlPAG may contribute to the antihypertensive effect of acupuncture at LR3. However, our previous research observed that acupuncture could lower BP

via decreasing the nNOS in RVLM [8]. Furthermore, several studies [46–48] reported that nNOS in the paraventricular and supraoptic nuclei of the hypothalamus or the RVLM induced pressor responses by elevating sympathetic excitation in conscious rabbits or rats, which means nNOS may play different roles in different brain regions of different animal models. Therefore, further researches are needed to explore the specific mechanisms involved in links between acupuncture-induced antihypertensive effect and nNOS in the different brain regions of SHR rats.

In conclusion, our study demonstrates that acupuncture at Taichong (LR3) induces better antihypertensive effect than Zusanli (ST36) and Fengchi (GB20) in SHR rats. The underlying antihypertensive mechanism of acupuncture is probably correlated with the enhancement of nNOS in ARC and vlPAG. Nevertheless, whether other acupoints or combination of acupoints will produce better antihypertensive effect remains to be further explored. Besides, we only focused on the antihypertensive effect of acupuncture twirling for 30 seconds on acupoints; whether retaining needles will exert a better antihypertensive effect is also worth further study. We did not directly detect the expression of nNOS after applying the 7-NI, which may be a shortcoming in our study. Therefore, following studies will be carried out to explore the specific mechanism of elevated nNOS levels in ARC and vlPAG.

Data Availability

The data used to support the findings of this study are available from the corresponding author upon request.

Conflicts of Interest

The authors declare that they have no conflicts of interest.

Acknowledgments

This work was supported by the Key Project of Science and Technology Program of Beijing Municipal Education Commission (Grant no. KZ201710025025).

References

[1] R. Zack, O. Okunade, E. Olson et al., "Improving hypertension outcome measurement in low- and middle-income countries," *Hypertension*, vol. 73, no. 5, pp. 990–997, 2019.

[2] GBD 2016 Risk Factors Collaborators, "Global, regional, and national comparative risk assessment of 84 behavioural, environmental and occupational, and metabolic risks or clusters of risks, 1990-2016: a systematic analysis for the Global Burden of Disease Study 2016," *Lancet*, vol. 390, no. 10100, pp. 1345–1422, 2017.

[3] H.-M. Kim, S.-Y. Cho, S.-U. Park et al., "Can acupuncture affect the circadian rhythm of blood pressure? A randomized, double-blind, controlled trial," *The Journal of Alternative and Complementary Medicine*, vol. 18, no. 10, pp. 918–923, 2012.

[4] Y. Liu, J.-E. Park, K.-M. Shin et al., "Acupuncture lowers blood pressure in mild hypertension patients: a randomized, controlled, assessor-blinded pilot trial," *Complementary Therapies in Medicine*, vol. 23, no. 5, pp. 658–665, 2015.

[5] K.-Y. Huang, C.-J. Huang, and C.-H. Hsu, "Efficacy of acupuncture in the treatment of elderly patients with hypertension in home health care: a randomized controlled trial," *The Journal of Alternative and Complementary Medicine*, vol. 26, no. 4, pp. 273–281, 2020.

[6] G. Grassi, "Sympathetic neural activity in hypertension and related diseases," *American Journal of Hypertension*, vol. 23, no. 10, pp. 1052–1060, 2010.

[7] J. W. Yang, Y. Ye, X. R. Wang et al., "Acupuncture attenuates renal sympathetic activity and blood pressure via beta-adrenergic receptors in spontaneously hypertensive rats," *Neural Plasticity*, vol. 2017, Article ID 8696402, 9 pages, 2017.

[8] X.-R. Wang, J.-W. Yang, C.-S. Ji et al., "Inhibition of NADPH oxidase-dependent oxidative stress in the rostral ventrolateral medulla mediates the antihypertensive effects of acupuncture in spontaneously hypertensive rats," *Hypertension*, vol. 71, no. 2, pp. 356–365, 2018.

[9] P. Li, S. C. Tjen-A-Looi, Z. L. Guo et al., "Long-loop pathways in cardiovascular electroacupuncture responses," *Journal of Applied Physiology*, vol. 106, no. 2, pp. 620–630, 2009.

[10] P. Li, S. C. Tjen-A-Looi, and J. C. Longhurst, "Excitatory projections from arcuate nucleus to ventrolateral periaqueductal gray in electroacupuncture inhibition of cardiovascular reflexes," *American Journal of Physiology-Heart and Circulatory Physiology*, vol. 290, no. 6, pp. H2535–H2542, 2006.

[11] S. C. Tjen-A-Looi, P. Li, and J. C. Longhurst, "Processing cardiovascular information in the vlPAG during electroacupuncture in rats: roles of endocannabinoids and GABA," *Journal of Applied Physiology*, vol. 106, no. 6, pp. 1793–1799, 2009.

[12] P. Li, S. C. Tjen-A-Looi, Z.-L. Guo, and J. C. Longhurst, "An arcuate-ventrolateral periaqueductal gray reciprocal circuit participates in electroacupuncture cardiovascular inhibition," *Autonomic Neuroscience*, vol. 158, no. 1-2, pp. 13–23, 2010.

[13] Y. Wang and J. Golledge, "Neuronal nitric oxide synthase and sympathetic nerve activity in neurovascular and metabolic systems," *Current Neurovascular Research*, vol. 10, no. 1, pp. 81–89, 2013.

[14] Y. Nishida, Q.-H. Chen, M. Tandai-Hiruma, S.-i. Terada, and J. Horiuchi, "Neuronal nitric oxide strongly suppresses sympathetic outflow in high-salt Dahl rats," *Journal of Hypertension*, vol. 19, pp. 627–634, 2001.

[15] N. F. Rossi, M. Maliszewska-Scislo, H. Chen et al., "Neuronal nitric oxide synthase within paraventricular nucleus: blood pressure and baroreflex in two-kidney, one-clip hypertensive rats," *Experimental Physiology*, vol. 95, no. 8, pp. 845–857, 2010.

[16] S. H. H. Chan and J. Y. H. Chan, "Brain stem NOS and ROS in neural mechanisms of hypertension," *Antioxidants & Redox Signaling*, vol. 20, no. 1, pp. 146–163, 2014.

[17] S. H. H. Chan, L.-L. Wang, S.-H. Wang, and J. Y. H. Chan, "Differential cardiovascular responses to blockade of nNOS or iNOS in rostral ventrolateral medulla of the rat," *British Journal of Pharmacology*, vol. 133, no. 4, pp. 606–614, 2001.

[18] Z.-L. Guo and A. R. Moazzami, "Involvement of nuclei in the hypothalamus in cardiac sympathoexcitatory reflexes in cats," *Brain Research*, vol. 1006, no. 1, pp. 36–48, 2004.

[19] A. Ally, I. Powell, M. M. Ally, K. Chaitoff, and S. M. Nauli, "Role of neuronal nitric oxide synthase on cardiovascular functions in physiological and pathophysiological states," *Nitric Oxide*, vol. 102, pp. 52–73, 2020.

[20] X. F. Zhao, H. T. Hu, J. S. Li et al., "Is acupuncture effective for hypertension? A systematic review and meta-analysis," *PLoS One*, vol. 10, no. 7, Article ID e0127019, 2015.

[21] H. Lee, S.-Y. Kim, J. Park, Y.-J. Kim, H. Lee, and H.-J. Park, "Acupuncture for lowering blood pressure: systematic review and meta-analysis," *American Journal of Hypertension*, vol. 22, no. 1, pp. 122–128, 2009.

[22] H. Chen, F.-E. Shen, X.-D. Tan, W.-B. Jiang, and Y.-H. Gu, "Efficacy and safety of acupuncture for essential hypertension: a meta-analysis," *Medical Science Monitor*, vol. 24, pp. 2946–2969, 2018.

[23] C. S. Yin, H.-S. Jeong, H.-J. Park et al., "A proposed transpositional acupoint system in a mouse and rat model," *Research in Veterinary Science*, vol. 84, no. 2, pp. 159–165, 2008.

[24] T. Kawabe, K. Kawabe, and H. N. Sapru, "Tonic γ-aminobutyric acid-ergic activity in the hypothalamic arcuate nucleus is attenuated in the spontaneously hypertensive rat," *Hypertension*, vol. 62, no. 2, pp. 281–287, 2013.

[25] M. C. Martins-Pinge, M. R. Garcia, D. B. Zoccal et al., "Differential influence of iNOS and nNOS inhibitors on rostral ventrolateral medullary mediated cardiovascular control in conscious rats," *Autonomic Neuroscience*, vol. 131, no. 1-2, pp. 65–69, 2007.

[26] N. Pourshadi, N. Rahimi, M. Ghasemi, H Faghir-Ghanesefat, M Sharifzadeh, and A. R Dehpour, "Anticonvulsant effects of thalidomide on pentylenetetrazole-induced seizure in mice: a role for opioidergic and nitrergic transmissions," *Epilepsy Research*, vol. 164, Article ID 106362, 2020.

[27] N. Y. Chen, Y. Zhou, Q. Dong et al., "Observation on therapeutic effect of acupuncture in the treatment of German hypertension patients," *Zhen Ci Yan Jiu = Acupuncture Research*, vol. 35, no. 6, pp. 462–466, 2010.

[28] M.-H. Nam, C. S. Yin, K.-S. Soh, and S.-H. Choi, "Adult neurogenesis and acupuncture stimulation at ST36," *Journal of Acupuncture and Meridian Studies*, vol. 4, no. 3, pp. 153–158, 2011.

[29] W. Zhou and J. C. Longhurst, "Neuroendocrine mechanisms of acupuncture in the treatment of hypertension," *Evidence-based Complementary and Alternative Medicine*, vol. 2012, Article ID 878673, 9 pages, 2012.

[30] X. M. Xing, R. C. Wang, Q. W. Sun et al., "Effect on blood pressure and microcirculation of nail fold in primary hypertension patients treated with acupuncture according to syndrome differentiation," *Zhongguo Zhen Jiu*, vol. 31, no. 4, pp. 301–304, 2011.

[31] M. Yang, J. Yang, F. Zeng et al., "Electroacupuncture stimulation at sub-specific acupoint and non-acupoint induced distinct brain glucose metabolism change in migraineurs: a PET-CT study," *Journal of Translational Medicine*, vol. 12, no. 1, p. 351, 2014.

[32] J. Li, Y. Wang, K. He et al., "Effect of acupuncture at LR3 on cerebral glucose metabolism in a rat model of hypertension: a F-FDG-PET study," *Evidence-based Complementary and Alternative Medicine*, vol. 2018, Article ID 5712857, 8 pages, 2018.

[33] Y. Zheng, J. Zhang, Y. Wang et al., "Acupuncture decreases blood pressure related to hypothalamus functional connectivity with frontal lobe, cerebellum, and insula: a study of instantaneous and short-term acupuncture treatment in essential hypertension," *Evidence-based Complementary and Alternative Medicine*, vol. 2016, Article ID 6908710, 10 pages, 2016.

[34] F. Qadri, T. Arens, E.-C. Schwarz, W. H??user, A. Dendorfer, and P. Dominiak, "Brain nitric oxide synthase activity in spontaneously hypertensive rats during the development of hypertension," *Journal of Hypertension*, vol. 21, no. 9, pp. 1687–1694, 2003.

[35] Y. Hirooka, T. Kishi, K. Sakai, A. Takeshita, and K. Sunagawa, "Imbalance of central nitric oxide and reactive oxygen species in the regulation of sympathetic activity and neural mechanisms of hypertension," *American Journal of Physiology-Regulatory, Integrative and Comparative Physiology*, vol. 300, no. 4, pp. R818–R826, 2011.

[36] L. Wang, M. Henrich, K. J. Buckler et al., "Neuronal nitric oxide synthase gene transfer decreases [Ca2+]i in cardiac sympathetic neurons," *Journal of Molecular and Cellular Cardiology*, vol. 43, no. 6, pp. 717–725, 2007.

[37] N. Toda, K. Ayajiki, and T. Okamura, "Control of systemic and pulmonary blood pressure by nitric oxide formed through neuronal nitric oxide synthase," *Journal of Hypertension*, vol. 27, no. 10, pp. 1929–1940, 2009.

[38] H. S. Hwang, Y. S. Kim, Y. H. Ryu et al., "Electroacupuncture delays hypertension development through enhancing NO/NOS activity in spontaneously hypertensive rats," *Evidence-based Complementary and Alternative Medicine: eCAM*, vol. 2011, Article ID 130529, 7 pages, 2011.

[39] D. D. Kim, A. M. Pica, R. G. Durán, and W. N. Durán, "Acupuncture reduces experimental renovascular hypertension through mechanisms involving nitric oxide synthases," *Microcirculation*, vol. 13, no. 7, pp. 577–585, 2006.

[40] S. Chen and S.-X. Ma, "Nitric oxide in the gracile nucleus mediates depressor response to acupuncture (ST36)," *Journal of Neurophysiology*, vol. 90, no. 2, pp. 780–785, 2003.

[41] K. Chachlaki, S. A. Malone, E. Qualls-Creekmore et al., "Phenotyping of nNOS neurons in the postnatal and adult female mouse hypothalamus," *Journal of Comparative Neurology*, vol. 525, no. 15, pp. 3177–3189, 2017.

[42] D. Bajic, C. B. Berde, and K. G. Commons, "Periaqueductal gray neuroplasticity following chronic morphine varies with age: role of oxidative stress," *Neuroscience*, vol. 226, pp. 165–177, 2012.

[43] M. Deolindo, G. G. Pelosi, R. F. Tavares, and F. M. Aguiar Corrêa, "The ventrolateral periaqueductal gray is involved in the cardiovascular response evoked by l-glutamate microinjection into the lateral hypothalamus of anesthetized rats," *Neuroscience Letters*, vol. 430, no. 2, pp. 124–129, 2008.

[44] V. Vitcheva, R. Simeonova, M. Kondeva-Burdina et al., "Selective nitric oxide synthase inhibitor 7-nitroindazole protects against cocaine-induced oxidative stress in rat brain," *Oxidative Medicine and Cellular Longevity*, vol. 2015, Article ID 157876, 8 pages, 2015.

[45] T. Yoshida, V. Limmroth, K. Irikura, and M. A. Moskowitz, "The NOS inhibitor, 7-nitroindazole, decreases focal infarct volume but not the response to topical acetylcholine in pial vessels," *Journal of Cerebral Blood Flow & Metabolism*, vol. 14, no. 6, pp. 924–929, 1994.

[46] S. H. H. Chan, L.-L. Wang, and J. Y. H. Chan, "Differential engagements of glutamate and GABA receptors in cardiovascular actions of endogenous nNOS or iNOS at rostral ventrolateral medulla of rats," *British Journal of Pharmacology*, vol. 138, no. 4, pp. 584–593, 2003.

[47] J.-I. Kim, Y.-S. Kim, S.-K. Kang et al., "Electroacupuncture decreases nitric oxide synthesis in the hypothalamus of spontaneously hypertensive rats," *Neuroscience Letters*, vol. 446, no. 2-3, pp. 78–82, 2008.

[48] D. N. Mayorov, "Selective sensitization by nitric oxide of sympathetic baroreflex in rostral ventrolateral medulla of conscious rabbits," *Hypertension*, vol. 45, no. 5, pp. 901–906, 2005.

Hindawi
Evidence-Based Complementary and Alternative Medicine
Volume 2021, Article ID 5515396, 15 pages
https://doi.org/10.1155/2021/5515396

Research Article

Systematic Pharmacology Reveals the Antioxidative Stress and Anti-Inflammatory Mechanisms of Resveratrol Intervention in Myocardial Ischemia-Reperfusion Injury

Zuzhong Xing,[1] **Qi He**,[2] **Yinliang Xiong**,[3] **and Xiaomei Zeng**[2]

[1]*Brain Hospital of Hunan Province, The Second People's Hospital of Hunan Province, Changsha, Hunan, China*
[2]*People's Hospital of Ningxiang City, Ningxiang, Hunan, China*
[3]*Traditional Chinese Medicine Hospital of Ningxiang City, Ningxiang, Hunan, China*

Correspondence should be addressed to Zuzhong Xing; xzz5186@163.com and Qi He; heqi.ningxiang@outlook.com

Received 6 March 2021; Revised 10 April 2021; Accepted 17 April 2021; Published 21 May 2021

Academic Editor: Thanasekaran Jayakumar

Objective. To explore the oxidative stress and inflammatory mechanisms of resveratrol intervention in myocardial ischemia-reperfusion injury (MIRI). *Methods*. The potential targets of resveratrol were predicted by PharmMapper. The MIRI genes were collected by Online Mendelian Inheritance in Man (OMIM), GeneCards is used to collect related disease genes, and String is used for enrichment analysis. Animal experiments were then performed to verify the systematic pharmacological results. Hematoxylin-eosin (HE) staining was used to observe myocardial damage. The levels of serum interleukin-1β (IL-1β), IL-6, and tumor necrosis factor-α (TNF-α) in each experimental group were detected. The protein and mRNA expressions of Toll-like receptor 4 (TLR4), nuclear factor-kappa (NF-κB) p65, IL-1β, IL-6, and TNF-α in rat myocardial tissue were measured. *Results*. The results of systematic pharmacology showed that insulin resistance, FoxO signaling pathway, adipocytokine signaling pathway, insulin signaling pathway, PI3K-Akt signaling pathway, ErbB signaling pathway, T-cell receptor signaling pathway, peroxisome proliferator-activated receptors (PPAR) signaling pathway, Ras signaling pathway, TNF signaling pathway, and so on were regulated to improve MIRI. The results of animal experiments showed that the myocardial cells of the sham operation group were arranged in fibrous form, and the myocardial ischemia-reperfusion injury group had obvious cell morphology disorder. Compared with the MIRI group, the resveratrol group had a certain degree of relief. Compared with the MIRI group, serum IL-1β, TNF-α, and IL-6 in the resveratrol group was significantly reduced ($P < 0.05$), and myocardial tissue TLR4, NF-κB p65, IL-1β, IL-6, and TNF-α mRNA and protein expressions were significantly reduced ($P < 0.05$). *Conclusion*. Resveratrol can effectively improve MIRI, and its mechanism may be related to antioxidative stress and anti-inflammatory.

1. Introduction

Coronary artery disease (CAD) refers to heart disease caused by coronary artery atherosclerosis that causes lumen stenosis or occlusion, leading to myocardial ischemia, hypoxia, or necrosis, also known as ischemic heart disease [1]. When the larger branch of the coronary artery is completely occluded (or thrombosis), the myocardium supplied by this blood vessel becomes necrotic due to the lack of blood nutrition, and myocardial infarction (MI) will occur [2]. Myocardial infarction, as a high incidence of cardiovascular disease, is one of the diseases with the highest mortality rate in the world [3]. With the trend of population aging in the future, the prevalence and mortality of cardiovascular diseases will continue to rise for a long time, and the number of patients with cardiovascular diseases will continue to increase rapidly in the next 10 years [4].

The current effective strategy for the treatment of acute MI is to perform early coronary reperfusion through primary percutaneous coronary intervention (PCI) or thrombolysis [5, 6]. However, after the blood flow of the ischemic myocardium is restored, the myocardial injury does not alleviate and recover, but aggravates it, leading to other fatal injuries. This pathological syndrome is called

myocardial ischemia-reperfusion injury (MIRI) [7, 8]. The factors leading to MIRI damage include inflammation, oxidative stress, calcium overload, mitochondrial permeability transition pore (mPTP) opening, and energy metabolism disorders [9–11]. The intervention of these pathological processes that lead to MIRI damage is a potential strategy to prevent cardiomyocyte death during MIRI [12, 13]. At present, natural plant ingredients have shown potential advantages in the treatment of MIRI [14]. Resveratrol, as a polyphenolic oxidant (nonflavonoid polyphenol organic compound), has been identified in the extracts of many plants and their fruits, such as grape (red wine), knotweed, peanut, and mulberry [15, 16]. The biological activity of resveratrol has antioxidative stress, anti-inflammatory, heart protection, immune regulation, anti-diabetic, antiaging, and anticancer properties [17–19], especially playing an important role in the protection of myocardial damage [20, 21]. However, its molecular mechanism is not fully understood; especially, the biological network of resveratrol in regulating MIRI is still unknown. This study will first construct the biomolecular network of resveratrol intervention in MIRI through the strategy of systematic pharmacology and then further verify the molecular mechanism of resveratrol intervention in MIRI animal models.

2. Materials and Methods

2.1. Resveratrol Target Prediction and MIRI Disease Gene Acquisition. The structure of resveratrol was retrieved in PubChem (https://pubchem.ncbi.nlm.nih.gov/) and saved in sdf format. Resveratrol's sdf format file is imported into PharmMapper using reverse molecular docking technology to obtain predicted targets [22, 23]. GeneCards (http://www.genecards.org) [24] and OMIM database (http://omim.org/) [25] were utilized to obtain the MIRI genes [22]. Relevance score > 1 was used as the criterion to include MIRI-related genes when searching GeneCards. MIRI gene and resveratrol target protein were imported into UniProt (https://www.uniprot.org/) to get their official gene symbol (Table S1 and Table S2) [22].

2.2. Network Construction and Analysis Methods. The protein-protein interaction (PPI) data of resveratrol target and MIRI gene was collected from String (https://string-db.org/) [22, 26]. The String database was used to construct and analyze the PPI network. Database for Annotation, Visualization and Integrated Discovery (David) ver. 6.8 (https://david.ncifcrf.gov/) was used for Gene Ontology (GO) enrichment and Kyoto Encyclopedia of Genes and Genomes (KEGG) pathway enrichment analysis [22, 27]. String is used for Reactome pathway enrichment analysis.

2.3. Experimental Materials

2.3.1. Experimental Animal. Ninety (90) clean-grade male Sprague Dawley (SD) rats were purchased from Hunan Slack Jingda Experimental Animal Co., Ltd., animal certificate number, Sheng Chan Xu Ke (SCX) (Xiang): 2017–0013). The rats weigh 290~330 g, and they are kept in separate cages in a sterile animal breeding room after purchase. The temperature is controlled at 22~26°C, the light and darkness are each 12 h, and the humidity is 40~60%. All experiments were carried out in accordance with the "Guidelines for the Care and Use of Laboratory Animals" (National Institutes of Health Publication, No. 86–23, revised in 1996) and were approved by the Animal Ethics Committee of Hunan University of Chinese Medicine.

2.3.2. Reagents and Instruments. Resveratrol (34092–100 MG) was purchased from Sigma Company in the United States. 3% sodium pentobarbital was obtained from China Pharmaceuticals Shanghai Chemical Reagent Company. Rat interleukin 1-beta (IL-1β) enzyme-linked immunoassay kit (ELISA) (bsk00027), tumor necrosis factor-α (TNF-α) kit (bsk00163), and IL-6 kit (bsk 0411) were purchased from Beijing Boaosen Biotechnology Co., Ltd. Creatine Kinase Isoenzyme-MB Isozyme (CK-MB) Assay Kit (E006-1-1), Lactate Dehydrogenase (LDH) Assay Kit (A020-2-2), Malondialdehyde (MDA) Assay Kit (A003-1-2), and Superoxide Dismutase (SOD) Assay Kit (A001-3-2) were purchased from Nanjing Jiancheng Institute of Biotechnology. Bicinchoninic acid (BCA) whole protein extraction kit (Cat. no.: 20170613) and BCA protein content detection kit (Cat. no.: 20170528) were purchased from Jiangsu Keygen Biotechnology Co., Ltd. Rabbit anti-Toll-like receptors (TLR)_4 polyclonal antibody (catalog number: ab13867), rabbit anti-β-actin antibody (catalog number: ab8227), and anti-histone H3 (methyl K37) antibody (catalog number: ab215728) were purchased from Abcam Inc. Rabbit anti-nuclear factor-kappa (NF-κB) p65 monoclonal antibody was purchased from Cell Signaling Technology. Horseradish enzyme-labeled secondary antibody was purchased from Beijing Zhongshanjinqiao Biotechnology Company (catalog number: ZB2306). Polyvinylidene fluoride (PVDF) membrane (0.45 μm, product number: 101123-1) was purchased from Shanghai Yantuo Biotechnology Co., Ltd.; primers were obtained from Shanghai Biotech; RNA extraction kit was purchased from Tiangen Biochemical Technology (Beijing) Co., Ltd., (DP419). TransScript One-Step gDNA Removal and cDNA Synthesis SuperMix Kit (Cat. no.: J21201), 2 x EcoTaq PCR SuperMix Kit (Cat. no.: L20719), TransStart Tip Green qPCR SuperMix Kit (Cat. no.: K31213), and Gelstain staining solution (Cat. no.: GS101) were purchased from TransGen Biotech Inc.

HX-300 animal ventilator and BL-420 biological signal acquisition system were purchased from Chengdu Taimeng Technology Co., Ltd. Visible fluorescence imager was purchased from Azure Biosystems, USA; SDS-PAGE electrophoresis instrument, Quantity One 4.6.2 image analyzer, and electromembrane transfer instrument were obtained from Bio-Rad Inc.; SW-CJ2-1F ultraclean table was purchased from Suzhou Antai Bioscience and Technology Company;

and EASYCYCLER 96 PCR instrument was obtained from Jena Company.

2.4. Experimental Methods

2.4.1. Animal Modeling Methods. The rats were fasted for 12 hours before the operation, and the rats were anesthetized by intraperitoneal injection of 3% pentobarbital sodium 30 mg/kg. The rat was fixed on the operating table in the supine position and connected to the BL-420 biological function system, electrocardiograph (ECG) standard II lead, tracheal intubation, and ventilator-assisted breathing were recorded, the third and fourth ribs on the left side of the sternum were incised, and the pericardium was separated. Then the left anterior descending coronary artery (LAD) was ligated with 6.0 silk thread, and both ends of the thread were threaded into the PE tube, and the polyethylene (PE) tube was clamped with a needle holder and pushed forward to cause cardiac compression ischemia. If ECG monitoring shows that the ST segment is significantly elevated, it is considered to be successful. After 30 minutes of ischemia, the PE tube was released and the PE tube was reperfused for 3 hours. The rat's ECG showed significant elevation of the ST segment, that is, the MIRI model was successfully constructed, and then blood was taken from the abdominal aorta; the left ventricular tissue of the heart was taken.

2.4.2. Animal Grouping and Intervention. First, resveratrol was dissolved in dimethyl sulfoxide and diluted with saline. After 1 week of adaptive feeding, the rats were divided into five groups according to the random number method, with 18 rats in each group: sham group: the LAD coronary artery of the heart is only threaded and not ligated. MIRI group: myocardial ischemia is 45 minutes and reperfusion is 3 hours. Low-resveratrol, high-dose preconditioning + MIRI group: resveratrol 40 mg/kg or 80 mg/kg was injected intraperitoneally before myocardial ischemia-reperfusion injury. The sham operation group and MIRI group were pretreated with the same dose of normal saline for intraperitoneal injection. Rats of different groups were raised in separate cages, and each rat was labeled with picric acid serial number on the limbs.

2.4.3. Echocardiography. Before and 3 hours after making the model, the rats were intraperitoneally anesthetized with 3% sodium pentobarbital (30 mg/kg), and the two-dimensional ultrasound system was used to detect the cardiac function of the rats. A probe with a frequency of 10 MHz and a depth of 2 cm is placed on the animal's left chest. The short-axis papillary muscles are recorded on 2D ultrasound, and the left ventricle and tissue Doppler imaging is recorded from the level of the papillary muscles with M-mode ultrasound. Left ventricular ejection fraction (LVEF) and left ventricular fractional shortening (LVFS) were measured.

2.4.4. Animal Specimen Collection and Processing. After the completion of the perfusion, blood was drawn from the abdominal aortic artery. After collection, the blood was centrifuged in a low-temperature high-speed centrifuge at 4°C and 3000 g for 15 minutes, and the serum was separated. After the serum was collected, it was placed in a −20°C low-temperature refrigerator for the detection of biochemical indicators. After blood collection, the rats were sacrificed by neck dislocation, and the myocardial tissue was quickly taken out, washed with normal saline, partly fixed with 4% paraformaldehyde, and partly stored in an ultralow-temperature refrigerator (−80°C) for testing.

2.4.5. Pathological Observation. The heart was uniformly cut about a quarter of the apex and placed in 4% neutral formalin solution for fixation. After 48 hours, it was taken out for dehydration and paraffin-embedded section. Then, the slices were soaked in xylene I and xylene II for 5 minutes, soaked in absolute ethanol I and absolute ethanol II for 2 minutes each, and soaked in 95% ethanol, 85% ethanol, and 75% ethanol for 3 minutes. After the sections were immersed in distilled water, they were stained with hematoxylin for 5 min, differentiated with 1% hydrochloric acid for 30 s, soaked in warm water for 10 min and eosin for 2 min, washed with three distilled water, dehydrated, transparent, mounted with neutral gum, and dried overnight. The sections were observed under an optical microscope and filmed.

2.4.6. Detection of Serum LDH and CK-MB. The inflammatory factors IL-1β, IL-6, and TNF-α are determined by ELISA double-antibody sandwich method. All operations are carried out in strict accordance with the instructions provided by the kit. The blood collected from the abdominal aorta was centrifuged at 3000 r/min for 10 min, and the serum was collected and stored at −20°C. The detection steps were performed in strict accordance with the ELISA kit instructions, using double-well determination, measuring the absorbance (OD) value of each well, and calculating the concentration of IL-1β, IL-6, and TNF-α according to the standard curve.

2.4.7. Detection of Myocardial Tissue Glutathione Peroxidase (GSH-Px), MDA, and SOD. The myocardial tissue was ground into a homogenate with a glass homogenizer, and then the protein concentration of each group of cells was measured according to the instructions of the BCA kit. The working fluid is then configured according to the kit instructions. Then, the reaction initiation solution in the kit is melted and mixed, and diluted according to the ratio of the reaction initiation solution of each kit to the detection buffer of each sample solution, and the mixed liquid is the reaction initiation working solution. Then, the sample measurement is performed: the sample wells and control wells are set up in a 96-well plate, the sample and working solution are added, and finally, the reaction starter solution is added. The sample was incubated at 37°C for 30 minutes. Finally, the absorbance at 532 nm and 560 nm was measured with a microplate reader, and the GSH-Px, SOD, and MDA values were calculated.

2.4.8. Detection of TLR4, NF-κB p65, IL-1β, TNF-α, and IL-6 mRNA Expression in Myocardial Tissue. 50 mg of the infarct area of the heart tissue was selected, and the total RNA was extracted with the total RNA kit. After extraction, it was quantified and leveled, and then each group took 20 μg for reverse transcription. After the reverse transcription is completed, the amplification reaction can be carried out. The amplification conditions are as follows: 95°C predenaturation for 2 min; 95°C denaturation for 10 s, 56°C annealing for 30 s, 72°C extension for 35 s, repeated cycles of 38 times, and finally 72°C extension for 5 min. The results were calculated according to $(2 - \Delta\Delta Ct)$: ΔCt value = Ct value target gene − Ct value GAPDH; $\Delta\Delta Ct = \Delta Ct$ value of experimental group − ΔCt value of the sham group; ratio $= 2 - \Delta\Delta Ct$. The primer is shown in Table 1.

2.4.9. Detection of TLR4, NF-κB p65, IL-1β, TNF-α, and IL-6 Protein Expression in Myocardial Tissue. 500 mg of myocardial tissue was extracted with a tissue total protein extraction kit. After completion, it was quantified and leveled. After that, 60 μg of each group was heated and denatured. Then SDS-PAGE was performed. After the electrophoresis is completed, the required strips are cut and transferred to the PVDF membrane, and the PVDF membrane is sealed with skim milk for 2 hours. After washing three times, the PVDF membrane was placed in the primary antibody diluent (TLR4, NF-κB p65, beta-actin, and histone H3 were diluted at a ratio of 1 : 500, and IL-1β, IL-6, and TNF-α were all 1 : 200), shaken at room temperature for 1 h, and put in 4°C environment overnight. After the primary antibody was recovered, the PVDF membrane was washed 4 times with Tris-buffered saline with Tween (TBST) (1 time in 15 minutes and 3 times in 5 minutes). The PVDF membrane was then placed in the secondary antibody diluent on a horizontal shaker at room temperature for 2 h, and the membrane was washed 4 times. Finally, the PVDF film was completely immersed in the luminescent liquid for about 30 s (protected from light), and then the film was placed in a UVP gel imaging exposure instrument for development. ImageJ software is used to analyze the ratio of the gray value of the target protein band to the β-actin band, which reflects the protein expression level.

2.5. Statistical Analysis. Statistical analysis was performed using SPSS 20.0 software package, GraphPad prism software 7.0 was used for graphing, and the measured results were expressed by mean + SEM. The data of multiple groups were compared by one-way analysis of variance, and the pairwise comparison between groups was mostly by the SKN-q method, and $P < 0.05$ was considered statistically significant.

3. Results

3.1. Resveratrol-MIRI PPI Network Analysis

3.1.1. Resveratrol-MIRI PPI Network Construction. A total of 171 resveratrol targets and 93 MIRI genes were obtained. They were input into String to construct Resveratrol-MIRI PPI Network (Figure 1). In this network, the top 30 nodes in degree are as follows: ALB (127 edges), TNF (110 edges), MAPK1 (99 edges), EGFR (96 edges), SRC (95 edges), FN1 (93 edges), STAT3 (92 edges), MAPK8 (84 edges), IGF1 (84 edges), MMP9 (81 edges), ESR1 (77 edges), HSP90AA1 (76 edges), IL10 (72 edges), NOS3 (72 edges), MAPK14 (72 edges), TLR4 (71 edges), CAT (70 edges), ICAM1 (60 edges), IL2 (58 edges), RELA (57 edges), STAT1 (57 edges), KDR (57 edges), PPARG (55 edges), MMP2 (54 edges), MPO (53 edges), PIK3R1 (53 edges), JAK2 (50 edges), AR (50 edges), IFNG (48 edges), and NR3C1 (48 edges).

Table 1: The primer.

Gene	Direction	Sequence
TLR4	Forward primer	5′-GCCTTTCAGGGAATTAAGCTCC-3′
	Reverse primer	5′-GATCAACCGATGGACGTGTAAA-3′
NF-κB p65	Forward primer	5′-ATGGCAGACGATGATCCCTAC-3′
	Reverse primer	5′-CGGAATCGAAATCCCCTCTGTT-3′
IL-1β	Forward primer	5′-TTGGGCTGTCCAGATGAGAG-3′
	Reverse primer	5′-CACACTAGCAGGTCGTCATCAT-3′
TNF-α	Forward primer	5′-GTGCCTCAGCCTCTTCTCATT-3′
	Reverse primer	5′-CCAGTTGGTTGTCTTTGAGATCC-3′
IL-6	Forward primer	5′-GTATGAACAGCGATGATGCACT-3′
	Reverse primer	5′-AACTCCAGAAGACCAGAGCAG-3′
β-Actin	Forward primer	5′-GACTATGACTTGAATGCGGTCC-3′
	Reverse primer	5′-TCAGCACCCAAAGTCACCAAGT-3′

3.1.2. Enrichment Analysis of Resveratrol-MIRI PPI Network. The targets and genes in Resveratrol-MIRI PPI Network are imported into DAVID and String for enrichment analysis. A total of 89 MIRI-related biological processes, 25 MIRI-related cell components, 24 MIRI-related molecular functions, 31 MIRI-related signaling pathways, and 37 MIRI-related Reactome pathways were returned (Table S3 and Table S4 and Figure 2). The biological processes include steroid hormone-mediated signaling pathway, cellular response to lipopolysaccharide, negative regulation of the apoptotic process, positive regulation of ERK1 and ERK2 cascade, positive regulation of cell proliferation, aging, leukocyte migration, peptidyl-tyrosine phosphorylation, intracellular receptor signaling pathway, positive regulation of gene expression, positive regulation of nitric oxide (NO) biosynthetic process, positive regulation of PI3K signaling, response to hypoxia, activation of mitogen-activated protein kinase (MAPK) activity, positive regulation of vasodilation, and so on. The cell components include cytosol, extracellular space, extracellular region, extracellular exosome,

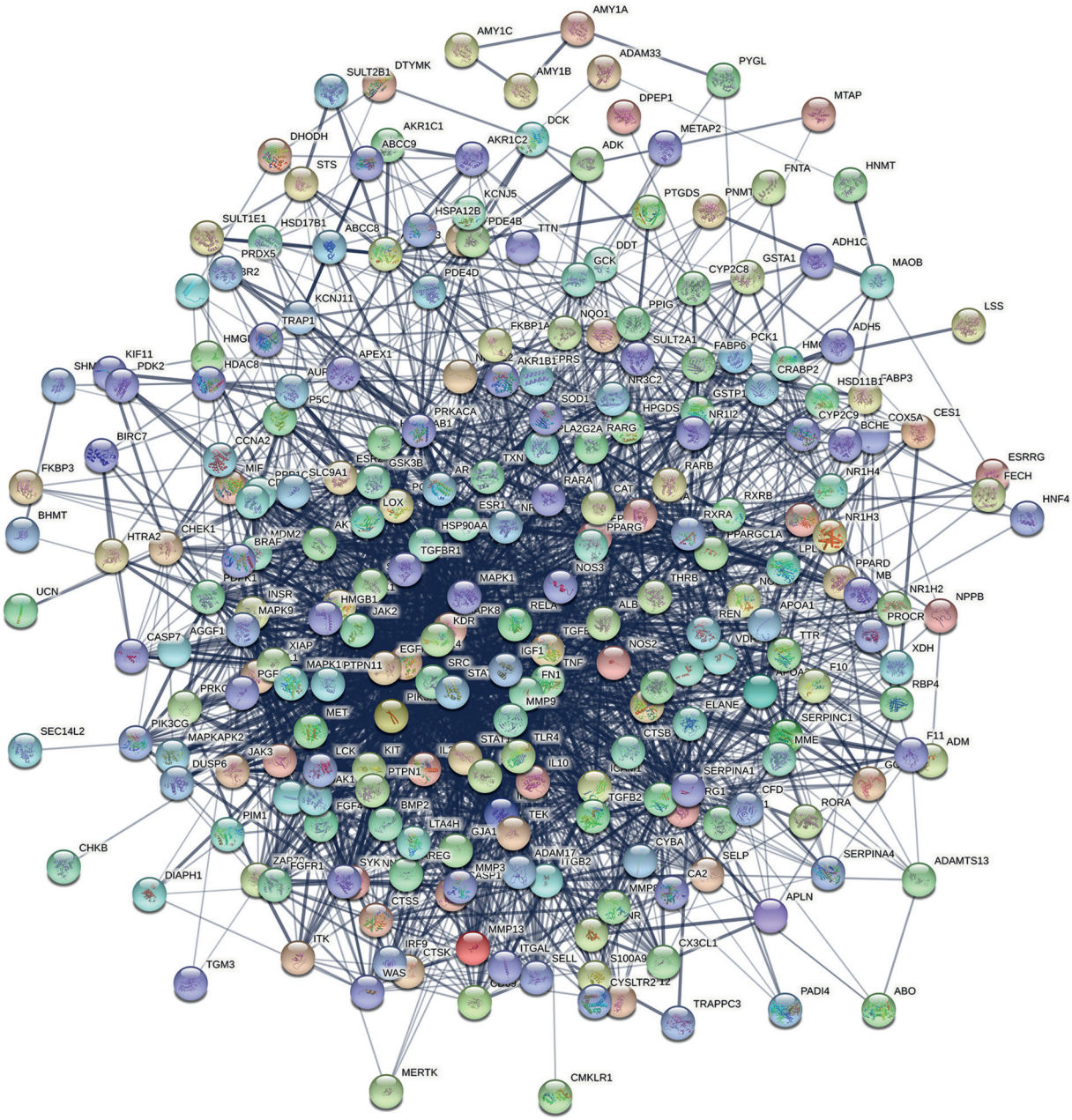

Figure 1: Resveratrol-MIRI PPI Network.

nucleoplasm, cell surface, extrinsic component of cytoplasmic side of plasma membrane, membrane raft, mitochondrion, cytoplasm, platelet alpha granule lumen, nuclear chromatin, plasma membrane, focal adhesion, and so on. The molecular functions include steroid hormone receptor activity, protein tyrosine kinase activity, protein binding, receptor binding, drug binding, enzyme binding, ATP binding, zinc ion binding, protein kinase activity, steroid binding, and so on. The signaling pathways include insulin resistance, FoxO signaling pathway, adipocytokine signaling pathway, insulin signaling pathway, PI3K-Akt signaling pathway, ErbB signaling pathway, T-cell receptor signaling pathway, PPAR signaling pathway, Ras signaling pathway, estrogen signaling pathway, TNF signaling pathway, and so on. The Reactome pathways include signal transduction, nuclear receptor transcription pathway, immune system, signaling by interleukins, metabolism, hemostasis, innate immune system, cytokine signaling in the immune system, signaling by receptor tyrosine kinases, diseases of signal transduction, SUMOylation of intracellular receptors, generic transcription pathway, metabolism of lipids, and so on. The fold enrichment, count, and false discovery rate (FDR) of the biological processes, cell components, molecular functions, and signaling pathways are shown in Figure 2. The strength, FDR, and count of the Reactome pathway are shown in Figure 3. The targets and genes in Toll-like receptor signaling pathway are shown in Figure 4 as an example.

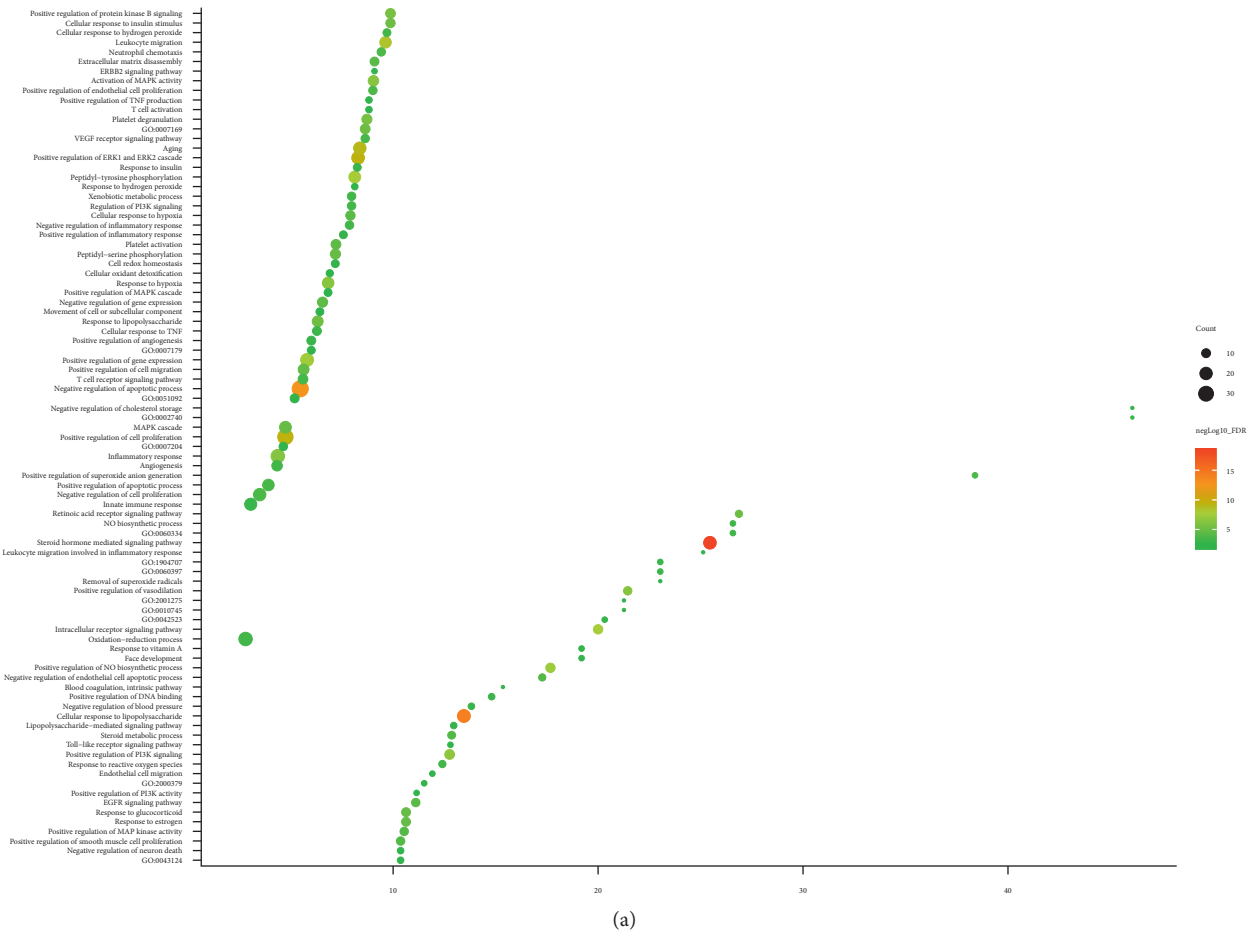

(a)

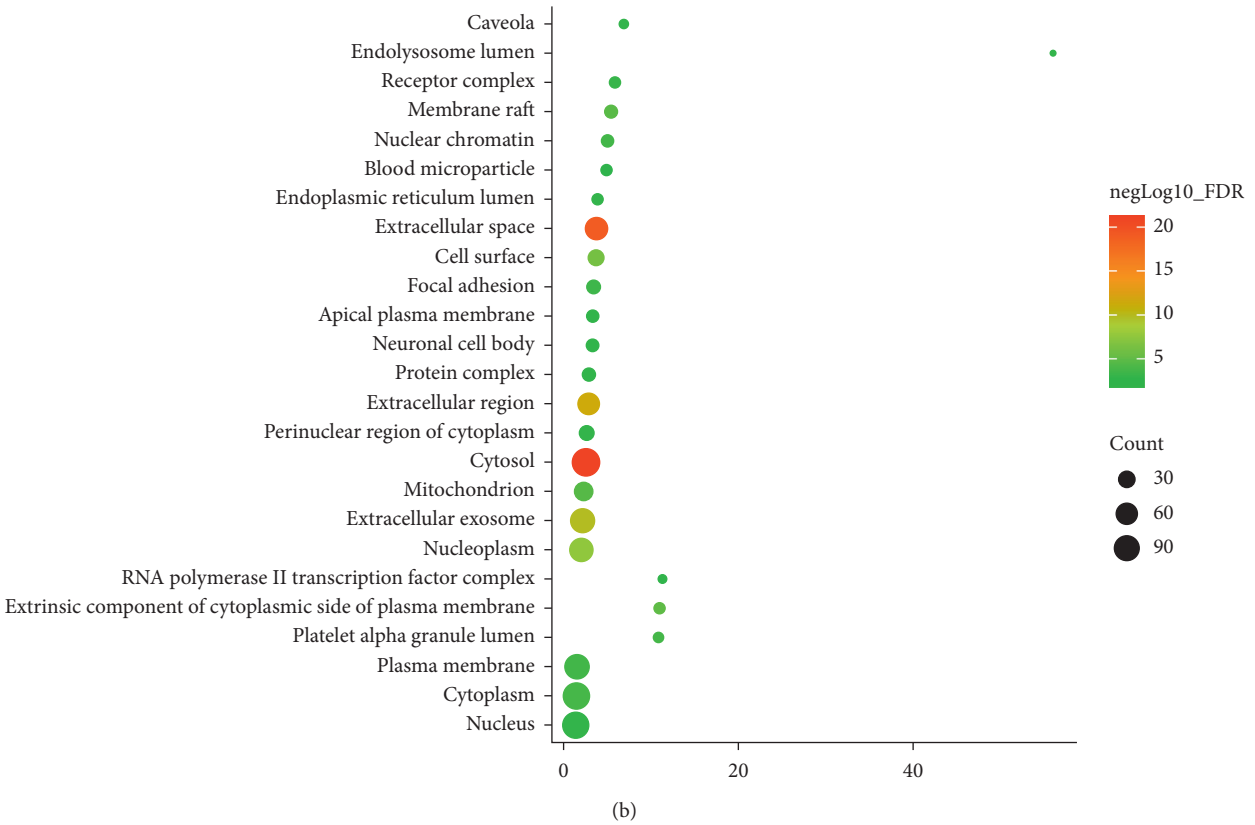

(b)

Figure 2: Continued.

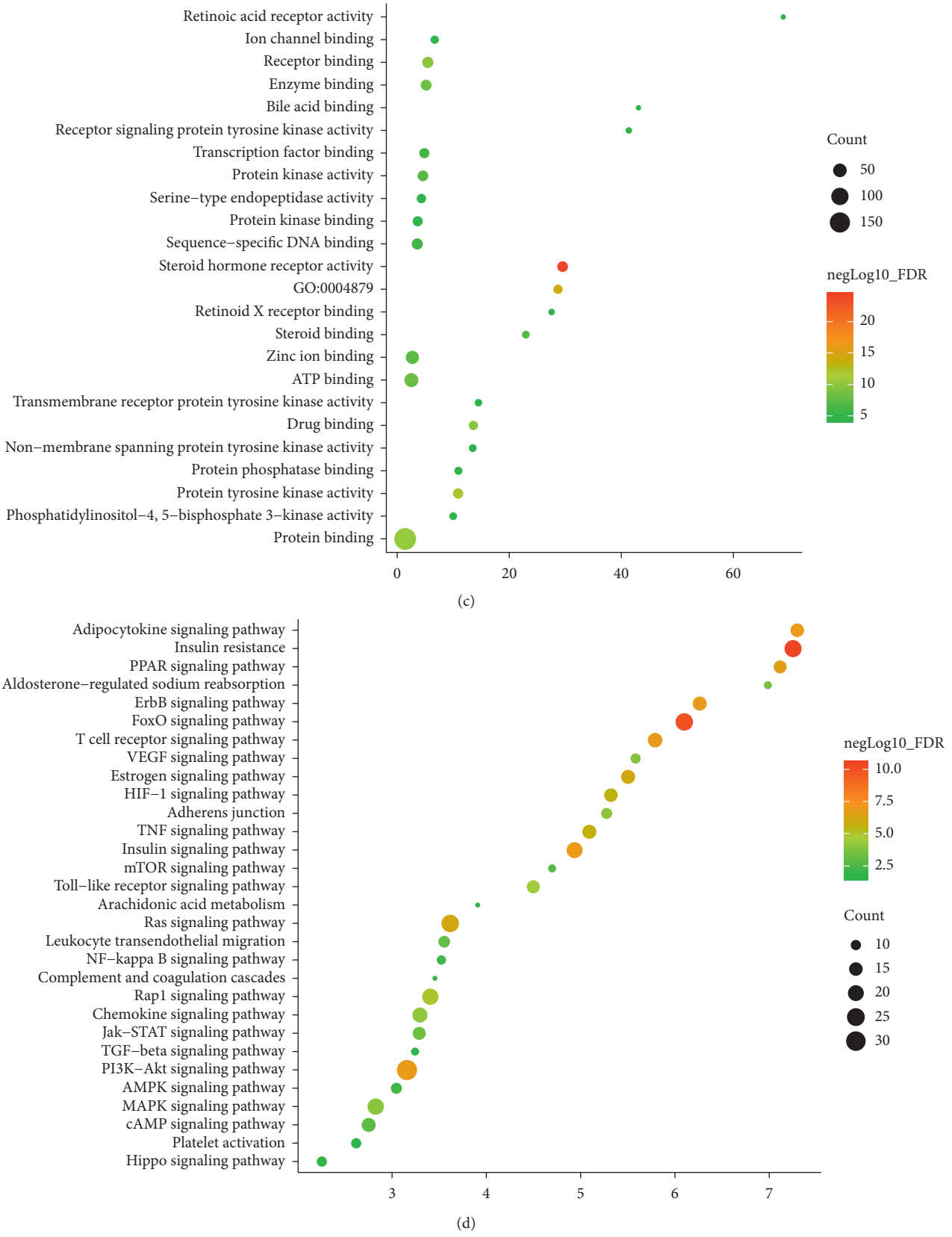

Figure 2: Bubble chart of enrichment analysis. (a) Biological processes; (b) cell components; (c) molecular function; (d) signaling pathways; *X*-axis is fold enrichment.

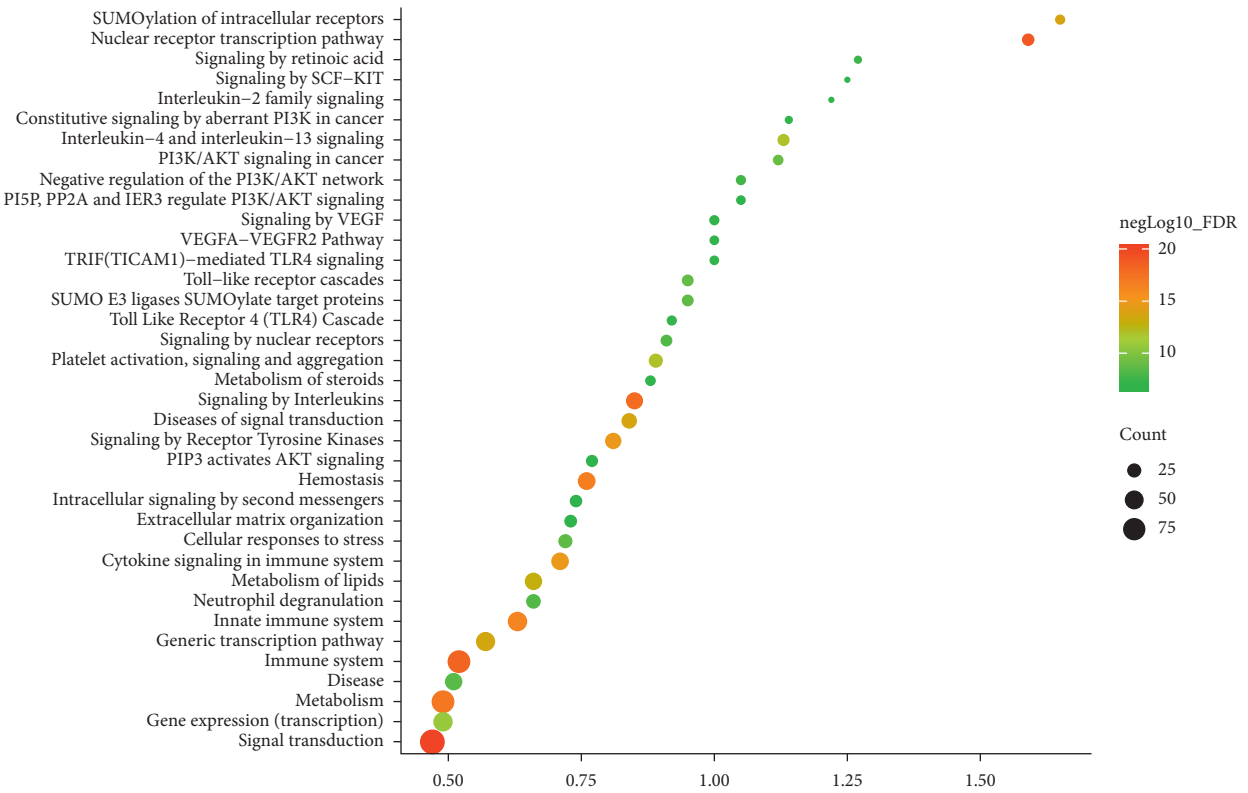

Figure 3: Bubble chart of Reactome pathway (*X*-axis is strength).

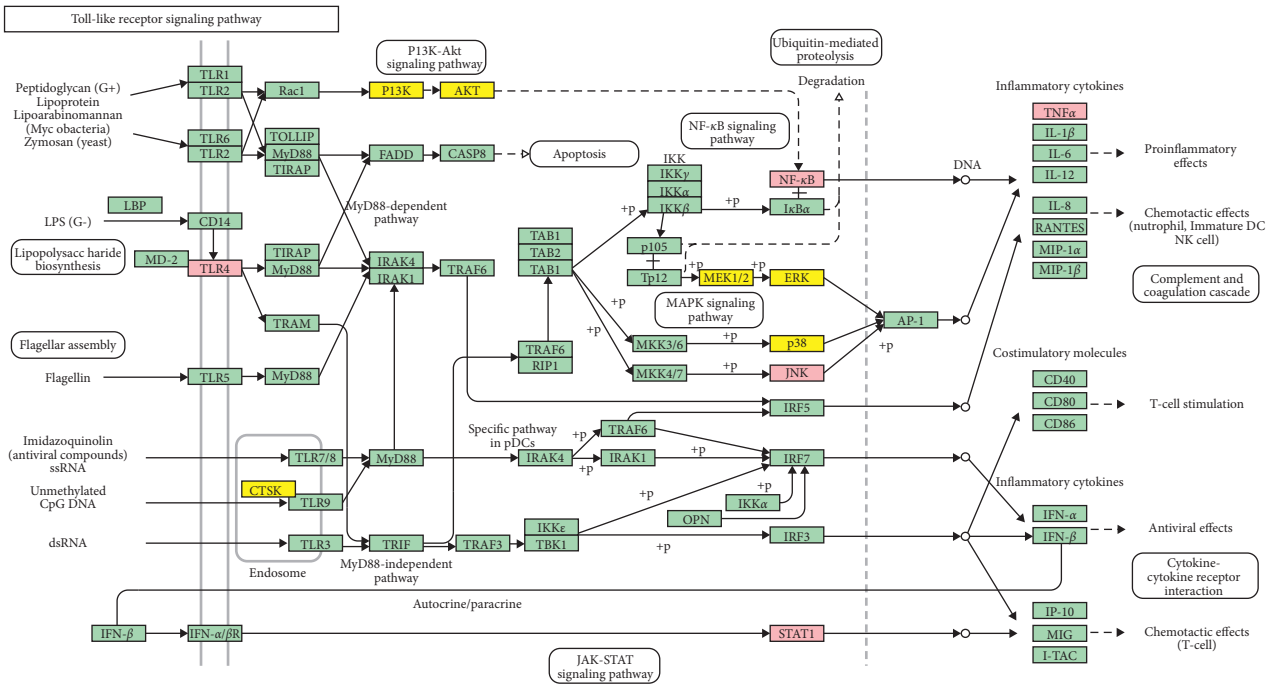

Figure 4: Toll-like receptor signaling pathway adapted from KEGG (ID: hsa04620) (MIRI gene is marked in pink, and the resveratrol target is marked in yellow).

3.2. Effects of Resveratrol on Heart Function. Before operation and 24 hours after operation, echocardiography showed that the heart function of rats in each group did not change significantly before operation, and there was no statistical difference. Echocardiogram at 24 hours after operation showed that LVFS and LVEF were lower in the sham group than in the MIRI group. LVFS and LVEF increased significantly after treatment with resveratrol ($P < 0.05$). The above results indicate that resveratrol improves heart dysfunction caused by MIRI (Figure 5).

3.3. Histopathological Changes. In the sham operation group, the morphology of the cells was tightly arranged in a fibrous shape without inflammatory factors. In the MIRI group, there was an obvious disorder of cell morphology, the horizontal stripes disappeared, and there was some inflammatory cell infiltration. Compared with the MIRI group, the other groups have a certain degree of relief; especially, the resveratrol high-dose group has the most obvious improvement, but there is still a certain difference compared with the sham operation group (Figure 6).

3.4. Effects of Resveratrol on Myocardial Injury Markers. The CK-MB and LDH values in the sham group were lower, and the CK-MB and LDH values in the MIRI group were significantly increased. Compared with the model group, resveratrol was significantly reversed after pretreatment, and the resveratrol high-dose group was significantly lower than the low-dose group (Figure 7).

3.5. Effects of Resveratrol on Myocardial Tissue MDA, GSH-Px, and SOD. The level of MDA in the myocardial tissue of rats in the MIRI group increased significantly ($P < 0.05$), and the activities of GSH-Px and SOD decreased significantly ($P < 0.05$). The MDA level of the resveratrol group was significantly lower than that of the MIRI group ($P < 0.05$), and the activities of GSH-Px and SOD were significantly increased ($P < 0.05$) (Figure 8).

3.6. Effects of Resveratrol on Serum IL-1β, TNF-α, and IL-6. Compared with the sham group, the levels of IL-1β, TNF-α, and IL-6 in the MIRI group increased significantly ($P < 0.05$). Compared with the MIRI group, the levels of IL-1β, TNF-α, and IL-6 in the high and low doses of resveratrol decreased significantly ($P < 0.05$). Among them, compared with the low-dose group, the high-dose group was also significantly reduced ($P < 0.05$), indicating that resveratrol has the anti-inflammatory ability (Figure 9).

3.7. Effects of Resveratrol on the Expression of Myocardial Tissue TLR4, NF-κB p65, IL-1β, TNF-α, and IL-6 mRNA and Protein

3.7.1. Effects of Resveratrol on Myocardial Tissue TLR4 and NF-κB p65 mRNA. Compared with the sham operation group, the expression of TLR4 and NF-κB P65 mRNA in the MIRI group increased ($P < 0.05$). Compared with the MIRI group, the expression of TLR4 and NF-κB P65 mRNA in the resveratrol low-dose and high-dose groups was significantly reduced ($P < 0.05$). In addition, the TLR4 and NF-κB P65 mRNA in the resveratrol high-dose group were lower than those in the resveratrol low-dose group ($P < 0.05$) (Figure 10).

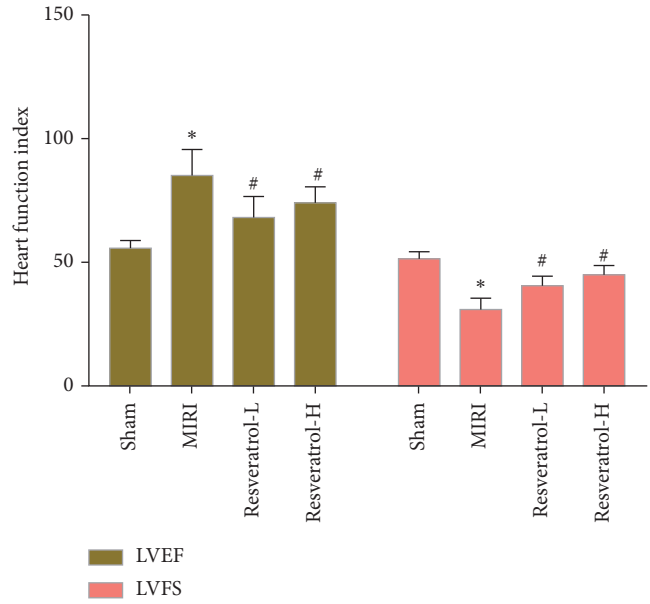

Figure 5: Effects of resveratrol on heart function (*compared with the sham operation group, $P < 0.05$; #compared with the MIRI group, $P < 0.05$).

3.7.2. Effects of Resveratrol on Myocardial Tissue IL-1β, TNF-α, and IL-6 mRNA. Compared with the sham group, the expression levels of IL-1β, TNF-α, and IL-6 mRNA in the MIRI group increased ($P < 0.05$). Compared with the MIRI group, the levels of IL-1β, TNF-α, and IL-6 mRNA in the resveratrol group were decreased ($P < 0.05$) (Figure 10).

3.7.3. Effects of Resveratrol on Myocardial Tissue TLR4 and NF-κB p65 Protein. Compared with the sham operation group, the expression of TLR4 and NF-κB P65 protein in the MIRI group increased ($P < 0.05$). Compared with the MIRI group, the expression of TLR4 and NF-κB P65 protein in the resveratrol low-dose and high-dose groups was significantly reduced ($P < 0.05$) (Figure 11).

3.7.4. Effects of Resveratrol on Myocardial Tissue IL-1β, TNF-α, and IL-6 Protein. Compared with the sham group, the expression levels of IL-1β, TNF-α, and IL-6 protein in the MIRI group increased ($P < 0.05$). Compared with the MIRI group, the levels of IL-1β, TNF-α, and IL-6 protein in the resveratrol group were decreased ($P < 0.05$) (Figure 11).

4. Discussion

With the rapid development of medical technology, the continuous popularization and promotion of PCI, coronary

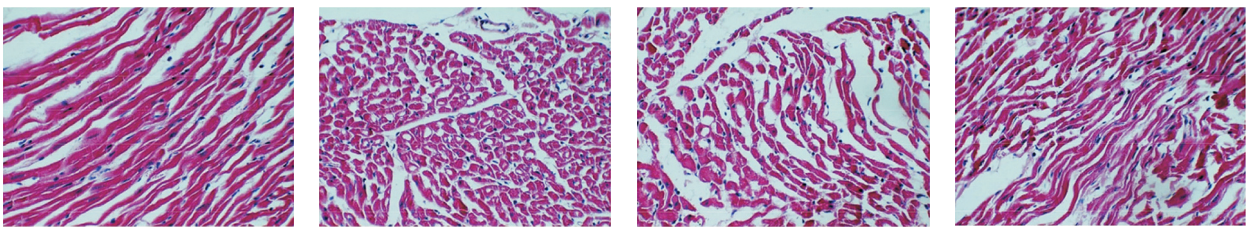

Figure 6: Histopathological changes (HE staining 100X). (a) Sham. (b) MIRI. (c) Res-L. (d) Res-H.

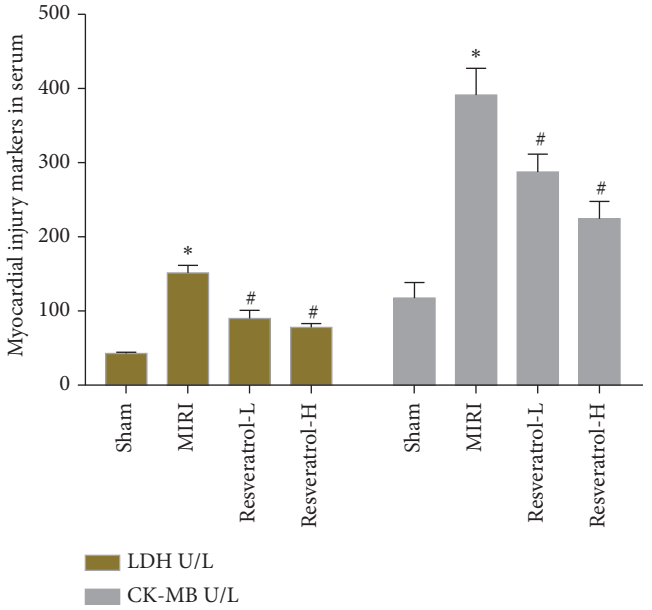

Figure 7: Effects of resveratrol on myocardial injury markers (*compared with the sham operation group, $P < 0.05$; #compared with the MIRI group, $P < 0.05$).

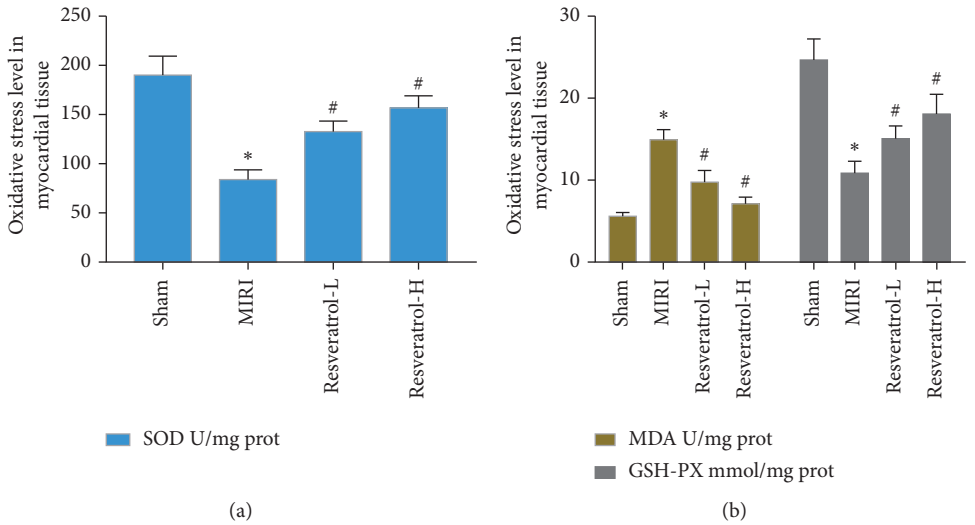

Figure 8: Effects of resveratrol on myocardial tissue MDA, GSH-Px, and SOD (*compared with the sham operation group, $P < 0.05$; #compared with the MIRI group, $P < 0.05$).

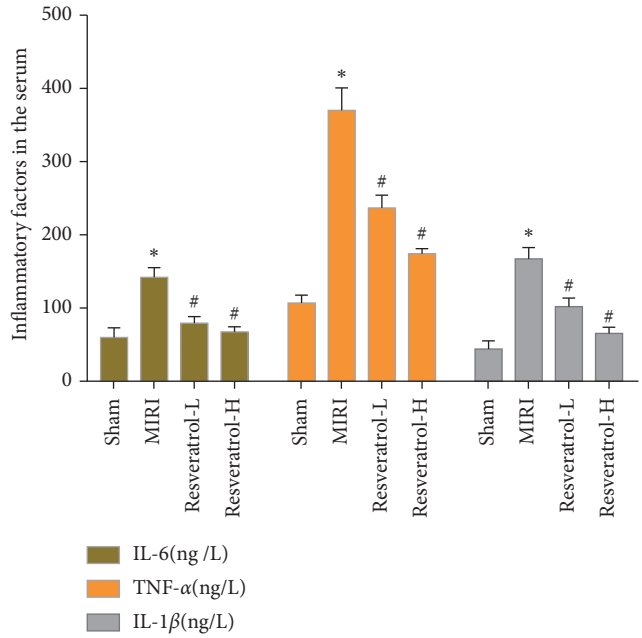

Figure 9: Effects of resveratrol on serum IL-1β, TNF-α, and IL-6 (*compared with the sham operation group, $P < 0.05$; #compared with the MIRI group, $P < 0.05$).

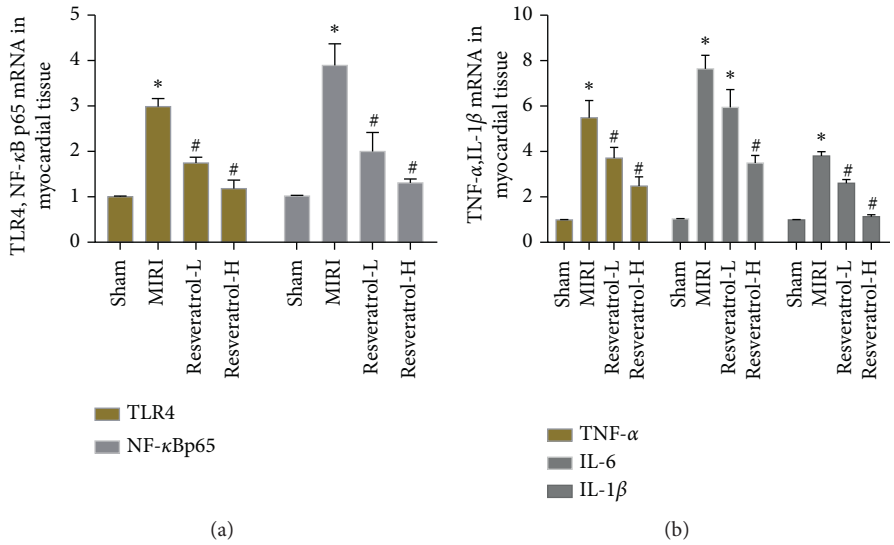

Figure 10: Effects of resveratrol on the expression of myocardial tissue TLR4, NF-κB p65, IL-1β, TNF-α, and IL-6 mRNA (*compared with the sham operation group, $P < 0.05$; #compared with the MIRI group, $P < 0.05$).

artery bypass grafting (CABG), and coronary thrombolysis technologies and drugs have brought great help to patients with ischemic cardiomyopathy [28]. But in clinical, MIRI is an unavoidable problem, which is also a problem that needs to be solved urgently in clinical practice. Reperfusion injury is the key to determining myocardial viability after ischemic myocardial blood flow reconstruction. Existing studies have found that ischemia-reperfusion can exacerbate the irreversible cell necrosis of damaged cardiomyocytes [29, 30]. Studies of cellular molecular mechanisms have shown that there is a causal relationship between MIRI and intracellular calcium overload, inflammation, and oxidative stress [13, 31, 32]. Mitochondrial dysfunction is considered to be the main source of reactive oxygen species in the pathogenesis of reperfusion injury, and it also promotes inflammation and endothelial damage [33]. At the same time, the opening of mPTP and subsequent release of cytochrome c from damaged mitochondria triggers the intrinsic apoptotic process by activating the caspase-9/3 signaling pathway, leading to cardiomyocyte apoptosis. Apoptosis combined with other programmed cell deaths together leads to the expansion of the infarct size after MIRI injury [34]. In

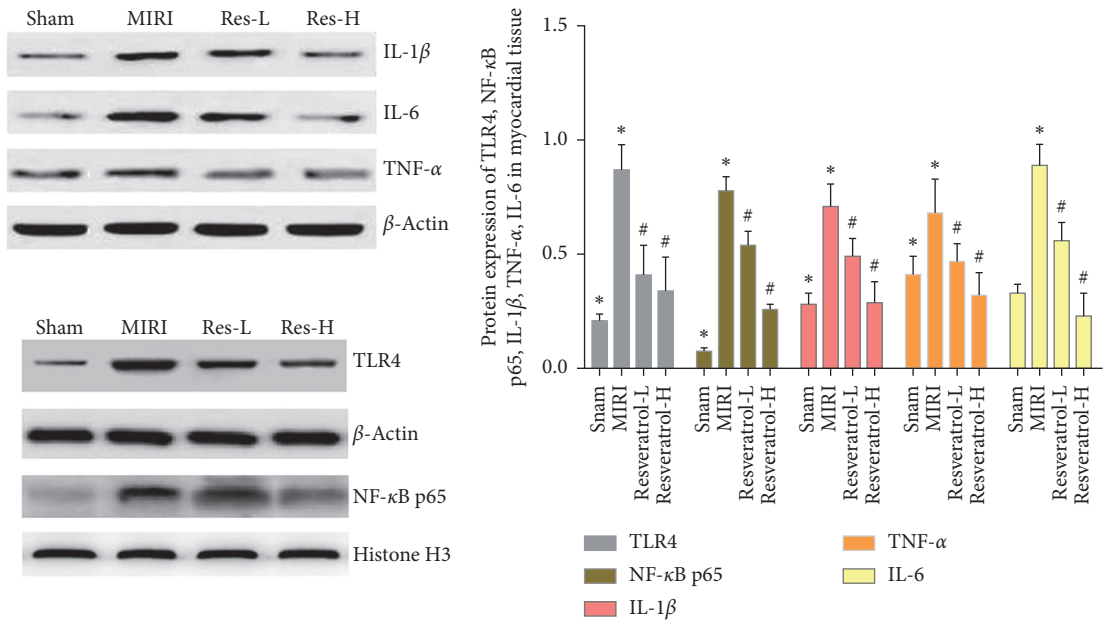

Figure 11: Effects of resveratrol on the expression of myocardial tissue TLR4, NF-κB p65, IL-1β, TNF-α, and IL-6 protein (*compared with the sham operation group, $P < 0.05$; #compared with the MIRI group, $P < 0.05$).

addition to the apoptotic pathway, autophagy, a process of programmed cell death caused by energy metabolism after ischemia, plays an important role in the occurrence of reperfusion injury. The activation or inhibition of autophagy may have beneficial or harmful effects in the case of MIRI [35]. In addition, platelet aggregation caused by MIRI leads to microvascular obstruction, which is characterized by microcirculation spasm, intraluminal thrombosis, and obvious endothelial cell swelling and dysfunction, which ultimately leads to slow blood flow [36]. After reperfusion injury, inflammation and oxidative stress mainly lead to a large loss of cardiomyocytes, which leads to the expansion of the infarct area. Among them, neutrophils are also closely related to the inflammatory response, and the large accumulation of neutrophils in the reperfusion area will cause a negative impact on the survival of cardiomyocytes [37]. In addition, damage to mitochondria and immune cell infiltration can lead to a large amount of ROS generation, which leads to excessive oxidative stress [38].

In this study, we found that resveratrol can regulate steroid hormone-mediated signaling pathway, cellular response to lipopolysaccharide, negative regulation of the apoptotic process, positive regulation of ERK1 and ERK2 cascade, positive regulation of cell proliferation, aging, leukocyte migration, peptidyl-tyrosine phosphorylation, intracellular receptor signaling pathway, insulin resistance, FoxO signaling pathway, adipocytokine signaling pathway, insulin signaling pathway, PI3K-Akt signaling pathway, ErbB signaling pathway, T-cell receptor signaling pathway, PPAR signaling pathway, Ras signaling pathway, estrogen signaling pathway, TNF signaling pathway, and so on. Previous studies also provided many evidences that resveratrol protects MIRI. For example, in terms of inflammation, it shows that resveratrol protects the myocardium by inactivating NALP3 inflammasomes and inhibiting the inflammatory cascade mediated by IL-1β and IL-18 [39]. Evidence from previous studies shows that resveratrol is an antioxidant that can regulate the multistep process of redox stress [40]. In vivo and in vitro MIRI models, resveratrol pretreatment reduces ROS levels, inhibits the formation of MDA, and is negatively correlated with the increase in antioxidant enzyme expression [41, 42]. Meanwhile, inflammation and/or oxidative stress trigger the apoptotic cascade through internal or external apoptotic signaling pathways, leading to cardiomyocyte apoptosis and poor ventricular remodeling and further worsening the contractile function after MIRI [43]. Existing studies have also shown that resveratrol significantly reduces apoptosis in MIRI heart models by eliminating ROS production and inhibiting inflammation [44]. Resveratrol can also prevent the opening of mPTP, the release of cytochrome c from the mitochondria, and subsequent activation of caspase-3 during I/R injury, thereby preventing cell death caused by mitochondrial dysfunction [20]. In terms of angiogenesis caused by myocardial ischemia-reperfusion, resveratrol reduces MIRI by upregulating vascular endothelial growth factor B [42]. In terms of endothelial dysfunction caused by MIRI, resveratrol inhibits I/R-induced iNOS and upregulates the expression of eNOS and nNOS to improve myocardial ischemia-reperfusion injury [45]. When NOS inhibitors (NG-nitro-L-arginine methyl ester, L-NAME) or cGMP inhibitors (MB) are used, the cardioprotective effects of resveratrol are counteracted. This indicates that resveratrol is essential in promoting angiogenesis and inhibiting vascular endothelial dysfunction [46]. In terms of oxidative stress, resveratrol can reduce myocardial oxidative stress by stimulating Sirtuin1 (SIRT1) or inhibiting GSK3β in diabetic cardiac ischemia-reperfusion injury models and increasing

nuclear factor E2-related factor 2 (Nrf2) expression [47]. In terms of apoptosis, resveratrol protects myocardial cell apoptosis from ischemia-reperfusion injury by regulating the phosphorylation level of proteins relative to the PI3K/Akt/e-NOS pathway [48]. In terms of autophagy, resveratrol can reduce the ischemia/reperfusion injury of diabetic myocardium by inducing autophagy [49]. In terms of calcium signal pathway, resveratrol inhibits STIM1-induced intracellular Ca^{2+} accumulation, exerts antiapoptotic activity, and improves cardiac function recovery after MIRI [50].

The mechanism of ischemia-reperfusion injury and therapeutic drugs has positive significance for the treatment of patients with heart disease for noncardiac surgery. Current studies have shown that the main signaling pathways of MIRI are Ca^{2+} signaling pathway, mTOR signaling pathway, JAK-STAT signaling pathway, MAPK signaling pathway, NRF2 signaling pathway, JAK-STAT signaling pathway, SIRT signaling pathway, nitric oxide signaling pathway, TLR4/NF-kB signaling pathway, etc. [51–55]. Current studies have shown that the rapid increase of TLR4 and NF-kB can occur during transient cardiac ischemia. In addition, the two did not decrease after reperfusion, but increased further [56]. It was found in animal models of acute MIRI that the TLR4/NF-kB signaling pathway is closely related to cardiomyocyte apoptosis. Reactivation of the TLR4/NF-kB signaling pathway can directly induce the occurrence of cardiomyocyte apoptosis, and inhibiting the expression of TLR4 and NF-xB can inhibit apoptosis [57]. Further studies have shown that the activation of TLR4 and NF-kB in cardiomyocytes can lead to a significant increase in downstream inflammatory factors TNF-α and IL-6, which in turn directly cause damage to myocardium and vascular endothelial cells. Similarly, resveratrol inhibits the inflammatory response after MIRI by inhibiting the expression of TLR4 and NF-kB, thereby reducing myocardial ischemia-reperfusion injury [58]. Our research also observes the changing characteristics of the above indicators. Compared with the sham operation group, the myocardial ischemia-reperfusion injury group showed significant increases in TLR4, NF-KB, IL-1β, TNF-α, and IL-6. Resveratrol can effectively reduce the expression of the above five indicators. In addition, resveratrol can also regulate oxidative stress markers (such as MDA, GSH, and SOD) in myocardial tissue. Therefore, resveratrol may inhibit the expression of TLR4 and NF-kB in the myocardium, thereby inhibiting the production of inflammatory factors IL-1β, TNF-α, and IL-6 in the myocardium, and ultimately protect myocardial cells.

5. Conclusion

Resveratrol can effectively improve MIRI, and its mechanism of action may be related to reducing the expression of TLR4/NF-kB in the myocardium, thereby improving inflammation. However, this study also has certain limitations, that is, MIRI is the result of multiple effects, involving multiple signal pathways. In the future, we will conduct further in-depth research on other signal pathways.

Data Availability

The data that support the findings of this study are openly available in supplementary materials.

Disclosure

Zuzhong Xing, Qi He, and Yinliang Xiong are considered as joint first authors.

Conflicts of Interest

The authors declare no conflicts of interest.

Authors' Contributions

Zuzhong Xing, Qi He, and Yinliang Xiong were responsible for the study concept and design. Zuzhong Xing, Qi He, Yinliang Xiong, and Xiaomei Zeng were responsible for the data collection, data analysis, and interpretation. Zuzhong Xing and Yinliang Xiong drafted the paper; Qi He supervised the study; all authors participated in the analysis and interpretation of data and approved the final paper.

Acknowledgments

This research was supported by the Special Clinical Research Project of the Health Industry of the Health Commission of Ningxiang City (no. 201840230), Scientific Research Project of Hunan Provincial Health and Family Planning Commission (no. 20191030201), and Longitudinal Project of Hunan Provincial Health Commission (no. 20201100).

Supplementary Materials

Table S1: predicted potential targets of resveratrol. Table S2: MIRI genes. Table S3: enrichment analysis of Resveratrol-MIRI PPI Network. Table S4: Reactome pathway of Resveratrol-MIRI PPI. (*Supplementary Materials*)

References

[1] J. E. Tamis-Holland, H. Jneid, H. R. Reynolds et al., "Contemporary diagnosis and management of patients with myocardial infarction in the absence of obstructive coronary artery disease: a scientific statement from the American heart association," *Circulation*, vol. 139, no. 18, pp. e891–e908, 2019.

[2] G. Heusch, "Coronary microvascular obstruction: the new frontier in cardioprotection," *Basic Research in Cardiology*, vol. 114, no. 6, p. 45, 2019.

[3] J. E. Dalen, J. S. Alpert, R. J. Goldberg, and R. S. Weinstein, "The epidemic of the 20th century: coronary heart disease," *The American Journal of Medicine*, vol. 127, no. 9, pp. 807–812, 2014.

[4] GBD 2019 Viewpoint Collaborators, "Five insights from the global burden of disease study 2019," *Lancet*, vol. 396, no. 10258, pp. 1135–1159, 2020.

[5] R. K. Al-Lamee, A. N. Nowbar, and D. P. Francis, "Percutaneous coronary intervention for stable coronary artery disease," *Heart*, vol. 105, no. 1, pp. 11–19, 2019.

[6] C. P. McCarthy, M. Vaduganathan, K. J. McCarthy, J. L. Januzzi Jr., D. L. Bhatt, and J. W. McEvoy, "Left

ventricular thrombus after acute myocardial infarction," *JAMA Cardiology*, vol. 3, no. 7, pp. 642–649, 2018.

[7] D. J. Hausenloy and D. M. Yellon, "Myocardial ischemia-reperfusion injury: a neglected therapeutic target," *Journal of Clinical Investigation*, vol. 123, no. 1, pp. 92–100, 2013.

[8] S. Toldo, A. G. Mauro, Z. Cutter, and A. Abbate, "Inflammasome, pyroptosis, and cytokines in myocardial ischemia-reperfusion injury," *American Journal of Physiology-Heart and Circulatory Physiology*, vol. 315, no. 6, pp. H1553–H1568, 2018.

[9] A. Frank, M. Bonney, S. Bonney, L. Weitzel, M. Koeppen, and T. Eckle, "Myocardial ischemia reperfusion injury," *Seminars in Cardiothoracic and Vascular Anesthesia*, vol. 16, no. 3, pp. 123–132, 2012.

[10] B. Shin, D. B. Cowan, S. M. Emani, P. J. Del Nido, and J. D. McCully, "Mitochondrial transplantation in myocardial ischemia and reperfusion injury," *Advances in Experimental Medicine and Biology*, vol. 982, pp. 595–619, 2017.

[11] M. Neri, I. Riezzo, N. Pascale, C. Pomara, and E. Turillazzi, "Ischemia/reperfusion injury following acute myocardial infarction: a critical issue for clinicians and forensic pathologists," *Mediators of Inflammation*, vol. 2017, Article ID 7018393, 14 pages, 2017.

[12] B. Ibáñez, G. Heusch, M. Ovize, and F. Van de Werf, "Evolving therapies for myocardial ischemia/reperfusion injury," *Journal of the American College of Cardiology*, vol. 65, no. 14, pp. 1454–1471, 2015.

[13] H. K. Eltzschig and T. Eckle, "Ischemia and reperfusion-from mechanism to translation," *Nature Medicine*, vol. 17, no. 11, pp. 1391–1401, 2011.

[14] A. Mokhtari-Zaer, N. Marefati, S. L. Atkin, A. E. Butler, and A. Sahebkar, "The protective role of curcumin in myocardial ischemia-reperfusion injury," *Journal of Cellular Physiology*, vol. 234, no. 1, pp. 214–222, 2018.

[15] J. Breuss, A. Atanasov, and P. Uhrin, "Resveratrol and its effects on the vascular system," *International Journal of Molecular Sciences*, vol. 20, no. 7, p. 1523, 2019.

[16] N. Xia, A. Daiber, U. Förstermann, and H. Li, "Antioxidant effects of resveratrol in the cardiovascular system," *British Journal of Pharmacology*, vol. 174, no. 12, pp. 1633–1646, 2017.

[17] L. Malaguarnera, "Influence of resveratrol on the immune response," *Nutrients*, vol. 11, no. 5, p. 946, 2019.

[18] A. Rauf, M. Imran, M. S. Butt, M. Nadeem, D. G. Peters, and M. S. Mubarak, "Resveratrol as an anti-cancer agent: a review," *Critical Reviews in Food Science and Nutrition*, vol. 58, no. 9, pp. 1428–1447, 2018.

[19] M. Springer and S. Moco, "Resveratrol and its human metabolites-effects on metabolic health and obesity," *Nutrients*, vol. 11, no. 1, p. 143, 2019.

[20] Z. Liao, D. Liu, L. Tang et al., "Long-term oral resveratrol intake provides nutritional preconditioning against myocardial ischemia/reperfusion injury: involvement of VDAC1 downregulation," *Molecular Nutrition & Food Research*, vol. 59, no. 3, pp. 454–464, 2015.

[21] T. Adam, S. Sharp, L. H. Opie, and S. Lecour, "Loss of cardioprotection with ischemic preconditioning in aging hearts: role of Sirtuin 1?" *Journal of Cardiovascular Pharmacology and Therapeutics*, vol. 18, no. 1, pp. 46–53, 2013.

[22] K. Yang, L. Zeng, A. Ge et al., "Integrating systematic biological and proteomics strategies to explore the pharmacological mechanism of danshen yin modified on atherosclerosis," *Journal of Cellular and Molecular Medicine*, vol. 24, no. 23, pp. 13876–13898, 2020.

[23] X. F. Liu, S. S. Ouyang, Y. Biao et al., "PharmMapper server: a web server for potential drug target identification using pharmacophore mapping approach," *Nucleic Acids Research*, vol. 38, pp. W609–W614, 2010.

[24] G. Stelzer, R. Rosen, I. Plaschkes et al., "The GeneCards suite: from gene data mining to disease genome sequence analysis," *Current Protocols in Bioinformatics*, vol. 54, pp. 1301–1303, 2016.

[25] A. Hamosh, A. F. Scott, J. S. Amberger et al., "Online Mendelian Inheritance in Man (OMIM), a knowledgebase of human genes and genetic disorders," *Nucleic Acids Research*, vol. 33, pp. D514–D517, 2005.

[26] D. Szklarczyk, A. Franceschini, S. Wyder et al., "STRING v10: protein-protein interaction networks, integrated over the tree of life," *Nucleic Acids Research*, vol. 43, no. D1, pp. D447–D452, 2015.

[27] D. W. Huang, B. T. Sherman, and R. A. Lempicki, "Systematic and integrative analysis of large gene lists using DAVID Bioinformatics Resources," *Nature Protocols*, vol. 4, no. 1, pp. 44–57, 2009.

[28] A. Katbeh, G. Van Camp, E. Barbato et al., "Cardiac resynchronization therapy optimization: a comprehensive approach," *Cardiology*, vol. 142, no. 2, pp. 116–128, 2019.

[29] M.-Y. Wu, G.-T. Yiang, W.-T. Liao et al., "Current mechanistic concepts in ischemia and reperfusion injury," *Cellular Physiology and Biochemistry*, vol. 46, no. 4, pp. 1650–1667, 2018.

[30] S. K. Powers, Z. Murlasits, M. Wu, and A. N. Kavazis, "Ischemia-reperfusion-induced cardiac injury," *Medicine & Science in Sports & Exercise*, vol. 39, no. 9, pp. 1529–1539, 2007.

[31] A. T. Turer and J. A. Hill, "Pathogenesis of myocardial ischemia-reperfusion injury and rationale for therapy," *The American Journal of Cardiology*, vol. 106, no. 3, pp. 360–368, 2010.

[32] N. R. Madamanchi and M. S. Runge, "Redox signaling in cardiovascular health and disease," *Free Radical Biology and Medicine*, vol. 61, pp. 473–501, 2013.

[33] G. Pagano, A. Aiello Talamanca, G. Castello et al., "Oxidative stress and mitochondrial dysfunction across broad-ranging pathologies: toward mitochondria-targeted clinical strategies," *Oxidative Medicine and Cellular Longevity*, vol. 2014, Article ID 541230, 27 pages, 2014.

[34] P. Jia, C. Liu, N. Wu, D. Jia, and Y. Sun, "Agomelatine protects against myocardial ischemia reperfusion injury by inhibiting mitochondrial permeability transition pore opening," *American Journal of Translational Research*, vol. 10, no. 5, pp. 1310–1323, 2018.

[35] T. Li, Y.-R. Jiao, L.-H. Wang, Y.-H. Zhou, and H.-C. Yao, "Autophagy in myocardial ischemia reperfusion injury: friend or foe?" *International Journal of Cardiology*, vol. 239, p. 10, 2017.

[36] N. Takaya, Y. Katoh, K. Iwabuchi et al., "Platelets activated by collagen through the immunoreceptor tyrosine-based activation motif in the Fc receptor γ-chain play a pivotal role in the development of myocardial ischemia-reperfusion injury," *Journal of Molecular and Cellular Cardiology*, vol. 39, no. 6, pp. 856–864, 2005.

[37] M. Dobaczewski, C. Gonzalez-Quesada, and N. G. Frangogiannis, "The extracellular matrix as a modulator of the inflammatory and reparative response following myocardial infarction," *Journal of Molecular and Cellular Cardiology*, vol. 48, no. 3, pp. 504–511, 2010.

[38] A. Singh, R. Kukreti, L. Saso, and S. Kukreti, "Oxidative stress: a key modulator in neurodegenerative diseases," *Molecules*, vol. 24, no. 8, p. 1583, 2019.

[39] W. Dong, R. Yang, J. Yang et al., "Resveratrol pretreatment protects rat hearts from ischemia/reperfusion injury partly via a NALP3 inflammasome pathway," *International Journal of Clinical and Experimental Pathology*, vol. 8, no. 8, pp. 8731–8741, 2015.

[40] P. Silva, A. Sureda, J. A. Tur, P. Andreoletti, M. Cherkaoui-Malki, and N. Latruffe, "How efficient is resveratrol as an antioxidant of the Mediterranean diet, towards alterations during the aging process?" *Free Radical Research*, vol. 53, no. 1, pp. 1101–1112, 2019.

[41] L. Cheng, Z. Jin, R. Zhao, K. Ren, C. Deng, and S. Yu, "Resveratrol attenuates inflammation and oxidative stress induced by myocardial ischemia-reperfusion injury: role of Nrf2/ARE pathway," *International Journal of Clinical and Experimental Medicine*, vol. 8, no. 7, pp. 10420–10428, 2015.

[42] L. Yang, Y. Zhang, M. Zhu et al., "Resveratrol attenuates myocardial ischemia/reperfusion injury through up-regulation of vascular endothelial growth factor B," *Free Radical Biology and Medicine*, vol. 101, pp. 1–9, 2016.

[43] G. Ndrepepa, "Myeloperoxidase—a bridge linking inflammation and oxidative stress with cardiovascular disease," *Clinica Chimica Acta*, vol. 493, pp. 36–51, 2019.

[44] J. Li, C. Xie, J. Zhuang et al., "Resveratrol attenuates inflammation in the rat heart subjected to ischemia-reperfusion: role of the TLR4/NF-κB signaling pathway," *Molecular Medicine Reports*, vol. 11, no. 2, pp. 1120–1126, 2015.

[45] L.-M. Hung, M.-J. Su, and J.-K. Chen, "Resveratrol protects myocardial ischemia-reperfusion injury through both NO-dependent and NO-independent mechanisms," *Free Radical Biology and Medicine*, vol. 36, no. 6, pp. 774–781, 2004.

[46] I. P. G. Botden, H. Oeseburg, M. Durik et al., "Red wine extract protects against oxidative-stress-induced endothelial senescence," *Clinical Science*, vol. 123, no. 8, pp. 499–507, 2012.

[47] G. Xu, X. Zhao, J. Fu, and X. Wang, "Resveratrol increase myocardial Nrf2 expression in type 2 diabetic rats and alleviate myocardial ischemia/reperfusion injury (MIRI)," *Annals of Palliative Medicine*, vol. 8, no. 5, pp. 565–575, 2019.

[48] X. Zhang, L. F. Huang, L. Hua, H. K. Feng, and B. Shen, "Resveratrol protects myocardial apoptosis induced by ischemia-reperfusion in rats with acute myocardial infarction via blocking P13K/Akt/e-NOS pathway," *European Review for Medical and Pharmacological Sciences*, vol. 23, no. 4, pp. 1789–1796, 2019.

[49] X. Qu, X. Chen, Q. Shi, X. Wang, D. Wang, and L. Yang, "Resveratrol alleviates ischemia/reperfusion injury of diabetic myocardium via inducing autophagy," *Experimental and Therapeutic Medicine*, vol. 18, no. 4, pp. 2719–2725, 2019.

[50] H. Xu, J. Cheng, X. Wang et al., "Resveratrol pretreatment alleviates myocardial ischemia/reperfusion injury by inhibiting STIM1-mediated intracellular calcium accumulation," *Journal of Physiology and Biochemistry*, vol. 75, no. 4, pp. 607–618, 2019.

[51] D. Zhao, J. Yang, and L. Yang, "Insights for oxidative stress and mTOR signaling in myocardial ischemia/reperfusion injury under diabetes," *Oxidative Medicine and Cellular Longevity*, vol. 2017, Article ID 6437467, 12 pages, 2017.

[52] Y. Zheng, B. Shi, M. Ma, X. Wu, and X. Lin, "The novel relationship between Sirt3 and autophagy in myocardial ischemia-reperfusion," *Journal of Cellular Physiology*, vol. 234, no. 5, pp. 5488–5495, 2019.

[53] R. Bolli, B. Dawn, and Y. T. Xuan, "Role of the JAK-STAT pathway in protection against myocardial ischemia/reperfusion injury," *Trends in Cardiovascular Medicine*, vol. 13, no. 2, pp. 72–79, 2003.

[54] P. Weerateerangkul, S. Chattipakorn, and N. Chattipakorn, "Roles of the nitric oxide signaling pathway in cardiac ischemic preconditioning against myocardial ischemia-reperfusion injury," *Medical Science Monitor*, vol. 17, no. 2, pp. RA44–RA52, 2011.

[55] G. Vilahur and L. Badimon, "Ischemia/reperfusion activates myocardial innate immune response: the key role of the toll-like receptor," *Frontiers in Physiology*, vol. 5, p. 496, 2014.

[56] X. Li, J. Yang, J. Yang et al., "RP105 protects against myocardial ischemia-reperfusion injury via suppressing TLR4 signaling pathways in rat model," *Experimental and Molecular Pathology*, vol. 100, no. 2, pp. 281–286, 2016.

[57] X. Guo, H. Jiang, J. Yang et al., "Radioprotective 105 kDa protein attenuates ischemia/reperfusion-induced myocardial apoptosis and autophagy by inhibiting the activation of the TLR4/NF-κB signaling pathway in rats," *International Journal of Molecular Medicine*, vol. 38, no. 3, pp. 885–893, 2016.

[58] L. Y. Dong, F. Chen, M. Xu, L. P. Yao, Y. J. Zhang, and Y. Zhuang, "Quercetin attenuates myocardial ischemia-reperfusion injury via downregulation of the HMGB1-TLR4-NF-κB signaling pathway," *American Journal of Translational Research*, vol. 10, no. 5, pp. 1273–1283, 2018.